SUPLLYMANTARY INFORMATION (SI) FOR:

Astrophysical S factor and Reaction Rate of ^{12}C (α, γ) ^{16}O Calculatted with Reduced R-matrix Theory

Zhenpeng Chen[1], Zhendong An[2], Jiankai Yu[3], Yeying Sun[4], Gongtao Fan[2], Yugang Ma[2], Kan Wang[3]

Preface

This SI includes 8 chapters of main body and 7 sections of appendix, part of the content is in the text briefly introduces, described in detail in the appendix, strive to be complete and rigorous, in order to facilitate the review and application. This work is essentially a kind of nuclear data evaluation with high accuracy, it is the pursuit of scientific, objective and accurate. If need be, you can run the Code RAC2015 to make verification for all examples which are relative to this work, we are glad to send all relative files to you.

This work is of scientific significance as follow: The astrophysical S factors of ^{12}C (α, γ) ^{16}O are the most important basic data for determining the result of cosmogony, determination of accurate values of the S factors (error < 10%) has been regard as a 'holy grail' of nuclear astrophysics for decades. The world's tremendous efforts over 40 years have not reached this goal. We skillfully combines the formulae of the classical R-Matrix theory and the γ transition theory, with the coordination of covariance statistics and error propagation theory, a global fitting for almost all available experimental data of ^{16}O system formed by ^{12}C+α have been done. A set of reliable, accurate S factors and reaction rate of ^{12}C (α, γ) ^{16}O have been obtained. At E=0.3 MeV total S factor is 159.7±9.2 keV b with error <5.9%, reaction rate is 7.82±0.44 mol.s^{-1}.cm^{-3} (5.7 %), for the first time meet the required precision.

Three effective approaches for using global fitting and a powerful Code RAC2015 have been developed to get a set of unique, reliable, accurate and self-consistent S factors and Reaction Rate of ^{12}C (α, γ) ^{16}O. The principal value and error of STOT depend on the data-base used principally, on the width information of bound states (1_1^{-1} *and* 2_1^{+1}) especially, on the cross sections of ^{12}C (α, γ) ^{16}O for E<1.5 MeV very sensitively. Keep going to make new measurements about these data will have possibility to improve the accuracy of STOT. As long as the data-base and the global fitting are good enough, the obtained S factors must be very well. Anyway we believe that if you want to resolve the problem about ^{12}C (α, γ) ^{16}O you have to do with the ways created in this paper.

For this project, two groups of researchers, Tsinghua University and SINAP (Shanghai Institute of Applied Physics), by using the same RAC13 Code and according to the same principle and method, independently carry out analysis, fitting and operation. The purpose is to get through the comparison of two independent sets of results, Determining and improving the objectivity and reliability of the final recommendation values. They work together on the scheme **RAC-Lane-all,** which is a kind of pure phonominalogical fitting, then more schemes ware studied in more detail independently. The schemes **RAC-Lane-11234 and RAC2015** in this paper were finished by Tsinghua University group. The SINAP group adoped different way to calculate the cross section of (α, γ), but **the final obtained S factors are very close to these obtained** by Tsinghua University group, the results of SINAP group will be published elsewhere.

In this paper all SF is with unit keV b, all energy is in CM system and with unit MeV, The keV b and MeV may be omitted sometimes.

Welcome to get more information by E-Mail to zhpchen@tsinghua.edu.cn.

Index 1

1. Introduction

In the first stage of stellar helium burning the triple-α reaction is the dominating process, while in the later stage of this phase the $^{12}C(\alpha,\gamma)^{16}O$ reaction then converts part of the ^{12}C nuclei into ^{16}O nuclei and the ratio of the rates of these two reactions effectively determines the mass fractions of ^{12}C and ^{16}O at the end of helium burning. When the $3\alpha \rightarrow {}^{12}C$ process is relatively fast, the end product of helium burning will be mainly ^{12}C and when it is relatively slow, the end product will be mainly ^{16}O, because of the absence of appropriate states (resonances) near the $^{16}O + \alpha$ threshold. The $^{12}C(\alpha,\gamma)^{16}O$ cross section has been called 'the single greatest experimental uncertainty in explosive nucleosynthetic' at low energies (*W. Arnett1973*). W. Fowler, a Nobel laureate in physics in 1983, definitely held the view that the ratio of oxygen to carbon and the solar neutrino problem are serious difficulties in the most basic concepts of nuclear astrophysics (*Claus1983*), and consequently refer to $^{12}C(\alpha,\gamma)^{16}O$ reaction as the 'holy grail' of nuclear astrophysics. Numerous studies have shown that the ratio of the cross sections for the two reactions, and the resultant $^{12}C/^{16}O$ abundance ratio, are extremely important and sensitive parameter in the later aspects of stellar evolution, not only the nucleosynthetic of elements up to the iron core region but also the subsequent evolution of massive stars, the dynamics of a supernova, and the kind of remnant after a supernova explosion, e.g. a direct influence on type II Supernova (SN) nucleosynthetic (*Woosley2007, Tur2007*), the yield of the neutrino-process isotopes ^{7}Li, ^{11}B, ^{19}F, ^{138}La, and ^{180}Ta in core-collapse supernovae (*Austin2011*), the production of the important radioactive nuclei ^{26}Al, ^{44}Ti, and ^{60}Fe (*Tur2010*), the maximum luminosity and kinetic energy of type I SN (*Inma2001*), weak s-process yields occurring at the end of convective core-He burning and during shell carbon burning (*Pignatari2010*), the composition of C/O white dwarfs in the case of intermediate mass stars (*Metcalfe2002*), and the final state of massive stars: neutron stars, or black holes (*Brown2001*).

As usual, the astrophysical S-factor (SF) is given in terms of the cross section by

$$S(E) = E.\exp(2\pi\eta).\sigma(E) \qquad \text{S1.1}$$

An uncertainty of ≤10% in the astrophysical $S(E = 0.3MeV)$ of ^{12}C (α, γ) ^{16}O reaction is needed to advance the modeling, despite five decades of experimental and theoretical investigations yet, the uncertainty associated with the ^{12}C (α, γ) ^{16}O reaction continues to be an obstacle, which the published values of SF and reaction rate in the Table S1 and S2 contradict each other strongly and their uncertainties are 2 times larger than the required precision.

The most direct and trustworthy way to obtain the astrophysical rate of the $^{12}C(\alpha,\gamma)^{16}O$ reaction is to measure the cross section for that reaction to as low an energy as possible, and to extrapolate to energies of astrophysical interest. However, the difficulty in experimentally determining the rate of ^{12}C (α, γ) ^{16}O for quiescent helium burning, which typically takes place around center-of-mass-energies of 0.3 MeV in the α+^{12}C system, arises from the fact that the cross section is very small (≈ 10^{-17} b) and far beyond direct measurements. In recent two collaborations have pursued complementary approaches to measuring the inverse ^{16}O (γ, α) $^{12}C^{16}O(\gamma,\alpha)^{12}C$ reaction to energies lower than currently achieved at HIGS, which could offer significant advantages over traditional approaches (*Rehm2012, Gai2012*). No longer before, a proposal *(6)* suggest to measure the SF of ^{12}C (α, γ) ^{16}O at lower energy than that have done before, it will need a very reliable theory model to deal with data. R-matrix analysis is the most effective method for the fitting of existing data of ^{16}O system and the absolutely necessary progress for extrapolation at present, creating a new model to get satisfactory SF and RR of ^{12}C (α, γ) ^{16}O is the object of this work.

The classical R-Matrix theory (*lane1958*) deduced the standard R-matrix formulae (SRF) to describe two body nuclear reaction, but it thinks that these formulae are not justified for γ radiative capture, because maybe particles are created or destroyed, and it is hard to select suitable channel radium for electromagnetic interaction. After that, Ref. (*Lane1960*) described the collision matrix for radiative capture in a sum of three parts, internal resonant, external resonant and direct radiative capture (ETRT). Based on this conclusion, the detailed formulae are deduced for angle-integrated cross section in the Ref. (*Holt1978, Barker1991*), which include adjustable parameter of external collision matrix in practical applications. On the models mentioned above, a vital progress in R-matrix code AZURE allows simultaneous analysis the integrated and differential data (*Azmua2010, deBoer2013*), but has not be used to produce the SF down to 0.3 MeV (App. VII. 3). Some papers (*Schurmann2012*) think the E1 and E2 multipoles in ETRT have different energy dependencies, one must have an independent and precise information on each multipole for an extrapolation to E≈0.3MeV, so only the secondary data of E10 and E20 multipoles were used

for the R-matrix analysis, which were got from Legendre polynomials fitting for experimental angular distribution (AD) of ^{12}C (α, γ) ^{16}O. In addition, the literature (*Katsuma2008*) Questions the R- matrix fitting of previous work with enhanced contribution of SE10 in advance, then Using the potential theory to calculate S factor, but the calculated results and the experimental data have very large differences. The detail introductions for previous works are put in Appendix. V.II. Due to the R-Matrix model is based on a complete level-set, and the channels and levels have intimate correlation and strong interference, its analysis result can be accurate and unique only when it can describe the whole database for a nuclear system simultaneously (called global fitting). Examples for detail explain include that, if the used theory model is not complete, if the selected level scheme is not complete, if the types of channel and the set of sub-channel are not complete, if the types of dataset and the energy region of data are not complete, and so on, these defects will bring out the results with multi-values and have very larger uncertainty. These problems existing in the previous works.

In recent 40 years, ETRT have got popular application with the procedure mentioned above, but the produced results have very larger difference and very larger uncertainty (Table S1.1, S1.2), and have not anyone use it to do a global fitting for whole ^{16}O system. For that reason, based on (*Lane1958*) we create a 'Reduced R-matrix theory with relativistic calculation for energy' (RRRT), with the most advanced theory and methods for evaluation nuclear data (*Smith1991, Carlson2007*), which include the theory for systematical error distribution the theory for error propagation, the formulae for covariance fitting, the theory of generalized least squares, the experience method for modification of PPP, and the Lettes criteria for minimize the effect from occasional 'outliers', the test for the definite of covariance matrix, and so on, by using the powerful R-Matrix code RAC which were used to produce the accurate (error<1%) International Neutron Cross section Standards (*NDS-IAEA2007*), to make the global fitting for the special problem to search the SF of $^{12}C(\alpha,\gamma)^{16}O$. A very complete global database has been used for fitting. All available ED about ^{16}O system formed by α+^{12}C and the previous works were evaluated in detail, the sets of evaluated integrated data have complete types, inter-consistent values and continuous data in whole energy region. Near all of ED are selected to use, which include 12 types, 4404 data for E = -1.113 to17.51 MeV (Table S6.3). For example, STOT, $S_{g.s.}$, $S_{6.05}$, $S_{6.13}$, $S_{6.92}$, $S_{7.12}$, AD of $^{12}C(\alpha,\gamma 0)^{16}O$, α-Spectrum, AD of ^{12}C (α, α) ^{12}C, and width information for 31 levels. Have obtained unique, accurate and consistent astrophysical SF of $^{12}C(\alpha,\gamma)^{16}O$ with high precision, At E=0.3 MeV total S factor is 159.7±9.2 keV b with error <5.9%, reaction rate is 7.78±0.44 mol.s^{-1}.cm^{-3} (5.7 %), for the first time meet the required precision. (Table. S1.1, S1.2).

Table S1.1 Astrophysical SF of $^{12}C(\alpha,\gamma)^{16}O$ (keV b, E =300keV)

Reference	STOT	SE10	SE20	$S_{6.05}$	$S_{6.13}$	$S_{6.92}$	$S_{7.12}$
RAC2015	159±7.3	≈94	≈61	0.35±0.14	0.15±0.10	2.41±1.25	0.80±0.51
Schurman2012	161±21	83.4	73.4	0.3	0.3	3.3	0.5
Oulebsir2012	175±63	100±28	50±19				
Katsuma2008		3	150				
Sayre2012			$62^{\pm 9}_{-6}$				
Tang2010		84±21					
Matei2008						7±1.6	
Belhout2007		$80.6^{\pm 17}_{-16}$					
Matei2006				$25^{\pm 15}_{-16}$			
Hammer2005	162±39	77±17	81±22	4±4			
Tischhau2002	149±29	80±20	$53^{\pm 13}_{-18}$	16±16			
Kunz2001	165±50	76±20	85±30	4±4			
NACRE1999	$224^{\pm 97}_{-96}$	79±21	120±60				
Brune1999	$170^{\pm 52}_{-55}$	101±17	$44^{\pm 19}_{-23}$				
Ouellet1996		79±16	36±6				

Buchmann1996	165±39	79±21	70±70	16±16	
Azuma1994		79±21			
Barker1991	$280^{\pm 230}_{-140}$	$150^{\pm 170}_{-50}$	$120^{\pm 60}_{-70}$		
Redder1987	219	$140^{\pm 120}_{-80}$	80±25		
Kettner1982	$430^{\pm 160}_{-120}$	Sg. s = $420^{\pm 160}_{-120}$			12±2
CF88		$60^{\pm 60}_{-30}$	$40^{\pm 40}_{-20}$		
Average difference	>25%	>20%	>45%	>600%	>99%

Table S1.2. The Reaction Rate (10^{-15} mol/ s/cm^3) at T=0.2*10^9 K

	Adopted	High	Low	Error/ %
RAC2015	7.81	8.4	7.4	5.70*
NACREII	6.78	8.98	5.59	25.0
Katsuma2012	8.20	10.2	7.30	17.7
Kunz2002	7.58	10.2	5.25	32.7
Buchmann96	7.04	13.4	3.04	71.0
CF88	11.3	no	no	no

* Up limit, the calculated principal value is 4.10

2. Reduced R-matrix theory with relativistic calculation for energy

This paragraph give the experimental and theoretical basis of the Reduced R-matrix theory with relativistic calculation for energy.

2.1 The reaction mechanism of α+^{12}C

The α and ^{12}C particle collide each other with the center-of-mass energy E to form the entrance channel α+^{12}C. The elastic scattering of α +^{12}C include Coulomb scattering, potential elastic scattering and compound nuclear elastic scattering. In the entire meaningful analysis energy region, from E=0.6 MeV to 8.5 MeV, the elastic scattering is overwhelmingly dominant. According to partial wave expansion of the orbital angular momentum *l*, seven the partial waves (0 to 6) should be considered in the entrance channel α+^{12}C, to corresponding to the initial state spin and parity 0^+, 1^-, 2^+, 3^-, 4^+, $5^-$and 6^+ respectively.

The probability of resonance elastic scattering changes with the center-of-mass energy E, which is well represented by $\gamma_{\alpha,}$ reduced amplitude of elastic scattering. The value of γ_α is determined by fitting the ED. The scattering states γ_α describe the real nuclear reaction that exist in the scattering states, which constitutes the major part of the level width of the scattering state. The γ_α^2 of bound state is α reduced width, the elastic scattering width is defined as zero.

The compound nucleus capture occupy a dominant position in the capture reaction of ^{12}C (α, γ) ^{16}O, direct capture also exist in some extent. The following excited state need to be considered throughout the whole analytical energy region (Fig. S3.1).

The first 4 excited states of $J^\pi = 0^+$ are considered. For the ground state ($J^\pi = 0^+$), the γ transition is forbidden. The E1 and E2 cascade transition to the bound state $0^+_{1\,(-1.113)}$ have been measured in experiments. The transition from $0^+_{1\,(-1.113)}$ to 0^+_0 is by (e^+, e^-) effect with very small probability. Overall the contribution of excited states 0^+ are very weak for the SF.

The first 5 excited states of $J^\pi = 1^-$ are considered. For the ground state, the levels of $J^\pi = 1^-$ can produce E10 transitions. The E1 and M1 cascade transition to the bound state $1^-_{1\,(-0.045)}$ have been measured. The levels $1^-_{1\,(-0.045)}$ and $1^-_{2\,(2.423)}$ at the 2 sides of the **Gamow of E=0.3** MeV, occupy a dominant role for E10 capture processes into the ground state. Owing to the large binding energy(7.2 MeV) of the ^{16}O with respect to the α+^{12}C threshold, its wave function decreases rapidly when the radium larger than a certain value, and the effective charge for 1^- state near zero (Barker1991), so the external contribution and direct capture of E10 can be neglected. The levels $1^-_{3\,(5.280)}$ and $1^-_{4\,(5.858)}$ play dominant function in higher energy rigion.

The first 5 excited states of $J^{\pi}=3^{-}$ are considered of ^{16}O. For the ground state, the levels of $J^{\pi}=3^{-}$ can produce E30 transitions. The E1 and E2 cascade transition to $3^{-}_{1\,(-1.032)}$ have been measured. Overall the contribution of excited states 3^{-} is weak for the SF, the external contribution and direct capture can be ignored.

The first 4 excited states of $J^{\pi}=4^{+}$ are considered. For the ground state, the level $4^{+}_{1\,(3.194)}$ can produce E40-transitions. The overall contribution of excited states 4^{+} is very weak for the SF, the external contribution and direct capture can be ignored.

The first 2 excited states of $J^{\pi}=5^{-}$ and $J^{\pi}=6^{+}$ are considered, but they have elastic scattering width data only, no observed γ transitions.

So except the states of 2^{+} the states of $J^{\pi}=0^{+}$, 1^{-}, 3^{-}, 4^{+} , 5^{-} and 6^{+} can be well described by the standard R matrix theory for the system formed by α+12C.

The first 5 excited states of $J^{\pi}=2^{+}$ are considered. For the ground state, the levels 2^{+} can produce E20 transitions; The E1, E2 and M1 cascade transition to the bound state $2^{+}_{1\,(-0.242)}$ have been measured The width of the level $2^{+}_{2\,(2.683)}$ is very narrow, has little effect on the S-factor at E=0.3 MeV. The levels $2^{+}_{1\,(-0.242)}$ and $2^{+}_{3\,(4.385)}$ at the 2 sides of the **Gamow of E=0.3** MeV occupy a dominant role for E20. Some literature suggest that, for the 2^{+} states external contribution and direct capture are non-negligible. However, Ref. *(Angulo2000, Dufour2008)* think the external contribution can be neglected; (*Buchmann1996*) indicate that the direct capture part is about 4 keV b, about 2.5% of STOT(0.3MeV) only; (*Kettner1982*) and this work shown that the contribution from direct capture is less than 2.5% of STOT(0.3MeV) (refer to S5.1.9). For these reasons, it is reasonable to describe the direct capture of E20 with the parameters of distant levels. Due to the contribution of E10 and E20 play absolute dominate function for of $^{12}C(\alpha,\gamma)^{16}O$, So there is such possibility that a global fitting for whole ^{16}O system formed by α+12C can be done using the Standard R-matrix formula with a suitable channel radium.

One distant levels for each state were introduced for representing the contribution of all the distant level, which form a smooth background in the low energy scales.

2.2 The reduced R-matrix theory with relativistic calculation for energy

For the special problem to search the SF of $^{12}C(\alpha,\gamma)^{16}O$, we create a Reduced R-Matrix Theory. This paragraph give the derivation of a qualitative description for the model of physical concepts. In the subsequent paragraphs, the quantitative description will be given.

The sum of probability for all $\gamma_n+^{16}O_n$ just is the production cross section of $^{16}O_0$. It is not necessary to consider how to decay to $^{16}O_0$ finally, so the problem of 'particles are created or destroyed' is avoided. The reactions of primary radioactive decay to ground or 4 bound states are regards as 'two body particle reaction channels', denoted by $\gamma_n+^{16}O_n$, the reduced masses of these channels are represented by relativistic energy. The sum of integral cross sections of each reaction channel equal to the cross section of ^{16}O production. The primary wave function Ψ can be unfold with Ψ_c, set $c=\{\alpha,s,l\}$, where α refer to particle pair, s is channel spins and l is channel orbital angular momentums. Ψ_c Can be expended with level wave function $\Psi_{\alpha sl\lambda}$, which have different total angular momentum and parity J^{π} and E_λ. Finally Ψ is expressed with the equation V.2. (2.6) in *(7)*:

$$\Psi=\sum_c\left[\sum_\lambda\frac{X_\lambda\gamma_{\lambda c}}{E_\lambda-E}\right] \qquad \text{S2.2.1}$$

The total wave function for the initial state of ^{16}O can be expanded by the complete orthogonal set, the coefficient of the expanded formula represent the probability of different reaction channel of all sorts of resonance energy state. Formula (S2.2.1) demonstrates that, if the primary gamma decay ($\gamma_n+^{16}O_n$) as the independent two body reaction channel, the ^{16}O initial state can be expanded with Ψ_c and Ψ_c can be unfold with level wave function $\Psi_{\alpha sl\lambda}$, the wave function set of the theoretical model contain all types of γ- transition, whether direct decay to the ground state transition or cascade transition, both the compound nuclear transition or direct transition.

To sum up, the characteristics of ' Reduced R- matrix Theory' as follows:

A. The sum of probability for all $\gamma_n+^{16}O_n$ primary radiative is just the production cross section of $^{16}O_0$, it's not necessary to consider how to decay to $^{16}O_0$ finally, so the problem of 'particles are created or destroyed' is avoided;

B. All particles and gamma mass using energy representation by the relativistic method, so the reactions of primary radioactive decay to ground or 4 bound states can be regarded as two body particle reaction channels to calculate easily.

C. The wave function set contain all the ground gamma transition and cascade gamma transition in this model;

D. Using distant level parameter of compound nucleus to represent the smooth contribution of direct capture;

E. Using the total width of reduced channel Γ_λ^e to represent all other reaction channel except the ^{12}C (α, α) ^{12}C, ^{12}C (α, γ) ^{16}O, ^{12}C (α, α1)^{16}O and ^{12}C (α, p) ^{16}O reaction, so it's convenient to expend the analysis to higher energy region;

F. It can analyze and calculate all ED of ^{16}O systems to achieve the enhanced reliability S-factors at Gamow window.

G. The covariance fitting and error propagation theory are adopted, which can accurately give the expected value and the covariance of SF.

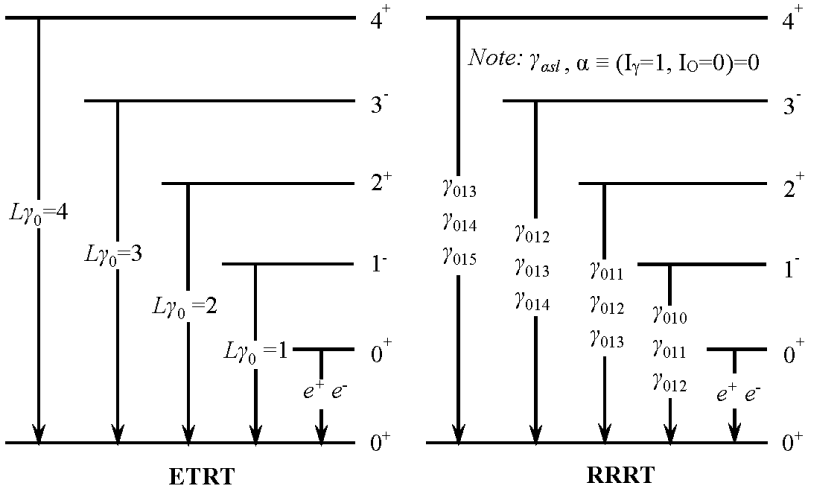

Figure 2.2 shows the transition processes to ground-state (0^+_0) described by ETRT and RRRT for ^{16}O system. In ETRT model *L* only has one value for each initial state. In the RRRT model, the 'relative orbital angular momentum *l*' is introduced in formulae, the angular momentum coupling mechanism is considered, the quantum state set which RRRT can provide are complete for each state, there are 3 sub-reaction channels included in the states 1^-, 2^+ and 3^- respectively. When ι_{max}=4, these reaction channel sets are able to describe all kinds of data directly and perfectly.

3. Construction of the best set of sub-reaction channel

To construct optimal sub reaction channel set is the key point in the R- matrix analysis. Sub reaction channel set in our work is strict set up in accordance with the decay scheme of ^{16}O energy levels. The details are as follows.

3.1. Level scheme of the ^{16}O nucleus and the gamma transition

Figure S3.1 show the position, width or life of ^{16}O levels below the 17.5MeV energy region. Except the level $J^\pi=2^-$(Ex=8.872 MeV), the other 31 levels contain α+^{12}C reaction channel. The blue line with arrow on the left side represent the reaction channel of the initial transition to the ground and four bound states. The red line represents the calculation of total SF in the analysis area. The branching ratio for the β-delayed α decay spectrum of ^{16}N shown on the right with the green lines. There are 4 bound states close to the threshold 7.162 MeV with respect to ^{12}C(α, α)^{12}C reaction, however these states are positive energy state for transfer reaction which have many ED of reduced width. For low-energy region (Ex<11.6 MeV), only ^{12}C (α, α) ^{12}C and ^{12}C (α, γ) ^{16}O are opened, more than 11.60 MeV and 12.13 MeV the ^{12}C (α, α1) ^{12}C* and ^{12}C (α, p) ^{15}N will be opened respectively. If the contribution of other reactions, such as ^{12}C (α, α2)^{12}C*, are represented by the total width of reduced channelΓ_λ^e, the analysis area can be extended to the Ex = 14.2 MeV, where have many ED. The region from Ex = 14.2 MeV to 17.5MeV, there are 12 levels which the widths of different reaction channel can be used to restrain the

contribution of background levels. The above energy region from 7.2 MeV to 17.5MeV are just to satisfy this requirement of the calculation of the reaction rate of $^{12}C(\alpha,\gamma)^{16}O$ from T_9=0.01 to 10.

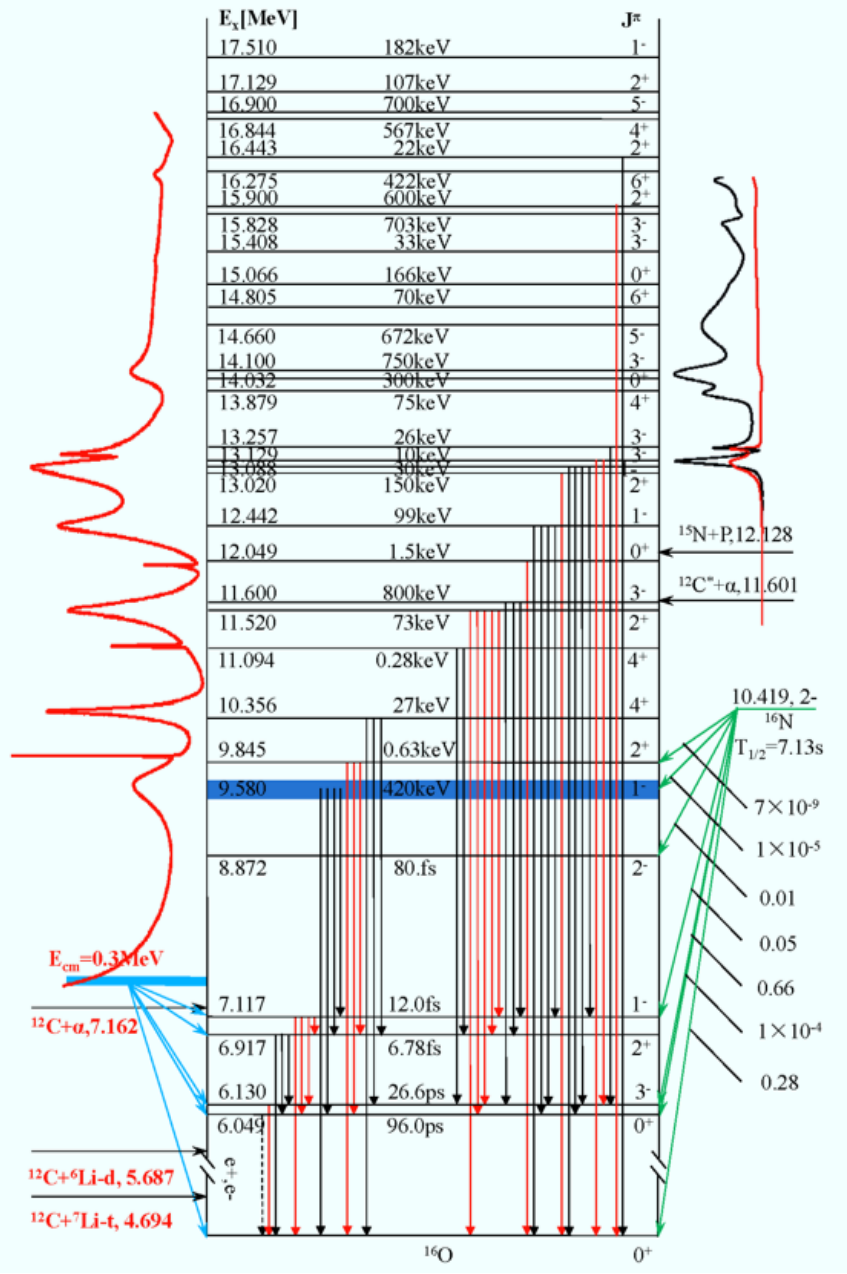

Fig. S3.1. Level scheme of the ^{16}O nucleus. All states relevant for the analysis are indicated. All published gamma transition (vertical line with arrows) are shown in Figure S3.1, which contain a latest confirmed cascade transition exists ($3^- \rightarrow 1^-$ vertical dotted line with an arrow), a pair decay ($e^+ + e^- \rightarrow \gamma$). The sub reaction channel of gamma particles in this analysis are strictly set up by referring to figure S3.1 data, and some new results (*deBoer2013*), . So this analysis has strong objectivity.

The relationship between width and life or half-life is:

$$T_{1/2}=0.693147\tau, \qquad \text{S3.1.1}$$

$$\Gamma = \hbar/\tau\,,\ \hbar=6.582173\times10^{-22}\ \text{MeV·s} \qquad \text{S3.1.2}$$

Using the above relationship the level lifetime is converted to energy level width in this fitting.

3.2. Construction of the best set of reaction channel

The considered levels of compound nucleus ^{16}O in the analysis are determined by the incident channel α+^{12}C. The intrinsic spin of α and ^{12}C are zero, so the channel spin S is constant 0. The total angular momentum of α+^{12}C, J≡ *l*, where *l* is the relative orbital angular momentum. The parity π of α and ^{12}C are +1 respectively, then the parity of compound nuclear of α+^{12}C is $\pi_{\alpha*}\pi_{C*}(-1)^{l}$. When *l* =0, 2, 4 and 6, the spin and parity J^{π} are 0^+, 2^+ , 4^+ and 6^+ respectively; when *l* =1, 3, 5, the $J^{\pi}=1^-$, 3^- and 5^- respectively .In the work the levels only of the actual measured with accurate information are set up in the energy region for the analysis. According to the Table 16.15: *Resonances in* $^{12}C+\alpha$, in [Tilley1993], 31 level with available information up to 17.52 MeV are adopted in our analysis. There are six kinds of levels, 0^+, 1^-, 2^+, 3^-, 4^+, 5^-, and 6^+. In addition to 6^+, each type of J^{π} Level is set up a distant level for making contribution of background. Hence, 37 levels in the complete set are considered in our fitting.

The decay channel of compound nucleus have the same total angular momentum J and parity as the entrance channel. The intrinsic spin of γ is 1. Supposing the compound nucleus decay a gamma ray from initial state φ_i to the final state φ_f, according to the principle of conservation of parity, the definition of parity of the emitted γ_n particle is

$$\pi_{\gamma} = \pi_i/\pi_f, \qquad \text{S3.2.1}$$

According to the principle of conservation of angular momentum, the angular momentum of gamma particles is

$$J_{\gamma}=|I_i - I_f|,\ |I_i - I_f|+1,\cdots |I_i + I_f| \qquad \text{S3.2.2}$$

If the γ_n+$^{16}O_n$ as a class of two body reaction channel, due to the intrinsic spin I_{γ} is 1, the intrinsic spin of $^{16}O^*_n$ Io=Jn, the channel spin γ_n+$^{16}O_n$ is

$$S_n=|1 - I_o|,\ |1 - I_o|+1,\cdots |1 + I_o| \qquad \text{S3.2.3}$$

The relative orbital angular momentum, L_n, of γ_n+$^{16}O^*_n$ meet the formula of vector summation:

$$L_n=|J_n - S_n|,\ |J_n - S_n|+1,\cdots |J_n - S_n| \qquad \text{S3.2.4}$$

For the heavy particle decay channel, due to its parity of angular momentum is $(-1)^{l}$ only, in a resonant level, the *l* can only be odd or even. For the γ particle decay channel, the symbol [ ] = $\frac{1}{2}[1+(-1)^{L'+L+k+\epsilon+\epsilon'}]$ indicates a parity restrication, in a resonant level, the *l* might be odd and even.

In each resonance state, according to the constraints of conservation law, can meet the requirements of gamma is a transverse wave, and actual need, the following reaction channels are set up:

A. elastic scattering channel α+^{12}C, which must be set up in each resonance states;

B. gamma particles channel γ_0+$^{16}O_0$, the first decay from initial state to the ground state;

C. gamma particles channel γ_1+$^{16}O_1$, the first decay from initial state to the first excited state (0^+, 6.05 MeV);

D. gamma particles channel γ_2+$^{16}O_2$; the first decay from initial state to second excited states (3^-, 6.13 MeV);

E. gamma particles channel γ_3+$^{16}O_3$, the first decay from initial state to third excited states (2^+, 6.92 MeV);

F. gamma particles channel γ_4+$^{16}O_4$, the first decay from initial state to fourth excited states (1^-, 7.12MeV);

G. inelastic scattering channel α_1+$^{12}C^*$, which is set up in the opened levels for the α_1+$^{12}C^*$;

H particles channel p+^{15}N, which is set up in the opened levels for the p+^{15}N;

I. reduced channel α+x, the total width Γ_{λ}^{e} represent the contribution of other reaction channel except the above channels mentioned.

For settings of sub-reaction channel and relevant parameter, the following principles should be obeyed:

A. The following conservation laws: the parity conservation, angular momentum conservation, energy conservation, momentum conservation and the conservation of charge should be satisfied. For gamma particle reaction channel the γ - transition selection rule should be met simultaneously.

B. The data should be obtained in the relevant experiment. Those reaction channel which meet the theoretical requirements, but no measured ED are not set up in this fitting.

C. In the distant level, the sub reaction channel are set up to describe the sum of smooth background of resonance capture and non-resonance capture.

D. The reduced width Γ_λ are established in the necessary energy area which can improve the fitting.

E. According to the physical principles, some parameters can be fixed with constants

For example, the radius value (7 parameters), the position of bound state and distant level (15 parameter), reduced total width of high level without competition from the other ED (8 parameters)

F. Using the error propagation law and covariance calculation to reduce the non-essential parameter as far as possible.

By using the error propagation law and covariance calculation the relative error of a reduced width amplitude $\gamma_{c\prime s\prime\iota\prime}$ can be obtained. The $\gamma_{c\prime s\prime\iota\prime}$ which must be set up in the physical and with Rerr≥200% should be keep; The $\gamma_{c\prime s\prime\iota\prime}$ which is not must b e set up in the physical and with Rerr≥200% should be given up; After getting rid of this kind of parameter, there may be sli ght increase the total χ^2, the average χ^2 per degree of freedom could be reduced. The detail information about reduced width amplitude $\gamma_{cs\iota}$ and $\gamma_{c\prime s\prime\iota\prime}$ are put in Table S3-C for RAC2015.

3.3. The R-Matrix parameters for RAC13

The formula S3.3.1 and S3.3.2 are the concrete expression in the RAC code, where asl and $a's'l'$ are the entrance and exit channel respectively ($a = c$), $\Delta_{\lambda\mu}$ is energy matrix, E_{el} is the position of resonance level, $\Delta_{\lambda\mu}$ is the energy shift, $\Gamma^e_{\lambda\mu}$ the total reduced channel width.

$$[R^J_{(E)}]_{\alpha's'l',asl} = \sum^N_{\lambda\mu} \gamma^J_{\alpha's'l'}\gamma^J_{asl}A_{\lambda\mu}\delta_{JJ_0} \quad \text{S3.3.1}$$

$$[A^{-1}]_{\lambda\mu} = \left[E^r_\lambda - E - \Delta^r_{\lambda\mu}(E^r_\lambda)\right]\delta_{\lambda\mu} + \Delta^e_{\lambda\mu}(E^r_\lambda) - \frac{i}{2}\Gamma^e_{\lambda\mu} \quad \text{S3.3.2}$$

$$\Delta_{\lambda\mu} = -\sum^N_{\alpha sl}[S_{\lambda\mu} - B_\alpha]\gamma_{\alpha's'l'}\gamma_{asl} \quad \text{S3.3.3}$$

About details R-matrix parameters see the Table S3-A, -B, -C, which is the input parameters file of our RAC program. For the first level of different J^P, let $S_{\lambda\mu} \equiv B_\alpha$ to get$\Delta_{\lambda\mu} \equiv 0$, but other levels will have$\Delta_{\lambda\mu} \neq 0$, which are called **Standard R-matrix formula**. When let $\Delta_{\lambda\mu} \equiv 0$ for all level, the standard R-matrix formula will be simplified to **R-matrix Physical formula**.

Table S3-A. The parameters of reaction channel

NO.	Channel	R(fm)	l_{max}	Th(MeV)	NO.	Channel	R(fm)	l_{max}	Th(MeV)
C1	α, ^{12}C	6.5	6	0.0000	C5	γ3, $^{16}O_3$	6.5	2	0.3449
C2	γ0, $^{16}O_0$	6.5	4	7.1620	C6	γ4, $^{16}O_3$	6.5	2	0.1452
C3	γ1, $^{16}O_0$	6.5	3	1.2126	C7	α_1, $^{12}C^*_1$	6.5	3	-4.4380
C4	γ2, $^{16}O_1$	6.5	2	1.1321	C8	p, ^{15}N	6.5	3	-4.9680

Table S3-B. The parameters of reaction channel

Channel	M_T	M_I	Th(MeV)	R(fm)	l_{max}	Z_T	Z_I	S_T	S_I	P_T	P_I
α, ^{12}C	12.0000648499	4.0015063286	0.0000	6.5	5	6	2	0	0	+	+
γ_0, $^{16}O_0$	15.9970233044	0.0000000000	7.1620	6.5	4	8	0	0	1	+	
γ_1, $^{16}O_1$	16.0035163226	0.0000000000	1.2126	6.5	2	8	0	0	1	+	
γ_2, $^{16}O_2$	16.0036076157	0.0000000000	1.1321	6.5	2	8	0	3	1	-	
γ_3, $^{16}O_3$	16.0044561723	0.0000000000	0.3449	6.5	6.5	8	0	2	1	+	
γ_4, $^{16}O_4$	16.0046677857	0.0000000000	0.1452	6.5	6.5	8	0	1	1	-	

α_1, $^{12}C^*_1$	12.0047583003	4.0015063286	-4.4380	6.5	6.5	6	2	2	1	+	-
p, ^{15}N	15.0004677857	1.0076000000	-4.9680	6.5	6.5	7	1	1/2	1/2	-	+

Table S3-C. Level position E_λ, Total Reduced width Γ_λ and Reduced Width Amplitude γ of sub-reaction channel

Note: **JP** refer to total spin and parity, E_λ the position of level, Γ_λ total width of reduced channels; Csl (csl) refer to Reduced Width Amplitude γ of sub-reaction channel, c is channel number, s is spin, l is orbital angular momentum. $+\gamma_n$ means l is even number, $-\gamma_n$ means l is odd number. Both the $+\gamma_n$ and $-\gamma_n$ are used to represent the γ_n.

1. '^{12}C (α, α) ^{12}C ', l=0 to 6.
2. '^{12}C (α,+γ_0)$^{16}O_0$ ', l is even number.
3. '^{12}C(α,-γ_0)$^{16}O_0$ ', l is odd number.
4. '^{12}C(α,+γ_1)$^{16}O^*_1$ ', l is even number.
5. '^{12}C(α,-γ_1)$^{16}O^*_1$ ', l is odd number.
6. '^{12}C(α,+γ_2)$^{16}O^*_2$ ', l is even number.
7. '^{12}C(α,-γ_2)$^{16}O^*_2$ ', l is odd number.
8. '^{12}C(α,+γ_3)$^{16}O^*_3$ ', l is even number.
9. '^{12}C(α,-γ_3)$^{16}O^*_3$ ' l is odd number.
10. '^{12}C(α,+γ_4)$^{16}O^*_4$ ', l is even number.
11. '^{12}C(α,-γ_4)$^{16}O^*_4$ ', l is odd number.
12. '^{12}C(α, α_1)$^{16}O^*$ ', l=0 to 3.
13. '^{12}C(α, p)^{15}N ', l=0 to 3.

JP(+0) E_1=-1.112600 Γ_1=0.000000
Csl(100) γ=-1.37357022221E-1
Csl(311) γ= 2.21482433448E-5

JP(+0) E_2= 4.653949 Γ_2=0.000250
Csl(100) γ= 1.26144826647E-3
Csl(311) γ=-1.08499237494E-1

JP(+0) E_3= 6.912000 Γ_3=0.020000
Csl(100) γ= 1.08337226583E-1

JP(+0) E_4= 7.904000 Γ_4=0.000030
Csl(100) γ= 1.32983007346E-1
Csl(1222) γ= 7.77723722468E-2
Csl(1311) γ= 2.78468615985E-1

JP(+0) E_5=30.577400 Γ_5=0.000000
Csl(100) γ= 3.12572752454E+0
Csl(311) γ= 8.08269108368E-4
Csl(1311) γ= 1.79296986129E+0

JP(-1) E_1=1-0.045150 Γ_1=0.000000
Csl(101) γ= 8.44370207619E-2
Csl(211) γ=-1.58448049396E-3
Csl(411) γ=-5.62112989995E-5
Csl(622) γ= 6.21361657784E-2
Csl(811) γ= 3.40285001537E-4
Csl(1010) γ=-5.34083118643E-5

JP(-1) E_2= 2.291539 Γ_2=0.000100
Csl(101) γ= 3.39925845722E-1
Csl(211) γ= 9.97525491644E-5
Csl(310) γ=-2.12573539295E-4
Csl(312) γ= 2.75626200896E-3
Csl(411) γ= 5.07192357190E-4
Csl(510) γ= 8.15736162362E-5
Csl(512) γ=-2.76161883245E-3
Csl(811) γ= 2.61449522821E-4
Csl(910) γ=-2.36222128253E-5
Csl(912) γ= 1.22209102885E-3
Csl(1010) γ= 1.15307356084E-4
Csl(1012) γ= 2.60956141574E-3

JP(-1) E_3= 5.280427 Γ_3=0.000010
Csl(101) γ= 1.09146620649E-1
Csl(211) γ=-5.65442297691E-4
Csl(310) γ= 1.08188648159E-3
Csl(312) γ= 1.80523326359E-2
Csl(411) γ=-1.79724663738E-3
Csl(510) γ=-9.62373998192E-4
Csl(622) γ= 3.31591811335E-2
Csl(1010) γ= 2.11600514649E-4
Csl(1012) γ=-3.72938086476E-3
Csl(1221) γ= 1.04128928160E-1
Csl(1223) γ= 1.59063021315E-1
Csl(1310) γ= 7.68436255639E-2

JP(-1) E_4= 5.873027 Γ_4=0.000100
Csl(101) γ=-6.63761389403E-2
Csl(211) γ=-1.86181898909E-3
Csl(310) γ= 5.98173991573E-3
Csl(312) γ=-4.40211735360E-2
Csl(411) γ=-1.71631841388E-3

JP(-1) E_5= 9.710000 Γ_5=0.153000
Csl(101) γ=-1.02545132591E-1

JP(-1) E_6=11.417600 Γ_6=0.000000
Csl(101) γ= 1.25001655375E+0
Csl(211) γ=-7.55125346307E-4
Csl(312) γ= 1.21693323256E-3
Csl(411) γ=-4.17054092420E-3
Csl(510) γ= 1.07127529613E-4

Csl(510) γ = 5.04165132058E-4
Csl(622) γ = 6.21724864416E-2
Csl(1101) γ =-1.00599912529E-2
Csl(1221) γ =-5.33725325864E-2
Csl(1223) γ = 2.40957646982E-1
Csl(1310) γ = 1.61843128628E-1
Csl(1312) γ = 3.47009993614E-2

Csl(512) γ = 8.31928561650E-3
Csl(622) γ = 2.91641743544E-2
Csl(910) γ =-7.62940983415E-5
Csl(1010) γ = 3.93033119104E-5
Csl(1310) γ =-4.73171801302E-2
Csl(1312) γ = 6.48034733891E-2

JP(+2) E_1=-0.2449000 Γ_1=0.00000
Csl(102) γ = 1.67923100136E-1
Csl(212) γ = 3.76420733969E-2
Csl(511) γ = 2.45764253686E-3
Csl(513) γ = 8.39205117920E-2
Csl(621) γ = 4.71733773052E-4

JP(+2) E_2= 2.6854552 Γ_2=0.00001
Csl(102) γ = 1.80332798509E-2
Csl(212) γ =-2.33008909808E-3
Csl(311) γ =-1.32999435887E-4
Csl(313) γ =-2.60717478928E-3
Csl(412) γ = 2.00269029024E-2
Csl(511) γ =-1.64874946783E-3
Csl(820) γ =-4.92653642416E-2
Csl(911) γ =-1.28426002736E-4

JP(+2) E_3= 4.3157254 Γ_3=0.00682
Csl(102) γ = 6.79653901836E-2
Csl(212) γ = 2.14186458616E-2
Csl(311) γ = 1.16302632848E-3
Csl(313) γ =-1.23536768531E-2
Csl(412) γ = 3.21421164882E-2
Csl(511) γ = 9.28287231701E-4
Csl(621) γ = 6.53503659796E-4
Csl(722) γ = 1.24416624317E-3
Csl(820) γ = 2.01222186976E-3
Csl(911) γ = 6.11734218678E-4
Csl(1011) γ = 5.67189563373E-4

JP(+2) E_4= 5.7847193 Γ_4=0.00010
Csl(102) γ = 1.15811078787E-1
Csl(212) γ =-1.06004370152E-2
Csl(311) γ = 1.94661501123E-3
Csl(313) γ =-1.56626245372E-2
Csl(1220) γ =-4.44948552966E-2
Csl(1222) γ = 6.19365068121E-2
Csl(1311) γ =-1.09992849621E-1
Csl(1313) γ = 1.90557933653E-1

JP(+2) E_5= 8.3000000 Γ5=0.00100
Csl(102) γ = 2.30560181580E-1
Csl(212) γ = 1.10871682149E-2

JP(+2) E_6=22.5322000 Γ_6=0.00000
Csl(102) γ = 2.43492902626E+0
Csl(212) γ = 2.74341571961E-2
Csl(311) γ =-4.48966698410E-3
Csl(313) γ =-8.67125381330E-2
Csl(412) γ =-4.13860940097E-2
Csl(511) γ = 1.53928858057E-2
Csl(621) γ = 2.61409608720E-3
Csl(812) γ =-1.16163111579E-1
Csl(820) γ = 1.52857928413E-2
Csl(911) γ = 6.91209289724E-3
Csl(1011) γ = 5.78246357892E-3
Csl(1220) γ =-4.23867016757E-2
Csl(1222) γ =-8.52532915671E-1
Csl(1311) γ =-6.99750335353E-1
Csl(1313) γ =-6.57242078420E-1

JP(-3) E_1=-1.0321000 Γ_1=0.00000
Csl(103) γ =-7.58573378626E-2
Csl(312) γ =-7.57434384405E-4

JP(-3) E_2= 3.9814730 Γ_2=0.04577
Csl(103) γ = 3.15699626669E-1
Csl(622) γ = 1.07763846271E-3
Csl(932) γ = 1.44330831315E-3
Csl(1022) γ = 4.08327680512E-2

JP(-3) E_3= 6.0935188 Γ_3=0.00005
Csl(103) γ = 1.02590858250E-1
Csl(312) γ = 3.81680145936E-3
Csl(622) γ =-2.04100966590E-2
Csl(721) γ = 2.83721511100E-3
Csl(1221) γ =-2.78642900324E-1

		Csl(1223) γ=-4.53693627698E-2
		Csl(1312) γ= 1.44205077016E-3
JP(-3) E_4= 6.0637369 Γ_4=0.00005	JP(-3) E_5= 6.9380000 Γ_5=0.00010	JP(-3) E_6=26.0851000 Γ_6=0.00000
Csl(103) γ=-3.81775480296E-2	Csl(103) γ= 4.80647188706E-2	Csl(103) γ=-1.83818521282E+0
Csl(622) γ= 1.23128495415E-2	Csl(1221) γ=-2.73841800415E-1	Csl(512) γ=-4.12072112241E-2
Csl(721) γ= 1.46963833925E-2	Csl(1223) γ= 4.29660963150E-1	Csl(622) γ= 3.08386819710E-2
Csl(1221) γ= 4.37076466020E-2		Csl(1223) γ= 4.50728380213E-1
Csl(1223) γ= 4.75674935781E-2		
Csl(1312) γ= 3.99081285942E-1		
JP(+4) E_1= 3.1956118 Γ_1=0.00300	JP(+4) E_2= 3.9339949 Γ_2=0.00020	JP(+4) E_3= 6.7373100 Γ_3=0.00060
Csl(104) γ= 2.16252005682E-1	Csl(104) γ= 7.24137908365E-3	Csl(104) γ=-5.15781085230E-2
Csl(313) γ= 1.47324734860E-4	Csl(641) γ= 6.77771308113E-4	Csl(1222) γ=-2.48574249270E-1
Csl(722) γ= 3.12895915419E-4	Csl(832) γ=-1.80637833527E-2	
Csl(822) γ=-1.40291047964E-1		
Csl(832) γ=-6.54674651634E-2		
JP(+4) E_4= 9.6820000 Γ_4=0.40800	JP(+4) E_5=30.4404000 Γ_5=0.00000	
Csl(104) γ= 1.00077927154E-1	Csl(104) γ= 2.23470318620E+0	
	Csl(513) γ= 4.74240166724E-1	
	Csl(822) γ=-2.32369380649E+0	
	Csl(832) γ=-5.00150284383E-1	
	Csl(1222) γ=-4.67653436371E-1	
JP(-5) E_1= 7.4980000 Γ_1=0.00000	JP(-5) E_2= 9.7480000 Γ_2=0.00000	JP(-5) E_3=23.3775000 Γ_3=0.00000
Csl(105) γ= 3.93028414880E-1	Csl(105) γ= 2.93138753413E-1	Csl(105) γ= 1.19299405418E+0
Csl(1223) γ=-1.26957859941E-1		
JP(+6) E_1= 7.6430000 Γ_1=0.04800	JP(+6) E_2= 9.1330000 Γ_2=0.02950	
Csl(106) γ= 8.30814046411E-2	Csl(106) γ= 2.85943713264E-1	

4. Advanced theory and Code RAC for evaluation of nuclear data

4.1. Covariance statistic, Generalized least squares and error propagation law (Smith1991)

The book (*Smith1991*) is the modern classical literature which include the most advanced theory for evaluation of nuclear data, and an Encyclopedia to guide program composition. The literatures (*Carlson2009;* STD-NDS-IAEA-2007) are the best example of applied the theory and summary of experiences. In the theory and self-contained methods, the theory for error distribution, the theory for error propagation, the formulae for covariance fitting, the theory of generalized least squares, the experience method for modification of PPP, and the Lettes criteria for minimize the effect from occasional 'outliers', the test for the definite of covariance matrix, and so on, are the key elements for trying to get accurate evaluating value, in which no anyone can be ignored. This is because only with a suitable model in which using these theories and methods the experimental nuclear data can be described objectively with high precision. The basic evidence is that in the measure process for nuclear data, the long range error, middle range error and short range error of observables are existing objectively, which are never be avoided absolutely. The long range and middle range error have correlation ship. The code RAC13 make use of the suitable theory model, employ the most advanced evaluation theory and methods, is able to use the most complete global database, the obtained evaluated values must be the closest to the expectation value, and the obtained error information must be the most reasonable. The previous work are the 'ordinary least squares' fitting, in theory which cannot give the unbiased estimation for complex

samples, but without the PPP problem introduced under the paragraph. In our work the 'covariance fitting' is quoted, this is because, in theory, the system error does always exist no matter how exact the evaluation of ED is. As long as the system error existed, the correlation of ED and the off-diagonal elements of the covariance matrix can never be removed. The ‘ordinary least squares’ fitting only considered the diagonal elements of the covariance matrix, which ignore the off-diagonal element and the part of correlation of ED. So the optimal calculation is only a rough approximation of the expected value according to the 'maximum like lihood principle'. The covariance fitting is an accurate method, inverse of the covariance matrix using in the optimization, the obtained values of SF are expected to the accurately estimate value. Table 4.1 shows the significant difference of SF between the ‘Common least squares fitting (DIA)’ and the ‘Covariance Fitting’ (COV). In next section to introduce how to construct covariance matrix with error information of experimental data.

Suppose U_i^2, S_i^2, L_i^2, M_i^2 and Y_i^2 are total variance, statistical variance, long-range component (LERC) of systematic variance, medium-range component (MERC) of systematic variance and total systematic variance of the i[th] ED point respectively, and let $U_i^2 = S_i^2 + L_i^2 + M_i^2$, $Y_i^2 = L_i^2 + M_i^2$. The diagonal elements C_{jj} of correlation coefficient matrix C are 1 for all. The non-diagonal elements for integral cross section are

$$C_{ij} = C_{ij}^L + C_{ij}^M \quad \text{S4.1.1}$$

Here C_{ij}^L refers to the LERC of systematic errors, C_{ij}^M to the MERC of systematic errors, and

$$C_{ij}^L = L_i L_j / (U_i U_j) \quad \text{S4.1.2}$$

$$C_{ij}^M = M_i M_j / (U_i U_j) \cdot f_{ij} \quad \text{S4.1.3}$$

$$f_{ij} = \text{Exp}\{-[(E_i - E_j)/\text{W}]^2/2\} \quad \text{S4.1.4}$$

Where, W is a distribution width parameter, and E_i and E_j stand for energy points of the data. The non-diagonal elements of C for AD are

$$C_{ij} = \left(C_{ij}^L + C_{ij}^M\right) \cdot G_{ij} \quad \text{S4.1.5}$$

$$G_{ij} = \text{Exp}\{-[(\theta_i - \theta_j)/160]^2/2\} \quad \text{S4.1.6}$$

Here 160 is a distribution parameter related to angle, θ_i and θ_j are angle values.

It can be seen from the formulas given above that correlation coefficient is determined by total error and systematic error, and a larger systematic error leads to a larger correlation coefficient. The absolute covariance matrix elements of simulation data can be calculated from the corresponding correlation coefficients as follows:

$$V_{ij} = C_{ij} \cdot U_i \cdot U_j \quad \text{S4.1.7}$$

The theoretical formula about error propagation with R-matrix model fitting is as following:

$$\text{y} - y_0 = D(P - P_0) \quad \text{S4.1.8}$$

$$D_{ki} = (\partial y_k / \partial P_i)_0 \quad \text{S4.1.9}$$

Here y refers to vector of calculated values, D to sensitivity matrix, P to vector of R-matrix parameters. Subscript 0 means optimized original value, k and i are for fitted data and R-matrix parameter subscript respectively. The covariance matrix of parameter P is

$$V_P = (D^+ V^{-1} D)^{-1} \quad \text{S4.1.10}$$

Here *V* refers to covariance matrix of the data to be fitted, and its inversion matrix can be expressed as following:

$$V^{-1} = \begin{pmatrix} V_1^{-1} & & 0 \\ & V_2^{-1} & \\ 0 & & \ddots \\ & & & V_k^{-1} \end{pmatrix} \quad \text{S4.1.11}$$

Here V_1, $V_2 \cdots V_k$ refer to the covariance matrixes of the sub-set data, which are independent with each other. The covariance matrix of calculated values is

$$V_y = D V_P D^+ \quad \text{S4.1.12}$$

Formula adopted for optimizing with R-matrix fitting is

$$\boldsymbol{\chi^2} = (\boldsymbol{\eta} - \boldsymbol{y})^{+}\boldsymbol{V^{-1}}(\boldsymbol{\eta} - \boldsymbol{y}) \Rightarrow minimun \qquad \text{S4.1.13}$$

Here η refers to the vector of ED, y refers to the vector of calculated values.

4.2. Modification about Peelle Pertinent Puzzle

The fact that the principal values of fitting lower than the experimental value was called Peelle Pertinent Puzzle (PPP) in the field of evaluation of nuclear data. In theory, the basis of covariance fitting is maximum likelihood principle which apply to the statistical sample, and the PPP is due to the large systematic error of ED depart from the statistical sample. For the ordinary least squares fitting, a big χ^2 data stem from only the contribution of the diagonal matrix element itself; For the covariance fitting, the source of a large χ^2 data are the large contribution of line and column of matrix element from this point. The great dimensions of the matrix the stronger influence of χ^2 value, so it is a disadvantage for a large number of ED analysis.

The PPP occurrence for the data sets is mainly due to the existence of some data points which are very much discrepant from others. In the data sets, all errors are given in percentage, so that for a datum value higher than its expected value, it has a larger absolute error and a larger associate covariance, and consequently has a relative smaller weight. On the contrary, for a datum lower than its expected value, it has a relative larger weight. When both the errors and discrepancy of a data sets are sufficiently large to some extent, the PPP may occur.

So any method, which is able to remove the phenomena mentioned above, will have the effect to avoid PPP.

As long as the covariance fitting, the fitting have PPP in varying degrees, and require revision. For the comprehensive fitting to the huge ED, there are many methods created to the PPP revision, one of the simplest way: the expected value times the relative error as the absolute error (*IAEA-NDS2009*).

The Table S4.2 shows the SF (E=0.3MeV, keV) and Chi square information of three fitting methods. The RAC2014-COV refers to a fitting procedure with covariance and with PPP modification. The RAC2014-DIA refers to a fitting procedure with variance and without PPP modification, its calculated STOT (153.52) is lower than that of RAC2014-COV (158.64) .The RAC2014-PPP refers to a fitting procedure with covariance and without PPP modification, its calculated STOT (148.82) is much lower than that of RAC2014-COV (158.64), and its Chi squares are much higher than those of RAC2014-COV. The Fig. 4.2 shows the calculated STOT of the three methods. It is very clear that the fitting values of RAC2014-PPP are lower than the experimental values systematically in the energy range of peak 1^-_2 (2.35).

These results explain that using the fitting procedure with covariance and with PPP modification is necessary absolutely.

Table S4.2. The SF (E=0.3MeV, keV) and χ^2 information of the three fitting methods

Method	STOT	SE10	SE20	Scas	STOTED	Sαγ0	αγ0AD	ScasED	αSpec	ααAD	SAllαγ	All*ED	Width
RAC2014*COV	158.64	108.49	46.16	3.99	1.6116	1.8699	1.9834	1.2129	1.3978	1.3189	1.7814	1.4729	1.2328
RAC2014*PPP	148.82	099.37	45.25	4.20	1.9596	2.0095	2.2533	1.1980	1.2951	1.2377	1.9840	1.4879	1.3663
RAC2014*DIA	153.52	102.73	46.58	4.21	1.4573	2.0887	2.2577	1.2478	3.0732	1.2812	1.9616	1.6304	1.5470

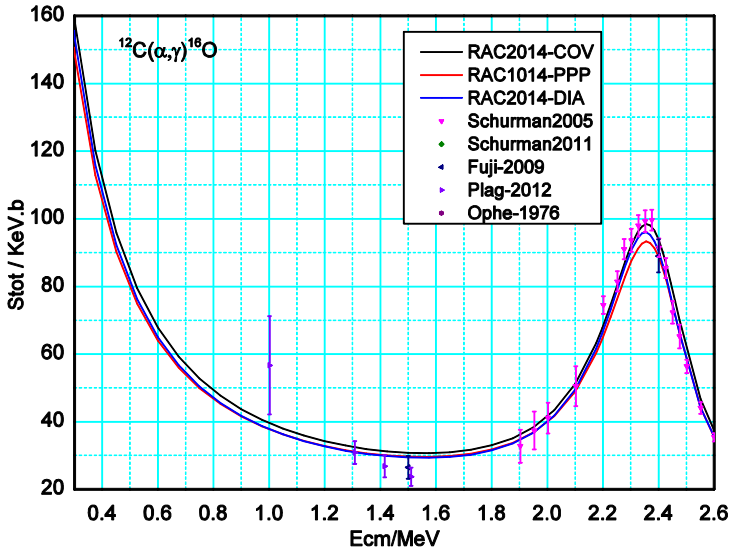

Fig. 4.2. Calculated STOT of the three methods.

In this paper, the character string as follow in Table S4.2 and all other Tables have definite meaning.

STOT--The total S factor at E=0.3 MeV for all (α, γ) reaction channel;

SE10--The S factor at E=0.3 MeV for the (α, $\boldsymbol{\gamma_0}$) from all 1^- levels to ground state 0^+_0;

SE20--The S factor at E=0.3 MeV for the (α, $\boldsymbol{\gamma_0}$) from all 2^+ levels to ground state 0^+_0;

Scas--The S factor at E=0.3 MeV for (α, $\boldsymbol{\gamma_1}$) + (α, $\boldsymbol{\gamma_2}$) + (α, $\boldsymbol{\gamma_3}$) + (α, $\boldsymbol{\gamma_4}$);

STOTED--All the STOT factor data;

A-Spec--Alpha Spectrum;

Sαγ0--The S factor for the (α, $\boldsymbol{\gamma_0}$) from all levels to ground state 0^+_0;

αγ0AD--The angular distribution for (α, $\boldsymbol{\gamma_0}$) from all levels to ground state 0^+_0;

ScasED--The S factor for all cascade data; some data are normalized;

ααAD--The angulear distribution for the ($\boldsymbol{\alpha, \alpha}$) reaction channel;

SAllαγ--The S factor for all data which are reletive to (α, $\boldsymbol{\gamma}$) reaction directly;

AllED--Whole data-base;

Width--Width data set for a level or a sub-reaction channel;

4.3. The new formulae for level width, energy shift and normalized

4.3.1. The level width and energy shift

The width formulas as follow, only approximate solutions may be obtained even in the single level.

$$\Gamma_\lambda = \sum_c \Gamma_{\lambda c},\ \Gamma_{\lambda c} = 2P_c\gamma^2_{\lambda c} \qquad \text{S4.3.1.1}$$

The literature (*Lane1958, P273, 1.17, 1.18, 1.19*) gives the correction formula on the level width and level shift:

$$\Gamma_{\lambda c} = 2P_c\gamma^2_{\lambda c}/d_c \qquad \text{S4.3.1.2}$$

$$\Delta_{\lambda c} = \frac{P_c(R^0_{cc}P_c)-S^0_c(1-R^0_{cc}S^0_c)}{d_c}\gamma^2_{\lambda c} \qquad \text{S4.3.1.3}$$

$$d_c = (1-R^0_{cc}S^0_c)^2 + (R^0_{cc}P_c)^2 \qquad \text{S4.3.1.4}$$

Here, λ is the level of c reaction channel, and notation zero is the constant background. These formulas is workable only on an approximation of single level. RAC is the multi-channel and multi-level R- matrix formula without constant background. Therefore, in the calculation of an energy level's width and shift, the remaining level value as a constant background, it is an accurately replaceable algorithm. Due to the involved algorithm extremely complex, the calculation time of adjustment parameter increases more than 5 times in the fitting. This work uses all level widths and branching ratios of experimental information, which is absolutely essential to accurately calculate the width and shift.

$$\Gamma_{\lambda\gamma}^{obs} = 2\mathrm{P}_c\,\gamma_{\lambda c}^2/(1+\sum k\ \gamma_{\lambda k}^2\ (\frac{dS_k}{dE})_{E_\lambda}) \qquad \text{S4.3.1.5}$$

In Eqs. S4.3.1.5 the $\Gamma_{\lambda\gamma}^{obs}$ represent observed width, $\mathsf{P_c}$ is the penetrability, $\gamma_{\lambda c}^2$ the reduced width amplitudes in calculation.

The accurate wave functions of positive energy were mainly obtained by the continued fractions method in the channel of (α, α) and gamma particle channel. Ensures that wave functions calculated by RAC are in conformance with the results of [Barnett1974], more than fourteen significant figures.

4.3.2. The formula of α-particles spectrum

The number of α-particles per unit energy is given by the expression

$$W_\alpha(E) = f_\beta(E)\sum_{l=1,3} P_l(E,a_l)\left|\frac{\sum_{\lambda=1}^{q_l}\frac{A_{\lambda l}}{E_{\lambda l}-E}}{1-[S_l(\mathrm{E},a_l)-B_l-iP_l(\mathrm{E},a_l)]R_l(\mathrm{E})}\right|^2 \qquad \text{S4.3.2.1}$$

Where, $f_\beta(E)$ is the integrated Fermi function, and $A_{\lambda l}$are the β-feeding amplitudes.

$$R_l(\mathrm{E}) = \sum_{\lambda=1}^{q_l}\frac{\gamma_{\lambda l}^2}{E_{\lambda l}-E} \qquad \text{S4.3.2.2}$$

$$f_\beta(W_0,Z) = \int_1^{W_0} F(W,Z)PW(W-W_0)^2dW \qquad \text{S4.3.2.3}$$

$$A_{1l}^2 = \frac{N_\alpha Y_{1l}}{Y(9.59)I_{1l}f_{1l}} \qquad \text{S4.3.2.4}$$

$$I_{1l} = \pi\gamma_{1l}^{-2}(1+\gamma_{1l}^2)_{E_{1l}}^{-1} \qquad \text{S4.3.2.5}$$

$$\Gamma_{1\gamma}^{obs} = \Gamma_{1\gamma}(1+\gamma_{1l}^2\frac{dS_l}{dE})_{E_{1l}}^{-1} \qquad \text{S4.3.2.6}$$

Here N_α is the total number of counts in the α spectrum, $Y_{1l}/Y(9.59)$ is the branching ratio to the sub threshold level relative to that of the level with E_x= 9.59 MeV in ^{16}O, the $f_{1l} = f_\beta(E_{1l})$.

The first 3 levels and 1 distant level of J^π=1$^-$ were adopted in the fitting than the previous analysis using third level; the first 2 levels and 1 far level of J^π=3$^-$, as in previous analysis were used in the fitting. The Fermi function, $F_\beta(E)$ (S4.5.2) were calculated by the interpolation with the Fermi function table in the literature (*Gove1971*). In the bound states of (α, α), the Wittaker function (S4.5.3), partial differential of negative energy were obtained by the formula (4-5.1) and formula (4-5.4) respectively.

$$W\left(-\eta, l+\frac{1}{2}, 2\rho\right) = \frac{exp(-\rho-\eta log 2\rho)}{\Gamma(1+l+\eta)}\int_0^\infty t^{l+\eta}e^{-t}(1+\frac{t}{2\rho})^{l-\eta} \qquad \text{S4.3.2.7}$$

$$\frac{\mathrm{dW}}{\mathrm{dE}} = \frac{\{[\mathrm{W(E+3\Delta)-W(E-3\Delta)}]+9[\mathrm{W(E+2\Delta)-W(E-2\Delta)}]+45[\mathrm{W(E+\Delta)-W(E-\Delta)}]\}}{60\Delta} \qquad \text{S4.3.2.8}$$

4.4 The comparison of R matrix Codes

4.4.1 The comparison for RAC13 with EDA, SAMMY and NJOY

EDA is an R-matrix program for light nucleus system evaluation at LANL of the United States, which hold the absolute dominant position in the work of international light nuclear evaluation. A systematic comparison between EDA and RAC was finished in the international cooperation projects about ' Neutron cross section standards ' hold by the International Atomic Energy Agency. The calculation of ^{6}Li (t, α) ^{4}He neutron standard section reaches a value of 5 or 6 digits consistent. In figure S4.4-A the black line indicates calculated values of EDA, the red line represents the calculation by RAC, two lines are agreement with each other without significant difference.

SAMMY (*Larson2006*) is the R-Matrix code of ORNL (USA) used to evaluate resonance parameter, which hold the absolute dominant position in the work of international resonance parameter evaluation. NJOY (*MacFarlane1994*) is an R-Matrix code of USA used to reconstructive resonance cross section, which hold the absolute dominant position in the work of international macroscopic nuclear data evaluation. Using the same R-Matrix parameters produced by SAMMY, the reconstructed cross section of RAC and NJOY have the same 4 to 6 effective figures. In figure S4.4-B the black line indicates calculated values of NJOY, the red line represents the calculation by RAC, and these two lines are agreement with each other without significant difference.

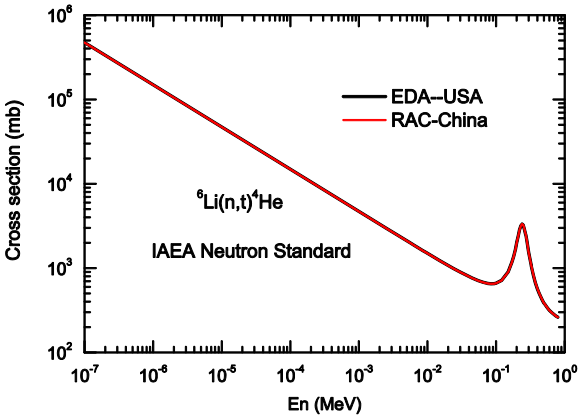

S4.4-A. The calculation of cross section of RAC and EDA with the same parameters.

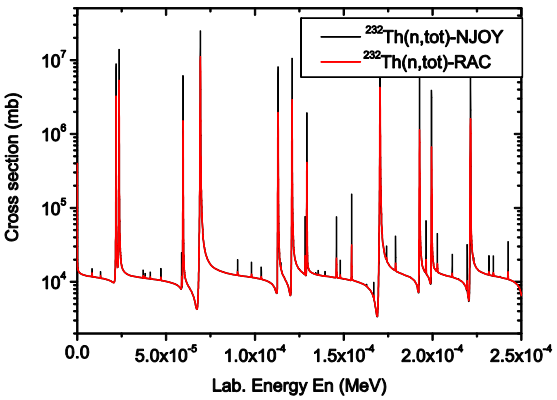

Fig. S4.4-B. The reconstructive resonance cross section of RAC and NJOY with the same parameters of SAMMY.

4.4.2. Comparison between RAC and [Tang2010] for Alpha spectrum

The delay Alpha spectrum follow β decay in ^{16}N (Alpha spectrum) are calculated by RAC with the original parameters given in (*TANG2010*). Fig. S4.4-C show the curve of Alpha spectrum of RAC is very similar to that curve of (*TANG2010*), and is very close to the normalized Alpha spectrums of the 3 groups. The calculated wave contribution of RAC is similar to that of (*Buchmann2009*) very much. The conclusion is that the calculation for Alpha spectrum of RAC is complete correct.

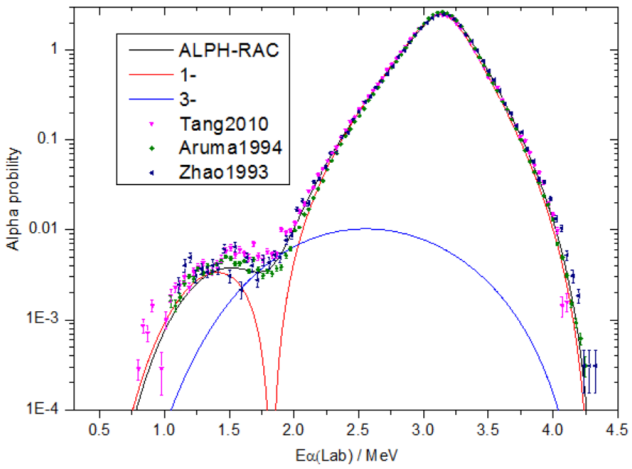

S4.4-C. The data and calculated normalized Alpha spectrum

4.5. How to describe 'external contribution' and 'direct capture'

For 'external contribution' and 'direct capture', many literatures have many views and different treatment methods, It is because of this cause great differences were produced in their works, so this work gives a detailed study on the problem. The external and direct capture being very small is the main physical basis for creating RAC2015 model.

Physically speaking, the 'direct capture' is a direct collision of α and ^{12}C, where γ releases by electromagnetic interaction and residual nucleus directly converts into ^{16}O in the ground state or some excited states. Since no other ^{16}O excited states of compound nucleus are involved, 'direct capture' cross section, starting from 0, increases with the increase of energy of α particle, then in certain energy point more than a Coulomb barrier, it rises to a maximum. After that, 'direct capture' cross section decline as 'resonance capture' competition is more and more strengthening and low wave component decreases with increase of energy. Such type of direct capture is a smoothly varying with energy, but mixed together with the tail contribution from high energy level resonance capture, which is hard to be distinguished from them. Therefore, direct capture for ^{12}C (α, γ) ^{16}O has no their own characteristic experimental information.

In the currently popular theory (*Barker1991*), for the 'external contribution' and 'direct capture' to the ground-state transition, the 1^- and 3^-can be ignored, but 2^+ states cannot. Document (*Angulo2000*) states theoretically that for the low-energy collisions of α and ^{12}C, due to a high threshold (7.17 MeV) of formation of ^{16}O, external contribution of capture reaction is negligible. Literature (*Schürmann2012*) states that, for the cascade transitions ($S_{6.92}$) to 2^+_1 bound state, direct capture plays a dominant role. Some Literature (deboer2013) states for the cascade transitions ($S_{7.13}$) to 1^-_1 bound state, direct capture has contribution too. The methods to deal with the non-resonant capture in this work are depicted as follows.

Some of the literatures add 'direct capture' part in the theoretical calculation formula. Literature (*Barker1991*) gives (*Kettner1982*) and his own description of ‘direct capture ‘empirical formula’ for SF the ground state, their calculated values being varying very smoothly, but more than five times in the overall difference (Fig. S4.5-F). In E = 0.3MeV area, the result of (Barker1991) for direct capture accounted for 16% of STOT, (*Barker1991*) accounting for about 1.8%, *(Buchmann1996)* states that direct capture in 2^+ is 4keV.b, accounting for 2.5% of STOT (165keV.b). These cases illustrate to a certain extent that, plus the currently envisaged description part of direct capture in the theoretical calculation formula, did not get the desired benefits, but increased multi-value characteristic of fitting and uncertainty of the results instead.

Since the R-Matrix analysis is a kind of phenomenological fitting, some special ‘background parameter R^j_0/ $(E-E^j_0)$’ which changed along with the change of energy and ‘reduced width amplitude γ^j_{dis}’ in distant levels can be settled to simultaneously describe the background of resonant capture and non-resonant capture contribution. E^j_0 can select a suitable value by some test fitting just same as done for the energy parameter of distant level. The R^j_0 and γ^j_{dis} have to be searched by multi-iteration procedure to take the best values.

The Table. S4.5 shows the final results of two fitting schemes. In A scheme the $R0_{E20}$, $R0_{6.92}$ and $R0_{7.12}$ are fixed as 0.0, the data for transition to ground state can be fitted very well, but the data for cascade transition about $S_{6.92}$ and $S_{7.12}$ cannot be fitted well. (Fig. S4.5-A, B). In B scheme the $R0_{E20}$, $R0_{6.92}$ and $R0_{7.12}$ are searched freely, the data for all transitions can be fitted very well (Fig. S4.5-C, -D, -E). It should be noted that the $R0_{E20}$ has a trend to be 0.

Table S4.5. The final results of the 2 schemes (E=0.3 MeV, E^{-1}_0 =0.3 MeV, E^{+2}_0=0.4 MeV)

	$R0_{E20}$	$R0_{6.92}$	$R0_{7.12}$	STOT	SE10	SE20	$S_{6.05}$	$S_{6.13}$	$S_{6.92}$	$S_{7.12}$	SE20dc	χ^2_{AG}	χ^2_{all}	All	χ^2_{AG3}
A.	0.00	0.00	0.00	159.5	101.9	56.8	0.52	0.28	0.047	0.001	2.54	2358	6676	3.01	2.69
B.	0.00	0.38	0.19	162.2	101.2	56.9	0.72	0.28	2.484	0.588	2.54	2140	6488	1.26	1.96

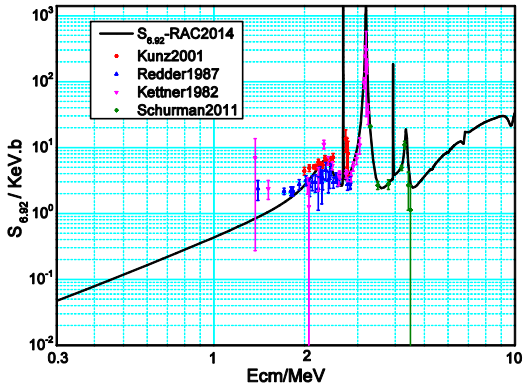

Table. S4.5-A. The result of $S_{6.92}$ with $R0_{6.92}$=0

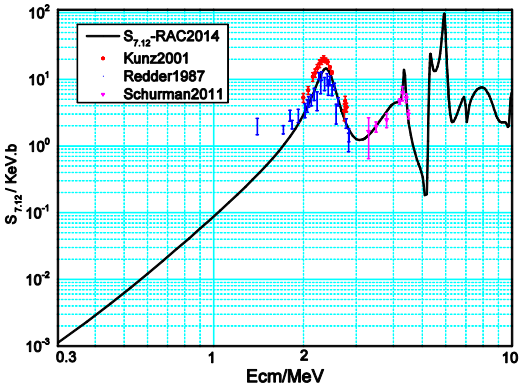

Fig. 4.5-B. The result of $S_{7.12}$ with $R0_{7.12}$=0

When all the reduced width amplitudes $\gamma^{2+}{}_c$ in resonant levels of 2^+were settled as 0.0, and only the $\gamma^{2+}{}_{dis}$ in distant levels and the background parameters $R^j{}_0/(E-E^j{}_0)$ were used to make calculation, the background of resonant capture and non-resonant capture contribution in low energy range(E<1 MeV)can be got.(Fig. S4.5- C).It is about 4.5 keV at E=0.3 MeV. When all the reduced width amplitudes $\gamma^j{}_c$ in resonant levels of 1^- and 2^+ were settled as 0.0, and only the $\gamma^j{}_{dis}$ in distant levels and the background parameters $R^j{}_0/(E-E^j{}_0)$ were used to make calculation, the background of resonant capture and non-resonant capture contribution in low energy range(E<1 MeV)can be got (Fig. S4.5- D, E). For $S_{6.92}$ and $S_{7.12}$, the contribution of $R^j{}_0/(E-E^j{}_0)$ is much larger than that of $\gamma^j{}_{dis}$, and the $\gamma^j{}_{dis}$ and $R^j{}_0/(E-E^j{}_0)$ have negative correction. In the bound states $2^+{}_1$ and $1^-{}_1$ not exist any correlative $\gamma^j{}_c$ and the $\gamma^j{}_{dis}$ about $S_{6.92}$ and $S_{7.12}$, so the calculated value are accurately.

In E=0.3 MeV GAMOW energy point, about the direct capture S factor S_{DC}, the value of [Kettner1982] is 9 keVb, the ratio for S_{DC}/STOT is 2.5% ; the value of (Buchmann1996) is 4 keVb, the ratio for S_{DC}/STOT is 2.5% ; the value of this work is 4.5 keVb, the ratio for S_{DC}/STOT is 2.8%. These data show that, due to very small contribution of direct capture for ^{12}C (α, γ) ^{16}O, it is entirely feasible for compound nucleus model to be used in the system ^{16}O produced by α+^{12}C.

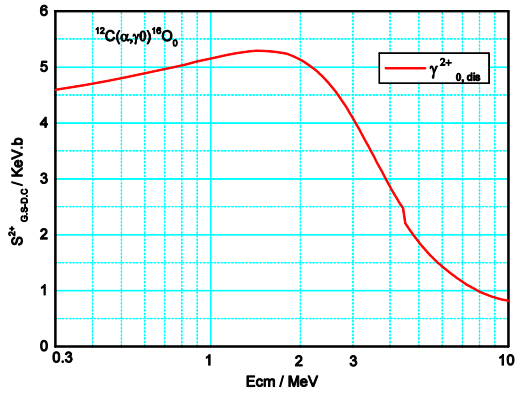

Fig. S4.5-C The background of resonant capture and non-resonant capture for $0^+{}_{0\ from}\ 2^+$ levels

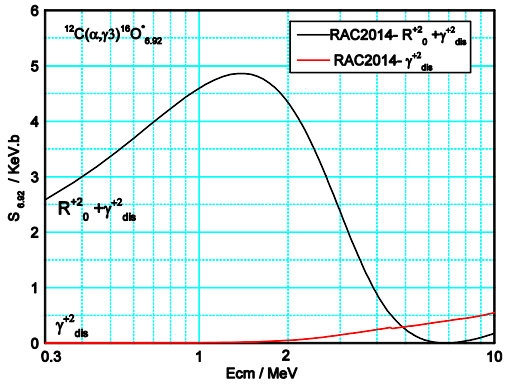

Fig. S4.5-D The background of resonant capture and non-resonant capture for $2^+{}_{6.92}$

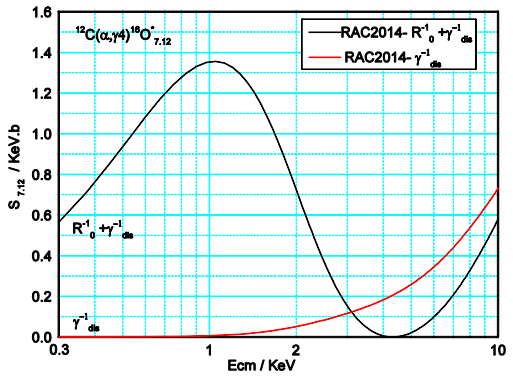

Fig. S4.5-E The background of resonant capture and non-resonant capture for $1^-_{7.12}$

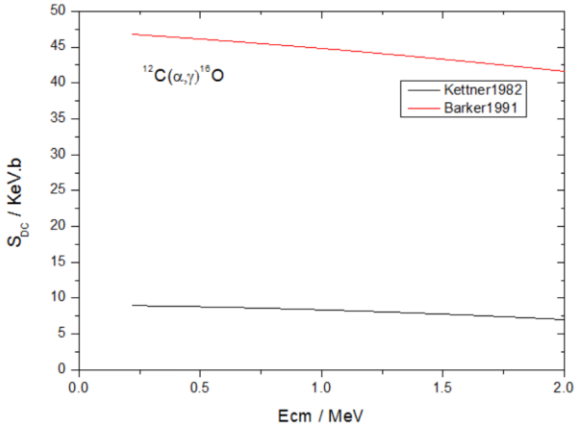

Fig. S4.5-F The calculated direct capture for 0^+_0 in Ref. Kettner1982 and Barker1991

4.6 Skillfully combines the formulae of the classical R-Matrix theory and γ capture theory

In this work we have adopted 3 schemes on the same data-base and energy level construction to calculate the cross section of ^{12}C (α, γ) ^{16}O.

The first scheme (RAC-Lane-all) is the formulae used for all channels are those in ref. 6, the formulae for AD **of** all channels are as follow:

$$d\sigma_{\alpha\alpha'}/d\Omega_{\alpha'} = 1/((2I_1+1)(2I_2+1))\sum_{ss'\nu\nu'}\left|A_{\alpha's'\nu',\alpha s\nu}(\Omega_{\alpha'})\right|^2 \qquad 4.6.1$$

$$A_{\alpha's'\nu',\alpha s\nu} = \sqrt{\pi}/\kappa_\alpha\,[-C_{\alpha'}(\theta_{\alpha'})\delta_{\alpha's'\nu',\alpha s\nu} + i\sum_{JMll'm'}\sqrt{2l+1}(sl\nu 0|JM)(s'l'\nu'm'|JM)T^J_{\alpha's'l',\alpha sl}Y^{(l')}_{m'}(\Omega_{\alpha'})] \qquad 4.6.2$$

Here, channel c ≡ (α s ι, *JM*), α refer to channel particle pair, s channel spin, ι channel relative orbital angular momentum, *J* and *M* total angular momentum and its project, This is a kind of pure phenomenological fitting, did not consider the demand for γ being transverse wave, this way include rather large approximation, but the fittings for all data sets are excellent, is the best one in the 3 ways used.

The second scheme (RAC-Lane-11234) is the formulae used for all channels are those in ref. 6, but for $J^\pi = 0^+, 1^-, 2^+, 3^-, 4^+$ levels the wave number of γ particle channel only take ι=1, 1, 2, 3, 4 respectively.

RAC2015 use the angular momentum coupling formulae defined in Literature (Lane1958[6]) as follow:

$$\vec{s}_i+\vec{s}_t=\vec{S}i, \qquad 4.6.3$$

$$\vec{\iota}_i+\vec{S}i=\vec{I}_i, \qquad 4.6.4$$

$$\vec{I}_\gamma+\vec{I}_f=\vec{s}_c \qquad 4.6.5$$

$$\vec{\iota}_c+\vec{s}_c=\vec{I}_i, \qquad 4.6.6$$

The γ is transverse wave, its intrinsic spin is 1, and it means that γ spin projection can be -1 and +1, cannot be 0. For the transition with $\vec{I}_f=0$, when $\nu'=0$ the γ spin projection is 0. So when using the formula 4.6.1 to calculate the angular distribution of γ, as long as ignored the loop for $\nu'=0$, that γ spin projection will not be 0 in calculation.

For $J^\pi = 0^+, 1^-, 2^+, 3^-, 4^+$ levels, the main contribution of γ transition to ground state (γ_0, $^{16}O_0$) and to the first bound state (γ_1, $^{16}O_1$) come from ι=1, 1, 2, 3, 4 respectively. Here has a very useful coincidence, that is if only use these partial wave, in the CG coefficients set which relative to the calculation about the transitions of (γ_0, $^{16}O_0$) and (γ_1, $^{16}O_1$), all the CG coefficients with $\nu'=0$ are 0! So the contribution to differential cross section from $\nu'=0$ is 0. This means that the AD of (γ_0, $^{16}O_0$) described by 4.6.1 and 4.6.2 essentially satisfactory the demand for γ being transverse wave, in the integral cross section of (γ_0, $^{16}O_0$) not exist the component from $\nu'=0$, the integrated cross section and AD of (γ_0, $^{16}O_0$) are essentially consistent. This is an especial useful result for calculating the Astrophysical SF.

Table 4.6.1. All CG coefficients $(s'\nu'l'm'|JM)$ used in calculation about (γ_0, $^{16}O_0$) and (+γ_1, $^{16}O_1$)

$(s'\nu'l'm'\|JM)$	CG	$(s'\nu'l'm'\|JM)$	CG	$(s'\nu'l'm'\|JM)$	CG	$(s'\nu'l'm'\|JM)$	CG
1-1 1 1|1 0	-0.707107	1-1 2 1|2 0	-0.707107	1-1 3 1|3 0	-0.707107	1-1 4 1|4 0	-0.707107
1 0 1 0|1 0	0.000000	1 0 2 0|2 0	0.000000	1 0 3 0|3 0	0.000000	1 0 4 0|4 0	0.000000
1 1 1-1|1 0	0.707107	1 1 2-1|2 0	0.707107	1 1 3-1|3 0	0.707107	1 1 4-1|4 0	0.707107

For the transitions (γ_2, $^{16}O_2$), (γ_3, $^{16}O_3$) and (γ_4, $^{16}O_4$), the spin of final state $\vec{I}_f>0$, so for $\nu'=0$ the projection value of spin of γ is not must be 0. Practical calculations show that for a part of l' (marked with l'_0) their all CG coefficients with $\nu'=0$ are 0, for a part of l' (marked with l'_0+1) their all CG coefficients with $\nu'=0$ are not 0. The ED for (γ_2, $^{16}O_2$), (γ_3, $^{16}O_3$) and (γ_4, $^{16}O_4$) only involve integral data, usually only using one l' is able to get satisfactory fitting. So if only using the l'_0 wave to fit the ED the demand for γ being transverse wave will be meet briefly. As long as the integrated ED are fitting very well, the obtained calculation value will be correct.

The third scheme (RAC- EMT-STET, RAC2015) is the formulae used for haven particle channels are those in ref. 6, but, for γ particle channels are those in Seyler1979 and Azuma2010**,** that is the Electric-Magnetic Transition Model (EMT) with Statistical-Tensor-Efficiency-Tensor Approach (STET). The expressions for the Legendre coefficients in the channel spin representation were derived as formulae 4.6.7 to 4.6.11, which satisfactory the demand for γ being transverse wave. It should be especially point out that the ι in ref. 6 and the $\vec{\iota}_\gamma$ in **ref.** Seyler1979 and Azuma2010 have different physical mean, the $\vec{\iota}_\gamma$ appear in formula $\vec{\iota}_\gamma+\vec{I}_\gamma=\vec{L}$, which is an indispensable angular momentum coupling formula for constructing the Electromagnetic vector potential, $\vec{\iota}_\gamma$ is called 'unobservable' orbital angular momentum, it never appears in the formulae used for calculation; $\vec{I}_\gamma$ the intrinsic spin of γ, $\vec{L}$ the total angular momentum of γ (Seyler1979, P20).

For γ particle channel $p \equiv (\varepsilon\, L\, \lambda_f)$, here λ_f refers to final state, ε to indicate magnetic or electric transitions, let $\Omega_p=1$. $\Gamma_{\lambda P} = 2k_\gamma^{2L+1}\gamma_{\lambda P}^2$ is the normal formula defined in EMT, it is accurate only for using Electromagnetic vector potential. In RAC2015 the wave function used is Coulomb wave function, so a modifying factor has to be used to get accurate fitting values for data set about AD. The formulae used for calculate AD of γ particle channels are

$$\Gamma_{\lambda P} = 2k_\gamma^{2L+1}\gamma_{\lambda P}^2 \quad (2L\text{-}1)/4 \qquad 4.6.\ 7$$

$$d\sigma_{\alpha\to\lambda_f}/d\Omega = 1/((2I_{\alpha 1}+1)(2I\alpha_2+1))\,\frac{1}{k_\alpha^2}\sum_k B_k P_k(\theta) \qquad 4.6.\ 8$$

With the definitions

$$B_k = \sum_{s,L,L',l,l'J,J'\epsilon,\epsilon'}[\,]\ (-1)^{1+s-J_f}/4\ Z_1(\iota,J,\iota',J';sk)$$

$$\times Z_2\left(L\ J\ L'\ J'\ ;\ J_f k\right)\ T^{*J'}_{\alpha s\iota',\epsilon' L'\lambda_f}\ T^{J}_{\alpha s\iota,\epsilon L\lambda_f}, \qquad 4.6.\ 9$$

$$Z_1(\iota\ J\ \iota'\ J';sk) = \hat{\iota}\ \hat{J}'\ \hat{\jmath}\ \hat{\jmath}'\ (\hat{\iota}\ 0\ \hat{\iota}'0\,|\,k0)\mathrm{W}(\mathrm{J}\iota J';sk), \qquad 4.6.\ 10$$

$$Z_2\left(LJL'J';J_f k\right) = \hat{L}\ \hat{L}'\ \hat{J}\ \hat{J}'\ (L1L'-1|\mathrm{k}0)W\left(LJL'J';J_f k\right). \qquad 4.6.\ 11$$

Where the symbol [ ] indicates a parity restriction defined by

$$[\,] = \frac{1}{2}\left[1+(-1)^{L'+L+k+\epsilon+\epsilon'}\right] \qquad 4.6.12$$

$$\hat{\iota} = (2\iota+1)^{1/2}, \hat{J} = (2J+1)^{1/2} \qquad 4.6.13$$

Here, α refer to incident particle pair (α1, α2), s incident channel spin, ι incident channel relative orbital angular momentum, J is total angular momentum. It should be especially point out that, for γ particle channel the calculated transition matrix elements $T^{J}_{\alpha' s' l', \alpha s l}$ are obtained with (α s ι, *JM*) scheme, the $T^{J}_{\alpha' s' l', \alpha s l}$ include all required $T^{*J'}_{\alpha s l', \varepsilon' L'\lambda f}$ and $T^{J}_{\alpha s l, \varepsilon L\lambda f}$, the formula [ ]=1/2(-1+(-1)$^{L+L'+k+\varepsilon+\varepsilon'}$) is used to select the suitable $T^{*J'}_{\alpha s l', \varepsilon' L'\lambda f}$ and $T^{J}_{\alpha s l, \varepsilon L\lambda f}$ which satisfactory the constraints of all conservation law, the selection is finished in the calculation process for AD of ^{12}C (α,γ) ^{16}O with formulae (4.6.9 to 4.6.11) above. In this scheme the original theory formula

for integrated data become inconsistent with the formula used above. The integrated data of ^{12}C (α, γ) ^{16}O is calculated by mathematical integrating corresponding calculated AD of ^{12}C (α, γ) ^{16}O, the integrating precision is better 0.5%.

It has been known that in the ^{16}O system formed by (α+^{12}C), s=0, $I_{\alpha 1}$=0, $I_{\alpha 2}$=0, all γ capture are electric transition, so ε≡1, ε' ≡1. When λ_f and k are selected already, for a selected set of (L, $L^{'}$, l, $l^{'}$, J, $J^{'}$), there have a pair relative $T^{*\,J'}_{\alpha s l',\varepsilon' L' \lambda f}$ and $T^{\,J}_{\alpha s l,\ \varepsilon L \lambda f}$, which have one or more corresponding $T^{\,J}_{\alpha' s' l',\,\alpha s l}$, these $T^{\,J}_{\alpha' s' l',\,\alpha s l}$ will be used in calculation actually. The final calculated result will satisfactory the constraints of all conservation law and the demand for γ being transverse wave. The AD of ^{12}C (α, γ_0)^{16}O at 66 energies have got good fitting, but the fitting is not as perfect as the fitting obtained in the first way.

4.7. How to get a unique evaluated Stot of ^{12}C (α, γ) ^{16}O

The optimization objective function for is

$$\boldsymbol{\chi^2 = (\eta - y)^{+} V^{-1} (\eta - y) \Rightarrow minimun} \qquad \text{S4.7.1.}$$

It is a multidimensional high order polynomial function determined by the initial parameter-set and data-base. With different parameter-set or data-base will have different local minimum. In order to get a unique evaluated Stot of ^{12}C (α, γ) ^{16}O, some methods have been adopted as follow.

A. The key data set Stot of Schurmann2005 and $S_{G.S}$ of Brochard1975 are set with higher weight in 2 times.

B. Some key data points are set with higher weight, which include:

$S_{G.S}$ at E_{lab}= 0.313384E+01, 0.318412E+01, 0.312451E+01 and 0.316585E+01 MeV for the main resonance level 1^-_2;

$S_{G.S}$ at E_{lab} =0.357000E+01 MeV for the resonance level 2^+_2;

$S_{G.S}$ at E_{lab} = 0.572250E+01 MeV for the main resonance level 2^+_3;

$S_{6.05}$ at E_{lab}= 0.321252E+01 MeV for the main resonance level 1^-_2;

AD of ^{12}C (α, γ0) ^{16}O at E_{lab} = 0.357000E+01 MeV for the resonance level 2^+_2;

$\Gamma^{2+}_{2,\alpha\gamma}$ at E_{cm} =0.268771E+01 MeV for the nerow resonance level 2^+_2;

C. The most important method is that the width information for bound states 2^+ and 1^- ($\gamma^2_{\alpha 1\text{-exp}}$, $\gamma^2_{\alpha 2\text{-exp}}$, $\Gamma^{1-}_{\gamma 1-exp,}$ $\Gamma^{2+}_{\gamma 1-exp}$) were used as ED to fit, the deviation have to be less 0.5 time of the original error, see 5.1.1.

D. For the 7 data of width without error information, a suitable error have been given out. A resonable way is to take Error=50% in iterative procedures.

5. Characteristic special research procedures

In order to get a unique and reliable SF, some special procedures are developed, which include:

5.1 Systematical study.

This item also includes '**the Research for six configurations of multi-channels and multi-levels**' and '**the Studying of eight schemes for practical application'**. The 2 items are very long, so put them in Appendix. III.

5.2 Iiteration fitting procedure.

5.1. Systematic study

The so-called 'systematic study' refers to research's in some types of identical conditions, which are performed by a variety of possibilities analysis for certain types of key factors in order to make the best choice; After all key factors are best choose, the most reliable results for overall analysis will be obtained.

5.1.1. Width information in bound states taking different weights

The width information for bound states, especially 2^+ and 1^- bound states, plays a particularly important role in the data fitting, which is done by some considerate researches.

Table S5.1.1-A. The *α*-reduced widths and SF

Experiment	γ_α^2 (0^+) /(keV)	γ_α^2 (3^-) /(keV)	γ_α^2 (2^+) /(keV)	$\gamma^2\alpha$ (1^-) /(keV)	SE10/ keV b	SE20/ keV b
Oulebsir2012	19.7±5.5	2.35±0.8	26.7±10.3	7.8±2.7	100±28	50±19
Belhout2007	/	/	$26.6^{+19.2}_{-17.2}$	4.59 ± 2.91	80.6^{+17}_{-16}	
Adopted Values	19.7±5.5	2.35±0.8	26.65±9.022	6.195±1.979		
Evaluated value	18.7±2	2.35±0.3	26.65±5.*86*	6.195±0.76		

Reduced width γ^2_α in bound states are the results (see Table S5.1.1 above) obtained by measuring and analyzing ^{12}C (^{7}Li, t) ^{16}O or ^{12}C (^{7}Li, d) ^{16}O transfer reaction data, and the data used is the weighted averaged values for the data of two experiments.

Fitting process shows that $\gamma^2_{\alpha 0}$ in 0^+_1 has a very little impact on the SF, Additionally, the ' γ width $\Gamma^{0+}_{\gamma 1}$ ' in 0^+_1 is a formal parameter representing the 'electron-pair transition ' possibility of actually happening in this energy level, so it has something very small to do with SF Similarly, for 3^-_1, the 'α reduced width $\gamma^2_{\alpha 3}$ ' and ' γ width $\Gamma^{3-}_{\gamma 1}$' hardly influence the SF.

Fitting process also illustrates that, the 'α reduced width' $\gamma^2_{\alpha 1}$ in bound states 1^-_1 and $\gamma^2_{\alpha 2}$ in bound states 2^+_1 are sensitive elements on the SF， but duo to $\gamma^2_{\alpha 1}$ and $\gamma^2_{\alpha 2}$ have relative larger error(33.4% and 34.4% respectively) and the delay Alpha spectrum is used, their effect is not much high.

Fitting process also illustrates that, the 'γ width' $\Gamma^{1-}_{\gamma 1}$ in bound states 1^-_1 and $\Gamma^{2+}_{\gamma 1}$ in bound states 2^+_1 are the most sensitive elements on the SF. The experimental values of $\Gamma^{1-}_{\gamma 1}$ and $\Gamma^{2+}_{\gamma 1}$ have relative small error (5.8% and 3.1% respectively).

There are two kinds of methods for using of such data. At first, used them as R- matrix parameter directly, so their original value are used to determine the scale of S factor. This approach ignores the contribution from other types of ED, that is overestimates the weights of the transfer reaction data mentioned above. The calculated S factors at E=0.3 MeV and the Chi-squares for the 3 schemes are shown In **Table S5.1.1-B** as RAC-LANE-All-ORI, RAC-LANE-11234-ORI, RAC-EMT-STET-ORI respectively.

Then on the base of data-sets and parameter-sets obtained in the first way, the experimental values $\gamma^2_{\alpha 1\text{-exp}}$, $\gamma^2_{\alpha 2\text{-exp}}$, $\Gamma^{1-}_{\gamma 1-exp}$ and $\Gamma^{2+}_{\gamma 1-exp}$ were used as ED to fit, in fitting procedure their corresponding fitting parameter walues will deviate from the original experimental values. The crition is that the deviation have to be less or eqval to 0.5 time of original error, that is $\gamma^2_{\alpha 1\text{-fit}} \approx \gamma^2_{\alpha 1\text{-exp}}(1\pm 0.167)$, $\gamma^2_{\alpha 2\text{-fit}} \approx \gamma^2_{\alpha 2\text{-exp}}(1\pm 0.172)$, $\Gamma^{1-}_{\gamma 1-fit} \approx \Gamma^{1-}_{\gamma 1-exp}(1\pm 0.029)$, $\Gamma^{2+}_{\gamma 1-fit} \approx \Gamma^{2+}_{\gamma 1-exp}(1\pm 0.016)$. This fitting process taking into account the effect from other types of ED which should have for the fitting parameter walues. The calculated S factors at E=0.3 MeV and the Chi-squares for the 3 schemes are shown In **Table S5.1.1-B** with RAC-LANE-All-0.5S, RAC-LANE-11234-0.5S, RAC-EMT-STET-0.5S respectively.

Table S5.1.1-B. The calculated S factors at E=0.3 MeV and the Chi-squares for the 3 schemes

	S Factor at E=0.3MeV(keV b)				Integrated χ^2		Mean χ^2			Mean χ^2			Err%
Scheme	Stot	Se10	Se20	Scas	SAll**αγ**	All_{ED}	Stot	S**αγ0**	**αγ0**$_{AD}$	Scas	**α** −Spec	**αα**$_{AD}$	Stot
RAC-LANE-All-ORI	149.87	088.94	57.03	3.89	1856	6346	1.346	1.574	1.867	1.458	1.607	1.393	6.1
RAC-LANE-11234-ORI	150.30	088.85	56.95	4.49	1858	6355	1.352	1.579	1.867	1.465	1.675	1.387	6.2
RAC2015-ORI	156.27	≈93.0	≈59.7	3.57	2430	6880	2.470	1.862	2.499	1.417	1.647	1.356	4.5
RAC-LANE-All-0.5σ	156.58±8.3	100.52	52.15	3.89	1780	6246	1.211	1.455	1.833	1.332	1.461	1.373	5.3
RAC-LANE-11234-0.5σ	158.96±8.3	104.62	48.57	5.76	1832	6298	1.320	1.486	1.842	1.513	1.511	1.370	5.2
RAC2015-0.5σ	**159.71**±9.3	≈94.2	≈61.4	4.10	2290	6809	1.299	1.867	2.421	1.622	1.447	1.415	5.9

Table S5.1.1-B Shows that in the second method (0.5σ) all kinds of Chi-squares are smaller than the corresponding Chi-squares in the first method (ORI). So the S factors obtained in the second method should be taken as the recommend values. In the second method (0.5σ), the astrophysical S Factors obtained in its 3 schemes are near identical. The first scheme **RAC-LANE-All-0.5σ** has the best fitting, the

integrated χ^2 of whole data-base is 6246, but it's a kind of pure phenomenological fitting; his scientific significant is that it verified the reliability of S Factors obtained in the 3 schemes in mathematical evaluation aspect. The fitting of the second scheme **RAC-LANE-11234-0.5σ** is better, the integrated χ^2 of whole data-base is 6298, the（γ_0,$^{16}O_0$）and（γ_1,$^{16}O_1$）naturally meet the requirements of gamma being a transverse wave, its contribution play dominate function. This is the most striking quantitative successes with this scheme. In other way, the AD of ^{12}C (α, γ_0)^{16}O at 66 energies have got the best fittings, and play very important role for ascertain of SE10 and SE20. The results show SE10 is much greater than SE20, they are the objective results obtained by fitting objective experimental data sets, there is no any subjective constraints, not set the SE10 with enhanced values in advance as that ref. 43 challenged. But, there exist a little approximation in calculation about cascade transition. **The fitting of the third scheme RAC2015-0.5σ is good too,** the integrated χ^2 of whole data-base is 6809**, it's the strictest one in theory formulae used. The S factors obtained in this scheme are taken as the final recommended values.**

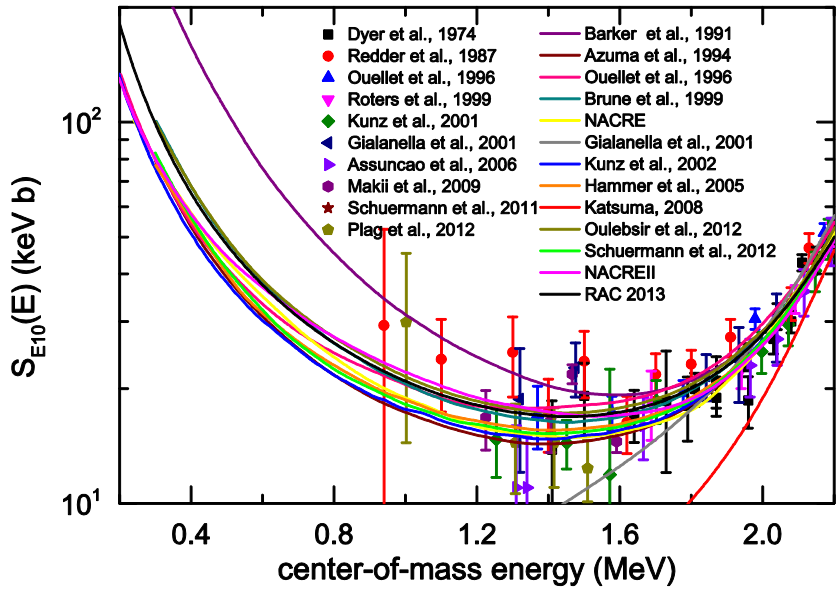

Fig. S5.1.1-A. ED and calculated values for SE10

Figure S5.1.1-A shows both ED and theoretical calculated values for SE10, where RAC2013, Brune1999 and Ouelebslr2012 use the ED values of α reduced width in bound state (γ^2_α). Consequently, in low energy extrapolation energy region (E <0.7 MeV), they agree very well with each other for the theoretical values. Additionally, in the energy area where existing ED, the calculated value of Brune1999 and Ouelebslr2012 show slightly high. Since others did not use the ED of α reduced width in bound state (γ^2_α), the calculated values are systematically lower in the low energy range (E <0.7 MeV). The calculated values of Schurmann2012 and Kunz02 show systematically lower in the energy range where there exist ED.

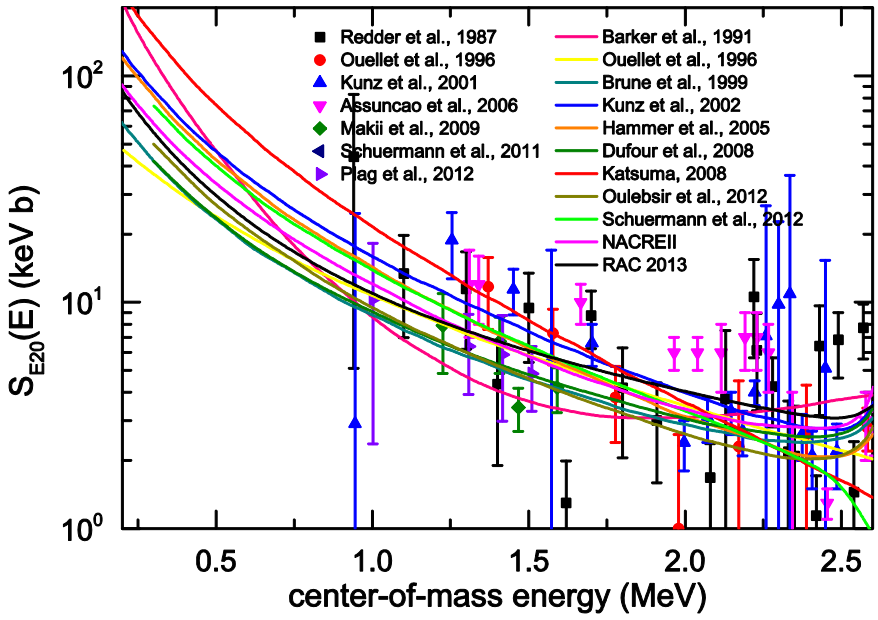

Fig. S5.1.1-B. ED and calculated values for SE20

Figure S5.1.1-B demonstrates the ED and theoretical values of SE20, where RAC2013, Brune1999 and Ouelebsir2012 use the ED values of α reduced width in bound state (γ^2_α). Therefore, in lower extrapolation energy region (E <0.7 MeV), they agree very well with each other. In the energy region where there exist ED, the calculated values by Brun1999 and Ouelebsir2012 are significantly lower. Since others did not use ED for α reduced width in bound state (γ^2_α), the calculated values are systematically higher in the low energy range (E <0.7 MeV). The theoretical values calculated by Schurmann12 and Kunz02 show systematically lower in the energy range where there exists ED.

As describe in the chapter 7.8, it is the RAC2013 that the theoretical calculations and ED show the closest.

5.1.2. Searching best Scaling factor of AD for ^{12}C (α, γ0)^{16}O

In the ED set, there are two units, 23 energy points, 120 data points of absolute values of AD for ^{12}C(α, γ_0)^{16}O, it is necessary to search the normalization coefficient for every unit.. Moreover, 7 units, 42 energy points, 493 data points of relative values of AD for ^{12}C (α, γ_0) ^{16}O, it is necessary to search the Scaling factor for every energy point. Analysis indicate that such type of data plays very important role in determining the proportion of SE10 and SE20, and STOT. One of the strengths for R-matrix analysis is that it can normalize the ED to the expected value, to obtain the 'Scaling factor' or 'normalization coefficients' for relative values, determining the systematic errors in the last. Thus, some particularly detailed studies are performed on these factors.

It is provided in this work that the in ' covariance fitting ' to take into account the ' long-range energy correlation and middle-range energy correlation ' of covariance, only the data in the same group is related to each other. For this reason, at first, with the condition that taking one energy point as a group, data fitting is performed to find the Scaling factor without the consideration of long-range correlation, then to get the primary absolute values of AD for every energy point. Secondly, in the case that taking a unit of data as a group, data fitting is performed to find preliminary normalization coefficients with the consideration ‘long-range correlation and middle-range energy correlation' for every unit. Next, repeating the first step to find improved Scaling factor for every energy point, repeating the second step to find improved normalization coefficients for every unit. Similar procedures are repeated several times to get the ideal Scaling factors set (including 42 elements) and the normalization coefficients set (including 7 elements) , and obtain the expected absolute value of AD for ^{12}C(α, γ0)^{16}O.

The Best Scaling factor is the term compared to fitted relative values. By principles of error propagation law, the uncertainty is addressed by using the systematic error of relevant data. Theoretical, the systematic error is equivalent to mean square error of fitted values. (Note: The systematic error here does not refer to that existed in experimental measurements). By using the best Scaling factor, relative values can be converted into absolute ones. When the absolute values are used in such type of data, the normalization coefficients should be 1. As the errors of 'Scaling factor' have been presented by the 'systematic error', 'Scaling factors' are no longer to be regards as adjustable parameters when calculating the errors of fitted values by 'error propagation law'. The 'Scaling factor' column in APPENDIX IV, The Table 2 list 'Scaling factor' for each energy and 'normalization coefficient' for each group in detail.

5.1.3. Determine the optimum Schürmann2011 normalization coefficient

S-factors of the reaction channel in ref. (Schürmann2005) and (Schürmann2011) are extremely important ED which influence whole fitting, providing their systematic errors are both 6.5%. Due to the experimental value of STOT in the main energy region (1.3 to 4MeV) is less than the sum = $S_{G.S}$. + $S_{6.05}$+$S_{6.13}$+$S_{6.92}$+ $S_{7.12}$, it can be identified that Schürmann's STOT is on the lower. To this end, the normalization coefficients for Schürmann's STOT were taken 1.01, 1.02, 1.03, 1.04 and 1.05 respectively to make testing run, and their systematic errors are taken the errors of the corresponding fitted values. It is found by fitting that the normalization coefficient of 1.03 can result in the minimum Chi-square for the most important data-set SAllαγ and All-ED, which is seen in Table S5.1.3.

Table S5.1.3. The results for different normalization coefficient of [Schürmann2005]

Schü-NF	STOT	SE10	SE20	Scas	SAllαγ	AllED	STOTED	Sαγ0	αγ0AD	ScasED	α-Spec	ααAD	Width
Sch-1.01	158.78	109.07	45.62	4.09	2050.6	6374.8	1.5557	1.8886	1.9851	1.2059	1.3997	1.3196	1.2459
Sch-1.02	158.69	109.49	45.15	4.05	2054.0	6374.8	1.6163	1.8904	1.9813	1.2026	1.4001	1.3197	1.2187
Sch-1.03	158.99	110.20	44.80	3.99	2049.7	6368.8	1.6052	1.8651	1.9810	1.2072	1.4008	1.3195	1.2054
Sch-1.04	159.06	110.41	44.69	3.96	2053.4	6371.4	1.6441	1.8604	1.9798	1.2123	1.4008	1.3196	1.1960
Sch-1.05	158.65	109.22	45.54	3.89	2061.0	6382.4	1.6808	1.8607	1.9826	1.2206	1.3983	1.3196	1.2020

5.1.4. Determining appropriate weights for AD of ^{12}C (α, α) ^{12C}

In this work we use 5 groups of elastic scattering AD for reaction ^{12}C (α, α) ^{12}C, their energy E_α (Lab) including from 1.446 to 10.00 MeV. For energy region larger than 4.5MeV, because of absence of ED of Alpha spectrum, the width of ^{12}C (α, α) ^{12}C is determined by the AD of ^{12}C (α, α) ^{12}C only. In the main energy range from 1.3 to 4 MeV, such type of ED along with three groups of Alpha spectrum ED jointly determines the width of ^{12}C (α, α)^{12}C in 1^-_2 level, but there is a competition between them, while ED of Alpha spectrum are dominant. The ED for ^{12}C (α, α) ^{12}C will be taken different weights so that the average chi-squared χ^2_{ela} are 0.50, 1.0, and 2.00 times of averaged value of chi-squared of Alpha spectrum separately. Since then, various SF factors show very close to each other (Table S5. 1.4), and in the end of iterative fitting, $\chi^2_{ela}$is made to be approximately to equal χ^2_{alp}.

Table S5.1.4. The different weights for AD of ^{12}C (α, α) ^{12}C

$\chi^2_{ela}/\chi^2_{alp}$	STOT	SE10	SE20	Scas	STOTED	Sαγ0	αγ0AD	ScasED	α-Spec	ααAD	SAllαγ	AllED	Width
0.50	157.97	110.87	43.31	3.79	1.5664	1.8451	1.9730	1.2030	1.4261	0.9342	1.7660	1.2416	1.1080
1.00	158.43	110.15	44.29	3.99	1.6575	1.8513	1.9775	1.2097	1.4404	1.3197	1.7790	1.4798	1.0823
2.00	157.62	110.33	43.51	3.78	1.6028	1.8499	1.9747	1.2095	1.4094	1.6806	1.7722	1.6956	1.1809

5.1.5. Determining appropriate weights for three groups of ED of Alpha spectrum

In this work we use three units of ED of Alpha spectrum, i.e. [Azuma1994], [Tang2010] and [Zhao1993]. In the energy region there existing ED of Alpha spectrum, both Alpha spectrum and ^{12}C (α, α) ^{12C} elastic scattering AD jointly determine channel width for (α, ^{12}C), where there is a very strong competition between them. Moreover, the normalized Alpha spectrum, in which the total error is very small,

plays a dominant role in determining channel width for (α, ^{12}C). These three units of normalized Alpha spectrum show different shapes, and real fitting procedures indicate that [Aruma1994] is the most accurate one, which is needed to be ensured to plays a dominant role. After Adjusting the weighting factor of 0.72, 1.00 and 1.43 for other two units compared to [Aruma1994] respectively, it is found that calculated values of all types of SF change very little (Table S5.1.5), thus, it can be determined that W is equal to 1.00.

Table S5.1.5. Alpha Spectrum taking different weights

α-Spec-w	STOT	SE10	SE20	Scas	STOTED	Sαγ0	αγ0AD	ScasED	α-Spec	ααAD	SAllαγ	AllED	Width
Alpha-w0.72	158.35	110.63	43.80	3.92	1.6440	1.8778	1.9801	1.2045	1.7800	1.3210	1.7819	1.4914	1.0950
Alpha-w1.00	158.43	110.31	44.20	3.92	1.6182	1.8618	1.9794	1.2152	1.4001	1.3195	1.7791	1.4676	1.0717
Alpha-w1.43	158.56	110.54	44.09	3.94	1.6484	1.8832	1.9753	1.2090	1.1241	1.3183	1.7812	1.4502	1.0902

5.1.6. Determining the appropriate weight for ED of [Plag2012]

By Fitting discovers that, the ED in the low-energy point of [Plag2012], especially AD for ^{12}C (α, γ0) ^{16}O, is the most sensitive data on SF in all kinds of cross sections, when change their weights can let SF change very significantly. Table S5.1.6 show the SF and χ^2 for its weight-factors are set as 2, 1, 0.25 and 0.01 respectively. It is very useful and necessary to make direct experimental measurements in low energy area, which is proved by the fact that ED in low energy area is the most sensitive to SF factors.

Table S5.1.6. The ED of [Plag2012] taken different weights

plag-wf	STOT	SE10	SE20	Scas	STOTED	Sαγ0	αγ0AD	ScasED	α-Spec	ααAD	SAllαγ	AllED	Width
plag-w2.00	154.30	106.87	43.43	4.00	1.7663	2.1075	2.1985	1.2124	1.4095	1.3185	1.9515	1.5072	1.2307
plag-w1.00	158.66	108.85	45.72	4.09	1.5523	1.8947	1.9852	1.2039	1.3966	1.3197	1.7787	1.4712	1.2362
plag-w0.25	160.72	110.31	46.25	4.16	1.4165	1.7928	1.8608	1.1957	1.4113	1.3207	1.6794	1.4364	1.2157
plag-w0.01	161.57	110.74	46.64	4.18	1.3459	1.7571	1.7987	1.1952	1.4090	1.3213	1.6323	1.4239	1.2010

5.1.7. Processing anomalies straggling ED by Leit's criteria

According to Letts criteria, when observational data follow a normal distribution, the probability of that residual lies in range of three times of standard deviation [± 3σ] is over 99.7 %, while the probability of lying outside this area is less than 0.3%. In some cases, the measured data, their residual lying outsides, can be considered the occasional 'outliers', which is maybe caused by the presence of large systematic errors in some data set , and the very little nominal error between them. For data points with a very large residual, they can be removed, or retained by increasing their nominal error, which is depending on the actual cause of them. In this work, we prefer the latter one to retain them. In the cases of using ± 2σ, ± 3σ, ± 4σ and ± 8σ as amended criteria, it is found that although the maximum difference of finally calculated STOT (7 keVb) (Table. S5.1.7) are smaller than the error of expecting value (about 11 keVb) obviously, but for the high accurate demand for SF, this difference should be considered carefully. The Table. S5.1.7 show that when taking ± 3σ as the amended criteria, the amended data number is 372, about 8.3% of total number, the STOT=159.02. Taking ± 2σ as amended criteria looks excessive, it make the STOT drops 1.1 keVb. The result for taking ± 2σ as amended criteria is very close to that for ± 3σ. It should be noted that using ±8σ has only 11 amended data, it is almost no making any amend. It make the STOT increase 6 keVb. So the conclusion is processing anomalies straggling ED by Leit's criteria is absolutely necessary.

Table S5.1.7. The results using 2σ, 3σ, 4σ and 8σ as criteria respectively

Method	STOT	SE10	SE20	Scas	STOTED	Sαγ0	αγ0AD	ScasED	α-Spec	ααAD	SAllαγ	AllED	Width	D-No.
Leit±2σ	157.93	109.25	44.63	4.04	1.1427	1.4075	1.5100	0.9093	0.8982	1.3162	1.3436	1.3045	0.9575	551
leit±3σ	159.02	109.57	45.39	4.06	1.5731	1.8788	1.9826	1.2019	1.3991	1.3194	1.7765	1.4701	1.2222	372
leit±4σ	159.25	109.78	45.39	4.07	1.7514	2.2532	2.2028	1.3828	1.9458	1.3225	2.0065	1.5708	1.2648	296

leit±8σ	165.14	113.65	47.20	4.28	1.7260	2.9586	2.5332	1.7878	3.8085	1.3245	2.3713	1.7917	1.6585	11

5.1.8. Determining the appropriate channel radius

In the R-matrix analysis, in the condition of only considering the effect of compound nucleus, only if ED is an ideal statistical sample, the channel radius can be taken any real number within a certain range, you can getting a better analysis result. In the contrary, in the case of considering the effect of non-nuclear complex with a complexity ED samples, the different channel radius result in different analyzed results, and there is a group of channel radius close to the best results. The study finds, for determining astrophysical SF of ^{12}C (α, γ) ^{16}O, channel radius, especially elastic scattering channel radius, is the very critical and very sensitive parameter. In the condition of taking the same value for all channel radius, 6.0, 6.5, and 7.00 fm were chosen in the parameter fitting, which is shown in Table S5.1.8. It is found the best results is in the case of 6.5fm. On the other hand, the experimental data of Alpha reduced width γ_α^2 in 4 bound states are given in the condition with channel radius equal 6.5 fm (Oulebsir2012), so all the channel radius are taken as 6.5 fm in this work.

Table S5.1.8. The SF and χ^2 with different radius

Radiixxx	**STOT**	**SE10**	**SE20**	**Scas**	**STOTED**	**Sαγ0**	**αγ0AD**	**ScasED**	**αSpec**	**ααAD**	**SAllαγ**	**AllED**	**Width**
Radi6.00	132.54	095.97	33.57	2.99	1.8189	1.9719	2.0072	1.2870	2.1438	1.3265	1.8427	1.5652	1.5498
Radi6.50	158.43	110.31	44.20	3.92	1.6182	1.8618	1.9794	1.2152	1.4001	1.3195	1.7791	1.4676	1.0717
Radi7.00	178.53	118.17	54.82	5.55	1.5474	1.9988	1.9890	1.2065	2.8542	1.3745	1.7954	1.5988	1.8259

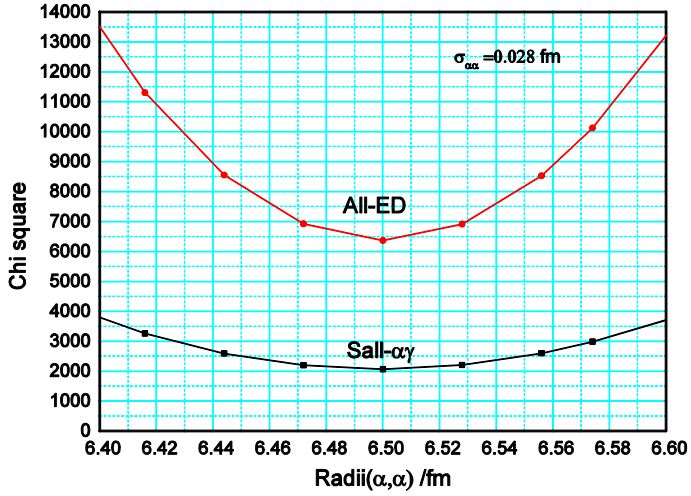

Fig. 5.1.8. The calculated SF and χ^2 for different radius with fixed parameters

In the Tables except 5.1.8, all the SF and χ^2 are the data in a local minimum point which is got by adjusting parameters to fit experimental data under the condition of fixed radius. The error propagation law is used to calculate the STD of parameters and s factors.

In the Table 5.1.8, all the SF and χ^2 are the data in a local minimum point which is got by adjusting parameters to fit experimental data under the condition of with a given radius. The error propagation law is used to calculate the STD of parameters and s factors.

In the Fig. 5.1.8, all the SF and χ^2 are the data calculated with the parameters of a selected local minimum point and a given $R_{\alpha\alpha}$ which changed with the step length$\sigma_{\alpha\alpha}$. The SF and χ^2 are not the calculated values a local minimum point. Using the error propagation law to calculate the STD of parameters and S factors will be of no practical value. But in the previous study works which did not use the error propagation law, the ways to get the STD of someone parameter just is this kind of calculus of differences for the parameter. Or was it, the calculus of differences for the parameter is used to select the best fitting. It is clear that, if we consider 2 Parameters will need 2

dimensional grid computing, if consider n parameters will need n dimensional grid computing. If each parameter considered in M grids, then will need operation for m^n times. The practical calculation shows that when all kinds of parameters have a good estimate, need to take $M \geq 7$. This work needs to consider 140 parameters, then need to do 7^{140} times operations, this is absolutely not feasible. Using the error propagation theorem in RAC13 , in a complete procedure for fitting data, each of the parameters need to adjust about 100 times, so will need a total of 14000 times operation. It can be completed in 6 hours with ordinary microcomputer.

5.1.9. The effect of systematic middle range correlation error (SMRCE)

The systematic long range correlation error (SLRCE) describe the systematic deviation of experimental condition or standard for deal with detected data, e.g., the used detect efficiency is lower than real value 2%; The systematic middle range correlation error (SMRCE) describe the inhomogeneity of experimental condition or standard for deal with detected data, e.g., the used detect efficiency changed 5% with energy change. The systematic short range error is just refer to the statistic error. In the detect process these error are existing objectively. Now a days in most of experimental articles, the SLRCE information is given out, but, very few article give out the information about SMRCE. In general, its estimate values is from 0% to 20%. Table S5.12 show the results for SMRCE taking 0%, 10%, 20% respectively. It looks that the SMRCE have little effect on STOT, taking mean value 10% is a good choice.

Table S5.1.9. The SF (E=0.3 MeV) and $\chi_i^2, \chi_{\alpha\gamma}^2$ for different middle range error item

SMRCE-%	STOT	SE10	SE20	Scas	STOTED	Sαγ0	αγ0AD	ScasED	α-Spec	ααAD	SAllαγ	AllED	Width
midl-00%	158.21	111.29	42.87	4.05	1.7289	1.8805	2.1415	1.2531	1.4514	1.3212	1.8920	1.5058	1.2139
midl-10%	158.19	111.22	42.90	4.07	1.6514	1.8700	2.0970	1.2464	1.4710	1.3213	1.8567	1.4963	1.2201
midl-20%	158.25	111.20	42.97	4.08	1.6122	1.8654	2.0932	1.2401	1.4997	1.3207	1.8491	1.4955	1.2047

5.2. Repeated Iterative fitting

With the use of systematic research, some of the best selection and the initial values of the key factors in the fitting are obtained, these best choices including: 8 reaction channels, 37 levels, 128 to 144 adjustable parameters, 6.5 fm of channel radius, ±3σ of Letts criteria , Schürmann STOT taking 1.03 as the normalization coefficient, and so on. The system error is the deviation from expectation value, due to the expectation value will be get only by global fitting, the deduced conclusion is that the systematic error for someone data set cannot be obtained by isolated analysis, it can be get only with systematical and accurate analysis. According to the error propagation law, if a sub-Dataset get its normalized absolute values, then its relative statistic errors take its original values, its systematic error takes the relative value of the root of its STD.

Two ED input files are needed in RAC. The file named CA12.AE--ORI is a fixed record file of the original ED, which function is to provide the original statistical error. File CA12.AE--EVA is a dynamic ED file recording the evaluation process, which role is to provide the actually used ED in fitting and is updated in the iterative process, where the original relative values of the ED are replaced with the new absolute value, the systematic error values are updated by the mean square errors of newly fitted values, the statistical errors are renewed with the original one at the beginning, but corrected according to the Letts criteria. The ratio of the corresponding data in there two documents is the new 'Scaling factor' or 'normalization coefficient'. The Scaling factor is adjustable in RAC, which is recorded in the parameter file CA12.APAR together with the new R-matrix parameters. Figure S5.2 shows the iterative fitting procedure flow chart.

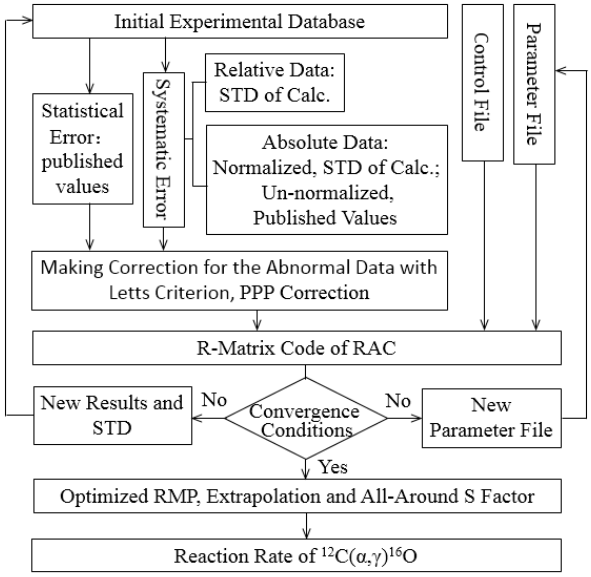

Table S5.2. The flow chart for the iterative fitting procedure.

So, with the continuity of iterative fitting, the variation of scaling factor will be getting smaller and smaller, and the principal values of relative ED will be closer to their expectations. Similarly, the variation of R-matrix parameters, fitted values and mean square error of fitted values will also be getting smaller and smaller, related systematic error of experiments data will be more accurate; their chi-squared smaller changes more and more slightly; at last, all calculated values tend to have very slight fluctuations. Finally take the .loop in which the averaged χ^2_m is smallest as the best one. Refer to Table S5.2.1, in which the loop with STOT=159.72 has the minimum of χ^2_m.

Table S5.2.1. The SF, χ^2_i and the average weighted value χ^2_m for Scheme S3-012-123-3-4

STOT	**SE10**	**SE20**	**Scas**	**STOTED**	**Sαγ0**	**αγ0AD**	**ScasED**	**α-Spec**	**ααAD**	**SAllαγ**	**AllED**	**Width**	χ^2_m	
157.52	103.64	49.88	4.00	1.852	1.763	1.906	1.202	1.421	1.324	1.742	1.460	1.125	1.6125	L
160.95	98.88	57.98	4.10	1.708	1.760	1.970	1.211	1.395	1.321	1.767	1.463	1.166	1.5896	H
160.82	99.11	57.61	4.10	1.712	1.751	1.973	1.209	1.396	1.321	1.767	1.463	1.163	1.5892	H
160.33	99.13	57.11	4.09	1.712	1.753	1.971	1.211	1.395	1.320	1.767	1.462	1.165	1.5893	H
160.22	99.56	56.57	4.09	1.712	1.753	1.971	1.210	1.396	1.320	1.767	1.462	1.163	1.5892	H
159.92	100.03	55.80	4.08	1.715	1.747	1.973	1.210	1.398	1.320	1.767	1.461	1.161	1.5892	H
159.72	100.05	55.60	4.08	1.715	1.746	1.971	1.210	1.398	1.320	1.766	1.461	1.163	1.5890	H
159.50	100.05	55.37	4.07	1.716	1.748	1.971	1.210	1.399	1.320	1.766	1.464	1.164	1.5900	H
159.32	100.04	55.20	4.07	1.719	1.748	1.972	1.209	1.395	1.319	1.767	1.464	1.173	1.5905	H
159.16	100.07	55.02	4.07	1.721	1.749	1.972	1.209	1.395	1.320	1.767	1.464	1.157	1.5902	H

As can be seen from the above description, through the 'systematic research' and 'iterative fitting', with the gradual optimization of parameters to fit the ED with gradually optimized factors, the probable priori factors and subjective factors being excluded in the analysis processing, instead the posterior factors, objective factors playing a decisive role, it is guaranteed that the objective, accurate, self-consistent and unique interior and good astrophysical SF will be obtained in the end.

6. Evaluation and selection of experimental data (ED)

Usally in a set of experimental data the largist uncertainty is its systematical error, becase it's very hard to give out the error accurately according to the experiment alone; and it's very hard to determine the error accurately by analisis of a few sets of data. In evaluation of nuclear data the most important problem is to ascertain the systematical error, which means to get the most reasonable normalization factor for absolute data, and the scaling factor for relative data. In order to approach this object the unique effective way is to do a gloable fitting for the whole data-sets of a nuclear system; the evaluation procedure is included in the gloable fitting procedure.

So far, about astrophysics SF of $^{12}C(\alpha,\gamma)^{16}O$, more than 30 experiments have been carried out with the minimum energy down to E= 0.9 MeV. There are two main experiment method of the capture reaction, direct measurement and indirect measurement. Indirect measurement included the β-delayed α decay spectrum of ^{16}N, Coulomb dissociation, and transfer reaction etc. In this work, The Experimental data have been evaluated very carefully, for the previous research did analysis and reference to very carefully, the specific situation is described in detail in Appendix VII. In this chapter only introduce the principles for evaluation and selection of ED.

6.1. The principle of data evaluation

The basic principle of the data evaluation is that the evaluation data set can reflect the information of nuclear structure and nuclear reaction accurately and objectively, no matter which is to use the original data or the appropriate amendment.

R-matrix fitting require the ED covering full energy region with complete energy points and continuous values, especially in the resonance peaks area with the different types of data. Reliable ED sub-set should satisfy the following requirements:

A. In the resonance peak area, the sum of SF in different reaction channel should be equal to the total SF;
B. The peak position of the different types of ED should be consistent within the range of error;
C. The principal value of different groups should be consistent within the range of uncertainty;
D. The width data of resonance peaks is matched to the implied width information of the other data;
E. The integral value of the differential data should be equal to the corresponding integral data within the range of error;
F. The integral data of different groups should span a broad energy range with a number of data points and have a good match with each other.

According to the principle of maximum likelihood, fitting a data set with many types and large amount of points needs to meet the approximate statistical distribution, so the revisions of some data set is reasonable.

A. If one experimental point deviates from the expectations obviously, such as the residual error larger than three times of uncertainty, the error of this point can be enlarged with the Letts' criteria;
B. In the same type of ED, if the difference of principal value are far greater than their uncertainties, the some error of corresponding data should be amplified in the fitting;
C. If the principal value in one group data deviate from the expected value wholly, the normalization to this data set is needed in the fitting;
D. If one high precision data set are selected as the standard data in the evaluation, then some data with systematic deviation should be normalized to the standard data.

6.2. The principle of ED selection

The basic principle of the data selection is that the fitting data set can reflect the information of nuclear structure and nuclear reaction accurately, wholly and objectively, no matter which is to use or to give up.

All the available data about the SF are adopted in the fitting, unless there is enough evidence to show the problem of one group data. The rare and important low-energy ED are paid special attention in our fitting.

The original and reliable data are paid attention to use, such as 4 group total STOT, 5 group AD of ^{12}C(α, α)^{12}C, 3 α-spectrum data, 71 width data, 7 groups AD of ^{12}C(α, γ_0)^{16}O, 7 groups of Sg.s , and 7 groups of cascade transition data about $S_{6.05}$, $S_{6.13}$, $S_{6.92}$ and $S_{7.12}$ etc.

6.3. The comprehensive information about experimental data set

The final fitting used 12 types, 55 groups of data-sets. The mass center energy range is -1.112→17.51 (MeV), 1282 energy points, 4404 data points, the details are shown in table S6.3 and Appendix IV.

Table S6.3. Channels and experimental database for making global fitting

Channel	ι_{max}	Thro. /MeV	Data types	E / MeV	E_α-No.	Data No.
$^{12}C(\alpha, \alpha)^{12}C$	6	0.0000	AD	1.002→7.500	83	2602
$^{12}C(\alpha, \gamma 0)^{16}O_0$	4	7.1620	AD AD-EX $S_{g.s.}$	1.362→6.075 4.898→6.103 0.940→6.413	67 160	514 146 160
$^{12}C(\alpha, \gamma 1)^{16}O_1$	3	1.2126	$S_{6.05}$	2.223→4.493	39	39
$^{12}C(\alpha, \gamma 2)^{16}O_2$	2	1.1321	$S_{6.13}$	2.222→4.493	15	15
$^{12}C(\alpha, \gamma 3)^{16}O_3$	2	0.3449	$S_{6.92}$	1.370→4.493	70	70
$^{12}C(\alpha, \gamma 4)^{16}O_4$	2	0.1452	$S_{7.12}$	1.399→4.493	48	48
$^{12}C(\alpha, \alpha 1)^{12}C^*_1$	3	-4.4380	CS AD AD-EX	5.904→6.317 5.962→6.105 5.789→6.164	22 14	22 198 67
$^{12}C(\alpha, p)^{15}N_0$	3	-4.9680	AD-EX	5.712→6.158	22	86
			STOT	1.002→5.918	105	105
			α-Spec.	0.600→3.240	259	259
			$\gamma_\alpha^2, \Gamma_{\lambda c}$	-1.113→17.51	31	81

Note: All channel radium is 6.5 fm. $S_{G.S.}$ Refer to SF for ground state capture, $S_{6.05}$, $S_{6.13}$, $S_{6.92}$ and $S_{7.12}$ to the four bound state captures respectively. Total S Factor STOT =$S_{g.s.} + S_{6.05} + S_{6.13} + S_{6.92} + S_{7.12}$, γ_α^2 is α reduced width of bound state, $\Gamma_{\lambda c}$ is width of channel.

7. Evaluation, fit and result for integrated data

Essentially, the fitting of R- matrix is a semi-classical phenomenological fitting. The criterions to assess the performance of an R-matrix model include whether it could fit the reliable ED sets of a nuclear system uniformly and accurately and give reliable extrapolation. Next, we will illustrate how we choose various kinds of integral ED, the agreement degree between the data value and the fitting value, and the contributions of each energy level and partial reaction channel to the fitting value. The situation about differential ED is described in detail in APPENDIX I. In this paper all SF is in keV b. all energy in CM system and MeV, The keV b and MeV will be omitted in sometime.

In this SI file the calculated STOT and $S_{g.s}$ of RAC2013 or RAC2014 are identical with these in RAC2015, the calculated $S_{6.05}$, $S_{6.13}$, $S_{6.92}$, $S_{7.12}$, of RAC2013 or RAC2014 are near identical with these in RAC2015. In order to make more items of comparisions, in this SI file the plots include the contributions of each energy level and partial reaction channel to the fitting value, and more evaluated values of previous wroks. The Ref. Kastuma, 2008 thinks that in previous wroks '*an enhancement of the E1 component in the cross section is presumed to fit the experimental data in the Ec.m. = 1–2 MeV region. The enhancement originates from the subthreshold 1−1 state (Ex = 7.12 MeV). The resulting low-energy extrapolation strongly depends on the expected contribution from this state.'* The SE10 of Kastuma2008 is very small (about 3 keV b), the SE20 is very high (about 150 keV b). The plots in SI Chp.7 will show the calculated S factors are far from corresponding ED.

7.1. Total S factor-ST

Figure S7.1 illustrates the ED of the total S-factor ST and the corresponding fitted value. In general, the fitting is perfect. Especially, all the energy levels are accurately described. Figure S7.1 shows the partial contributions of all kinds of energy levels for ST.

In this work we choose 4 groups of ST include (*Schürmann2005*), (*Schürmann2011*), (*Fuji2009*) and (*Plag2012*). The ST of (*Schürmann2011*) is obtained by adding of their component: ST= $S_{G.S}+S_{6.05}+S_{6.13}+S_{6.92}+S_{7.12}$, and it is consistent with the ST of (*Schürmann2005*) very well. The data about energy level 1^-_2 (E≈2.42) play the most important role in analysis. The (Schürmann2005) have not given definite numerical value of 3 narrow peak(2^+_2,4^+_1 and 0^+_2), and the author's personal communication consider that the relative

numerical value is difficult to determine, so the distribution for the data of this three peak is the estimated value which is obtained from figure reading.

In the peak region of the 1^-_2 energy level (E≈2.42±0.20), the evaluation of ED is as follow. We can learn the ST≈96.5 from (*Schürmann2005*); the evaluated $S_{G.S.}$≈76.0 from 6 groups of $S_{G.S}$; Estimating the $S_{6.05}$≈1.0, $S_{6.92}$≈6.89 and $S_{7.12}$≈20.2 from (*Matei2006*) and (*Kunz2001*); making assumption for S6.13≈0.8 from (*Matei2008*). In view of the above, the sum of the partial S-factor is 104.8 , which is 1.09 times of the calculated ST=96.5; that is to say, the experimental value of the total S-factor is significantly less than the sum of the experimental partial S-factor. Relevant literature (*Schürmann2005*) account for that the maximal systemic error is 6.5% , so we choose 1.03 as the normalization coefficient (NF) of (*Schürmann2005*), then the data become ST=99.4, it is lower than the sum of partial S factors.. The systematical studying shows that the $S_{6.92}$ of (*Kunz2001*) has the trend to increase, the $S_{7.13}$ of (*Kunz2001*) has the trend to decrease, when taking the NF of $S_{6.92}$ and $S_{7.12}$ as 1.00 and 0.95 respectively, then the sum of partial S-factor approximately equal to 99.5. So we can get a satisfied ED set which have complete types and numerical self-consistency for the main resonance peak 1^-_2. The ST data set constitute the skeleton of the whole database.

Another skeleton of the ED set is the data on the peak region of $\mathbf{2^+_3}$(4.358). In this region (*Schürmann2011*) has $S_{G.S}$, $S_{6.05}$, $S_{6.13}$, $S_{6.92}$ and $S_{7.12}$, the energy points distribute on both sides of the peak position. The test fitting shows that if we translate the energy for -5keV, then the agreement between fitted value and ED become much better, the sum of the partial S-factor for each energy is consistent with the ST of (*Schürmann2005*). All kinds of the data of (*Schürmann2011*) is used as standard dataapp:ds:criterion, the NF is 1.00.

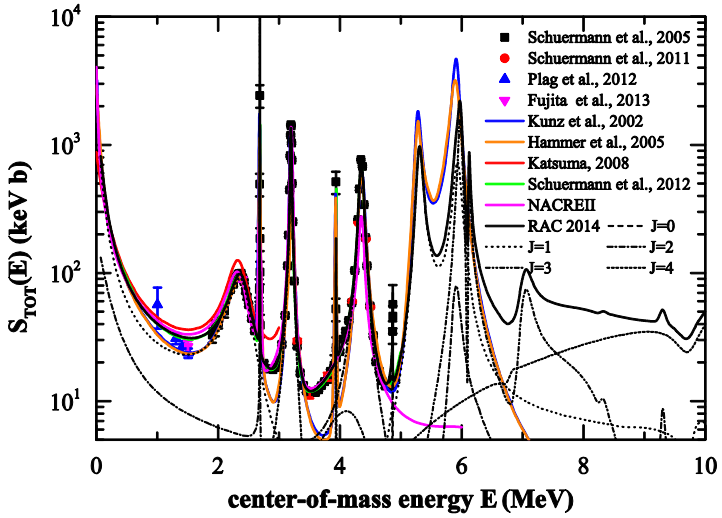

Fig. S7.1.1 the fitting situations for ED of 4 groups ST and 4 available previous calculated ST. The measurement of *(Schürmann2005, Schürmann2011,* Plag2012*)* in inverse kinematics using the recoil mass separator allowed to collect data with high precision in a wide energy range, which would make good restriction to the extrapolation and normalization of ground transition, cascade transitions and the total SF *(Schürmann2005)*. These data play a dominate function for determining of SF. The fitting of *(Schürmann2005)* is good up to 5.1 MeV, the $S_{0.3}$=161±19. The fitting of RAC2014 are very well, every peak and most of data are described perfectly up to5.2 MeV. The calculated ST of (*Hammer, Katsuma, and NACREII*) have larger deviation from the data of ST.

The ST of (*Fujita2009*) has only two energies, with rather large nominal errors, and the principal values are relatively close to expectations. (*Plag2012*) is the latest ED which has 4 low energies, which are 1.002, 1.308, 1.416 and 1.511 .The principal value of 1.002 is far above expectation, while the principal value of 1.416 and 1.511 are significantly below the expectations. Because this strange trend, it is difficult to normalize the ST satisfactorily.The error values given in (*Fujita2009*) are used as the systematic errors.

The RAC2014 in figure S7.1 indicates the fitted value of ST. Because the fitting is very good, it could be regard as the expectation of ST.

Other color lines in figure s7.1 denote the total contribution of all kinds of energy levels, which will be elaborated in the following relevant section.

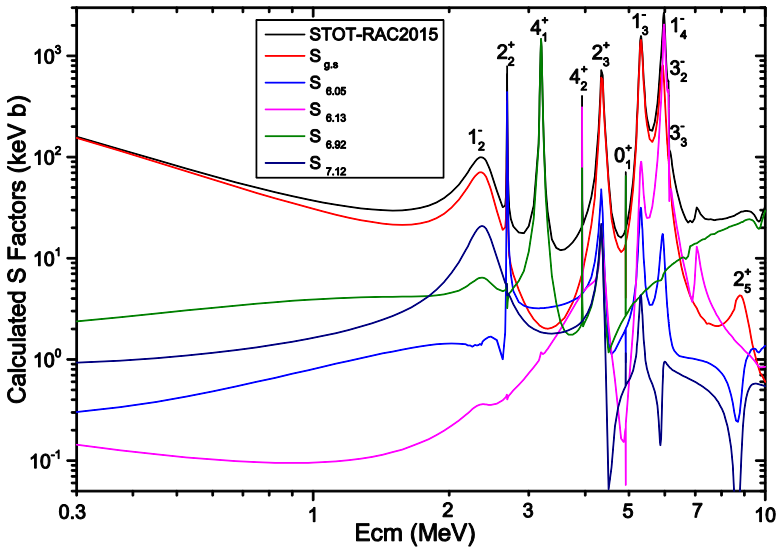

Fig. S7.1.2. Calculated STOT and the 5 primary transition S factor

Figure S7.1.2 shows the fitted value of the ST and the contribution of each reaction channel. The difference between Fig. S7.1.1 and Fig. S7.1.2. will be illustrated in following section.

In R-Matrix theory, the contributions of all energy levels to the AD are related, so there exist numerical competitions among them. And the numerical values cannot be indicated according to different energy levels respectively.

In R-Matrix theory, the contributions of all energy levels to the integral cross-section are related, so there also exist numerical competitions among them. But the numerical values can be indicated according to different energy levels respectively. The total SF equal to the sum of the S-factors of all energy levels by definition:

$$ST=SE0T+SE1T+SE2T+SE3T+SE4T, \quad \text{S7.2.1}$$

Where the items in the right denote the total contribution of 0^+, 1^-, 2^+, $3^-$and 4^+ respectively. In R-Matrix theory, the contributions of all reaction channels to the integral cross-section are related, so there exist numerical competition among them, but the numerical values could be indicated according to different reaction channels respectively. The total S-factor equal to the sum of the S-factors of each reaction channel by definition:

$$ST=S_{G.S}+S_{6.05}+S_{6.13}+S_{6.92}+S_{7.12} \quad \text{S7.2.2}$$

According to the definition, the first channel is the elastic scattering channel and the second to seventh channels are the γ particle channel which is relate to S-factor.

Since the integral quantities could be indicated according to energy levels and reaction channels, we could obtain the combined quantities of all kinds of integrations. e.g.: the total contribution of 1^- energy level is the sum of the contribution of each reaction channel of 1^- energy level:

$$SE1T=SE10+SE11+SE12+SE13+SE14 \quad \text{S7.2.3}$$

The total contribution of 2^+ energy level is the sum of the contribution of each reaction channel of 2^+energy level:

$$SE2T=SE20+SE21+SE22\ \ SE23+SE24 \quad \text{S7.2.4}$$

The total contribution of ground state is the sum of the contribution of each energy level to ground state:

$$S_{G.S}\ =SE00+SE10+SE20+SE30+SE40 \quad \text{S7.2.5}$$

The total contribution of 2^+_1 state is the sum of the contribution of each energy level to 2^+_1 state:

$$S_{6.92}=SE03+SE13+SE23+SE33+SE43 \qquad S7.2.6$$

In R-Matrix theory, there exists interference between each kinds of energy level. Hence the numerical value of integration could not be expressed strictly according to individual energy level. But we can determine which energy level contributes dominantly by the position of the energy point, besides, we could derive the coherent properties from the shape of the curve of integral values.

During the analysis, the figures of above various sum are drawn frequently in order to find out whether the fitting is right or not.

7.2. The comparison of Alpha energy spectrum

Figure S7.2 shows the ED and corresponding fitted values of Alpha energy spectrum.The fitting is good as a whole.

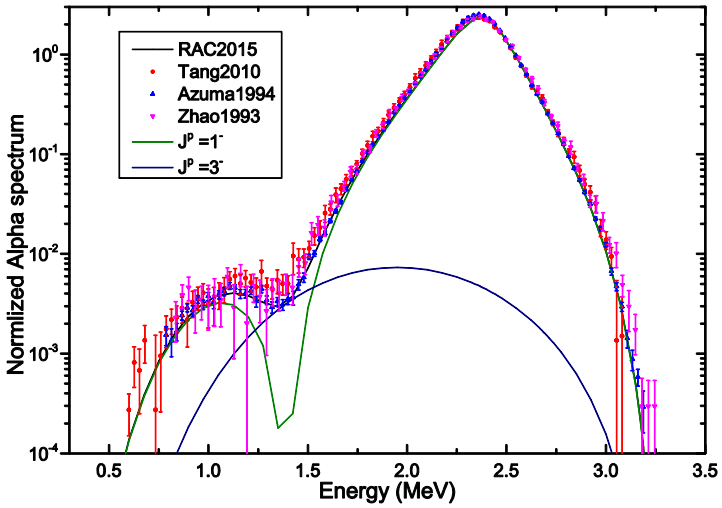

Fig. S7.2. Fitting situation for Alpha spectrum

Ref. (*Buchmann2009*) gives detailed evaluation about 6 different data of Alpha energy spectrum. In this work we choose the data of (*Azuma1994*), (*Tang2010*) and (*Zhao1993*) to use. This is because there exists better consistency between these data after being transformed to normalized spectrum. The other data are difficult to normalize due to have incomplete region of energy, so they not be used. The energy span of Alpha energy spectrum in the cm system is from 0.60 to 3.2. In this energy region the width of (α, ^{12}C) channel is determined by the Alpha energy spectrum and the Elastic scattering AD of ^{12}C (α, α) ^{12}C, which results in fierce competition. But the Alpha energy spectrum plays main role in the determination of the α+^{12}C width of 1^-(E=2.42). Most of the original data of the Alpha energy spectrum is particle number spectrum with 20keV interval. The normalizations of the data from different group have great systematic errors. The normalization for probability spectrum is obtained through dividing the number in each energy interval by the total counts, then transforming the quotient to the counts per unit energy. In this way the systemic error could be basically eliminated. The statistical errors of the original data remain unchanged in the normalization. The normalized spectrum is just the $W_\alpha(E)$ in the relevant formula (S4.3.2). The error of the fitted value is the systematic error, so the total error of Alpha energy spectrum is very small, which indicates that the Alpha spectrum plays an important role to determine the width of the (α, ^{12}C) channel

The line marked with J=1^- in Fig. S7.2 denotes the contribution of 1^- energy levels. We see that the elastic scattering channels of 1^-_1 and 1^-_2 are strongly negative coherent around 1.4 MeV. For determination of the width of (α, ^{12}C) in 1^-_1 and 1^-_2 they play an important role. The line marked with J= 3^- denotes the contribution of 3^- energy levels, which perfectly compensates the negative coherence of 1^-_1 and 1^-_2.

7.3. The S factor $S_{G.S}$ of Decay to the ground state

Figure S7.3 shows the ED and corresponding fitted value of the S-factor $S_{G.S.}$ Of decay to the ground state, which fit well as a whole. And the figure shows the contribution of each energy level.

In this work we choose 9 groups of $S_{G.S}$ data, which were obtained through data fitting and are more reliable. Some papers provide $S_{G.S}$ directly, some papers provide SE10 and SE20, we take $S_{G.S}$=SE10+SE20.

All the values of $S_{G.S}$ in Ref. (Redder1987), (Ouellet1996), (Kunz2001) and (Assuncao2006) include the most important resonance peak of 1^-_2 (2.42). These values are well consistent in the peak region and are all close to expectation value. In *E*=2.42±0.20 MeV there are 5 groups absolute ED about $\sigma_{\gamma 0}$, their weighted average value is $\sigma_{\gamma 0}$= 47±3nb *(*Redder1987*)*, these data play the key function to determine $S_{g.s.}$ In the peak region, the average value of SG.S is about 76.5, and can be regarded as a criterion for normalizing the ED. The NF of those 4 different data are fixed at 1.0, the systematic errors are the square errors of the fitted values. In Ref. (Brune2012i), the DE convolution method is used to correct the ED of in Ref. (Assuncao2006). The result changes little after the correction, but it is still used in this work.

Even though the $S_{G.S}$ of (Kettner1982) is systematically larger, it is dispensable since it is the only one that has the data points at above 3MeV. It is noteworthy that if the NF is fixed as 0.93, the data of 1^-_2(2.42) peak region is consistent with the above 4 different data, meanwhile the data at 3.3MeV is well consistent with the $S_{G.S}$ of Schürmann2011. This reasonably connects the data at low and high energy regions, and remarkably reinforces the consistence between this kinds of data, which develops a data set of $S_{G.S}$ covering full energy region with complete energies and continuous values.

The $S_{G.S}$ of Makii2009 has 4 energies with smaller nominal errors, the principal value are closer to expectation.

The latest $S_{G.S}$ of (Plag2012) has 4 energies with E at 1.002, 1.308, 1.416 and 1.511 MeV. The value of 1.002 point is significantly larger than the expectation, while the values of 1.416 and 1.511 points are much smaller than the expectations. This strange trend makes it very difficult to normalize the $S_{G.S}$.

The $S_{g.s.}$ of (Brochard1977) has 24 energies and with NF=1.00, the excitation function of (Ophel1976) are absolute value for 40 energies (NF=1.70, Fig. S8.2). These 2 absolute data and other AD (Larson 1964) and excitation function (Kern1961) of ^{12}C (α, γ0)^{16}O have rather strong non-consistent, the AD data have to be normalized. These 2 data sets locate in the energy region from 5.1 to 6.2 MeV, and cover the 5 levels 1^-_3, 1^-_4, 2^+_3, 3^-_3 and 3^-_4 , They play a dominate function for ascertain of $S_{g.s}$ for E>5 MeV. These 2 data sets have not be used by previous works. For example, (Kunz2001) did not use them, its calculated $S_{g.s}$ are 2 times that of ED. In this work these 2 data sets are used in first time, it is inevitable that the perfect fitting them must produce much better evaluated $S_{g.s.}$ than that have done before.

In this work, we choose 66 AD of ^{12}C (α, γ_0) ^{16}O from 9 different groups, which is crucial for the determination of $S_{G.S}$.

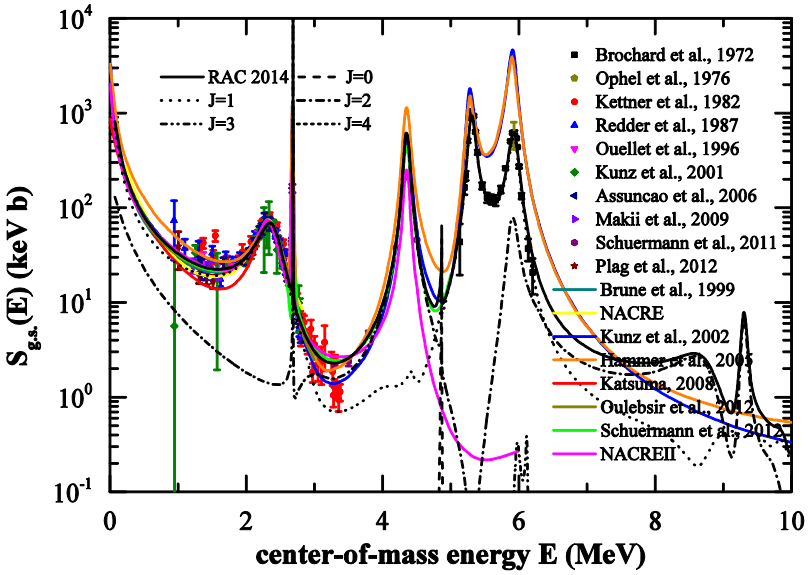

Fig. S7.3 shows the fitting situation for ED of $S_{g.s.}$ of 9 groups and other available calculated values of 8 groups In *E*=2.4±0.2 MeV there are 5 groups absolute ED about $\sigma_{\gamma 0}$, their weighted average value is $\sigma_{\gamma 0}$= 47±3nb *(*Redder1987*)*, these data play the key function to determine $S_{g.s.}$ The fitting for AD of ^{12}C (α, γ_0)^{16}O play very strong restrain effect too. Most of data have been described perfectly up to 6.5 MeV, it is the first time to use all the data from 0.8 to 6.5 MeV. The fittings of Schurmann2005 and Kunz2001 look good, but the up-energy for data is 5.2 MeV only. The result of Kunz2002 is too higher for E≥5.2 MeV. The result of Hammer2005 is too higher systematically for whole energy region. The result of NACREII2013 looks good for E<3.5 MeV, but it is too lower for E≥4.2 MeV. Other 5 groups have results up to 3 MeV only. So the reason is enough to say the result of RAC2014 is the best one.

In Fig. S7.3 the line marked with J=1 denotes the contribution of 1^- energy level. The 1^- has 5 resonant energy levels ($E_{1\lambda}$=-0.045, 2.423, 5.278, 5.928 and 9.710) and one distant level (E_{16}=12.3). The bound state (E_{11}=-0.045) and the second level (E_{12}=2.423) are vital in determining SE10. About the second 1^- energy level, there are a lot of reliable ED. The AD of ^{12}C (α, γ0) ^{16}O and the Alpha spectrum can determine the width of (α, ^{12}C) accurately. The AD of ^{12}C (α, γ0)^{16}O can precisely determine the width of (γ0, ^{16}O). In addition, the data of ST which with high precision and plenty of $S_{G.S.}$ Will provide strict constraints for determining the value. With the coordination of using α reduced width and γ width of bound state, the SE10 =94±7.63 is obtained in this work, which is a unique and reliable value based on the ground experiment data.

In Fig. S7.3, the line marked with J=2 denotes the contribution of 2^+ levels. 2^+ has 7 resonant energy level ($E_{2\lambda}$=-0.242, 2.683, 4.358, 5.858, 8.310, 9.281 and 9.967) and one distant level (E_{28}=22.1), the bound state (E_{21}=-0.242) and the third energy level (E_{23}=4.358) are vital in determining SE20. The AD of ^{12}C (α, α) ^{12}C is close related with the third energy level and can be used to determine the width of (α, ^{12}C) and the $S_{G.S}$ with considerable accuracy can determine the width of (γ0, ^{16}O).

In addition, ST width with high accuracy could provide strict constraints for determining the value. In this work, we have carefully studied the function of second nerow energy level (E_{22}=2.683). The data closely related with this energy level are as follows: 5 ST data points got from the figure, AD of ^{12}C (α, α) ^{12C}, $S_{G.S}$ and various width data in this energy level. The 7 AD data are much close to this energy level, which plays an important role to determine the coherence of this energy level and the contribution of SE20. The energy level presents 'high on the left and low on the right' kind of coherence, which is consistent with that in (Sayre2011). However, the coherence of (Schürmann2012) is 'low on the left and high on the right', which necessitates further study. Overall, the impact of the second energy level (E_{22}=2.683) on SE20 is not much, which is estimated to be within ±1.0 keV.

The line marked with J=3 in figure S7.3 denotes the contribution of energy level 3^-. The hump near the energy level (4.438) is produced by the interference, which has little contribution to ST factor

7.4. The S-factor $S_{6.05}$ of the decay to the first excited state

By now, the evaluated values of $S_{6.05}$ (0.3) from different groups differ greatly with each other. So it is necessary to give a detailed study and discussion. Refer to Fig. S7.4. In Matei2006, $S_{6.05}$ (0.3) =25^{+16}_{-15} is obtained by fitting the experimental results therein. It mainly comes from SE1 and partially from SE2 and is with large error. In (Schürmann2012), the $S_{6.05}$ is got by analysis the data in (Schürmann2011). $S_{6.05}$ (0.3) is less than 1.0, which is mainly contributed by SE02 while little by SE01. (Katsuma2008) is a potential model analysis, the deviation between calculated value and ED is very larger. The evaluated value of NACREII is close to ED for 2.6<E<4.5 MeV, but at the most important energy point (E=2.42 MeV) is much higher than ED, and it is much lower for E>5.2 MeV.

In this work, we obtain $S_{6.05}$ =0.78±0.14 keV b, and in the following we will give detailed illustration.

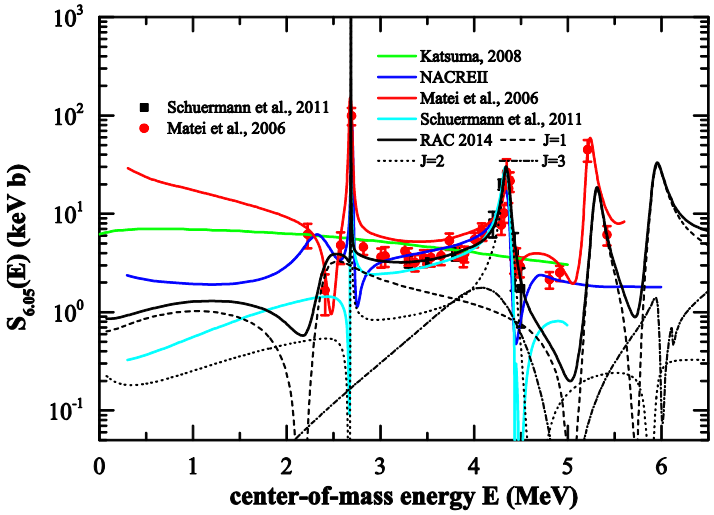

Figure S7.4 shows the fitting situation about $S_{6.05}$, and 5 groups of calculated values. The fitting of RAC2014 is good overall for E=2.4 to 5.5 MeV, the $S_{6.05}$ (0.3) =0.8±0.3 for RAC2014. The line of (schurmann2012) is close to the data set for 3 <E<4.5 MeV, there are larger deviation from data for E<3 MeV and E>4.5 MeV; the line of (NACREII2013) is close to the data set for 3 <E<4.5 MeV, but there are larger deviation from data for E<3 MeV and E>4.5 MeV; the line of (Matei2006) is got by fitting the data of himself only. The line of (Katsuma2008) just is an average value.

Ref. (Matei2006) and (Schürmann2011) use the same experimental method, and both their original data show the γ contribution of the first excited state (0^+_1, 6.05), but the result after analysis differs considerably. (Schürmann2011) concludes that the $S_{6.05}$ is negligible in the energy region less than 3.3 MeV, so it only gives the ED of $S_{6.05}$ above 3.3.

In figure S7.4, the data of (Schürmann2011) in high energy area is regarded as standard data and the NF is 1.03. The energy regions of the data in (Matei2006) and (Schürmann2011) have overlap around 3.5 MeV. The result of (Matei2006) can be normalized by that of (Schürmann2011), and the normalization is 0.70. This forms a data set of $S_{6.05}$ which covering full energy region with complete energy points and continuous values. From 2 to 5 MeV , the fitting of $S_{6.05}$ is restrained by lots of different kinds of ED. Above 5 MeV, the ED only include $S_{6.05}$, AD of $^{12}C(\alpha, \alpha)^{12}C$ and the data of width of 1^-_3 (5.278) and 1^-_4(5.928) energy level.

Of the ED in (Matei2006), the first 4 data are at 2.223, 2.409, 2.57 and 2.682 MeV respectively, which are at the peak region of the main excited state (1^-_2, 2.42) and play a particular role in determining $S_{6.05}$. The first point energy (E=2.223) is lower than the peak, but the $S_{6.05}$ data increases a lot in contrast, which means the $^{12}C(\alpha, \gamma_1)^{16}O$ channel of bound state(1^-_1, -0.0245) is 'positive interference' with the distant energy level (1^-_5, 12.20) which contributes the most and this increases the value of $S_{6.05}$. The second energy point(2.409) is very close to the peak, and the $S_{6.05}$ data value is the lowest one, which means that the $^{12}C(\alpha, \gamma_1)^{16}O$ channel of the excited state is ' negatively correlated' with the distant energy level which contributes the most, and infers that the contribution to $S_{6.05}$ must be small. (Schürmann2011) also explains that the $S_{6.05}$ data at 2.409 is very small. The third and the fourth energy point (2.682) located two sides of the level 2^+_2(2.685) which constrains the fitting very well.

The contribution of energy level 3^- is produced by the distant energy level, which can improve significantly the fitting of $S_{6.05}$ in intermediate energy region. The contribution of the energy level 2^+ is primarily from 2^+_3(4.358), whose interference state is 'higher left and low right', its shape is similar with that of (*Sayre2011*).

Of course, the results of RAC are obtained by using the entire parameter set to fit the whole ED set. Any reaction channel which exists in theory and has been observed in experiment has a set of expectations. These expectations rely not only on the direct ED of this reaction channel, but also the whole ED set. The whole ED set is normalized, and the sum of the contributions of the ground state and each discrete level to S-factor equals to the total S-factor. It can still give corresponding fitted value with improved precision even if the ED of

certain reaction channel is few or without sufficient precision, Comparing with previous analyses, this work has used more completed R-Matrix parameters and ED set. And the iterative fitting method is employed in this work, which doesn't describe certain energy level or reaction channel in isolation. Several fitting schemes show that there is not possibility to get $S_{6.05}(0.3) > 2$ keV b.

Fig. S7.4 show that for $S_{6.05}$ at E=0.3 MeV, 1^- levels produce main contribution, 2^+ levels produce very small contribution , The $S_{6.05}$ got by this work is from the systematic analysis of the whole $\mathbf{O^{16}}$ system. Hence compared with previous analyses, our result is much more firmly based on the experiments and must to be more reliable.

7.5. The S-factor $S_{6.13}$ of the decay to the second excited state

Figure S7.5 shows the ED and corresponding fitted value of the $S_{6.13}$, which represents the first decay to the second excited state (3^-_1, 6.13). The fitting is good as a whole. As for $S_{6.13}$, (Schürmann2011) is used as standard data at high energy region, and its NF is 1.03. At low energy region, there is no direct measurement yet. However, this kind of data is needed for precise determination of the S-factor of astrophysics. It is better to use estimated value than use none. By use of ^{19}F (p, αγ) ^{16}O reaction, the intensity ratios of 4 energy points for the decay of ^{16}O to 3 bound state (1^-_1, 2^+_1, 3^-_1) are attained (Matei2008), the average is about 70:23:7. The energy points are at about E=7.14±0.2, which is close to the bound state 1^-_1(E=7.12). At the peak (E=9.585±0.3) of 1^-_2, since the sum of partial S-factor $S_{G.S.}+S_{6.05}+S_{6.92}+S_{7.12}$ is larger than ST, we can deduce that the $S_{6.13}$ is very small though not 0, and its intensity ratio is lower than 7%.

With the assumption of 3.5% for the intensity ratio of $S_{6.13}$, we roughly obtain the estimated value of $S_{6.13}$ and the maximum value 0.8 at the peak of 1^-_2(E=9.585) by using $S_{6.92}$ and $S_{7.12}$ from (Kunz2001), which develops a data set of $S_{6.13}$ which covers full energy region with complete energy points and continuous values. The line marked J=1 in figure S7.5 denotes the contribution of the energy level 1^-, which dominates the SF in low energy region.

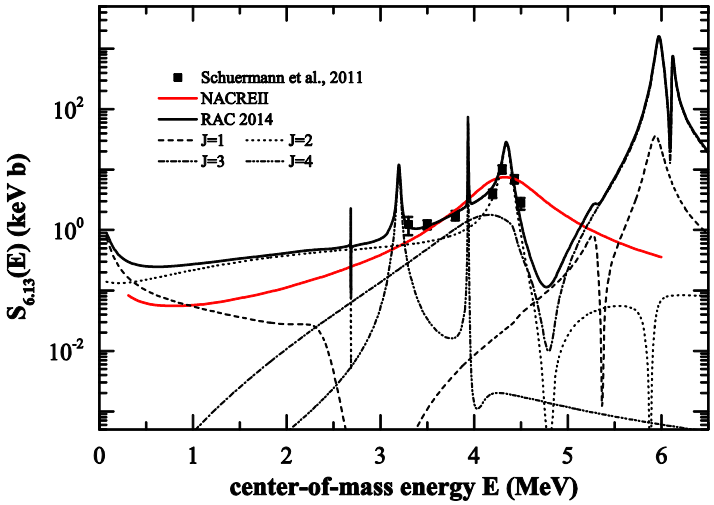

Fig. S7.5 shows the fitting situation about $S_{6.13}$ and 2 groups of calculated vales. The $S_{6.13}(0.3) = 0.28\pm0.05$ for RAC2014. The $S_{6.13}(0.3) \approx 0.08$ for NACREII2013.

7.6. The S-factor $S_{6.92}$ of the decay to the third excited state

Fig. S7.6 shows the fitting situation about $S_{6.92}$, and 7 groups of calculated values. The fitting of RAC2013 is good overall. The $S_{6.92}(0.3) = 2.48\pm0.22$. As for $S_{6.92}$, we use different ED from 4 groups of data sets. For (Schürmann2011) whose normalized coefficient is 1.030 are used as standard data in high energy region. Although (Kettner1982) and (Schürmann2011) doesn't have same energy point, they strictly match each other through the resonance level 4^+_1(3.19). In RAC2015 fitting, for Kettner1982[15] only the data points for E> 3 MeV are used with NF=1.00.

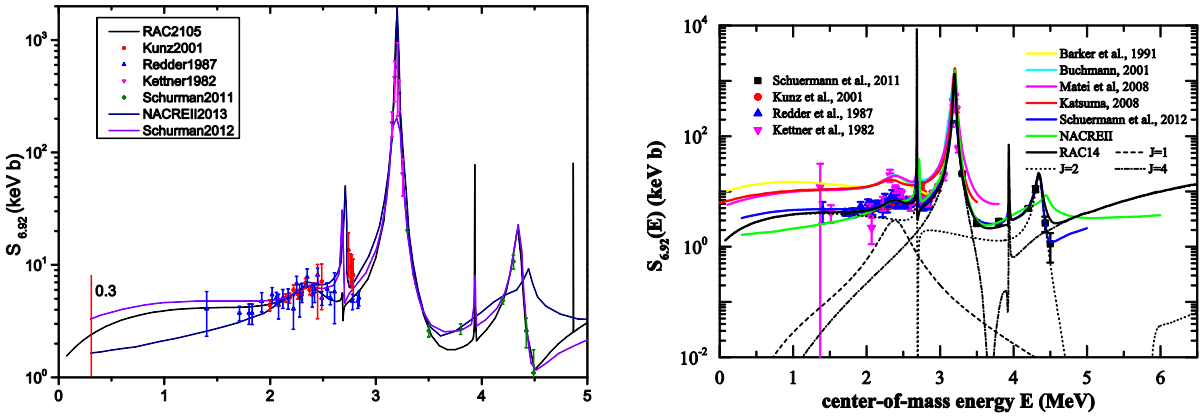

Fig. S7.6. Fitting situation about $S_{6.92}$ and 7groups of calculated vales.

According to the evaluation and fitting of the ED, we find that the $S_{6.92}$ of (Kunz2001) is more accurate, whose NF is fixed at 1.00. Then a data set of $S_{6.92}$ has been developed which covers full energy region with complete energy points and continuous values. The NF of (Redder1987) as an adjustable parameter is also determined by fitting.

Figure S7.6 (left) shows obviously that, the lug boss for E<2.5 can not be described by conpound nuclear model alon, in the extrapolation energy range (E<1.5 MeV) the $S_{6.92}$ mainly come from direct capture. So a background parameters R_{j0} / ($E-E_{j0}$) were used to make calculation for direct capture, E_{j0} is a constant less than 0, R_{j0} is an adjustable parameter. The background of resonant capture and non-resonant capture contribution in low energy range (E<1 MeV) can be got. (Fig. S4.5- C).

Figure S7.6 (right) shows that the contribution of the level 2^+ plays leading roles for the determination of the S-factor in low energy region. The $S_{6.92}$ (0.3) = 2.48±0.22. Several fitting schemes show that there is not possibility to get $S_{6.92}$ (0.3) > 4 keV b. The line of (schurmann2012) is very close to its data of (Schurmann2011), and is higher than that of RAC2013 a little. The lines of (Barker1991, Buchmann2001, Matei2008, Katsuma2008) are much higher than the ED for E<3 MeV. The line of NACREII2013 is much lower than ED for E<2.3 MeV.

7.7. The S-factor $S_{7.12}$ of the decay to the fourth excited state

As for $S_{7.12}$, we use 4 different ED data from (Schürmann2011) whose normalized coefficient is 1.030 are used as standard data in high energy region. According to the evaluation and fitting of the ED, we find that the $S_{G.S}$ and $S_{6.92}$ of (Kunz2001) are more accurate, but $S_{7.12}$ is a little higher. If the NF is fixed at 0.90, the $S_{G.S.}$ +$S_{6.92}$+$S_{7.12}$ of (Kunz2001) is consistent with the ST of (Schürmann2005) within the uncertainty. The NF of (Redder1987) as an adjustable parameter is determined by fitting, and its optimum value is 0.452. Then a data set of $S_{7.12}$ has been developed which covers full energy region with complete energy points and continuous values.

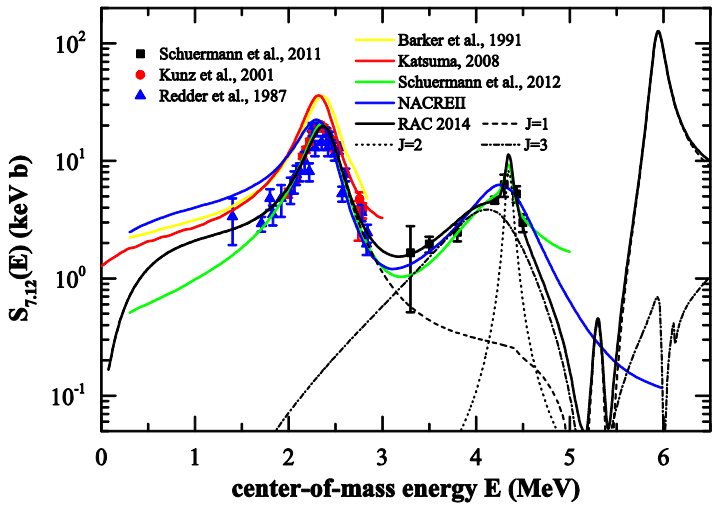

Fig. S7.7 shows the fitting situation for $S_{7.12}$, and 5 groups of calculated values. The fitting is good overall for E=1.4 to 4.5 MeV. The $S_{7.12}$ (0.3) =0.88±0.15. The line of Schurmann2012 is close to the data set. The lines of (Barker1991, Katsuma2008, NACREII2013) are much higher than the data set for E<3 MeV.

The figure S7.7 shows that the contribution of the energy level 1^+ play a leading role for the determination of S-factor in low energy region. In the extrapolation energy range (E<0.5 MeV) the $S_{7.12}$ partly come from direct capture. The contribution of the energy level 3^- which is produced by the scattering state 3^-_2. This kind of transition ($3^-_2 \rightarrow 1^-_1$) has not been reported normally. In this work the fitting is significantly improved after adding relevant parameters, which confirms the existence of this transition.

7.8. The comparison for width of level

7.8.1. The comparison for width of level

In this work, we have used all the relevant information about 74 widths in 31 energy levels published in (Tilley1993), and 7 new results(deboer2013), which include mean lifetime τ, life time $T_{1/2}$, level width Γ and branching ratio. Their relation is: $T_{1/2}=0.693147\tau$, $\Gamma=\hbar/\tau$, $\hbar=6.582173\times10^{-22}$ ·s. The modified formulae in (Lane1958) are used to calculate the width and energy shift of level.

$$\Gamma_{\lambda c} = 2P_c\gamma_{\lambda c}^2/d_c \qquad \text{S7.8.1.1}$$

$$\Delta_{\lambda c} = \frac{P_c(R_{cc}^0P_c)-S_c^0(1-R_{cc}^0S_c^0)}{d_c}\gamma_{\lambda c}^2 \qquad \text{S7.8.1.2}$$

$$d_c = (1-R_{cc}^0S_c^0)^2 + (R_{cc}^0P_c)^2 \qquad \text{S7.8.1.3}$$

$E_{\lambda c}$ And $\Gamma_{\lambda c}$ should be physical parameters, they should be able to describe the published evaluated experimental data in Tilley1993).

The problem about the width of bound states have been described in S5.1.1 in detail. In the energy region in which existing scattering and/or capture cross section data, there exist competition between cross section data and width data, but the cross section data play a dominate function, the parameter of energy of level and the parameter of width are ascertained by fitting the cross section data mainly and automatically. In the higher energy region in which there exist width data only, the parameters of width are ascertained by fitting the width data mainly automatically, but the parameters of energy of levels are ascertained by settings in iteration procedure, the method is that let the energy position of a level in the input parameter file equal to the calculated center energy of a peak of some observables (e.g. ($\alpha\gamma$) cross section). This means that in the higher energy region the R-Matrix parameter E_λ equal to the observed physical parameterE_λ^r, the real energy shift Δ_λ^r equal to 0, the calculated width is close to the observed physical width which is taken as a kind of ED in database.

7.8.2 Fitting situation about Width $\Gamma_{J^\pi_\lambda C}$ of Sub-reaction channel

Table S7.8.2. Fitting situation about Width $\Gamma_{J^\pi_\lambda C}$ of Sub-reaction channel

Width-$_{J^\pi_\lambda C}$ is Name of Width of Sub-reaction channel, J total spin of level, λ serial number, c Sub-reaction channel;
E_x/MeV is level position of level in ^{16}O system; WI-exp is experimental value of width in Ref. or
WI-cal is ftting value of width in this wrok RAC2015; Err.sys is systematical error evaluated in this wrok RAC2015;
Err.Sta is statiscal error of experimental data; σ is the mean square error of evaluated value.

Width -$_{J^\pi_\lambda C}$	Ex/ MeV	WI-exp/ MeV	WI-cal/ MeV	Err.Sys %	Err.Sta %	σ / 1.00	Width -$_{J^\pi_\lambda C}$	Ex/ MeV	WI-exp/ MeV	WI-cal/ MeV	Err.Sys %	Err.Sta %	σ / 1.00
'WI011'	6.049	1.8700E-02	1.8713E-02	0.03	27.92	0.01	'WI234'	11.491	3.0000E-08	2.6702E-08	1.00	16.67	0.49
'WI012'	6.049	6.8564E-12	6.8562E-12	0.03	7.29	0.01	'WI235'	11.491	2.0000E-08	2.0730E-08	1.00	50.00	0.05
'WI021'	12.059	1.5000E-03	1.5394E-03	1.00	33.33	0.06	'WI236'	11.491	2.9000E-08	2.9089E-08	1.00	24.14	0.01
'WI031'	14.032	2.0000E-01	2.2586E-01	1.00	7.50	1.02	'WI237'	11.491	5.0000E-09	1.8549E-09	1.00	50.00	1.06
'WI041'	15.062	1.6600E-01	7.0028E-01	0.03	18.07	2.89	'WI241'	13.002	2.5100E-01	2.1955E-01	1.00	13.88	0.69
'WI111'	7.117	6.1950E-03	6.7573E-03	0.00	8.01	0.71	'WI242'	13.002	7.0000E-07	6.4421E-07	1.00	28.57	0.20
'WI112'	7.117	5.3500E-08	5.2892E-08	0.00	5.83	0.14	'WI248'	13.002	5.0000E-04	6.0123E-04	1.00	50.00	0.24
'WI114'	7.117	3.0000E-13	2.9403E-13	1.00	33.00	0.05	'WI249'	13.002	1.5000E-03	2.4959E-03	1.00	13.33	0.94
'WI115'	7.117	4.6000E-11	2.5845E-11	0.03	21.74	1.56	'WI251'	15.900	6.0000E-01	9.2729E-01	1.00	12.00	1.95
'WI116'	7.117	5.5000E-13	1.8240E-13	1.00	33.00	1.37	'WI252'	15.900	4.0000E-07	5.4092E-07	1.00	12.00	1.49
'WI121'	9.447	3.8800E-01	2.9700E-01	1.00	16.00	1.28	'WI311'	6.130	5.7444E-03	5.7302E-03	0.03	34.04	0.01
'WI122'	9.447	1.5600E-08	3.3040E-07	1.00	50.00	1.28	'WI312'	6.130	2.4740E-11	2.4753E-11	0.03	22.63	0.01
'WI126'	9.447	1.4000E-09	1.4652E-09	1.00	50.00	0.07	'WI321'	11.356	8.0000E-01	6.6407E-01	1.00	12.50	1.14
'WI127'	9.447	5.4000E-09	5.0480E-09	1.00	50.00	0.10	'WI325'	11.356	1.0000E-08	9.1993E-09	1.00	50.00	0.11
'WI131'	12.442	1.0148E-01	1.6066E-01	5.83	0.99	3.00	'WI326'	11.356	1.0000E-08	9.9945E-09	1.00	50.00	0.01
'WI132'	12.442	1.1000E-05	4.0174E-05	1.00	37.90	1.28	'WI327'	11.356	1.0000E-08	9.1095E-09	1.00	50.00	0.14
'WI134'	12.442	1.2000E-07	7.2571E-08	1.00	33.33	1.31	'WI331'	13.256	9.4870E-02	1.3609E-01	1.00	14.58	1.35
'WI135'	12.442	7.0000E-08	5.8541E-08	1.00	43.33	0.38	'WI335'	13.256	8.0000E-06	9.3170E-06	1.00	50.00	0.25
'WI137'	12.442	1.3000E-07	1.4205E-07	1.00	38.33	0.17	'WI338'	13.256	2.1450E-02	7.2092E-02	3.88	3.88	3.01
'WI138'	12.442	3.0000E-05	3.5172E-05	1.00	6.67	1.47	'WI339'	13.256	1.5000E-03	1.4893E-03	1.00	5.58	0.09
'WI139'	12.442	1.4500E-03	6.8941E-05	1.82	2.10	3.32	'WI341'	13.356	2.4870E-02	2.4311E-02	1.00	34.58	0.05
'WI141'	13.122	1.3908E-01	7.7924E-02	9.80	1.51	2.99	'WI345'	13.356	8.0000E-06	8.0945E-06	1.00	16.30	0.05
'WI142'	13.122	3.2000E-05	2.7777E-04	1.23	15.62	3.01	'WI348'	13.356	2.5000E-03	1.8018E-03	1.00	30.48	0.87
'WI144'	13.122	2.6000E-07	7.2274E-08	1.00	34.62	1.97	'WI349'	13.356	9.8000E-04	1.1963E-02	3.59	5.58	2.03
'WI145'	13.122	4.0000E-07	3.1887E-07	1.00	50.00	0.22	'WI351'	14.656	7.5000E-01	8.2926E-01	1.00	26.67	0.25
'WI147'	13.122	1.4000E-06	1.4007E-06	1.00	28.57	0.01	'WI411'	11.357	2.7000E-02	2.6944E-02	1.00	11.11	0.01
'WI148'	13.122	9.8000E-04	8.6510E-04	1.00	12.26	0.74	'WI412'	11.357	5.6000E-14	5.4349E-14	1.00	35.71	0.06
'WI149'	13.122	1.0500E-01	1.7407E-02	1.24	2.26	2.69	'WI415'	11.357	4.7000E-10	4.7796E-10	1.00	22.00	0.06
'WI151'	17.542	1.8200E-01	2.4705E-01	1.00	34.51	0.50	'WI416'	11.357	6.2000E-08	6.1890E-08	1.00	9.68	0.01
'WI211'	6.917	2.6714E-02	2.6679E-02	0.00	8.01	0.01	'WI421'	12.092	2.8000E-04	2.8125E-04	1.00	17.86	0.01

'WI212'	6.917	9.8500E-08	1.0068E-07	0.00	3.09	0.47	'WI425'	12.092	3.1000E-09	3.8869E-09	1.00	41.94	0.41
'WI214'	6.917	2.7000E-11	2.6971E-11	0.03	11.11	0.04	'WI426'	12.092	2.5000E-09	2.3470E-09	1.00	24.00	0.18
'WI215'	6.917	9.0000E-12	9.2595E-12	0.03	33.00	0.39	'WI431'	13.856	7.5000E-02	7.8738E-02	1.00	9.33	0.35
'WI221'	9.850	6.8500E-04	1.1918E-03	0.03	16.10	1.79	'WI441'	17.040	5.6700E-01	5.2885E-01	1.00	10.58	0.45
'WI222'	9.850	5.7000E-09	5.6770E-09	0.03	10.50	0.04	'WI511'	14.660	6.7100E-01	6.7407E-01	1.00	1.64	0.17
'WI224'	9.850	1.9000E-09	1.8215E-09	1.00	21.05	0.14	'WI521'	16.910	7.0000E-01	6.9962E-01	1.00	2.24	0.01
'WI226'	9.850	2.2000E-09	3.1096E-09	1.00	18.18	1.42	'WI611'	14.860	7.0000E-02	6.9604E-02	1.00	11.00	0.04
'WI231'	11.491	7.2000E-02	6.8333E-02	1.00	15.50	0.23	'WI621'	16.295	4.2200E-01	4.2155E-01	1.00	3.30	0.01
'WI232'	11.491	6.1000E-07	6.0960E-07	1.00	3.28	0.01							

7.9. The comparison for RAC2013 and (Schürmann2012)

In the previous analysis works the **(Schürmann2012) can be regards as the best one.** The Ref. (Schürmann2012) think that the E1 and E2 multipoles in ETRT have different energy dependencies, one must have an independent and precise information on each multipole for an extrapolation to E≈0.3MeV, so only the secondary data of E10 and E20 multipoles were used for the R-matrix analysis, which were got from Legendre polynomials fitting for experimental AD of ^{12}C (α, γ_0) ^{16}O. The analysis of RAC2013 (RAC2013 is identical to RAC2014) explain that it is feasible to use the standard R-matrix formulae to describe all the ED about the ^{16}O system formed by $\alpha+^{12}C$ simultaneously. It can be seen in the 7th, 8th and 9th chapters that near all types of ED and almost of data have been described perfectly. The comparison between calculated value and ED about ST, $S_{G.S}$ and $S_{6.05}$ in paragraph 7.1, 7.3 and 7.4 show that the agreement situation of Katsuma2012, NACREII2013, Kunz2002 have defects evidently as a whole. Brune1999, Hammer2005 and Ouelbsir2012 fitted the data of $S_{G.S}$ in lower energy region only, did not fit any data of ST. But the ED of ST and $S_{g.s.}$ are the most relative and the most important observables for determining of astrophysical SF. So the follow sections involve the comparison and illustration about the fitting situation of RAC2013 and (Schürmann2012) in detail, not mention about other groups except **Kastuma2008.**

It should be indicated the fitted data of SE10 involve Dyer1974, Gialanella2001 and Roter1999 only, it looks very well for the agreement between ED and calculated value as a whole. The information in detail is that, The E<2.7 MeV energy region is the most important region for determining the energy-dependency of SF in extrapolation energy region. In which there are 105 data points. For comparing with calculated SE10 of RAC2013, there are 62 higher points , 53 lower points, the ratio of number is 62:53=1.17; Schuermann2012 has 69 higher points, 46 lower points, the ratio of number is 69:46≈1.5. So the fitting situation of RAC2013 looks better than the fitting situation of Schürmann2012. The calculated values about SE20 of Schürmann2012 are lower than these of RAC2013 systematically in extrapolation energy region. The calculated SE10 of Kastuma2008 is much lower than all ED of SE10.

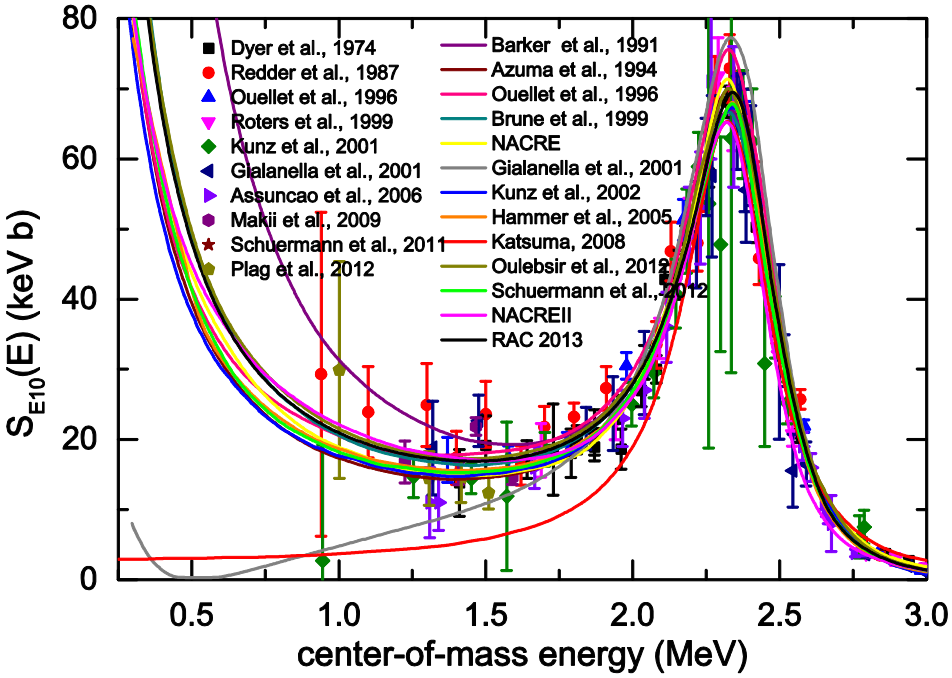

Fig. S7.9-A shows the ED and calculated values of SE10 for E< 3.0 MeV.

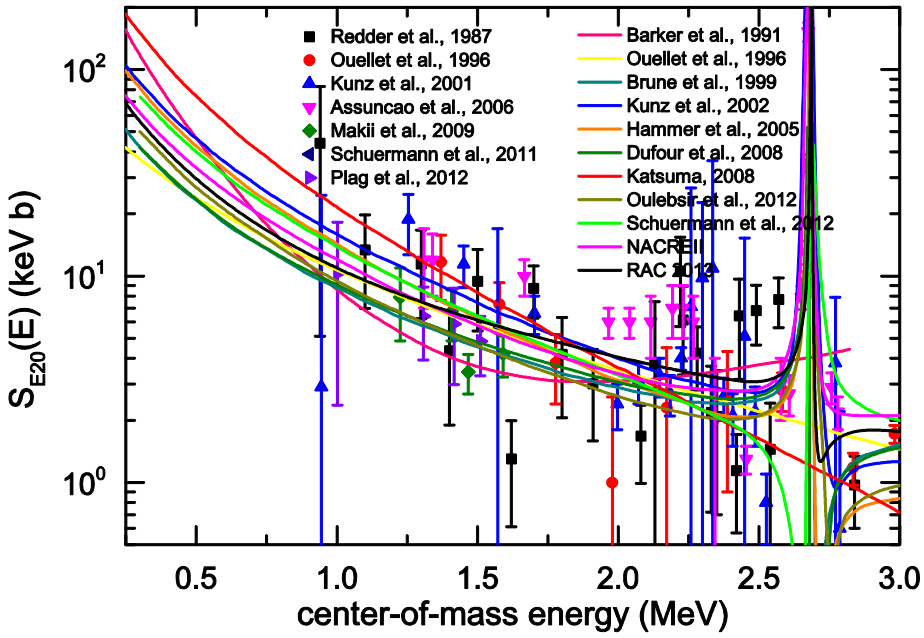

Fig. 7.9-B the ED and calculated values of SE20 for E<3.0 MeV.

It should be indicated that even though RAC13 did use the ED of SE20, but the agreement between fitting values and ED-set looks very well. The information in detail is that there are 70 data points for E<2.7 MeV, comparing with calculated SE20 of RAC2013, there are 35 higher points , 35 lower points, the ratio of number is 35:35=1; for (*Schuermann2012*) there 48 higher points, 22 lower points, the ratio of number is 48:22≈2.2. The main reason caused this very larger difference is that RAC2013 by fitting more types of ED, especially including the 66 groups AD of $^{12}C(\alpha, \gamma_0)^{16}O$, to determine the interference property of 2^+_2(higher left side and lower right side) , describe

the resonance characteristic of 2^+_2 accurately. The property is identical with those given out by Brune1999, Kunz2002, Hammer2005, Dufour2008, NACREII2013 and Ouelbsir2012. But the interference property of 2^+_2 given out by Schuermann2012 is reverse (lower left side and higher right side), on then left side of the resonance, its calculated values are lower than ED of SE20 evidently, it did not describe the resonance characteristic of 2^+_2 properly . The calculated values about SE20 of (Schuermann2012*)* are higher these of RAC2013 systematically. The calculated SE20 of Kastuma2008 has much higher diviation from all ED of SE20, it looks too higher for E<1.5 MeV.

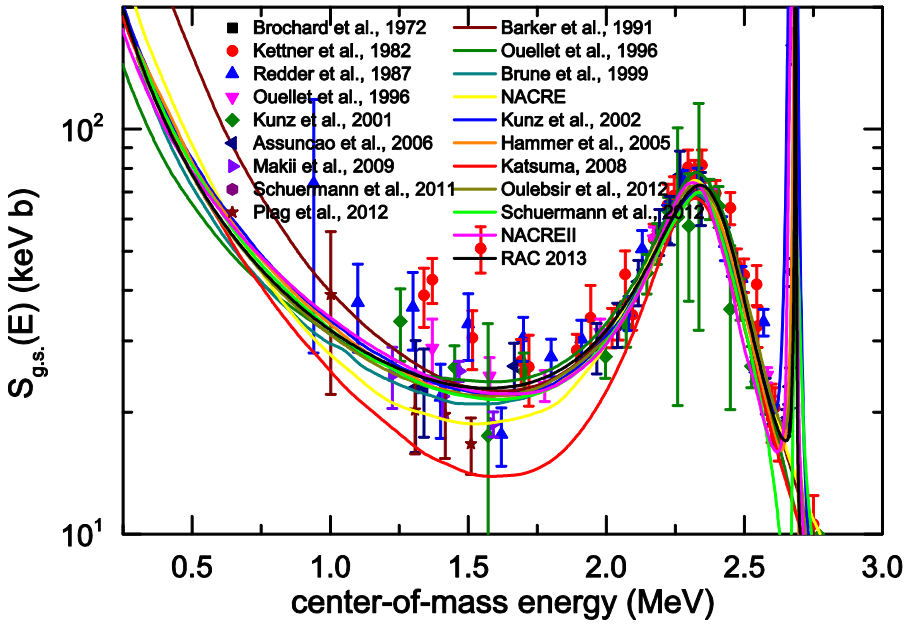

Fig. 7.9-C the ED and calculated values of S $S_{G.S.}$ For E<3.0 MeV. It can be seen that on the left side of resonance the calculated $S_{G.S.}$ of RAC2013 and Schurmann2012(block line and green line) are identical with each other, but on the right side the calculated SE10 of RAC2013 is higher than that of Schurmann2012, and it is more close to ED and SE10. The calculated $S_{G.S}$ of Kastuma2008 is much Lower than all ED of $S_{G.S}$.

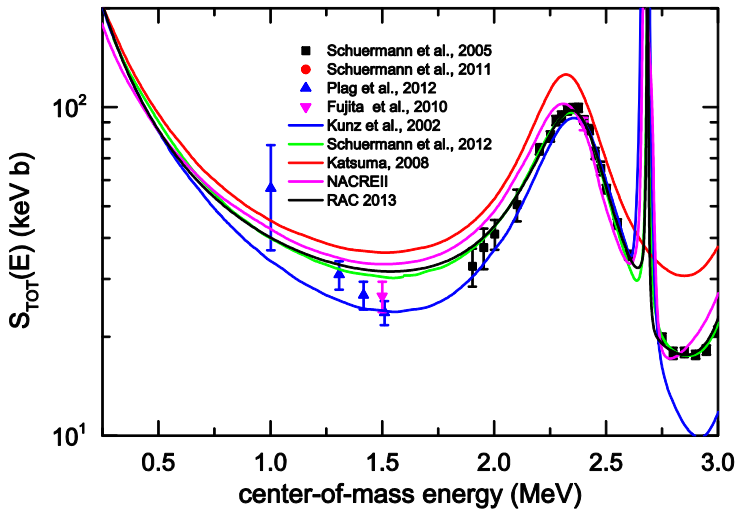

Fig. 7.9-D shows the ED and calculated values of ST for E<3.0 MeV. It can be seen that both fitting situations look very good for RAC2013 and Schurmann2012, no evident difference can be seen. On the left side of resonance the calculated ST of RAC2013 and Schurmann2012 has a little difference.

In summary, for the fitting situation about SE10, SE20, $S_{G.S}$ and $S_{6.05}$, RAC2013 is much better than that of Schurmann2012; for the fitting situation about $S_{6.13}$, $S_{6.92}$ and $S_{7.12}$, RAC2013 is close to that of Schurmann2012. The conclusion should be that the fitting values and extrapolation values down to lower energy region of RAC2013 have more reliable experimental basis, it should be more close to the expected values. The calculated STOT of Kastuma2008 is much higher than all ED of STOT.

8. The final result

8.1. The calculation of SF and Covariance matrix of ^{12}C (α, γ) ^{16}O at given 660 energies

The procedure for calculation of SF and Covariance matrix of ^{12}C (α, γ) ^{16}O as follow.

A. Using the best R-matrix parameter set P to calculate SF at given 660 energies (row *Y*)

B. Using the best R-matrix parameter set P and formula S4.3.10 for error propagation to calculate the Covariance Matrix of P

$$V_P = (D^+ V^- D\ )^{-1} \qquad \text{S 4.4.10}$$

Where, D refer to Sensitive matrix for database B relative to P, V is Covariance Matrix of B, superscript -1 refer to reverse Matrix. V_P Is positive definite through the test.

C. Using V_P and formula S4.3.12 to calculate Covariance Matrix of calculated SF V_y, its diagonal element just is the standard deviation, the root of standard deviation is the standard error.

$$V_Y = D\, V_P D^+ \qquad \text{S4.4.12}$$

Where, D refer to the Sensitive matrix for the calculated SF relative to P, the $V_{\bar{y}}$ is positive definite through test.

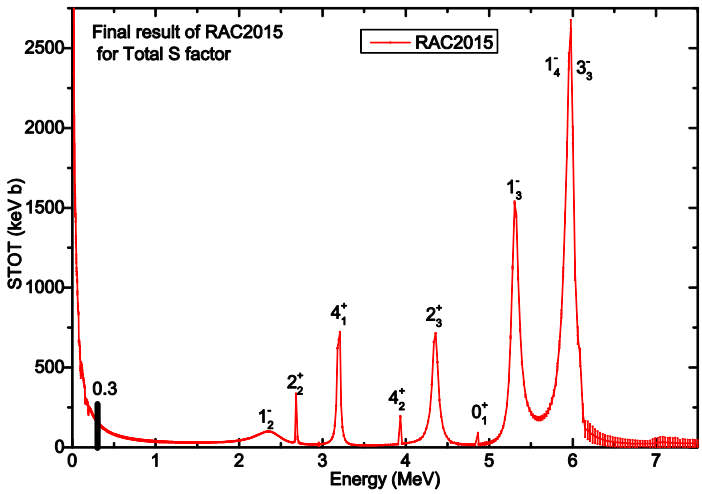

Fig. S8. 1. Calculated STOT and its Standard Deviation for ^{12}C (α, γ) ^{16}O at 660 energis.

8.2. Error analysis for STOT

8.2.1. The experience expression for error propagation

These can be observed intuitively in Fig. S8.1 that the standard error of STOT is very small for 1.5<E<6.5 MeV, the standard error of STOT is much larger for E≥7 MeV. In the extrapolate energy region 0.2≤E≤0.6 MeV the standard error of STOT is about 4.5 %(APE. Table 3).The error propagation law for covariance fitting in in Global model has been studied in detail by Ref. (Chen2003). An experience expression to describe standard error propagation was deduced as follow:

$$U_j^c = U_j^d * K_j * T * \sqrt{M}/\sqrt{N} \qquad \text{(S8.2.1)}$$

Here, *j* refer to the type of dataset or whole database, *M* the number of parameters, *N* the total number of the data, T the mean of absolute value of all sensitive matrix elements, it close to the mean of χ^2 and K_j is a positive real number which is called 'error propagation factor', U_j^c is the error of calculated value, U_j^d is the mean value for standard error of database.

According to the error propagation law the error of final calculated STOT are depending on some elements as follow.

A. The more the number of points of database N, the less the error of calculated value, the error is inverse proportion to the root of N approximately.

B. The more the data points of a unit energy (Data density DD), the less the error of calculated value. The larger the DD of a local energy region, the less the error for that region.

C. The less the error of data, the less of calculated value. The relative error is direct proportion to the mean relative error of database.

D. The less the χ^2 of optimized object function, the less the error of calculated value.

E. The less the number of adjusted parameters (m), the less the error of calculated value. The error is direct proportion to the root of m approximately.

F. The less the error of adjusted parameter, the less the error of calculated value.

G. The less the sensitivity of parameter related to data, the larger the error of calculated value.

A problem existed before 10 years ago is that the the error of calculated value in a globle fitting for a light neuclear system with R-Matrix is to lower to belive. Ref. (Chen2003) cast 3 years to explain and resolve this problem. In order to let the given error of calculated value is large enough to be much reliable, when to calculate the covariance matrix of calculated values, some non-adjusted parameters be taken as adjusted parameters, subsequently the relative error is increased about 1.0%. The errors of STOT listed in Appendix V. Table 5 are up-limit of errors. The main elements which have large influence to the error of calculated value include the number of adjusted parameters M, the number of points of database N, the mean primary error of data, the averaged value ofχ^2. The practical situation of this work are as follow, the number of parameters used in calculation M is about 160, the number of points of database N is about 4400, the mean primary error of data is about 8%, the averaged value of χ^2. is about 1.5. With these numbers to calculate the final error, that is ER $\approx \sqrt{160}/\sqrt{4400}$*8% ≈12.7/64.8*8%*1.5≈2.4%. So the estimated values are these as follow. In the energy region in which the data density (DD) near the mean value (DM) for whole database the ER≈2.4%; in which the DD larger than the DM the ER<2.4% (2<E<3 MeV); in which the DD larger than the DM the ER>2.4% (E<1.5 MeV or E≥6. MeV).

The RAC has been used to produce the neutron standard cross sections ^{6}Li (n, α) and ^{10}B (n, α), that process has accumulated much successful experience, methods, the obtained accurate (ERROR<1%) results which have been used to produce the Neutron Standard Cross Section of IAEA (22, 23). In this work the successful Code, experiences and methods are used to study the STOT of ^{12}C (α, γ) ^{16}O, the obtained results are reliable certainly.

8.2.2. The fitting quality examine and testing positive definite for covariance matrix

For an ideal pure statistic sample, if a variable Y is the function of variance of X_i, the distribution of Y is χ^2 distribution. The objective function for Ordinary least squares χ_i^2 just is a this kind of Y. the mean value χ^2 =1 is the most probable value. The χ_i^2 series obey χ^2 distribution. For a non-ideal statistic sample, e.g., the systematic error component is rather larger, if a variable Y is the function of the linear combination of $(X_i+a)^2$, the distribution of Y is uncertain until now. The objective function for general least squares χ_i^2 just is a this kind of Y, but it is a function of covariance. By now, the value of χ^2 is used to judge the quality of fitting, the smaller theχ^2, the better the fitting.

There is a theory criterion to judge the quality of fitting, that is the covariance of ED and its evaluated value must be positive definite, otherwise they have not physical mean. The code RAC13 test the positive definite for each sub-Dataset at first. The final output show that the covariance of the best parameter set and all SF set is positive definite. This explain the final results are reliable.

For the multi-channels and multi-levels R-Matrix analysis, the majority of data points which have rather larger χ^2 are the data points which located in the negative interference energy region. These data points usually have very small principal values, and have very small contribution to the practical physical quantity, it is very hard to get accurate measured value, but the nominal error is not larger. Even though by making PPP and Letts modification for them, χ^2 of them are larger than the meaning of χ^2 far away. So only use the value of χ^2 to judge the quality of fitting is not good enough. The most institutive and reliable method is to make comparison by drawing pictures, to make macro-judgment and micro-judgment simultiouslly. For the values distribute in 1 to 2 order of magnitude, using linear coordinate is good to show the difference between data and evaluated value, for the values distribute in more 3 order of magnitude, using logarithmic coordinate is good to show the difference between data and evaluated value.

8.3. Calculating the Reaction Rate (RR) of ^{12}C (α, γ) ^{16}O

Using the calculated value of STOT and its covariance matrix (APE. Table 3)and the formula used in(Kunz2002)as (10.1, 10.2) to calculate the RR of ^{12}C (α, γ) ^{16}O:

$$\langle v\sigma\rangle = (\frac{8}{\pi\mu})^{1/2}(\frac{1}{kT})^{3/2}\int_0^\infty S(E)\,exp(-\frac{E}{kT}-\frac{b}{E^{1/2}})dE \tag{8.3.1}$$

$$b = \frac{(2\mu)^{1/2}Z_1Z_2e^2}{\hbar} = 0.989\mu^{1/2}Z_1Z_2\ \ (\mathrm{MeV})^{1/2} \tag{8.3.2}$$

When to make integrating, the energy region E=0.01 to 11.25 MeV is divided with 660 nodes and different step length, the error propagation formulae(S4.4.10) are used to calculate the RR and its standard error. The formulae expressed with row and matrix are listed as follow.

$$R_j = (R_1, R_2, R_3, \cdots R_n),\quad j=1, 2, \cdots\cdots n \tag{8.3.2}$$

$$S_i = (S_1, S_2, S_3, \cdots S_m),\quad i=1, 2, \cdots\cdots m \tag{8.3.4}$$

$$D_{S_i}^{R_j} = \sum_{I=1}^{i=m} C^j{}_i S_i,\ \cdots\ j=1, 2, \cdots\cdots n, i=1, 2, \cdots\cdots m \tag{8.3.5}$$

$$D_{S_i}^{R_j}\ V_R = D_S^R\ V_S\ D_S^{R\text{-}} \tag{8.3.6}$$

D_S^R Is the n × m sensitive matrix for RR relative to STOT.

$$D_{S_i}^{R_j} = \partial R_j/\partial S_i = C^j{}_i \tag{8. 3.7}$$

$$C^j{}_i = (\frac{8}{\pi\mu})^{1/2}(\frac{1}{kTj})^{3/2} * exp\left(-\frac{Ei}{kTj}-\frac{b}{Ei^{1/2}}\right) * \Delta i \tag{8. 3.8}$$

$$V_{R,kl} = \sum_{o=1}^{o=m} * \sum_{p=1}^{p=m} * D_{S,ko}V_{S,op}D_{S,pl}^{R\text{-}} \tag{8. 3.9}$$

The essence of RR calculated with STOT is experimental value, so named $RR_{exp.}$

If the off-diagonal elements of covariance matrix are considered or ignored, the calculated principal RR are identical with each other, but the STD of calculated RR will have obvious difference. Fig. S8.3-A shows the relative errors in two situations mentioned above. Two relative errors are very close for $T_9 \leq 1$, at T_9=0.2, it is about 5.5% for both situations, but for $T_9 \geq 3.5$ have rather larger difference. Fig. S8.3-B shows that at T_9=0.2, the contribution of E10 is about 60% of total, the contribution of E20 is about 35%, the contribution of other transitions is about 2.5%.

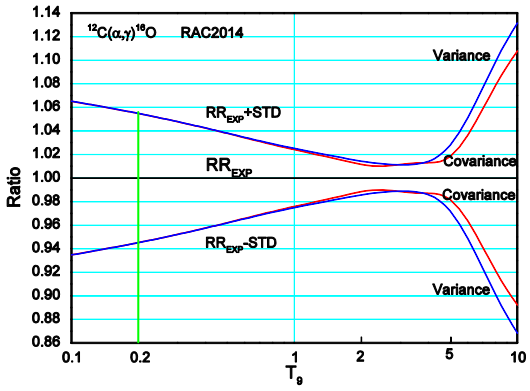

Fig. S8.3-A. The calculated RR with Covariance (red line） or with Variance (blue line) respectively

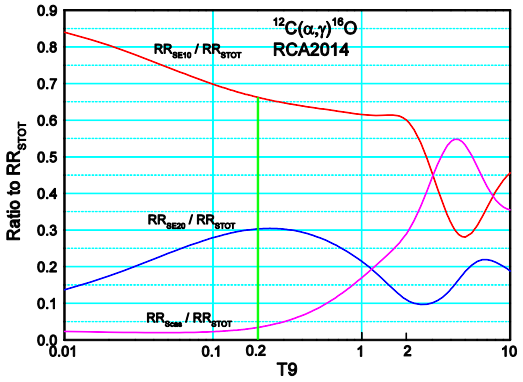

Fig. S8.3-B. the Contributions from E10, E20 and other kinds of transitions.

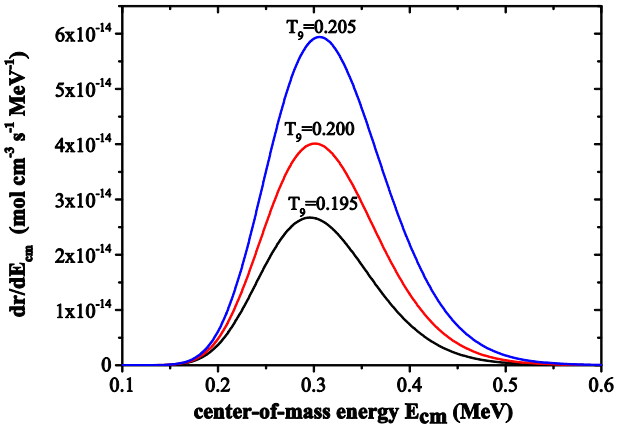

Fig. S8.3-C. RR/MeV at T_9=0.195, 0.200, 0.205

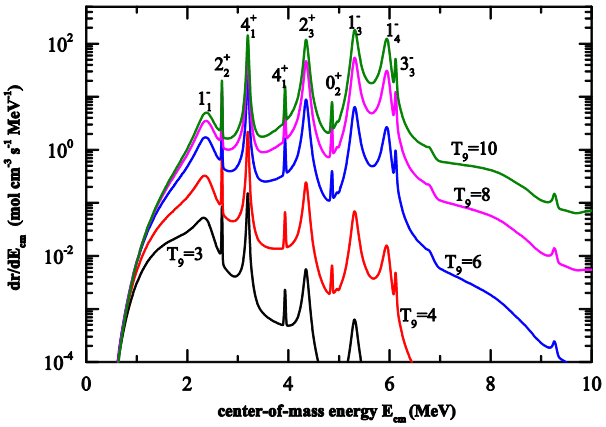

Fig. S8.3-D. RR/MeV at T_9=4, 6, 8, 10

Fig. S8.3-C show the reaction rate over unit energy MeV (RR/MeV) at T_9=0.195, 0.200, 0.205. Its integrated RR is R=5.09666E-015, 7.80818E-015 and 1.17926E-014 [mol.cm^{-3}.s^{-1}] respectively. For the Gamow window of T_9=0.2($GW_{0.2}$), the center energy E≈0.3 MeV, WH≈0.14MeV, The bottom energy region(0.15 to 0.55 MeV)is far away from the lowest energy(E=0.8 MeV) in which have direct ED. The RR in $GW_{0.2}$ are produced mainly by the interfering effect of the bound states $1^-_1$and 2^+_1 with the scattering states. In addition, it can be seen that in $GW_{0.2}$ the RR has dramatic changes with the T changed, When the T changed only 2.5% the RR changed 50%. This explain that to describe the dependence of STOT on energy accurately is very important, In order to get the accurate description the key element is to use the width data of the bound states, that is $\gamma^2_{\alpha 1}, \gamma^2_{\alpha 2}, \Gamma^1_\gamma$ and Γ^2_γ.

Fig. S8.3-C show the RR/MeV at T_9= T_9=4, 6, 8, 10. It can be seen that with the increasing of T the contribution of 1^-_3 and1^-_4 increasing, for T_9≥6 they become the ones of main ingredients of RR. This explain that only if the Ed in these two levels have been fitted perfectly, the accurate RR will be obtained.

The popular analytic formulae in (Kunz2002) (8.3.10) is used to fit the calculated RR with STOT (named RR_{exp}), and then obtain the coefficients a0 to a11 for the analytic expression. The calculated RR with the analytic expression is named RR_{ana}. It was found that if the denominate $T_9^{3/2}$ in the third item is replaced by T_9^2 as (8.3.11), will get more accurate results (Fig. S8.3-F), which make the total χ^2 decreased 50% at least.

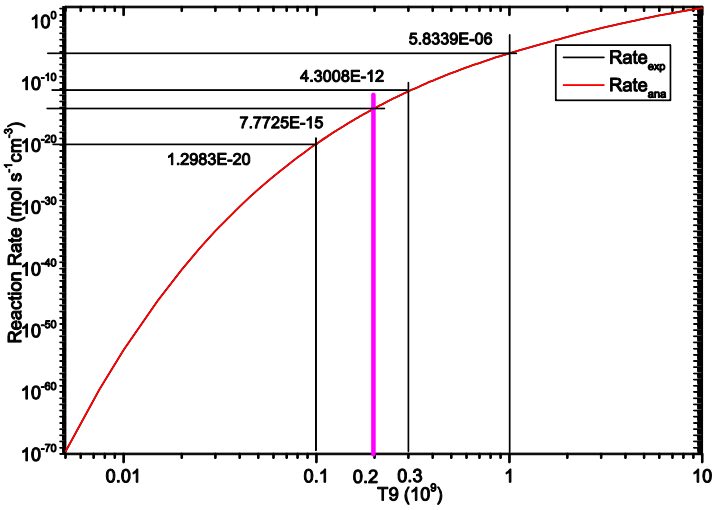

Fig. S8.3-E. Reaction Rate of RR_{ana} and RR_{exp} with absolute values

$$RR(T_9) = \frac{a_0}{T_9^2\left(1+a_1 T_9^{-2/3}\right)^2} exp\left[-\frac{a_2}{T_9^{1/3}} - \left(\frac{T_9}{a_3}\right)^2\right] + \frac{a_4}{T_9^2\left(1+a_5 T_9^{-2/3}\right)^2} exp\left(-\frac{a_6}{T_9^{1/3}}\right) + \frac{a_7}{T_9^{3/2}} exp\left(-\frac{a_8}{T_9}\right) + \frac{a_9}{T_9^{2/3}}\left(1 + a_{10} T_9^{1/3}\right) exp\left(-\frac{a_{11}}{T_9^{1/3}}\right) \quad 8.3.10$$

$$RR(T_9) = \frac{a_0}{T_9^2\left(1+a_1 T_9^{-2/3}\right)^2} exp\left[-\frac{a_2}{T_9^{1/3}} - \left(\frac{T_9}{a_3}\right)^2\right] + \frac{a_4}{T_9^2\left(1+a_5 T_9^{-2/3}\right)^2} exp\left(-\frac{a_6}{T_9^{1/3}}\right) + \frac{a_7}{T_9^2} exp\left(-\frac{a_8}{T_9}\right) + \frac{a_9}{T_9^{2/3}}\left(1 + a_{10} T_9^{1/3}\right) exp\left(-\frac{a_{11}}{T_9^{1/3}}\right) \quad 8.3.11$$

Fig. S8.3-E. The absolute value RR_{exp} (Exp-fitted value) and the absolute value RR_{ana} (Analytic expression). The pictures show clearly the RR for $T_9<1$ is very small, but it is the most interesting data for astrophysical study. The RR_{ana} is very close to the RR_{exp}, it is very hard to see the difference between them

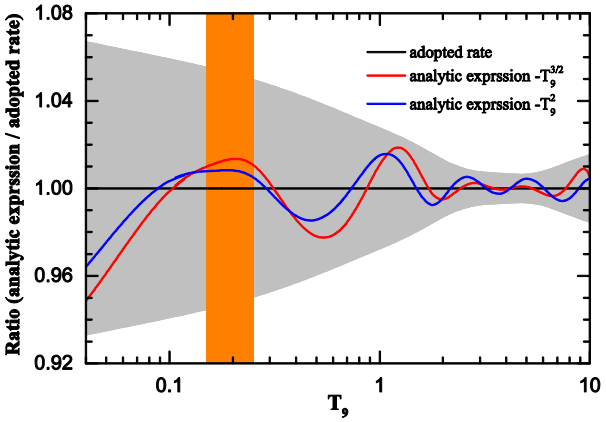

Fig. S8.3-F. Ratio for RR_{ana}/ RR_{exp} (Adopted rate)

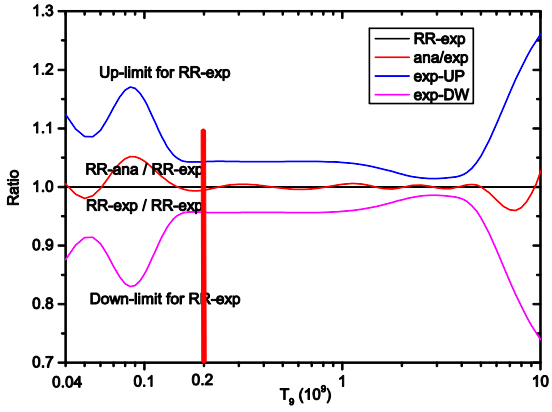

Fig. S8.3-G. Ratio for the RR_{ana} / RR_{exp}

Fig. S8.3-F. show that for $T_9 \leq 1.5$ region, the blue line (T_9^2 used) is more close to 1.0 then the red line ($T_9^{3/2}$ used) is, especially at the Gamow of $T_9=0.2$, which is the most interesting region for astrophysical study; for $T_9 \geq 2$ region, the red line ($T_9^{3/2}$ used) is more close to 1.0 then the blue line (T_9^2 used) is, but which is not the most interesting region for astrophysical study. So using T_9^2 (8.3.11) has practical benefit.

Fig. 8.3-G show the ratio for RR_{ana} to the original calculated value RR_{exp} with STOT., the process for fitting RR_{exp} is a kind of pure mathematical alternation, not is to fitting real statistic physical observable quantity, the variance of fitted value is very small, the most of

them is less 0.5%, it cannot be used as the STD of the final recommend value RR_{ana}. The STD**2 of RR_{ana} equal to the variance of the RR_{exp} plus the variance of fitted value. In Fig. 8.3-G, RR-High=RR_{exp}*(1+Error), RR-Low=RR_{exp}*(1-Error).

The Table 8.3.1 list the parameters a0 to a11 for analytic expression formula (8.11). By using formula (8.11) and the parameters a0 to a11 in Table 8.3.1 the corresponding RR in Fig.8.3.-G can be reproduced for T_9=0.01 to 10. The RR_{ana} in Appendix. V. 2. Will be got.

Table 8. 3.1 Parameters a0-a11 for analytic expression (8. 3. 10)

a0=0. 48918133D+9	a1=0. 39883022D+0	a2=0. 31680499D+2	a3=0. 40000000D+3	a4=0. 32415511D+16	a5=0. 31752720D+2
a6=0. 42114768D+2	a7=0. 13730056D+4	a8=0. 27350673D+2	a9=0. 23870846D+12	a10=-0. 99911666D+0	a11=0. 37586740D+2

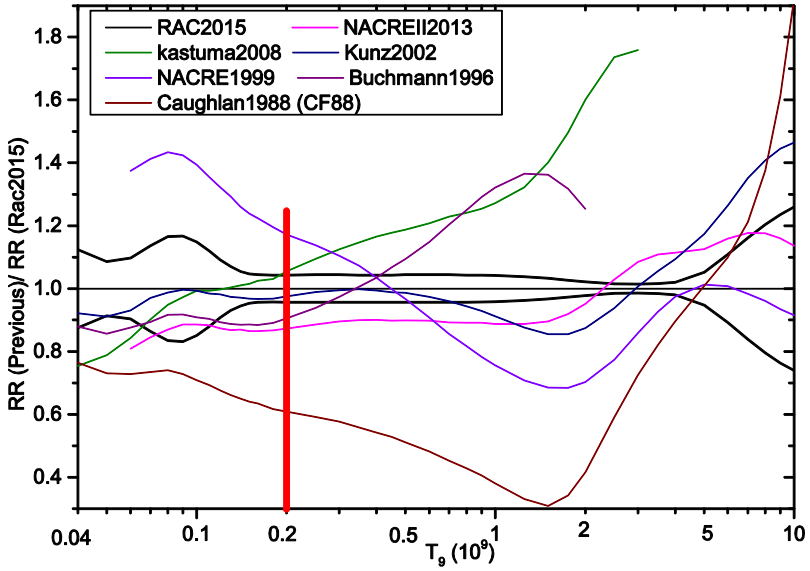

Fig. S8.3-I. The ratio for previous published RR to the calculated RR_{exp} of RAC2015

Fig. S8.3-I **Ratio for Reaction Rate (RR) of Previous Works over the RR of RAC2015.** T_9=0.2 corresponding to E=0.3 MeV is the most interesting temperature for nuclear astrophysics (Gamow window). The black lines represent the RR of RAC2015 with up-limit and down-limit, at T_9=0.2 RR is 7.77±0.32 mol.s^{-1}.cm^{-3} with error 4.4%. Schurmann2012 is a good analysis work, but did not publish its RR. Extended Data Table. 1.2 shows the minimum error of previous RR is 18% in Katsuma2008, but Katsuma2008 is a kind of pure theoretical calculation, the agreement between its theory values and ED is not good，refer to SI-Chapter 7. The RR of Kunz2002 is very close to RAC2015 for T_9<4, but it looks too higher for T_9>5, this is due to the data about $S_{G.S}$ of Brochard1975 did not be used in fitting, its error is 32.7%. NACREII2013 looks too lower for T_9< 2, but looks too higher for T_9> 4.5, the error is 25%. NACRE1999 looks too higher for T_9< 0.3. Bachmann1996 looks good for T_9<0.5, but looks too higher for T_9> 0.8, and its error is very larger (71%). The CF88 is a kind of groundbreaking work with very larger error (>80%). In summary, the RR of RAC2015 has the most reliable experimental basis and the best accuracy comparing to all previous works.

8.4. Conclusion

Three effective approaches for using global fitting and a powerful Code RAC2015 have been developed to get a set of unique, reliable, accurate and self-consistent S factors and Reaction Rate of ^{12}C (α, γ) ^{16}O. In present at E=0.3 MeV the best total S factor is 159.7 keV b with error < 5.9%, the **reaction rate is 7.82±0.44 mol.s^{-1}.cm^{-3}** with error < 5.7%. The principal value and error of STOT depend on the data-base used principally, on the width information of bound states (1_1^{-1} *and* 2_1^{+1}) especially, on the cross sections of ^{12}C (α, γ) ^{16}O for E<1.5 MeV very sensitively. Keep going to make new measurements about these data will have possibility to improve the accuracy of

STOT. As long as the data-base and the global fitting are good enough, the obtained S factors will be very well. Anyway we believe that if you want to resolve the problem about ^{12}C (α, γ) ^{16}O you have to do with the ways created in this paper.

Appendix

Appendix I. The fitting and comparison for ^{12}C (α, γ0)^{16}O and ^{12}C (α, α) ^{16}O

In [Dyer1974] the values of σ_{E1} and σ_{E2} were extracted by a least-squares fit to the measured AD by taking into account the interference between $E1$ and $E2$ transitions according to the relation given by

$$W(\theta_\gamma, E) = 1 - Q_2 P_2(cos\theta_\gamma) + \left[\frac{\sigma_{E2}(E)}{\sigma_{E1}(E)}\right] \times \left[1 + \frac{5}{7Q_2P_2(cos\theta_\gamma)} - \frac{12}{7Q_4P_4(cos\theta_\gamma)}\right] +$$
$$6/5[\sigma_{E2}(E)/\sigma_{E1}(E)]^{1/2} cos\Phi(E) \times \left[Q_1P_1(cos\theta_\gamma) - Q_3P_3(cos\theta_\gamma)\right] \quad \text{S-AP.I.1}$$

where *Pk*(cos $\theta\gamma$) are the Legendre polynomials, *Qk* are the experimental attenuation coefficients of the γ detectors and $\Phi(E)$ is the phase difference between the *d* and *p* wave and a Coulomb phase given as

$$\Phi(E) = \delta_2\,(E) - \delta_1\,(E) + \arctan(\eta/2) \quad \text{S-AP.I.2}$$

Here, η being the Somerfield parameter and δi being the nuclear phase shifts. Therefore a fit to a radiative AD in ^{12}C(α, γ)^{16}O is largely sensitive to the ratio of the E1 and E2 cross sections as phase shifts are known from elsewhere (elastic scattering). This 1^- and 2^+ levels formula has been got popular application.

In previous works, when the two channel and multiple levels R-Matrix formula were used to fit the E10 or E20, multiple coherent combination designed in advance were used, the taking which kind of coherence between energy levels was selected by the size of χ^2. e.g., 16 types of combinations were used in the literature [Hammer2005].

Where, α refer to particles pair, f_α is the Coulomb phase shift. As you seen about AD, each level, each reaction channel are all correlated, ignoring anyone item will get approximate results. In our work the strictly theoretical calculation was applied to fitting all the data available, the coherence between energy level is automatically determined by the procedures for fitting ED, the procedure did not suffer from any a priori and subjective elements. For determining the coherence property between energy levels, the AD of ^{12}C (α, α) ^{12}C and ^{12}C (α, γ_0) ^{16}O are the most sensitive elements.

Appendix.I.1. the AD of ^{12}C (α, γ0)^{16}O according to each group

Fig. APP. I.1. 2 to Fig. APP. I.1. 8 display all the AD of ^{12}C (α, γ_0)^{16}O calculated in RAC2015 and corresponding experimental data according to each group.

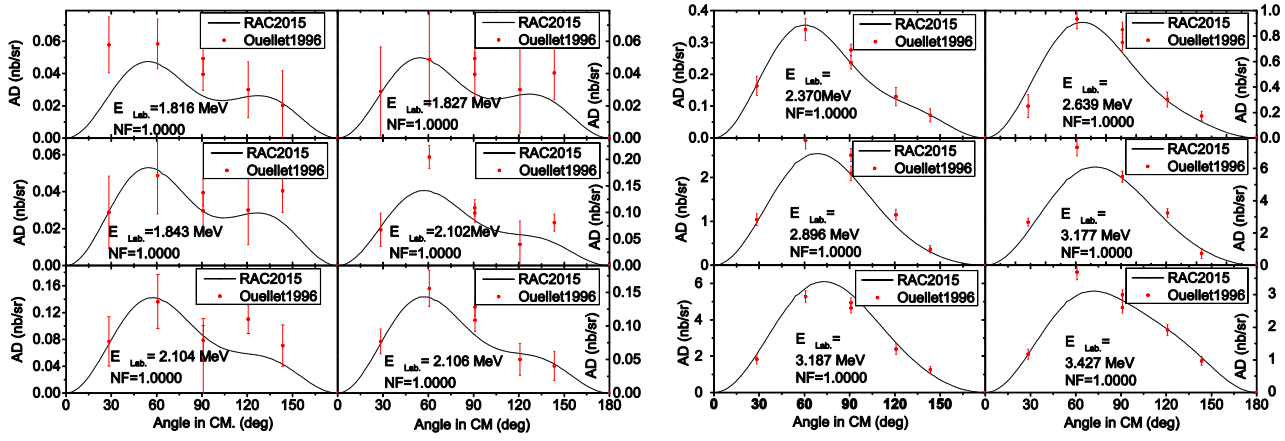

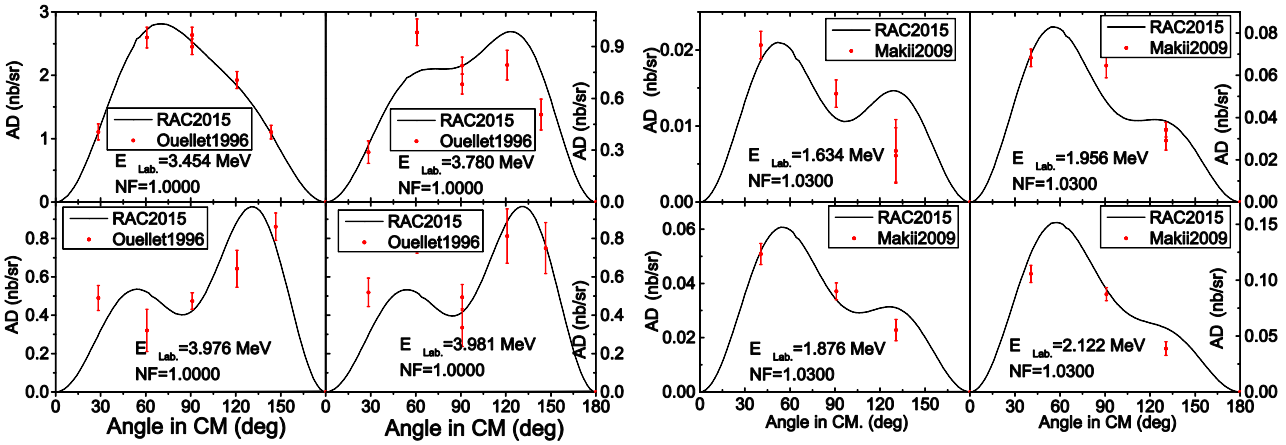

Fig. APP. I.1. 2. Fitting situations about the AD of ^{12}C (α, γ_0) ^{16}O for Ouellet1996 and Makii2009 in RAC2015, which are absolute value with NF=1.00 and 1.03 respectively. These two data sets play a key function to make unique evaluated values for the AD of ^{12}C (α, γ_0) ^{16}O.

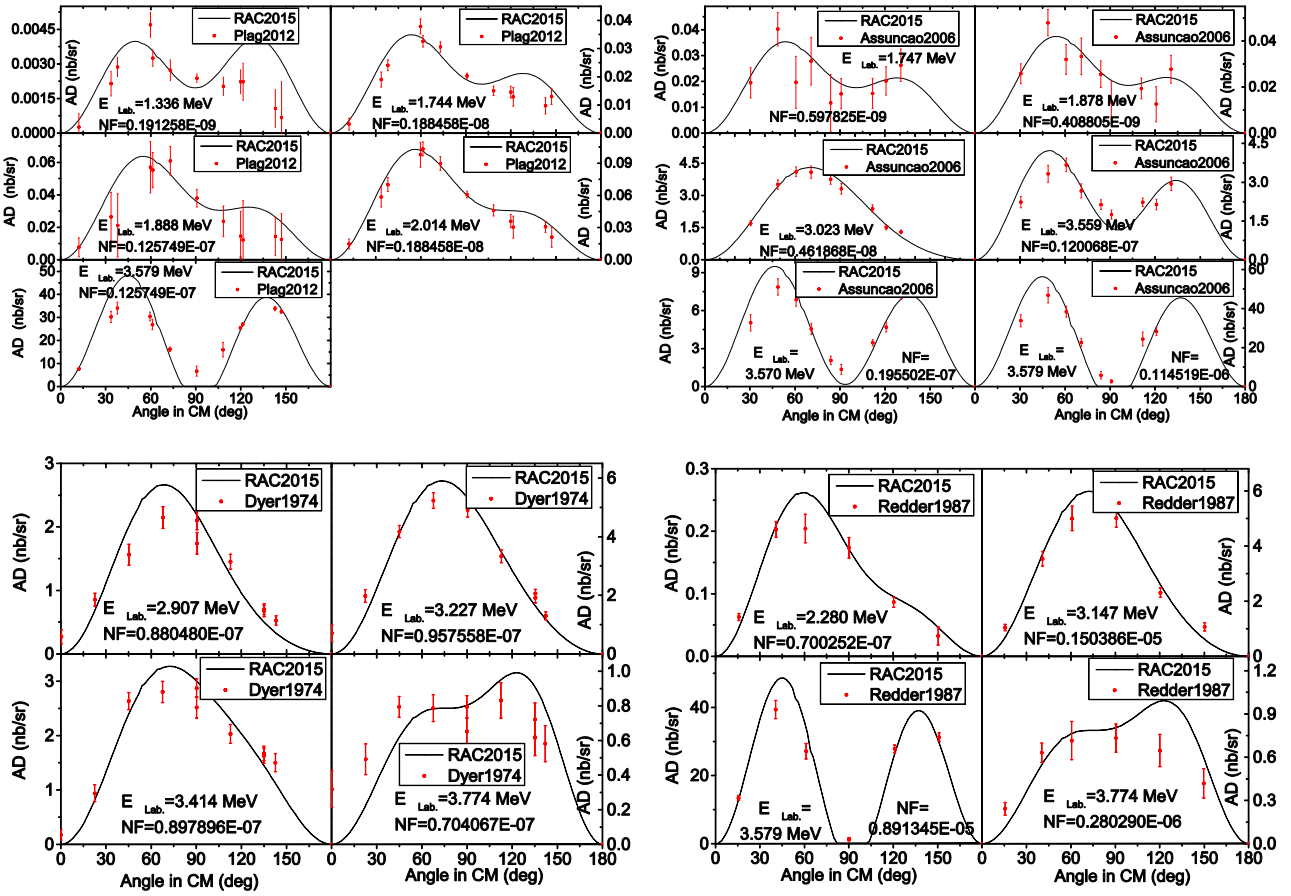

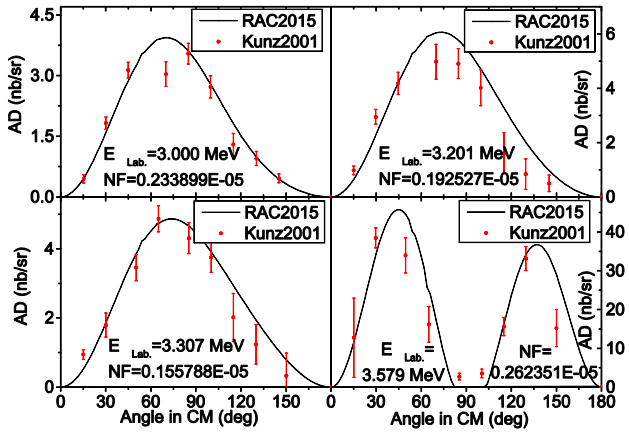

Fig. APP. I.1. 3. Fitting situations about the AD of ^{12}C (α, γ_0) ^{16}O for Plag2012, Redder1987, Kunz2001, Assuncao2006 and Dyer1974 in RAC2015, which are relative value with different scaling factors NF. At $E_{Lab} \approx 3.2\pm0.2$ MeV the contribution of 1^- play dominant function, the figure is a single peak with a bulge near 70^0 ; At $E_{Lab} \approx 3.570$ to 3.579 MeV the contribution of $2^+_{2,\ 3.574}$ play dominant function, the figure is a double peaks with a dent near 90^0, the calculated values near 90^0 are less than 10^{-7} keV b. The data set of Plag2012 at lower energy region is very sensitive to the STOT at E=0.3 MeV.

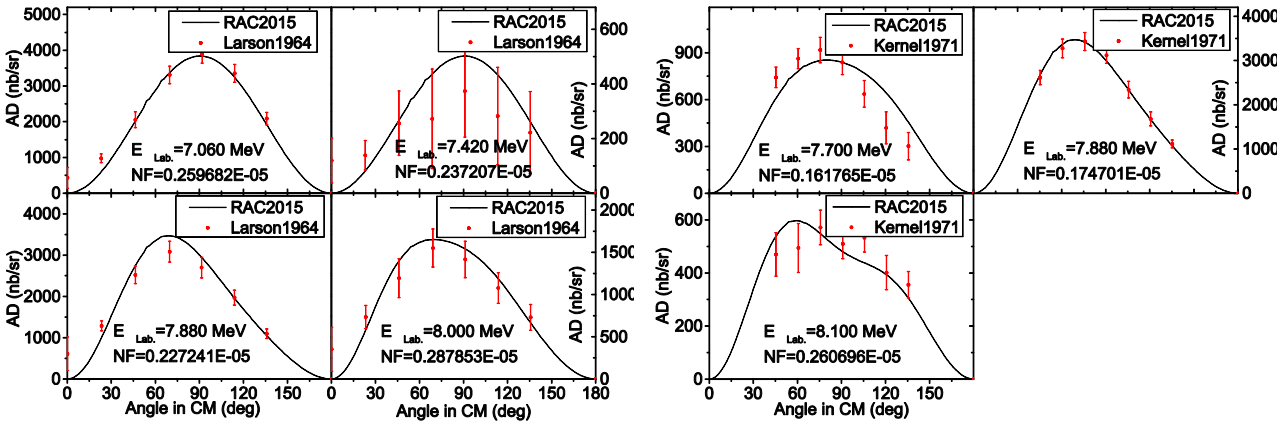

Fig. APP. I.1. 4. Fitting situations about the AD of ^{12}C (α, γ_0) ^{16}O for Larson1964 and, Kernel1971 in RAC2015, which are relative value with different NF. These two data sets play a key function to make unique evaluated values for the AD of ^{12}C (α, γ_0) ^{16}O at higher energy region. More figures are put in SI.

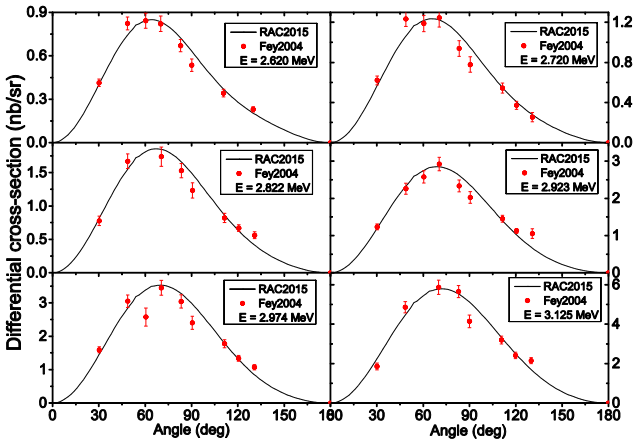

Fig. AP.I. 5. The AD of AGDA of Fey2004

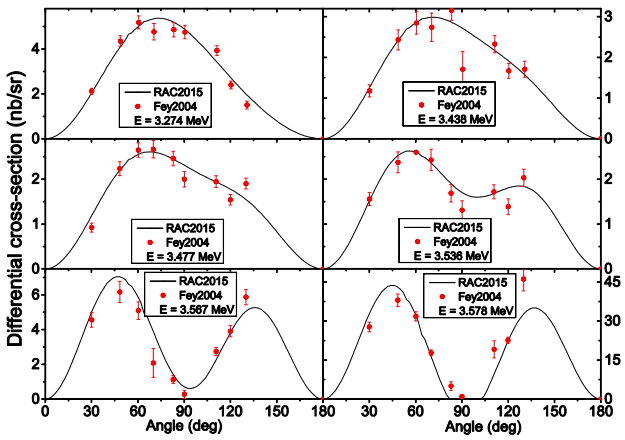

Fig. AP.I. 6. The AD of AGDA of Fey2004

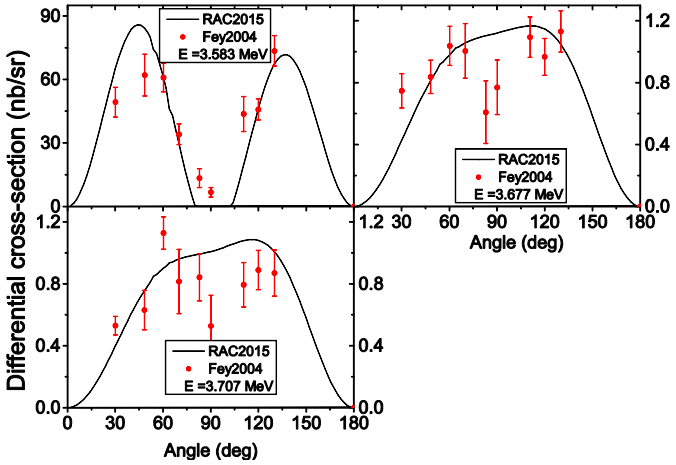

Fig. AP.I. 7. The AD of AGDA of Fey2004

Fig. AP.I. 8. The AD of AGDA of Ophell976

Fig. AP.I. 5 to Fig. AP.I. 7 display the AD of ^{12}C (α, γ0)^{16}O in（Fey2004） according to each group.In each group the energy increasing order. The Scaling factors for every energy are listed in the Expended Data Table 2.

Appendix.I.2. Comparison for the AD of ^{12}C (α, γ_0)^{16}O follow the increasing order of energy.

Fig. APP. I.2.-0 to APP. I.2.-5 show the fitting situation (RAC-Lane-2013) for the AD of ^{12}C (α, γ_0)^{16}O at 65 energies in E=1.002 to 6.075, follow the increasing order of energy. In the Fig. the fitted value and data at one energy are represented by the same color curve and symbol. The data value in vertical coordinate is the normalized absolute value, the scaling factor or normalizing factor have precision less than 1%.

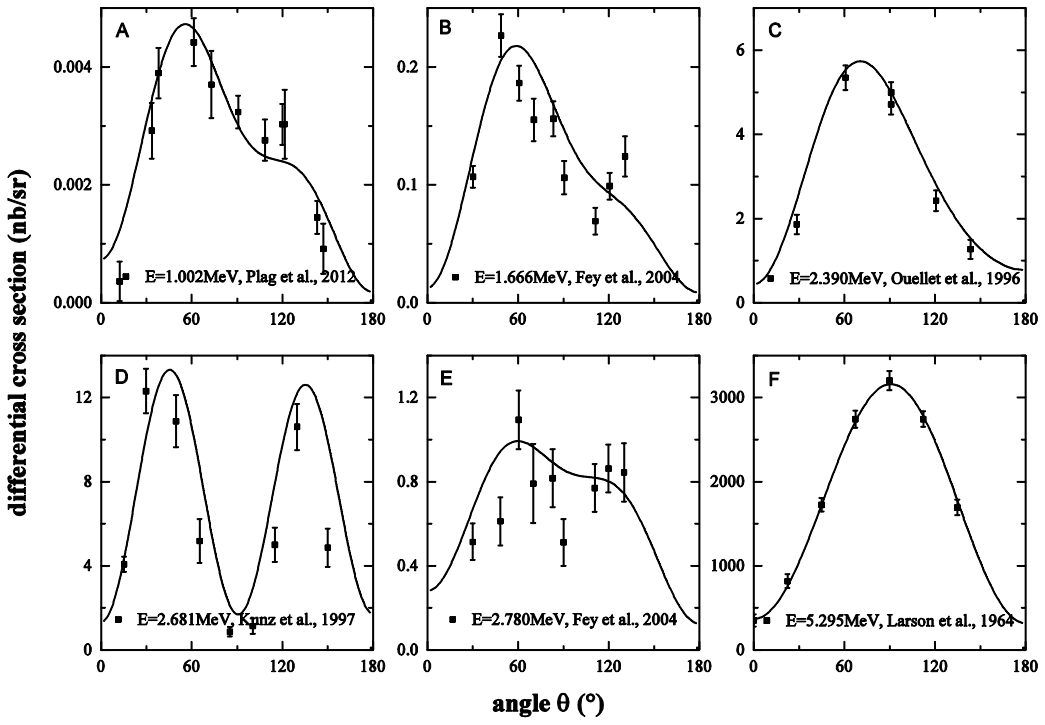

A 26.87/10.71=2.1 B 25.65/5.37=4.8 C 85.72/3.126=27.4

D 8.625/12674=0.0007 E 4.737/1.635=2.9 F 1492/0.1624=9187

Fig. APP. I.2.-0 Characteristic angular distribution of ^{12}C (α, γ_0)^{16}O at 6 energies

Fig. APP. I.2.-0 show the characteristic AD of ^{12}C (α, γ_0)^{16}O at six energies. The numbers in picture are the ratio for E10/E20, which is the value of calculated cross section of E10 transition over E20 transition. At the resonance peak of 1^-_3（Fig. F） in which the E10 play dominant function, the characteristic AD looks like ‘a single peak with a symmetry axis of θ=90^o ’. Due to the ratio is extremely large (E10/E20=9187), Fig. F is regard as the characteristic picture for pure E10 transition. At the resonance peak of 2^+_2 （Fig. D）in which the E20 play dominant function, it looks like ‘a double peaks with symmetry axis of θ=90^o’. Due to the ratio is extremely small (E10/E20=0.0007), Fig. F is regard as the characteristic picture for pure E20 transition. For the energies at which both E10 and E20 have significant contributions（Fig. A，B）, the shape of AD is the combination of E10 and E20, it looks like ‘a double bulges with topes at 60^o and 130^o separately’; the higher the amplitude of left bulge, the more contribution from E10. If the E10 is the main composition, it looks like ‘a single peak with a non-symmetry axis ’ （Fig. C）. The higher the amplitude of right bulge, the more contribution from E20 (Fig. C).The AD of ^{12}C (α, γ_0)^{16}O imply the ratio information about E20/E10，The AD of ^{12}C (α, γ_0)^{16}O at 65 energy points show the variation trend that the ratio E10/E20 changed with the change of energy. This work fitted these original AD, relative integrated data and other data accurately, the calculated E10 and E20 must be reasonable. It’s these data play dominate function to determine the SF.

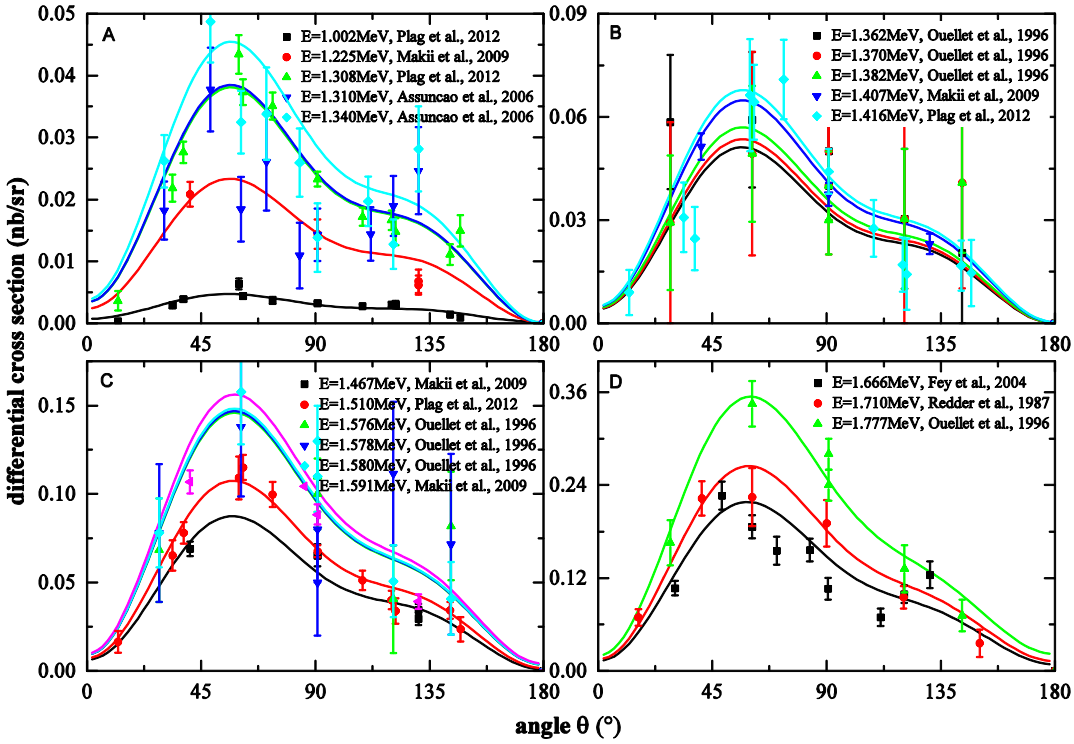

Fig. APP. I.2.-1 Angular distribution of ^{12}C (α, γ_0) ^{16}O in 1.002 to 1.591 MeV

Fig. APP. I.2.-1-（A，B）show that in the energy region E=1.002 to 1.416 MeV both E10 and E20 have significant contribution, The AD of 1.002 and 1.308 MeV have smallest error, they play a key function. Fig. APP. I.2.-1-（C，D） show that both E10 and E20 have significant contribution, Along with the energy increasing and close to the peak position of 1^-_2, the contribution of E10 increase. Fig. APP. I.2.-2 show that in the energy region E=1.965 to 2.480 MeV the contribution of E10 play dominate function, the contribution of E20 is very small, because these energies locate on the peak region of 1^-_2.

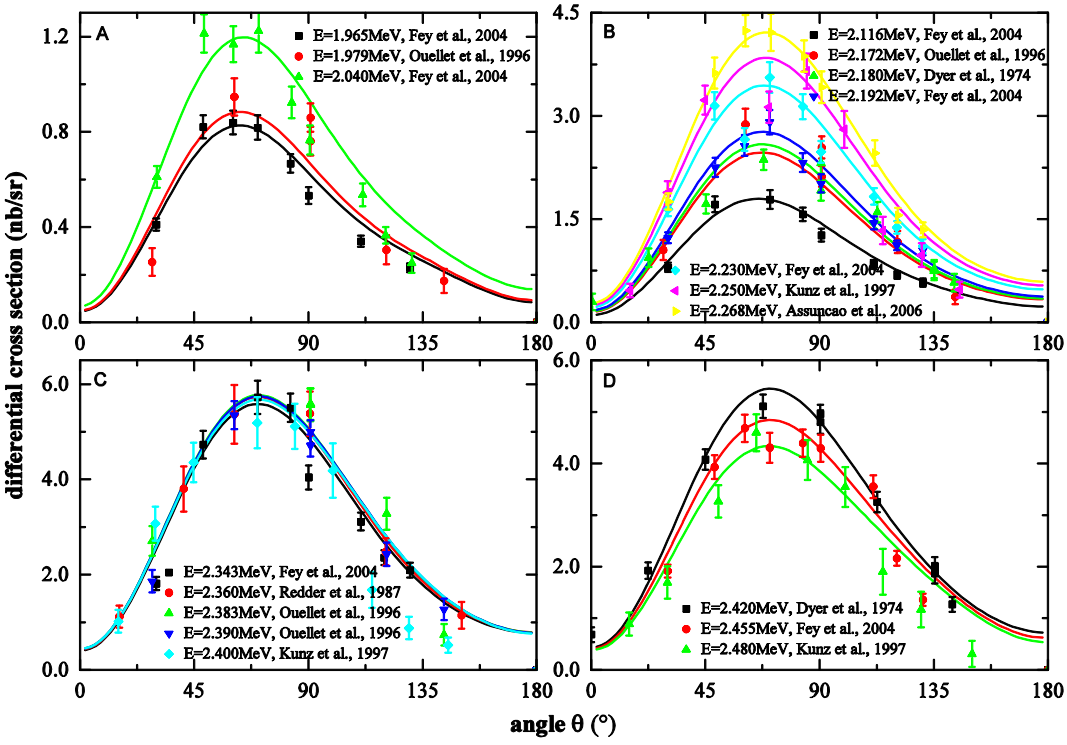

Fig. APP. I.2.-2 Angular distribution of ^{12}C (α, γ_0) ^{16}O in 1.965 to 2.480 MeV

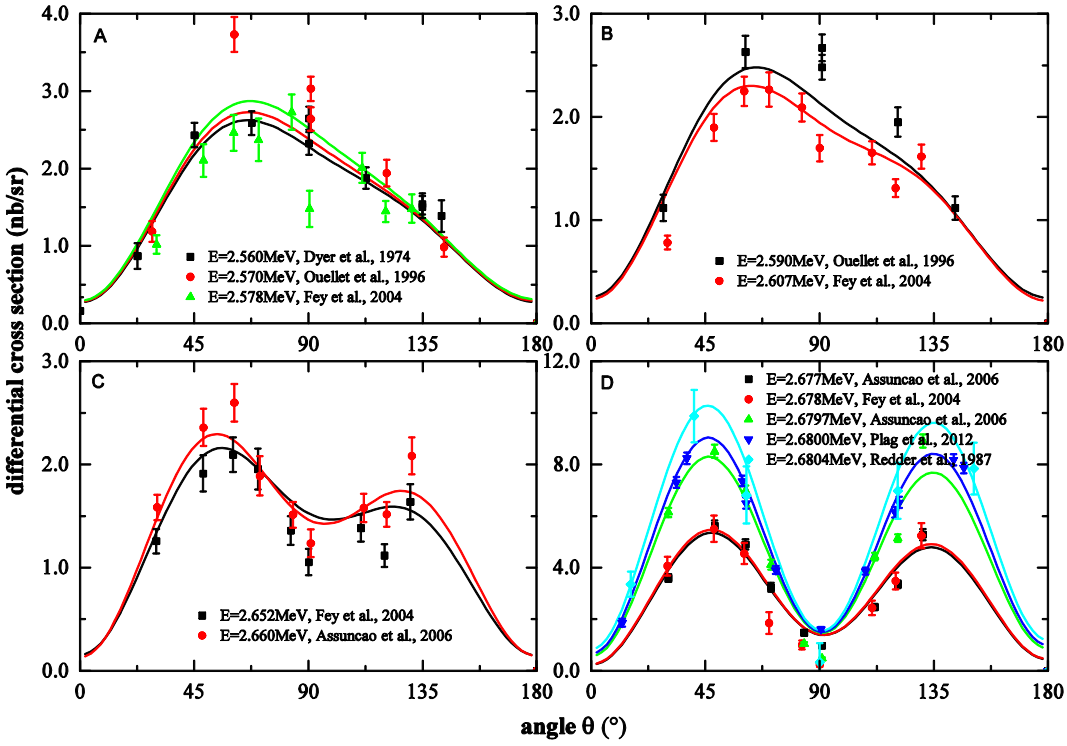

Fig. APP. I.2.-3 Angular distribution of ^{12}C (α, γ_0)^{16}O in 2.560 to 2.6804 MeV

Fig. APP. I.2.-3（A，B）show that along with the increasing of energy and gradually closing to the peak position of 2^+_2, the left bulge which characterize the contribution of E20 appear out. Fig. APP. I.2.-3（C）show that in the energy region which near peak position of 2^+_2, the contribution of E20 become significant. Fig. APP. I.2.-3（D）show that on the peak region of 2^+_2, the contribution of E20 play dominate function. The maximum cross section is at 2.6804 MeV, it means that it is the energy of the level 2^+_2.

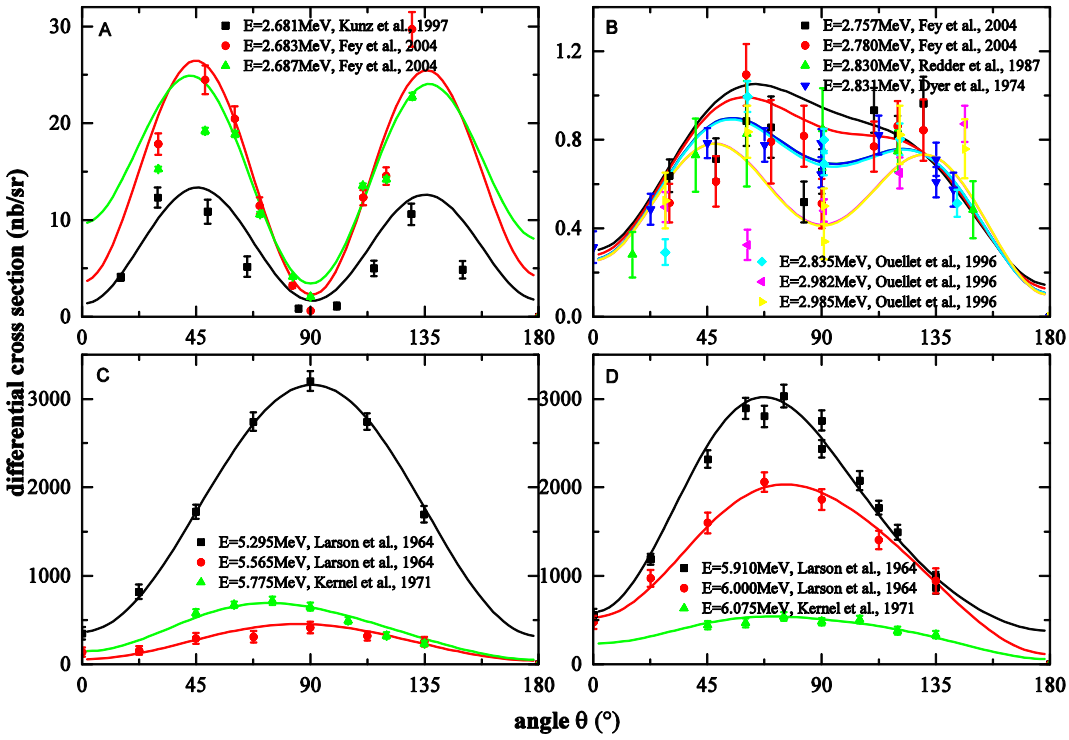

Fig. APP. I.2.-4. Angular distribution of ^{12}C (α, γ_0)^{16}O in 2.681 to 6.075 MeV

In Fig. S8. 1-4（A）the shape of AD explain the contribution of E20 play dominate function，the energies should locate in the peak region of 2^+_2. But their original nominal energies are larger than the up-limit of the peak energy, the fitting results are very bad always. If change the interference property of 2^+_2 artificially, the fitting situation for the AD of the 3 energies become better a little, but the fitting situation for the AD of the energies in Fig. S8. 1-become very bad. If shift the energies with -0.1 MeV, then the AD in all energies will get perfect fitting. The careful study demonstrate that the AD of the energies from 2.560 to 2.6875 MeV play dominate function for determining the interference property (positive for left side, negative for right side)。 If change the sign of the γ reduced width amplitude of 2^+_2 artificially, let the interference property change conversely as 'negative for left side, positive for right side', then the fitting situation become very bad for all AD mentioned above. But, by the process of adjusting parameter and fitting data automatically the related parameters and interference property restrain to original situation. The systematical study show that the total influence to $S_{0.3}$ produced by the interference property of 2^+_2 not larger than ±1.5 KeV b. Fig. S8. 1-4（B）shows that along with the energy increase and far away from the peak position of 2^+_2, the contribution of E10 increases and the contribution of E20 decreases.

The 3 energies in Fig.APP. I.2.-4（C）locate in the peak region of 1^-_3 level, the contribution of E10 play dominate function. The AD at 5.295MeV looks like 'a single peak with a symmetry axis of θ=90^o ', which is called the characteristic picture of pure E10. The 3 energies in Fig.APP. I.2.-4（D）locate in the peak region of 1^-_4 level. These 6 AD of $^{12}C(\alpha,\gamma_0)^{16}O$ and the integrated cross section in the same energy region[Brochard1975] play key function to determine the SF in high energy region.

In summary, this work make accurate analysis for the 65 AD of ^{12}C (α, γ_0)^{16}O, the shape and absolute values are reasonable in physics, subsequently the deduced SE10 and SE20 must be reasonable.

Appendix.I.3. Comparison for excitation function of ^{12}C (α, γ_0)^{16}O.

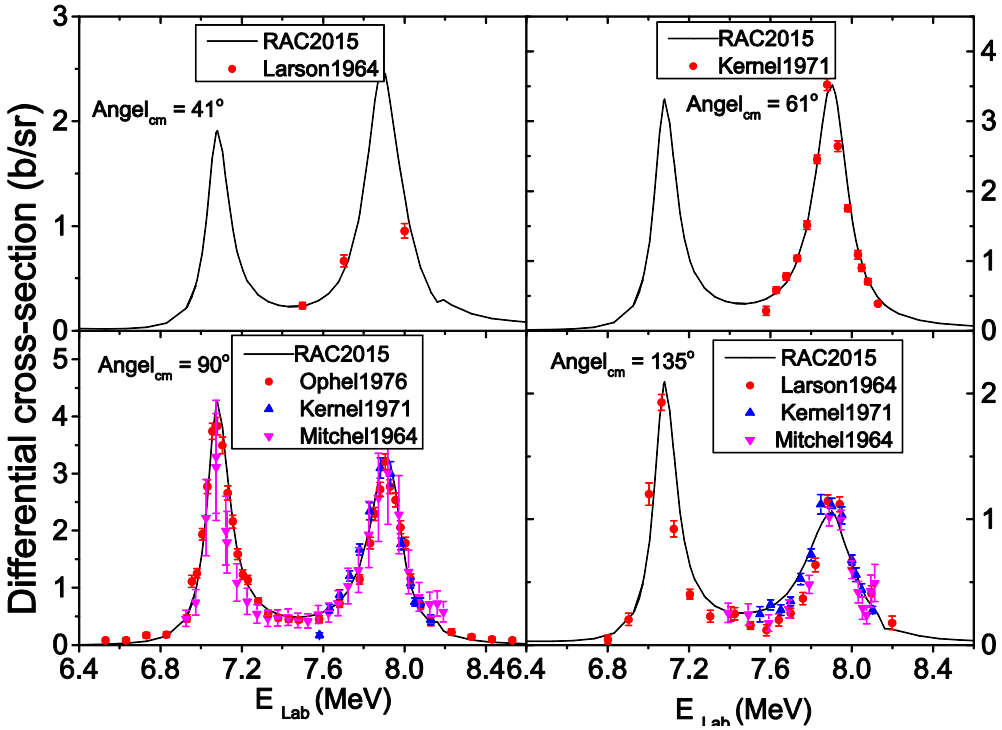

Fig. AP.I.3. 1. Shows the exciting function of ^{12}C (α, γ_0)^{16}O. The data of Ophell976 for θ_{CM}=90° are absolute value, it's NF=1.722. All Other data are relative values.

Appendix.I.4.Comparison for AD of ^{12}C (α, α) ^{12}C

Fig. S-AP.I.4.1 to Fig. S-AP.I.4.15 show the AD of ^{12}C(α, α)^{12}C at 83 energies, which include 51 energies of (*Plag1987*), 22 energies of (*MOrri2009*), 6 energies of (*Brunn2009*), they are absolute values, the NF fixed as 1.0; Also include 4 energies of (*Tischhauser2009*), which is relative values, the NF is 2.6748. In the Figs, lines refer to fitted values, samples refer to ED. The energy is from 1.00 to 7.5 MeV, which cover the all resonance peaks.

About the shape of AD of ^{12}C (α, α) ^{12}C, the characteristic of Coulomb scattering is 'very higher amplitude at small angle', this is very obvious for low energies region (E <1.87 MeV). The contribution of S wave (ι_α=0) is uniform distribution, it is a key element for describing the AD of ^{12}C (α, α) ^{12}C. But, in the scattering energy region less than 7.5 MeV only exist one very narrow 1^+, so the contribution of 1^+ mainly come from the distant levels, this exhibit the importance of considering complete level set. General speaking, the most of AD of ^{12}C (α, α) ^{12}C are fitted very well, especially in energy region in which no competition from the Alpha spectrum exist. This explain the deduced width of (α, α) are reliable.

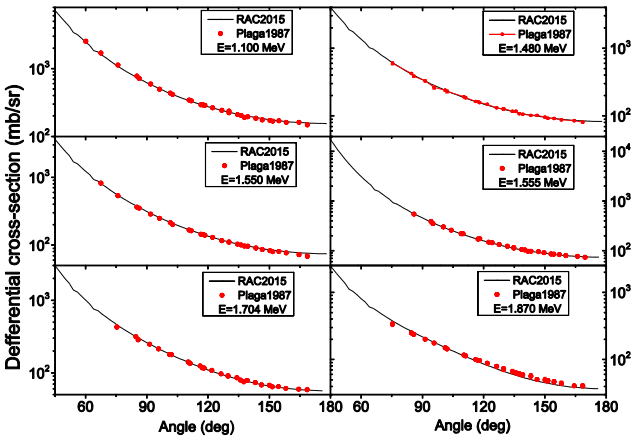

Fig S-AP.I.4.1 Fits to the AD of $^{12}C(\alpha,\alpha)^{12}C$ in (Plaga87)

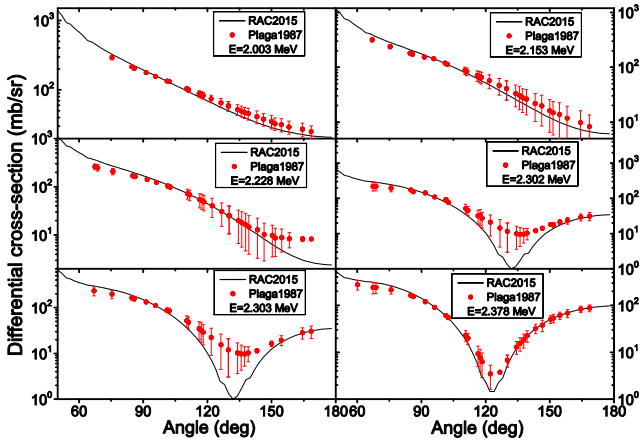

Fig S-AP.I.4.2 Fits to the AD of $^{12}C(\alpha,\alpha)^{12}C$ in (Plaga87)

In Fig S-AP.I.4.1 the 6 energies located the region in which the competition from Alpha spectrum is very weak, the agreement of data and fitted value is very well. In Fig S-AP.I.4.2 the 6 energies located in the peak region of 1^-_2, the agreement of data and fitted value is not good, this is because in the region there are a lot of ED take part in the stronger competition, the completing ability from Alpha spectrum is the one of most strong. The information of peak position implied in some ED have much larger difference, and no method to do modification for them.

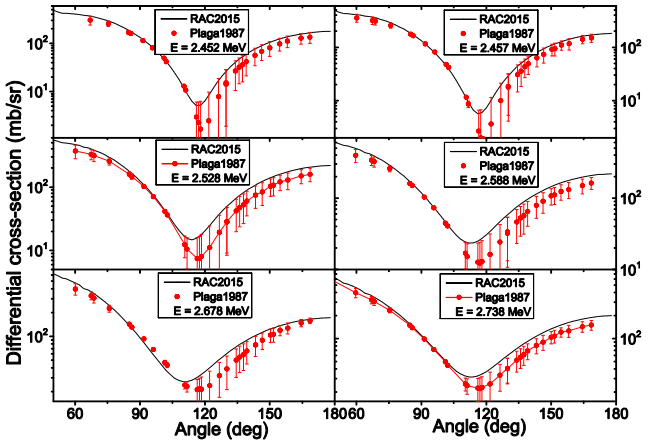

Fig S-AP.I.4.3 Fits to the AD of $^{12}C(\alpha,\alpha)^{12}C$ in (Plaga87)

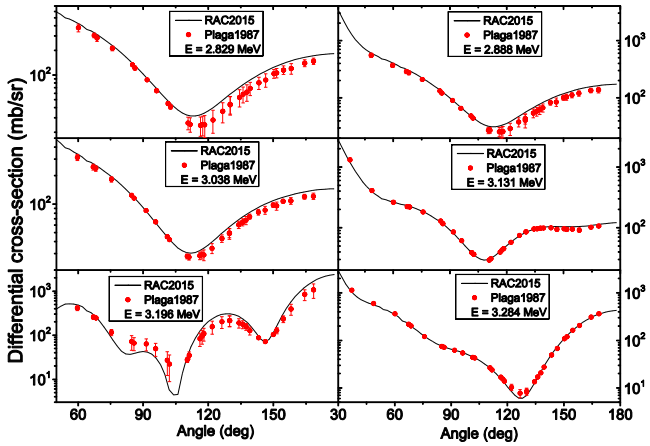

Fig S-AP.I.4.4 Fits to the AD of $^{12}C(\alpha,\alpha)^{12}C$ in (Plaga87)

In Fig S-AP.I.4.3 the 6 energies located in the peak region of 1^-_2, the agreement of data and fitted value is not good, this is because in the region there are a lot of ED take part in the stronger competition, the completing ability from Alpha spectrum is the one of stronger. The information of peak position implied in some ED have much larger difference, and no method to do modification for them. In Fig. S-AP.I.4.4 the 6 energies located the region in which the competition from Alpha spectrum is very weak, the agreement of data and fitted value is very well.

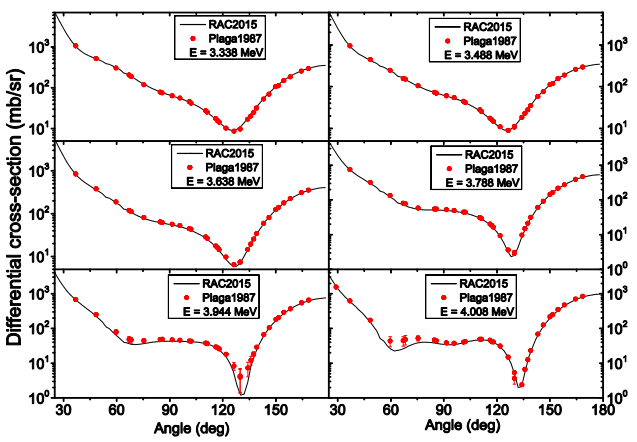

Fig S-AP.I.4.5 Fits to the AD of $^{12}C(\alpha,\alpha)^{12}C$ in (Plaga87)

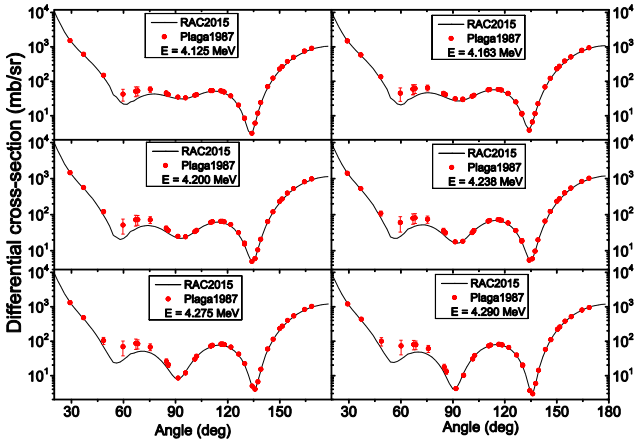

Fig S-AP.I.4.6 Fits to the AD of $^{12}C(\alpha,\alpha)^{12}C$ in (Plaga87)

In Fig. S-AP.I.4.5 and S-AP.I.4.6 (Plag87) for all energies the agreement of data and fitted value is perfect.

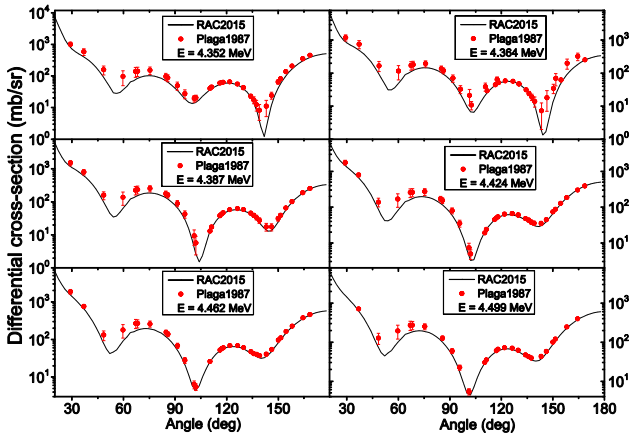

Fig S-AP.I.4.7 Fits to the AD of $^{12}C(\alpha,\alpha)^{12}C$ in (Plaga87)

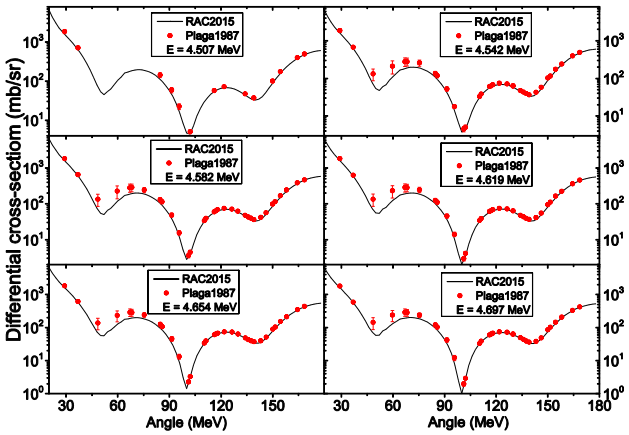

Fig S-AP.I.4.8 Fits to the AD of $^{12}C(\alpha,\alpha)^{12}C$ in (Plaga87)

In Fig. S-AP.I.4.7 and S-AP.I.4.8 (Plag87) for all energies, the agreement of data and fitted value is very well.

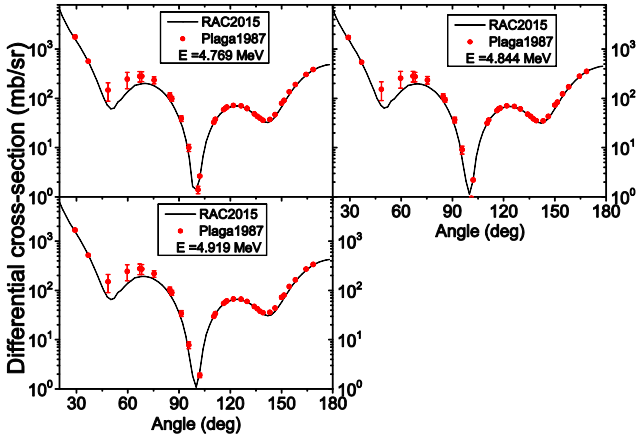

Fig S-AP.I.4.9 Fits to the AD of $^{12}C(\alpha,\alpha)^{12}C$ in (Plaga87)

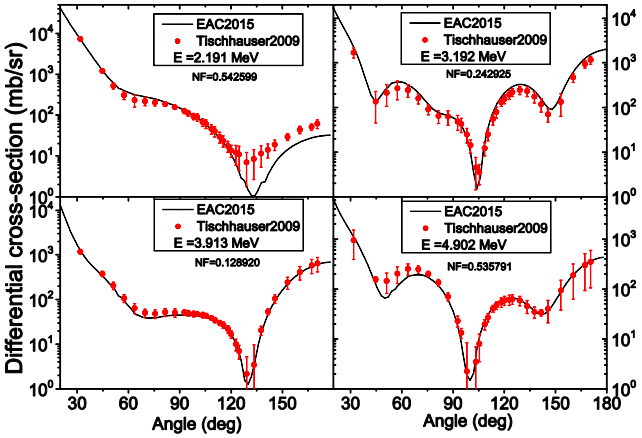

Fig S-AP.I.4.10 Fits to the AD of $^{12}C(\alpha,\alpha)^{12}C$ in (Tisc09)

In Fig. S-AP.I.4.9, for all energies, the agreement of data and fitted value is very well. In Fig. S-AP.I.4.10, the AD of ^{12}C (α, α) ^{12}C are relative value, the agreement of data and fitted value is very well

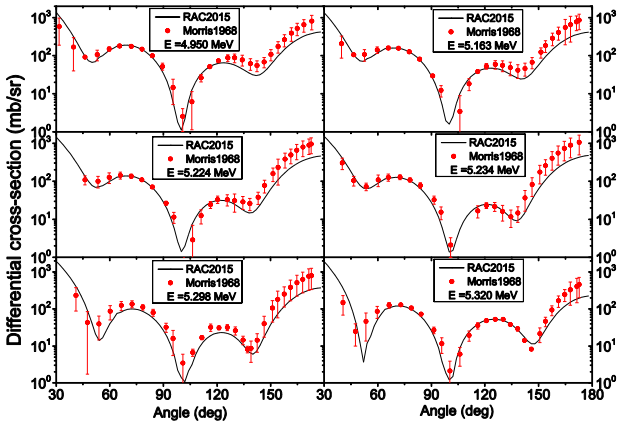

Fig S-AP.I.4.11 Fits to the AD of $^{12}C(\alpha,\alpha)^{12}C$ in (Morris1968)

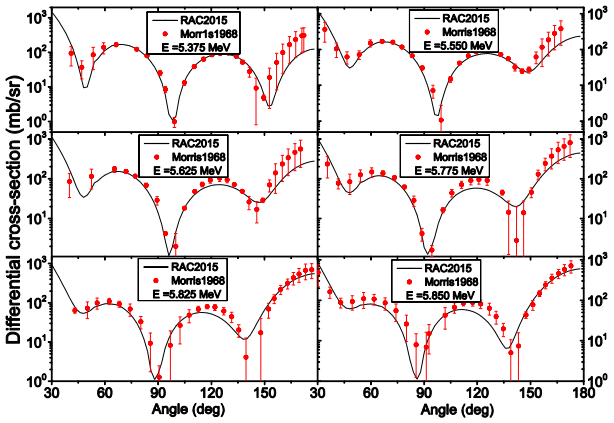

Fig S-AP.I.4.12 Fits to the AD of $^{12}C(\alpha,\alpha)^{12}C$ in (Morris1968)

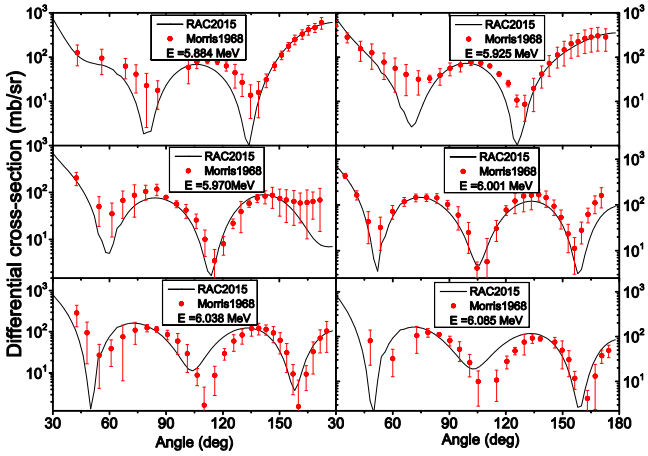

Fig S-AP.I.4.13 Fits to the AD of $^{12}C(\alpha,\alpha)^{12}C$ in (Morris1968)

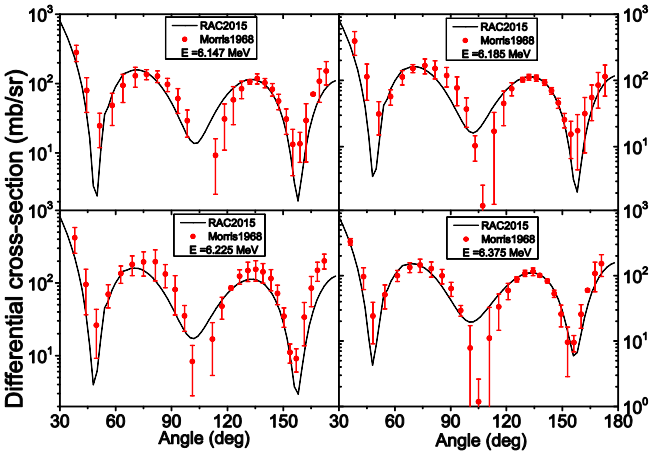

Fig S-AP.I.4.14 Fits to the AD of $^{12}C(\alpha,\alpha)^{12}C$ in (Morris1968)

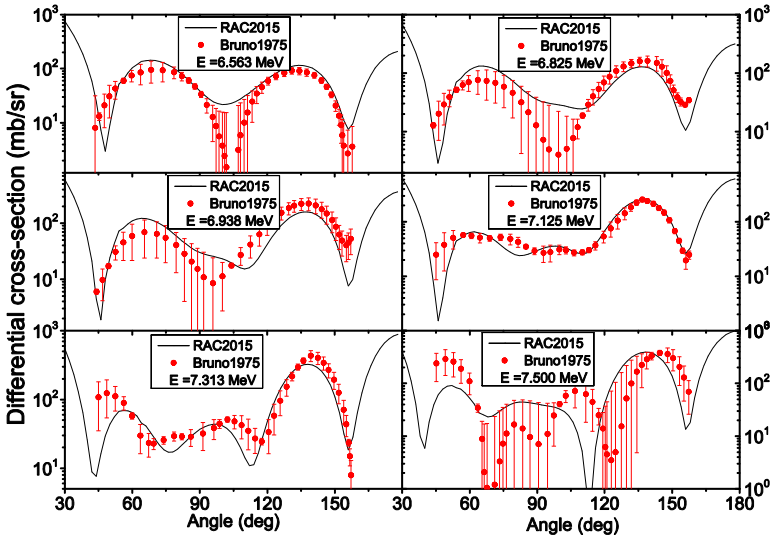

Fig S-AP.I.4.15. Fits to the AD of $^{12}C(\alpha,\alpha)^{12}C$ in (Bruno1975).

APPENDIX.II. The fitting and comparison for ^{12}C (α,α_1) ^{16}O* and ^{12}C (α, p) ^{15}N

It has been explained that in the higher energy region (E>5.5 MeV), using ED of ^{12}C (α, α1)^{16}O* and ^{12}C (α, p) ^{15}N minimize the contribution of reduced channel, and reduced the uncertainty of background from distant levels, subsequently to improve the fitting precision, in this effect the ED of ^{12}C (α, α_1)^{12}C* play a dominate role. The ED of ^{12}C (α, α_1)^{16}O* and ^{12}C (α, p) ^{15}N in the normal published articles have REF. (*Mitchell1965*) and (deBoer2012) only, and both are relative values, in the deBoer2012 all data are excitation function. These data play a dominate function in fitting for higher energy region.

APPENDIX.II.1. the fitting situation for ^{12}C (α, α_1)^{16}O*

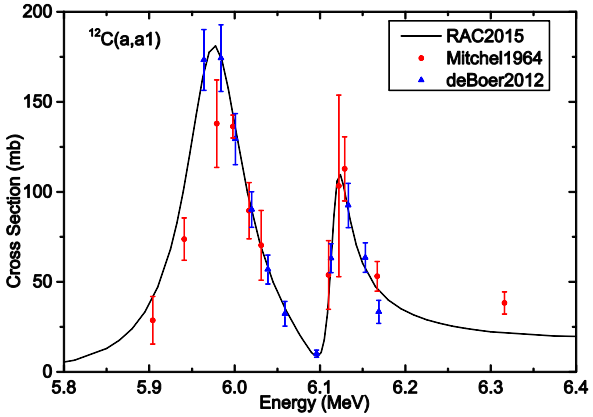

Fig S-AP.II.1.1 Fitting situation to the ED of integrated $^{12}C(\alpha,\alpha_1)^{12}C$ data in (Mitchel1964, deBoer2013). The data of (Mitchel1964) is relative value, the data of (deBoer2013) is absolute value, and the later play a dominate function in fitting for higher energy region.

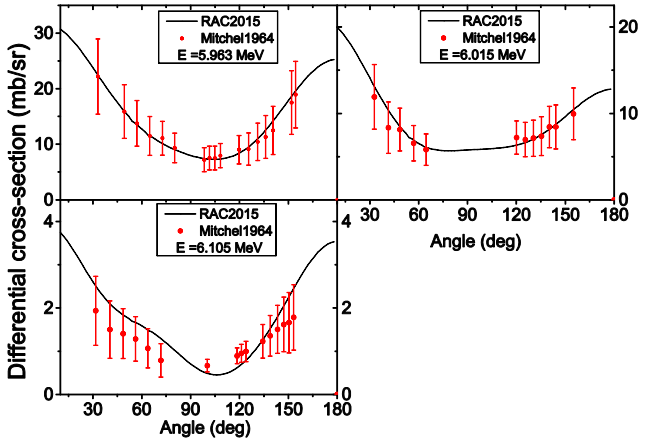

Fig S-AP.II.1.2 Fits to the AD of $^{12}C(\alpha,\alpha_1)^{12}C$ in Mitchel1964.

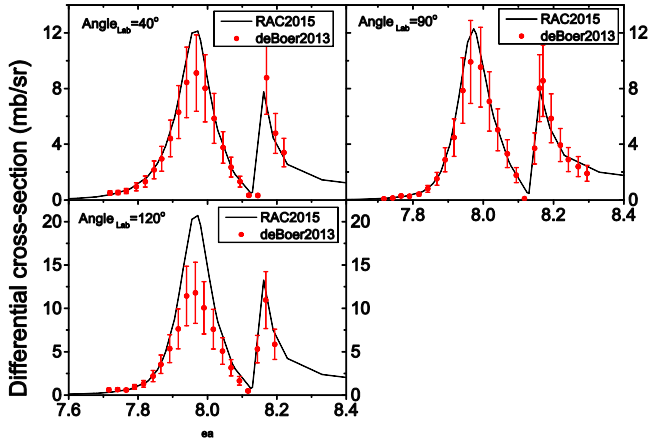

Fig S-AP.II.1.3 Fits to the AD of $^{12}C(\alpha,\alpha_1)^{12}C$ in deBoer2013

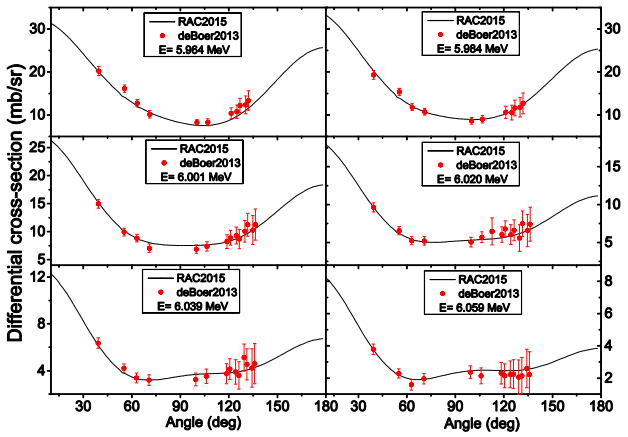

Fig S-AP.II.1.4 Fits to the AD of $^{12}C(\alpha,\alpha_1)^{12}C$ in (deBoer2013)

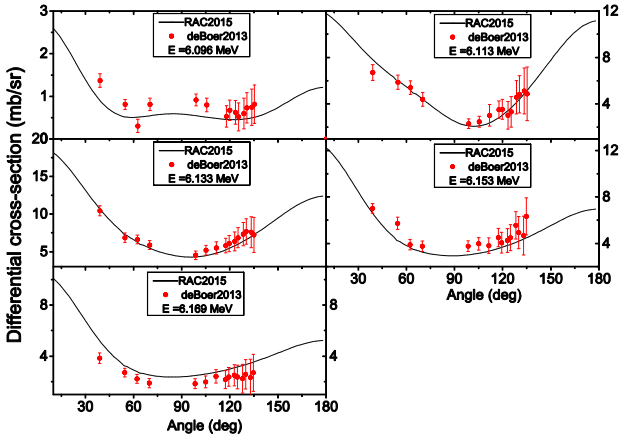

Fig S-AP.II.1.5 Fits to the AD of $^{12}C(\alpha,\alpha_1)^{12}C$ in (deBoer2013)

APPENDIX.II.2. the fitting situation for ^{12}C (α, p) ^{15N}

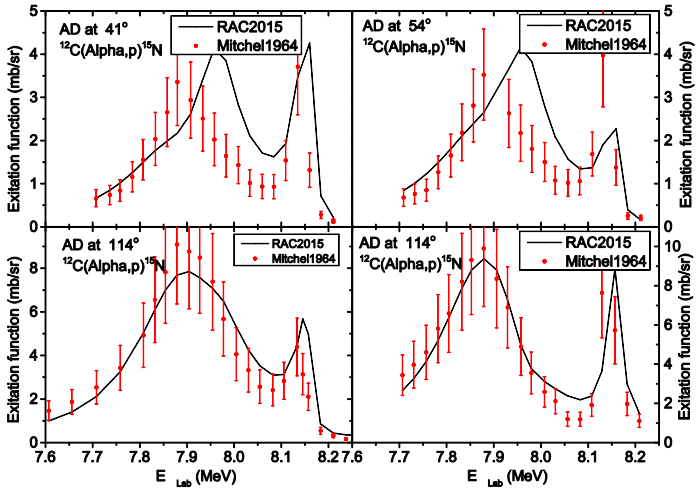

Fig S-AP.I.II.2.1 **Fitting situation about the AD of $^{12}C(\alpha,p)^{15}N$** excitation function in Mitchel1964[57] at 4 angles (41°, 54°, 114° and 140°) in RAC2015. In the higher energy region (E>5.5 MeV), by using the ED of ^{12}C (α, α$_1$)^{12}O* and ^{12}C (α, p) ^{15}N to minimize the contribution of reduced channel, and reduced the uncertainty of background from distant levels. Refer to 'Schemes for fit and calculation in basic study stage' in SI, Appendix. III.

Appendix. III. Schemes for fit and calculation

Appendix **III** display the results of basic research before 2014, the data samples are old ones, the results are old too, but the conclusions are correct, they are applied in the future research works. After 2013 a lot of improvements have been done on the base finished before.

Appendix. III.1. Six theoretical schemes

The reason for analysis of multi-channel and multi-types of level combination is to study the influence from the setting of reaction channels, selection of levels, selections of types of ED. The features of '**Combination**' are identified by string IcJeKd-a, where Ic

represents the I-th reaction channel, Je represents having J levels, Kd represents the number of ED to be fitted, -a indicates the presence of AD of (α, γ0) ED set, -i indicates the absence of AD of (α, γ0) data. All kinds of combinations are performed by using the '**Standard-R-matrix Formula**' and '**Covariance Fitting**'. Table S-AP.III.1-A lists unmarked feature points in these programs, Table S-AP.III.1-B lists calculated SF of these programs, and their mean square errors marked with $\chi^2_{\alpha\gamma}$-M. And Figure S0.1 illustrates the ratio of the RR in these programs.

Table S-AP.III.1-A. The characteristics of 6 combinations

Combination	**Reduced channel**	**ED energy/MeV**
9c37e4558d-a	(α, x)	E_α=1→10
8c37e4223d-a	(α, p), (α, x)	E_α=1→10
7c37e4104d-a	(α, α1), (α, p), (α, x)	E_α=1→10
7c37e3461d-i	(α, α1), (α, p), (α, x)	E_α=1→10
7c22e3104d-a	(α, α1), (α, p), (α, x)	E_α=1→6.5
7c22e2659d-i	(α, α1), (α, p), (α, x)	E_α=1→6.5

Table S-AP.III.1-B. SF (E=0.3MeV)/keV b for 6 combinations

Combination	STOT±ERR	SE10	SE20	Scas	$S_{6.05}$	$S_{6.13}$	$S_{6.92}$	$S_{7.12}$	$\chi^2_{\alpha\gamma}$-M
9c37e4558**d-a**	162.1±07.8	93.34	61.80	6.94	3.269	0.222	2.974	0.474	1.704
7e374223d-a	162.6±8.0	91.92	63.45	7.26	3.272	0.223	3.288	0.477	1.776
7c37e4104**d-a**	161.9±8.4	94.94	59.85	7.11	3.596	0.231	2.638	0.647	1.717
c37e3461d-i	163.±15.7	96.45	60.13	6.88	3.679	0.232	2.332	0.642	1.719
7c22e3104**d-a**	156.±12.0	94.64	54.39	7.16	3.401	0.332	2.759	0.664	1.804
7c22e2659d-i	158.±12.9	84.67	67.07	6.78	3.430	0.201	2.590	0.562	1.744

Among the above six kinds of combinations, 9c37e4558d-a used all the available ED in fitting (4558), and get the smallest average χ^2_{me} (1.704), STOT error being the minimal (162.10 ± 7.8). Literature (Chen2003) made some systematic researches on error propagation, and provided empirical formula like that: $ER_{fit} \approx \chi^2_{me}$*ERed*$\sqrt{M}/\sqrt{N}$, in which χ^2_{me} is the average error of fitted values, ERed the error of ED, M the square root of the number of adjusted parameters, N the square root of the number of ED. Thus, it is reasonable for 9c37e4558d-a case to get smallest error (4.8%), due to using all the available ED in iterative fitting.

The 8c37e4223d-a and 7c37e4104d-a have very close results to 9c37e4558d-a, it is mainly because the same level structure (37E) is used in these three combinations. Moreover, the fitting data set contains the same AD of ^{12}C (α, γ0)^{16}O, which includes the AD for 65 energy points, excitation function with 40 points in five angles. All of them play a decisive role in determining the contribution ratio of E10 to E20. Error of STOT in 7c37e3461d-i is quite large (163.49 ± 15.7), mainly due to absence of AD for ^{12}C (α, γ0) ^{16}O in the fitting data set.

The value of STOT given in 7c22e3104d-a is on the low side, but having a large error (156.22 ± 12.0), mainly due to that it does not use 37E level structure, which ignores 15 levels in the high energy region which having their width information. Then, the loss of binding impact from these levels on background of distant level will result in the fact that contribution from distant level is higher than the actual one and bring about a great uncertainty of their value.

The value of STOT given in 7c22e2659d-i is also on low side, but with a large error (158.68 ± 12.9). Additionally, there is a big difference of the contribution ratio of E10 to E20 compared with other five groups vary significantly, the smallest E10 and maximal E20. The cause is that the combination does not use complete level structure (37E), not fitting for AD of ^{12}C (α, γ_0)^{16}O.

Parameters construction and the fitting data used in 7c22e2659d-i is closest to (Schumman2011), and the result (SE10 = 84.67, SE20 = 67.07) and results of (Schumman2011) (SE10 = 83.4, SE20 = 73.4) are also the closest.

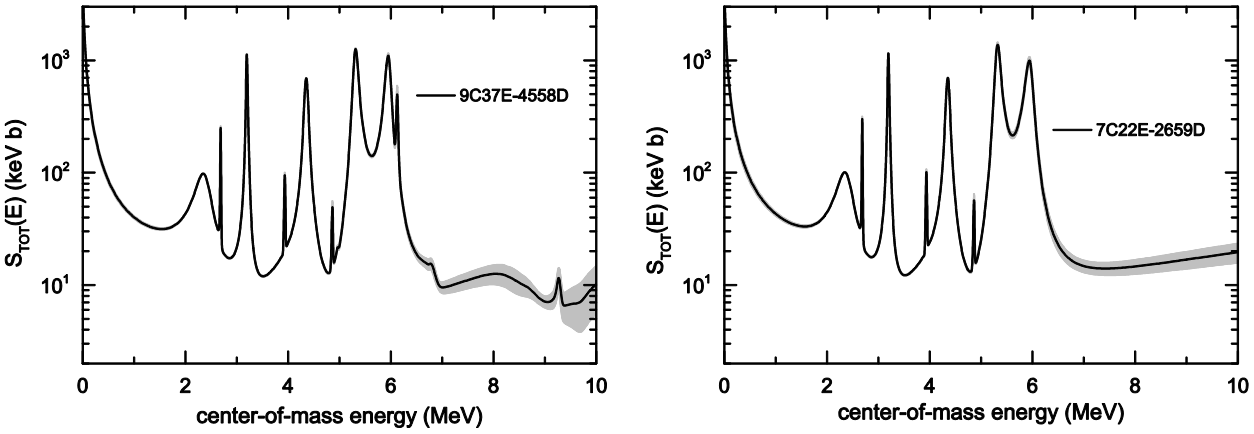

Fig. S-AP.III.1-A. Error for 9c37e4558d and 7c22e2659d

Figure S-AP.III.1-A illustrates intuitively STOT calculated values and their errors. From Ex = 0.01 to 10 MeV, equivalent to from Eα = 0.01 to 15 MeV, the energy range just right meets the computing demands for RR of ^{12}C (α, γ) ^{16}O from T_9 = 0.01 to 10. In the following description, the range from E_X = 0.01 to 0.5 MeV is called '**Extrapolated Area'**, because there is no direct ED in this energy region, but it is also interesting to study the evolution of stellar; the range from 0.5 to 7.2 MeV is called '**Middle- Energy Area'**, just because there is a lot of ED in this energy region; the range from 7.2 to 10 MeV is called '**High-Energy Area**', and in this energy region there exist AD data of ^{12}C (α, α) ^{16}O with six point and width data in scattering states with 15 points.

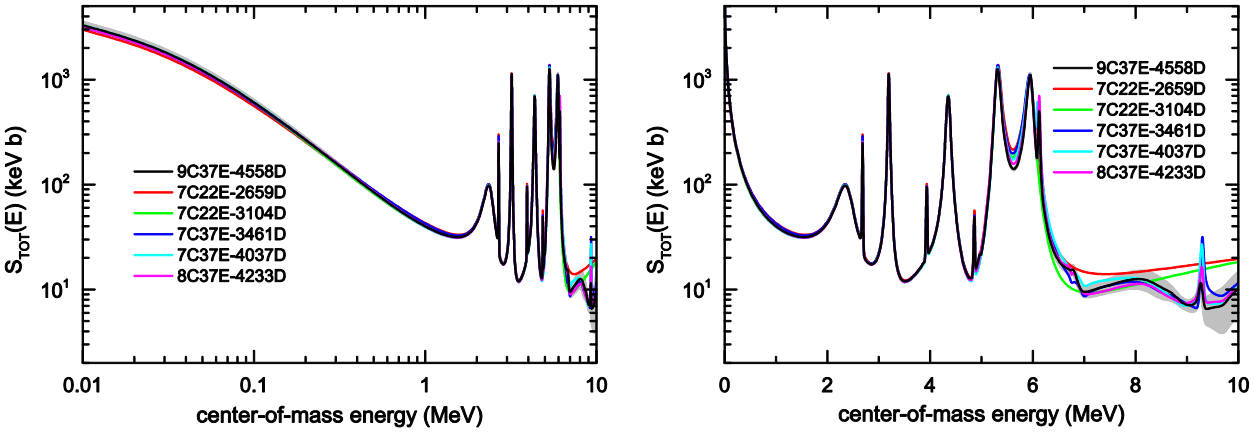

Fig. S-AP.III.1-B. the Calculated STOT for 6 combinations

Figure S-AP.III.1-B simultaneously displays and compares STOT calculated values in six combinations, which proves the effect from the number of levels. Left shows, in the extrapolation energy region, STOT calculated values are significantly different among them, and the right shows a significant difference of the calculated value STOT in high-energy area. The background of distant level in two combinations with use of 22E levels is significantly higher than that in combinations with use of full 37E levels. This is because 15 levels having width information in the higher-level region have a significant constraint impact on background from distant levels. It is obvious that it is more reasonable and more accurate for background from distant levels with 37E levels.

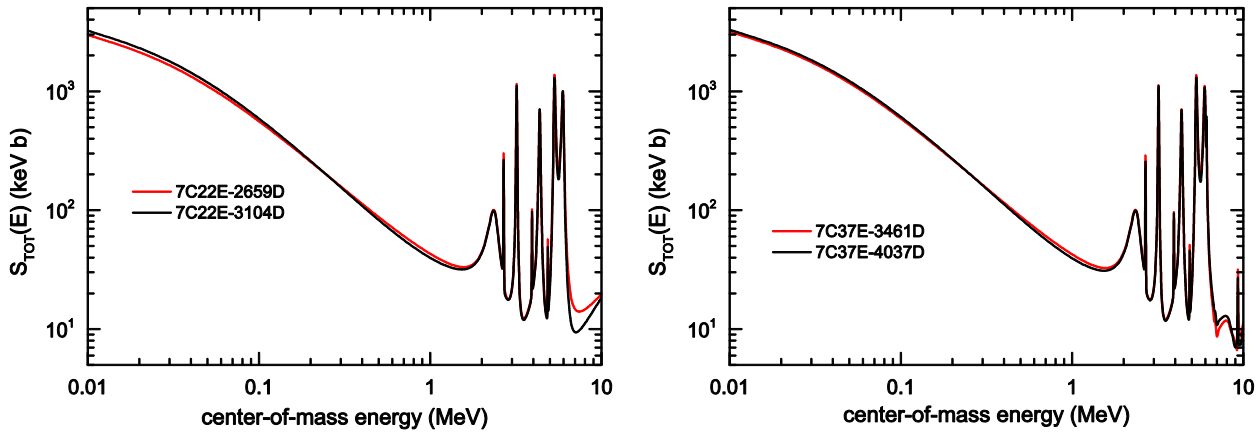

Fig. S-AP.III.1-C. Comparison of calculated STOT for 7c22e (left) to 7c37e (right)

Fig. S-AP.III.1-C shows the effect of using AD of ^{12}C (α, γ0)^{16}O. The case 7C22E3104D and 7C37E4031D take AD data of ^{12}C (α, γ_0)^{16}O, but the case 7C22E2659D and 7C37E3416D do not. As displayed in right figure above, STOT calculated value has significant differences in extrapolation area and high energy region. Since AD of ^{12}C(α, γ_0)^{16}O is the original data, with high reliability and a smaller error, Fitting AD of ^{12}C(α, γ_0)^{16}O can accurately determine the coherence between energy levels, and accurately distinguish the contribution of E10 and E20, so as to improve the accuracy and precision of the calculated value of STOT.

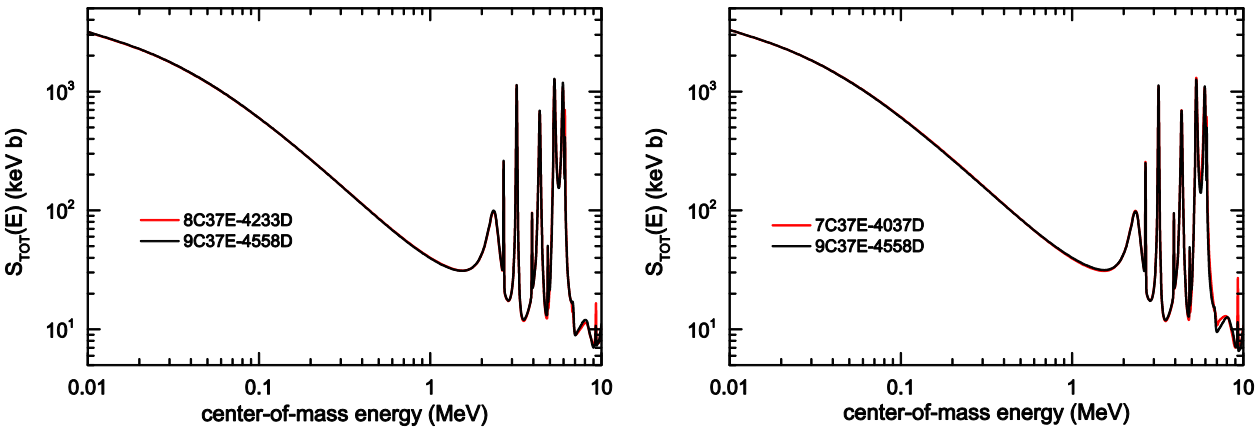

Fig. S-AP.III.1-D Comparison of calculated STOT for 8C37E/ 9C37E (left) and 7C37E/ 9C37E (right)

Figure S-AP.III.1-D depicts the influence of total width of reduced channel Γ and how to set the influence from reduce channel.

The data set of 8C37E4223D includes data of (α, α1), not data of (α, p). The contribution of (α, α1) is represented with specific R-matrix parameters. And the total width of reduced channel Γ represents the contribution of (α, p) and (α, x). The data set of 9c37e4558d contains (α, α1) and (α, p) data (from Eα= 6 to 8 MeV), the contribution of (α, α1) and (α, p) is represented with the specific R-matrix parameters, and the total width of the reduced channel Γ describes the contribution of (α, x) only. The left shows no difference between them in extrapolation area, but has a very slight difference in high-energy area. In case of 8C37E4223D, STOT is 162.66 ± 8.0, and 162.10 ± 7.8 in the case 9c37e4558d, which is indicated that the use of (α, p) data play small role in the improvement.

The data set in the case 7C37E4031D does not contains any data of (α, α1) or (α, p), total width of reduce channel Γ representing the total contribution of (α, α1), (α, p), and (α, x), which is the same as 9c37e4558d. The left shows a very little difference between them in extrapolation area, but visual difference in the high-energy area. STOT in 7C37E4031D is 161.93 ± 8.4, and 162.10 ± 7.8 in 9c37e4558d. Compared to the case 8C37E4223D, it play a bigger role in the improvement, which is mainly caused by the effect of (α, α1) data.

According to 'Reduced R-matrix Theory', the smaller is the contribution of the reduced channels, the smaller is the degree of approximation, and the more accurate is the formula, which leads to smaller uncertainty. For anyavailable ED, it is better to describe them with the specific R matrix parameters than by using corresponding Γ. The scheme 9c37e4558d has the smallest contribution from reduced channels, the average chi-squared is the smallest, the same with the error of STOT, which is consistent with the theoretical predictions.

In the following we use figures of ratio of STOT to show quantitative difference in six combinations to further prove that 9c37e4558d is the best one.

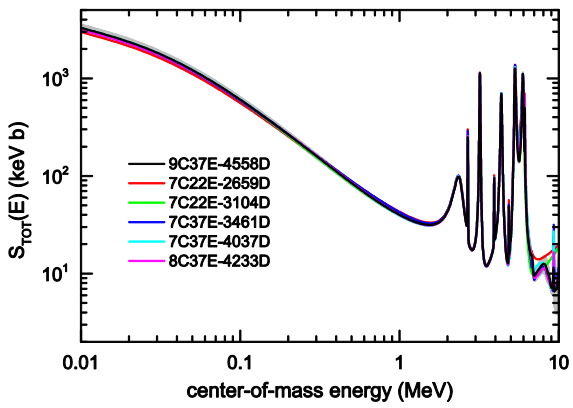

Fig. S-AP.III.1-E-L. STOT in six combinations

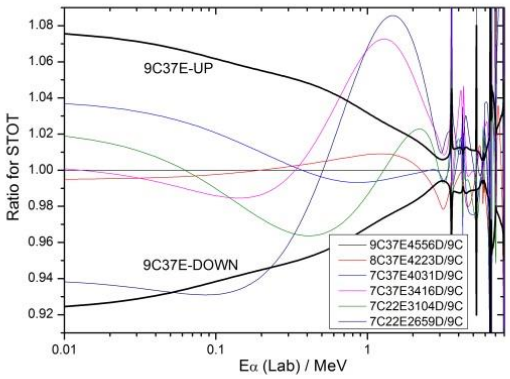

Fig. S-AP.III.1-E-R. Ratio for six combinations over **9c37e4558d**

Figure S-AP.III.1-E-L shows the ratio of STOT in six combinations. **Figure S-AP.III.1-E-R shows the ratio of STOT in six combinations to the case 9c37e4558d.** We can see that 9C37E-UP and 9C37E-DOWN represented upper and lower limits of standard error. Which is 4.7% in GAMOW window (E = 0.3 MeV). This standard error is sufficiently estimated value, because in the error propagation formula calculation, some fixed parameters are also used as adjustable ones to increase the value by about 1.5 percentage point. In extrapolation energy region, compared to 9c37e4558d, the difference in 8C37E4223D is less than 1.3%, and the difference in 7C37E4301D is less than 3.7%, 7C22E3104D less than 4%. Without the use of AD of ^{12}C (α, γ_0)^{16}O, both the case 7C22E2659D and 7C37E3416D have more than 7% of the difference. Thus it will lead to great uncertainty without use of the original AD data of ^{12}C (α, γ_0)^{16}O.

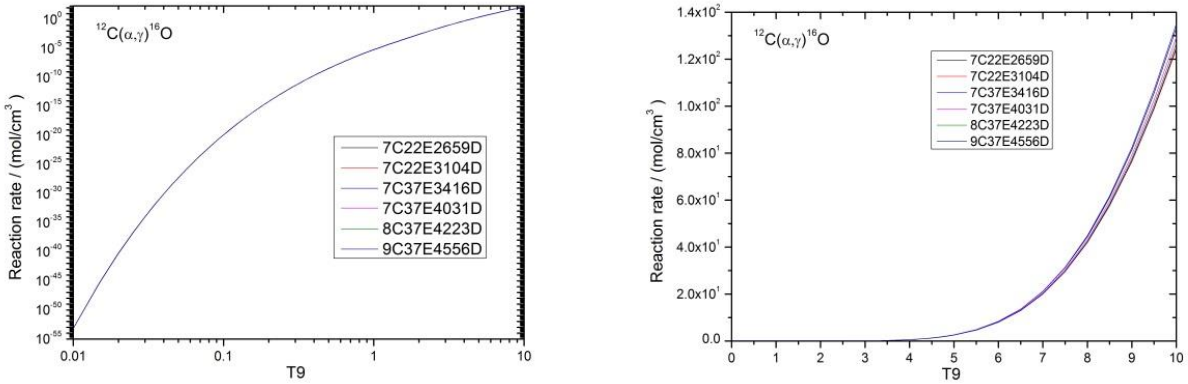

Fig. S-AP.III.1-F. Absolute calculated value of total RR for 6 combinations

Figure S-AP.III.1-F show absolute calculated values of total RR in six combinations. The rigth depicts a significant difference of total RR.

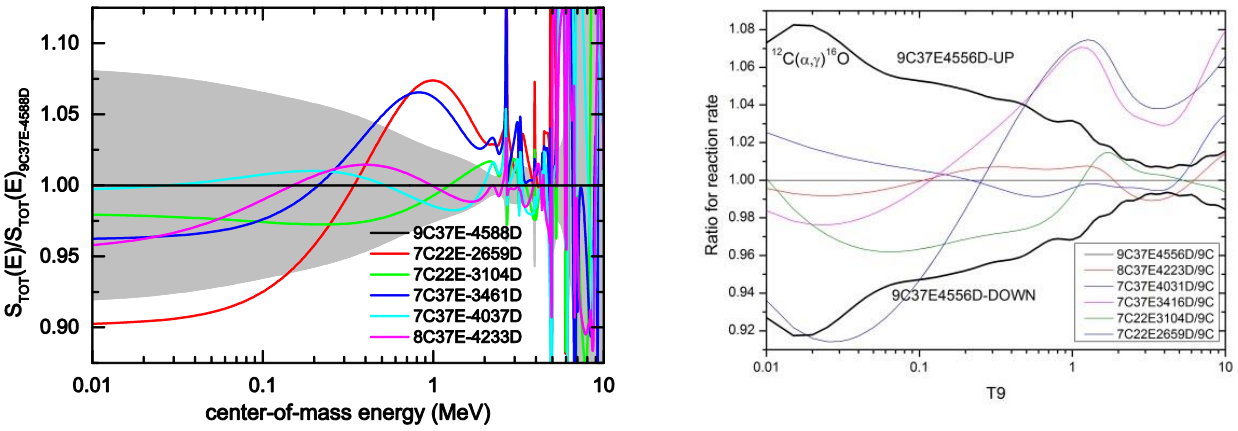

Fig. S-AP.III.1-G. The ratio of total RR in six combination to the case 9c37e4558d

Figure S-AP.III.1-G shows the ratio of total RR in six combination to the case 9c37e4558d. As shown in the figure, 9C37E4556-UP and 9C37E4556-DOWN expressed its standard error limit, 4.8% in GAMOW window (T_9 = 0.2). With comparison of 9c37e4558d, the difference of 8C37E4223D is less than 1% in T9 <8 energy region and difference of 7C37E4301D is less than 2.5%, 7C22E3104D less than 4%. Because of without use of AD of $^{12}C(\alpha, \gamma 0)^{16}O$, the differences in 7C22E2659D and 7C37E3416D are both as high as of 8% in the extrapolation region, which have a large RR in the region of T9> 0.6, caused by background from distant level of high energy levels.

Appendix. III.2. Eight applicable schemes

In order to analyze actual used programs, in this section we perform comparison study for influence generated by certain approximation of the **'standard R-matrix formula'**, by certain simplification of the 'complete set of parameters' , by certain abandonment of the 'complete ED set', and other widely used methods. Additionally to some extent, it is try to explain why so large differences exist in precious analysis works.

The **'Covariance Fitting'** in the 'Generalized least squared method', is to optimize parameters by using 'Covariance' to seek the minimal chi-squared, where we strictly considered the role of non-diagonal elements of 'Covariance' , that is to say, the impact of systematic errors are also taken into account. In essence, is to consider the objective existence relevance of data. According to 'maximum likelihood principle', the obtained best results can be regarded as the 'Expected Value' with the greatest probability of the existence. Advantage of such type of programs is theoretical rigorous, precise formula. But the drawback is its enormous amount of computation cost. In allthe previous conventional analysis works they did not adopt 'Covariance Fitting'.

All conventional analysis are based on a 'Common least squared fitting method', that is to say, the **'Statistical Variance Fitting**' method, where the systematic error is eliminated by 'normalization' method. In fact, they ignore the objective existence 'coherence' of data. Similarly according to 'maximum likelihood principle', the obtained results are not the 'Expected Values' with the greatest probability of the existence. The advantage of such programs is quite low amount of calculation, but the disadvantage is to introduce the hardly estimated uncertainty.

In the **'Physical R- matrix Formula'** used in previous section analysis, all the 'energy shift' factors are fixed to zero.

$$\Delta_{\lambda\mu} = -\sum_{\alpha sl}\left[S_{\lambda\mu} - B_{\alpha}\right]\gamma_{\lambda,\alpha sl}\gamma_{\mu,\alpha sl} \qquad \text{S-AP.III.2.1}$$

In this case, level position E_λ of a narrow level is very close to the real position of the resonance level $E_\lambda r$, that is $E_\lambda \approx E_\lambda r$, which has obvious physical meaning. When using such programs, let E_λ values be strict constrained by ED, equivalent to lose some freedom, so that

the finally obtained chi-squared will be greater than that with using of '**Standard R- matrix Formula**'. By judgment of 'maximum likelihood principle', the results obtained are not 'expected values' with the greatest probability of existence. However, the 'Physical R-matrix formula' can be used with the accordance of 'covariance' fitting or 'statistical variance' fitting.

This work was based on the same energy level structure and parameters set, based on the same set of ED, using the above four categories of formulas to fit the results respectively, and obtained the consistent results within a certain error range. Careful comparison of the results finds it best to apply **'Covariance fitting'** in the end.

Some of the previous analytical work are like as follows: first they adopt the 'Legendre function approximation expression' (Appendix S1.4.1) to fit AD of $^{12}C(\alpha, \gamma_0)^{16}O$, and get SE10 and SE20 in full energy area, then R-matrix formula comprehensive analysis of SE10, SE20, STOT and other types of integral ED was performed to get the finally recommended values. Some other analysis considers only the ED in low energy region (from 1 to 6.6 MeV). For these two situations, we have made a similar analysis and find that the calculated values of STOT and RR are very far from expected ones, so do their errors.

There Exists many units of ED for $^{12}C\ (\alpha, \alpha_1)^{16}O$ and $^{12}C\ (\alpha, p)^{15N}$, although they are in the higher energy region, and a very big difference among them, it can also get better results with the use of 'reduced channel' depicting their contributions. As is described above, 8C37E4223D and 7C37E3416D also have practical value for using.

The analysis results in above eight kinds of applicable programs, have some significant differences in some areas, but are consistent within a very small error range. We can choose the best solution by comparison. The 'Program name' in Table S –AP.III.2 has the same meaning with that in Table S5. Where the sign 'PHY' represents the use of 'Physical R-matrix formula', DIA refer to 'Statistical variance fitting'. Table S –AP.III.2 lists the characteristic points, which are not clearly identified in these programs. Table Table S –AP.III.2 displays calculated values SF, and Figure S0.1.2 illustrates ratio of RR among these programs.

Table S − AP. III. 2 − A Charectristic for eight kinds of applicable programs

Program name	shift	Data energy/MeV	Advantage/Defect	If have been used
9CSTD − COV	$\Delta e \neq 0$	$1 \rightarrow 10$	Most accurate / Need very long CPU time	Used by RAC2013
9CSTD − DIA	$\Delta e \neq 0$	$1 \rightarrow 10$	rather accurate / less CPU time	Popular
9CPHY − COV	$\Delta e = 0$	$1 \rightarrow 10$	rather accurate / less CPU time	Had similar works
9CPHY − DIA	$\Delta e = 0$	$1 \rightarrow 10$	rather accurate / less CPU time	Had similar works
9CSTD − COV	$\Delta e \neq 0$	$1 \rightarrow 6.5$	lower accurate / short CPU time	No
9CINT − COV	$\Delta e \neq 0$	$1 \rightarrow 10$	general accurate / less CPU time	Had similar works
8C37E − STD	$\Delta e \neq 0$	$1 \rightarrow 10$	rather accurate / less CPU time	Used by RAC2013
7C37E − STD	$\Delta e \neq 0$	$1 \rightarrow 7.5$	rather accurate / short CPU time	Used by RAC2013

Table S-AP.III.2-B. Calculated SF for eight kinds of applicable programs

Program name	STOT±ERROR	SE10	SE20	SCAS	$S_{6.05}$	$S_{6.13}$	$S_{6.92}$	$S_{7.12}$	χ_T^2-M
9CFSTCOV	161.40±6.7	93.17	61.16	7.05	3.382	0.224	2.965	0.480	1.701
9CSTDDIA	161.44±6.3	94.71	60.16	6.55	2.922	0.221	2.928	0.480	1.695
9CPHYCOV	161.07±7.0	83.95	69.89	7.16	3.459	0.233	2.950	0.521	1.851
9CPHYDIA	156.60±6.4	83.20	66.86	6.48	2.840	0.228	2.878	0.532	1.903
9CSTDINT	154.49±39.7	93.95	53.33	7.18	3.650	0.224	2.816	0.492	0.807
9CSTDLOW	162.00±6.5	95.39	59.27	7.32	3.651	0.223	2.942	0.504	1.496
8C37ESTD	162.55±7.1	91.81	63.46	7.25	3.266	0.223	3.288	0.476	1.775

7C37ESTD	161.93±8.0	94.94	59.85	7.11	3.596	0.231	2.638	0.647	1.714

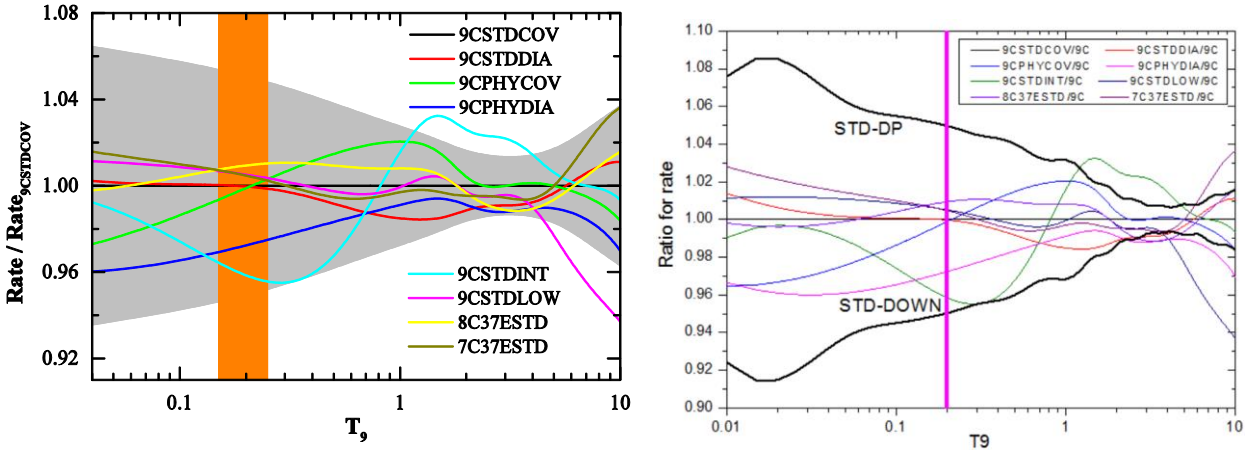

Fig. S-AP.III.2-A. Eight kinds of applicable programs

Figure S-AP.III.2-A depicts ratio of the RR eight kinds of applicable programs to the best solution (9CFSTCOV, referred 9C). As shown in the figure(right) , STD-UP and STD-DOWN represents the upper and lower limits of standard error in 9CFSTCOV respectively, its maximum being 4.8% in the GAMOW energy region (T_9 = 0.2). The error contains the error originally calculated values of RR, and the additional error calculated by using analytic formula (S10.11) in the original data fitting. Figure S0.1.2 clearly shows that, the case 9CSTDINT (green line) results in the biggest deviation without considering AD of ^{12}C (α, γ0) ^{16}O, which is followed by the case of 9CFSTCOV (blue line) and 9CSTDDIA (pink line), with the use of 'Physical R- matrix formula' having a large deviation. All these three types of programs should not be used. Without ED high-energy zone, the RR in 9CSTDLOW (dark blue line) is very close to the best selection in extrapolation energy region (T_9 <3). Unfortunately, the deviation increases rapidly in T9> 3 area, this is because there is constraints of ED in high-energy region. RR in 8C37ESTD (brown line) is very close to the value in the optimal solution in whole energy area, the error less than 1.5%. RR in 7C37ESTD (dark brown lines) is also very close to the value in optimal solution in most area (T9 <8), the error less than 3%. It is further illustrated that is feasible for using 'reduced channel' to represent the contribution of ^{12}C (α, α_1)^{16}O and ^{12}C (α, p) ^{15}N.

Appendix. IV. The information about R-matrix parameters and experimental database

Appendix.IV.1. Table. The digital information about R-matrix parameters

Table. App. IV.1.1 The digital information about Channel

Channel	Radii	Lmax.	Threshold	Mt	Mi	Chat	Chai	Spin	Spin	Parity	Parity
'α, ^{12}C'	0.6500D+01	6	0.000000	12.0000648499	4.0015063286	6.0	2.0	0.0	0.0	1.0	1.0
'γ$_0$, ^{16}O$_0$'	0.6500D+01	4	7.162000	15.9970233044	0.0000000000	8.0	0.0	0.0	1.0	1.0	
'γ$_1$, ^{16}O$_1$'	0.6500D+01	3	1.212600	16.0035163226	0.0000000000	8.0	0.0	0.0	1.0	1.0	
'γ$_2$, ^{16}O$_2$'	0.6500D+01	2	1.132100	16.0036076157	0.0000000000	8.0	0.0	3.0	1.0	-1.0	
'γ$_3$, ^{16}O$_3$'	0.6500D+01	2	0.344900	16.0044561723	0.0000000000	8.0	0.0	2.0	1.0	1.0	
'γ$_4$, ^{16}O$_4$'	0.6500D+01	2	0.145200	16.0046677857	0.0000000000	8.0	0.0	1.0	1.0	-1.0	
'α$_1$, ^{16}O*$_1$'	0.6500D+01	3	-4.438000	12.0047583003	4.0015063286	6.0	2.0	2.0	0.0	1.0	1.0
'P, ^{15}N$_0$'	0.6500D+01	3	-4.968000	15.0004677857	1.0076000000	7.0	1.0	0.5	0.5	-1.0	1.0

Appendix.IV.2. Table. The digital information about Data-sets

Ref.	Name	NF/SC	WF	ChiS	ChiC	Num.	Ref.		Name	NF/SC	WF	ChiS	ChiC	Num.
22	STOTschu	0.103000E+01	0.700	3.802	2.133	91	S52		AGDAfeyb	0.317869E-07	1.000	1.660	1.660	9
23	STOTsch3	0.100000E+01	1.000	4.946	2.939	7	S52		AGDAfeyc	0.360477E-07	1.000	7.435	7.440	9
25	STOTfuji	0.100000E+01	1.000	1.212	1.071	2	S52		AGDAfeyd	0.122886E-05	1.000	4.812	4.813	9
24	STOTplag	0.103000E+01	1.000	2.174	4.192	4	S52		AGDAfeye	0.112367E-07	1.000	2.361	2.361	9
20	ALPHtang	0.100000E+01	1.568	2.427	1.270	93	S52		AGDAfeyf	0.119041E-07	1.000	2.619	2.620	9
54	ALPHazum	0.100000E+01	1.000	3.384	1.436	91	24		AGDAplan	0.194177E-09	1.000	3.657	3.657	12
55	ALPHzhao	0.100000E+01	1.543	2.434	1.298	75	24		AGDApla1	0.285479E-09	1.000	3.377	3.379	12
50	AADApla1	0.100000E+01	1.000	1.419	1.803	823	24		AGDApla2	0.190457E-08	1.000	0.749	0.749	12
50	AADApla2	0.100000E+01	1.000	1.661	1.310	794	24		AGDApla3	0.410176E-09	1.000	0.838	0.838	12
51	AADAtisc	0.100000E+01	1.000	1.476	1.546	32	24		AGDApla4	0.313052E-07	1.000	4.631	4.789	12
51	AADAtis1	0.100000E+01	1.000	1.729	1.528	32	33		AGDAredd	0.705300E-07	1.000	2.724	2.739	6
51	AADAtis2	0.100000E+01	1.000	1.381	1.123	32	33		AGDAred1	0.148474E-05	1.000	3.742	3.742	6
51	AADAtis3	0.100000E+01	1.000	1.705	1.705	32	33		AGDAred2	0.214960E-04	1.000	3.296	3.298	6
54	AADAmorr	0.100000E+01	1.000	1.126	1.046	613	33		AGDAred3	0.283255E-06	1.000	3.838	3.839	6
53	AADAbrun	0.100000E+01	1.000	1.250	1.248	244	48		AGDAlars	0.259682E-05	3.000	1.412	1.406	7
33	SCG0redd	0.100000E+01	1.000	3.240	3.240	24	48		AGDAlar1	0.237207E-05	1.600	1.495	1.496	7
22	SCG0sch3	0.100000E+01	1.000	3.595	3.607	7	48		AGDAlar2	0.227241E-05	2.300	1.597	1.600	7
34	SCG0ouel	0.100000E+01	1.000	1.385	1.385	9	48		AGDAlar3	0.287853E-05	1.300	2.205	2.204	7
36	SCG0assu	0.100000E+01	1.000	1.802	1.803	20	49		AGDAkern	0.161765E-05	2.500	0.943	0.945	7
35	SCG0kunz	0.100000E+01	1.000	1.437	1.438	20	49		AGDAker1	0.174701E-05	1.000	0.651	0.626	7
24	SCG0plag	0.103000E+01	1.000	0.656	0.656	4	49		AGDAker2	0.260696E-05	1.100	1.674	1.675	7
31	SCG0maki	0.102999E+01	1.000	2.674	2.677	4	38		AGDAophe	0.172187E+01	2.000	0.845	0.844	40
15	SCG0kett	0.930571E+00	1.300	1.851	1.839	48	43		AGDAla45	0.226047E-05	2.000	1.530	1.530	4
32	SCG0broc	0.100000E+01	1.000	0.773	0.773	24	43		AGDAl135	0.241809E-05	2.100	1.570	1.572	20
38	SCG0ophe	0.100000E+01	1.000	0.497	0.497	1	49		AGDAke61	0.193794E-05	2.000	2.103	1.895	13
23	AGDAouel	0.100000E+01	1.000	2.267	2.289	96	49		AGDAke90	0.204952E-05	1.400	1.709	1.701	13
24	AGDAmaki	0.103007E+01	1.000	3.465	3.467	14	49		AGDAk135	0.241208E-05	1.000	1.489	1.599	13
36	AGDAassu	0.604415E-09	1.000	0.602	0.602	9	57		AGDAmi90	0.879282E-04	1.000	0.936	0.938	29
36	AGDAass1	0.413116E-09	1.000	0.783	0.784	9	57		AGDAm135	0.116424E-02	1.000	2.050	2.050	14
36	AGDAass2	0.455656E-08	1.000	1.299	1.299	9	39		SCG1mate	0.733601E+00	1.000	2.414	2.416	32
36	AGDAass3	0.114122E-07	1.000	4.269	4.273	9	23		SCG1sch3	0.100000E+01	1.000	0.431	0.431	7
36	AGDAass4	0.203269E-07	1.000	3.930	3.943	9	23		SCG2sch3	0.100000E+01	1.000	2.309	2.279	7
36	AGDAass5	0.311370E-06	1.000	6.042	6.046	9	35		SCG3kunz	0.100000E+01	1.000	0.657	0.649	16
35	AGDAkunz	0.230761E-05	1.000	2.025	2.026	9	33		SCG3redd	0.365951E+00	1.000	0.829	0.839	25
35	AGDAkun1	0.190541E-05	1.000	3.288	3.278	9	15		SCG3kett	0.451095E+00	1.000	0.694	0.696	5
35	AGDAkun2	0.155059E-05	1.000	1.635	1.635	9	23		SCG3sch3	0.100000E+01	1.000	0.890	0.899	7
35	AGDAkun3	0.543256E-05	1.000	4.484	4.485	9	35		SCG4kunz	0.100000E+01	1.000	2.560	2.697	16

47	AGDAdyer	0.872916E-07	1.000	5.109	5.111	10	33		SCG4redd	0.498559E+00	1.000	1.884	1.876	25
47	AGDAdye1	0.948589E-07	1.000	3.712	3.716	10	23		SCG4sch3	0.100000E+01	1.000	4.069	3.976	7
47	AGDAdye2	0.888921E-07	1.000	3.333	3.334	10	57		AA1Cmitc	0.176841E-01	1.400	1.790	1.808	11
47	AGDAdye3	0.697386E-07	1.000	4.922	4.874	10	56		AA1Cdebo	0.100000E+01	1.000	0.435	0.459	11
S52	AGDAfeyn	0.503108E-09	1.000	2.984	2.985	9	57		AA1Dmitc	0.357001E+01	1.000	0.040	0.040	17
S52	AGDAfey1	0.639139E-09	1.000	1.741	1.750	8	57		AA1Dmit1	0.372768E+01	1.000	0.062	0.062	12
S52	AGDAfey2	0.199498E-08	1.000	1.873	1.871	9	57		AA1Dmit2	0.167051E+00	1.000	1.080	1.072	16
S52	AGDAfey3	0.328845E-08	1.000	2.246	2.250	8	38		AA1Dophe	0.570640E+01	1.000	0.737	0.735	21
S52	AGDAfey4	0.250935E-08	1.000	2.264	2.265	9	38		AA1Doph1	0.540065E+01	1.000	0.812	0.812	25
S52	AGDAfey5	0.376141E-08	1.000	3.409	3.410	9	38		AA1Doph2	0.642512E+00	1.000	0.982	0.981	21
S52	AGDAfey6	0.470469E-08	1.000	3.175	3.177	8	56		AA1Ddebo	0.100000E+01	1.000	0.852	0.859	153
S52	AGDAfey7	0.583267E-08	1.000	2.370	2.375	9	57		APDAmitc	0.273387E+01	1.400	1.263	1.240	21
S52	AGDAfey8	0.186323E-07	1.000	1.144	1.144	9	57		APDAmit1	0.166021E+01	1.400	1.727	1.658	20
S52	AGDAfey9	0.440505E-08	1.000	2.553	2.553	9	57		APDAmit2	0.132442E+01	1.400	1.365	1.374	24
S52	AGDAfeya	0.127206E-07	1.000	1.619	1.619	9	57		APDAmit3	0.557257E+00	1.000	1.687	1.689	21

Note: For a data set in an article the energy is in increased order.

Ref. Order number of Reference in this paper. Name Name of data set in Parameter file of RAC2015.

NF/SF Normalization Factor for absolute or relative data. WF Weight Factor.

ChiD Mean Chi square for Statistic fitting. ChiC Mean square for Covariance fitting.

Num. Number of points in a Data set

Appendix. V. Table for the final calculated results of RAC2015

Appendix. V.1. Calculated RRexp of RAC2015 and previous published RR ($40T_9$) (in $mol.s^{-1}.cm^{-3}$)

T9	**Unit**	**RAC2015**	**NACREII**	**katsuma**	**Kunz**	**NACRE**	**Buchmann**	**Caughlan**
10^9	**$mol.s^{-1}.cm^{-3}$**	**2015**	**2013**	**2008**	**2002**	**1999**	**1996**	**1988**
0.4000E-01	0.1000E-30	0.9059E+01	0.0000E+00	0.6840E+01	0.8360E+01	0.0000E+00	0.7980E+01	0.6930E+01
0.5000E-01	0.1000E-27	0.5706E+01	0.0000E+00	0.4500E+01	0.5200E+01	0.0000E+00	0.4890E+01	0.4170E+01
0.6000E-01	0.1000E-24	0.7461E+00	0.6000E+00	0.6250E+00	0.6900E+00	0.1020E+01	0.6500E+00	0.5400E+00
0.7000E-01	0.1000E-23	0.3571E+01	0.2980E+01	0.3180E+01	0.3420E+01	0.4980E+01	0.3150E+01	0.2590E+01
0.8000E-01	0.1000E-21	0.8666E+00	0.7400E+00	0.8070E+00	0.8400E+00	0.1220E+01	0.7800E+00	0.6300E+00
0.9000E-01	0.1000E-20	0.1290E+01	0.1120E+01	0.1230E+01	0.1260E+01	0.1800E+01	0.1160E+01	0.9200E+00
0.1000E+00	0.1000E-19	0.1324E+01	0.1150E+01	0.1290E+01	0.1290E+01	0.1810E+01	0.1180E+01	0.9200E+00
0.1100E+00	0.1000E-18	0.1013E+01	0.8800E+00	0.9900E+00	0.9800E+00	0.1350E+01	0.9000E+00	0.6900E+00
0.1200E+00	0.1000E-18	0.6122E+01	0.5270E+01	0.6020E+01	0.5920E+01	0.7980E+01	0.5390E+01	0.4080E+01
0.1300E+00	0.1000E-17	0.3046E+01	0.2610E+01	0.3020E+01	0.2930E+01	0.3890E+01	0.2670E+01	0.1990E+01
0.1400E+00	0.1000E-16	0.1290E+01	0.1110E+01	0.1290E+01	0.1240E+01	0.1610E+01	0.1130E+01	0.8300E+00
0.1500E+00	0.1000E-16	0.4770E+01	0.4090E+01	0.4800E+01	0.4580E+01	0.5860E+01	0.4190E+01	0.3030E+01
0.1600E+00	0.1000E-15	0.1573E+01	0.1350E+01	0.1600E+01	0.1510E+01	0.1910E+01	0.1380E+01	0.9900E+00
0.1800E+00	0.1000E-14	0.1288E+01	0.1110E+01	0.1320E+01	0.1240E+01	0.1530E+01	0.1140E+01	0.7900E+00
0.2000E+00	0.1000E-14	0.7817E+01	0.6780E+01	0.8200E+01	0.7580E+01	0.9110E+01	0.7040E+01	0.4730E+01
0.2500E+00	0.1000E-12	0.2837E+01	0.2500E+01	0.3090E+01	0.2790E+01	0.3210E+01	0.2650E+01	0.1670E+01
0.3000E+00	0.1000E-11	0.4326E+01	0.3850E+01	0.4840E+01	0.4280E+01	0.4750E+01	0.4190E+01	0.2480E+01
0.3500E+00	0.1000E-10	0.3779E+01	0.3380E+01	0.4310E+01	0.3750E+01	0.4030E+01	0.3780E+01	0.2100E+01
0.4000E+00	0.1000E-09	0.2246E+01	0.2010E+01	0.2600E+01	0.2220E+01	0.2310E+01	0.2310E+01	0.1210E+01
0.4500E+00	0.1000E-08	0.1008E+01	0.9000E+00	0.1180E+01	0.9900E+00	0.1000E+01	0.1070E+01	0.5300E+00
0.5000E+00	0.1000E-08	0.3663E+01	0.3270E+01	0.4320E+01	0.3590E+01	0.3520E+01	0.3980E+01	0.1860E+01
0.6000E+00	0.1000E-07	0.3048E+01	0.2720E+01	0.3660E+01	0.2950E+01	0.2750E+01	0.3480E+01	0.1460E+01

0.7000E+00	0.1000E-06	0.1646E+01	0.1460E+01	0.2010E+01	0.1570E+01	0.1400E+01	0.1970E+01	0.7400E+00
0.8000E+00	0.1000E-06	0.6600E+01	0.5850E+01	0.8140E+01	0.6190E+01	0.5360E+01	0.8200E+01	0.2810E+01
0.9000E+00	0.1000E-05	0.2133E+01	0.1890E+01	0.2660E+01	0.1970E+01	0.1660E+01	0.2740E+01	0.8600E+00
0.1000E+01	0.1000E-05	0.5866E+01	0.5180E+01	0.7420E+01	0.5320E+01	0.4410E+01	0.7710E+01	0.2220E+01
0.1250E+01	0.1000E-04	0.4527E+01	0.4000E+01	0.5960E+01	0.3950E+01	0.3190E+01	0.6150E+01	0.1490E+01
0.1500E+01	0.1000E-03	0.2240E+01	0.2000E+01	0.3130E+01	0.1910E+01	0.1530E+01	0.3040E+01	0.6900E+00
0.1750E+01	0.1000E-03	0.8439E+01	0.7740E+01	0.1260E+02	0.7200E+01	0.5760E+01	0.1110E+02	0.2880E+01
0.2000E+01	0.1000E-02	0.2622E+01	0.2490E+01	0.4190E+01	0.2290E+01	0.1840E+01	0.3280E+01	0.1090E+01
0.2500E+01	0.1000E-01	0.1646E+01	0.1690E+01	0.2850E+01	0.1540E+01	0.1270E+01	0.0000E+00	0.9700E+00
0.3000E+01	0.1000E-01	0.6791E+01	0.7340E+01	0.1190E+02	0.6810E+01	0.5810E+01	0.0000E+00	0.4910E+01
0.3500E+01	0.1000E+00	0.2107E+01	0.2320E+01	0.0000E+00	0.2210E+01	0.1940E+01	0.0000E+00	0.1720E+01
0.4000E+01	0.1000E+00	0.5404E+01	0.5970E+01	0.0000E+00	0.5860E+01	0.5220E+01	0.0000E+00	0.4800E+01
0.5000E+01	0.1000E+01	0.2512E+01	0.2790E+01	0.0000E+00	0.2910E+01	0.2510E+01	0.0000E+00	0.2500E+01
0.6000E+01	0.1000E+01	0.8600E+01	0.9810E+01	0.0000E+00	0.1070E+02	0.8530E+01	0.0000E+00	0.9300E+01
0.7000E+01	0.1000E+02	0.2314E+01	0.2680E+01	0.0000E+00	0.3080E+01	0.2240E+01	0.0000E+00	0.2760E+01
0.8000E+01	0.1000E+02	0.5104E+01	0.5910E+01	0.0000E+00	0.7080E+01	0.4830E+01	0.0000E+00	0.6920E+01
0.9000E+01	0.1000E+02	0.9620E+01	0.1100E+02	0.0000E+00	0.1370E+02	0.8870E+01	0.0000E+00	0.1530E+02
0.1000E+02	0.1000E+03	0.1606E+01	0.1800E+01	0.0000E+00	0.2320E+01	0.1450E+01	0.0000E+00	0.3050E+01

Appendix. V. 2. Calculated RRexp and RR_{ana} of RAC2015 at $180T_9$ (in $mol.s^{-1}.cm^{-3}$)

T9	**RRana**	**Err/%**	**RRexp**	**Err/%**	**T9**	**RRana**	**Err/%**	**RRexp**	**Err/%**
10^9	$mol.s^{-1}.cm^{-3}$		$mol.s^{-1}.cm^{-3}$		10^9	$mol.s^{-1}.cm^{-3}$		$mol.s^{-1}.cm^{-3}$	
0.0050	0.3157D-69	41.33	0.2323D-69	41.33	0.2650	0.6923D-12	5.47	0.6911D-12	5.47
0.0075	0.3432D-59	30.12	0.3094D-59	30.12	0.2675	0.7978D-12	5.46	0.7963D-12	5.46
0.0100	0.7304D-53	28.09	0.6935D-53	28.09	0.2700	0.9178D-12	5.45	0.9159D-12	5.45
0.0150	0.6193D-45	13.83	0.6328D-45	13.99	0.2725	0.1054D-11	5.44	0.1052D-11	5.45
0.0200	0.6109D-40	8.66	0.6331D-40	9.34	0.2750	0.1208D-11	5.43	0.1205D-11	5.44
0.0250	0.2154D-36	9.96	0.2164D-36	9.97	0.2775	0.1383D-11	5.42	0.1379D-11	5.43
0.0300	0.1085D-33	15.23	0.1054D-33	15.51	0.2800	0.1580D-11	5.41	0.1576D-11	5.42
0.0350	0.1550D-31	17.13	0.1496D-31	17.50	0.2825	0.1802D-11	5.40	0.1797D-11	5.41
0.0400	0.9245D-30	14.66	0.9059D-30	14.81	0.2850	0.2052D-11	5.40	0.2047D-11	5.40
0.0450	0.2916D-28	11.62	0.2907D-28	11.62	0.2875	0.2333D-11	5.39	0.2327D-11	5.39
0.0500	0.5677D-27	9.93	0.5706D-27	9.94	0.2900	0.2649D-11	5.38	0.2642D-11	5.38
0.0550	0.7586D-26	9.78	0.7610D-26	9.78	0.2925	0.3003D-11	5.37	0.2995D-11	5.38
0.0600	0.7505D-25	10.95	0.7461D-25	10.96	0.2950	0.3400D-11	5.36	0.3390D-11	5.37
0.0650	0.5813D-24	13.06	0.5710D-24	13.19	0.2975	0.3843D-11	5.35	0.3832D-11	5.36
0.0700	0.3675D-23	15.55	0.3570D-23	15.82	0.3000	0.4338D-11	5.34	0.4326D-11	5.35
0.0750	0.1960D-22	17.77	0.1888D-22	18.17	0.3050	0.5505D-11	5.33	0.5490D-11	5.33
0.0800	0.9041D-22	19.29	0.8666D-22	19.77	0.3100	0.6949D-11	5.31	0.6930D-11	5.32
0.0850	0.3682D-21	19.91	0.3524D-21	20.41	0.3200	0.1091D-10	5.28	0.1088D-10	5.28
0.0900	0.1347D-20	19.67	0.1290D-20	20.15	0.3300	0.1680D-10	5.25	0.1676D-10	5.25
0.0950	0.4481D-20	18.76	0.4306D-20	19.19	0.3400	0.2543D-10	5.22	0.2537D-10	5.22
0.1000	0.1372D-19	17.40	0.1324D-19	17.78	0.3500	0.3786D-10	5.19	0.3779D-10	5.19
0.1025	0.2334D-19	16.63	0.2258D-19	16.97	0.3600	0.5552D-10	5.16	0.5544D-10	5.16
0.1050	0.3904D-19	15.83	0.3785D-19	16.13	0.3700	0.8026D-10	5.14	0.8019D-10	5.14

0.1075	0.6421D-19	15.01	0.6242D-19	15.28	0.3800	0.1145D-09	5.11	0.1144D-09	5.11
0.1100	0.1040D-18	14.20	0.1013D-18	14.44	0.3900	0.1613D-09	5.09	0.1613D-09	5.09
0.1125	0.1660D-18	13.41	0.1621D-18	13.62	0.4000	0.2245D-09	5.06	0.2246D-09	5.06
0.1150	0.2613D-18	12.65	0.2558D-18	12.82	0.4100	0.3091D-09	5.04	0.3094D-09	5.04
0.1175	0.4058D-18	11.92	0.3983D-18	12.07	0.4200	0.4212D-09	5.02	0.4217D-09	5.02
0.1200	0.6224D-18	11.24	0.6122D-18	11.37	0.4300	0.5682D-09	5.00	0.5691D-09	5.00
0.1225	0.9433D-18	10.61	0.9298D-18	10.71	0.4400	0.7595D-09	4.98	0.7609D-09	4.98
0.1250	0.1413D-17	10.03	0.1396D-17	10.11	0.4500	0.1006D-08	4.96	0.1008D-08	4.97
0.1275	0.2095D-17	9.50	0.2073D-17	9.56	0.4600	0.1322D-08	4.94	0.1325D-08	4.95
0.1300	0.3073D-17	9.02	0.3046D-17	9.07	0.4700	0.1723D-08	4.93	0.1728D-08	4.93
0.1325	0.4463D-17	8.59	0.4431D-17	8.62	0.4800	0.2229D-08	4.91	0.2235D-08	4.92
0.1350	0.6421D-17	8.21	0.6384D-17	8.23	0.4900	0.2862D-08	4.89	0.2871D-08	4.90
0.1375	0.9155D-17	7.87	0.9114D-17	7.88	0.5000	0.3651D-08	4.88	0.3663D-08	4.89
0.1400	0.1294D-16	7.57	0.1290D-16	7.58	0.5250	0.6524D-08	4.84	0.6547D-08	4.85
0.1425	0.1814D-16	7.31	0.1810D-16	7.32	0.5500	0.1124D-07	4.81	0.1128D-07	4.82
0.1450	0.2522D-16	7.09	0.2519D-16	7.09	0.5750	0.1875D-07	4.77	0.1882D-07	4.79
0.1475	0.3480D-16	6.89	0.3480D-16	6.89	0.6000	0.3038D-07	4.74	0.3048D-07	4.76
0.1500	0.4766D-16	6.72	0.4770D-16	6.73	0.6250	0.4794D-07	4.72	0.4808D-07	4.73
0.1525	0.6482D-16	6.58	0.6493D-16	6.58	0.6500	0.7386D-07	4.69	0.7403D-07	4.70
0.1550	0.8756D-16	6.46	0.8777D-16	6.46	0.6750	0.1113D-06	4.67	0.1115D-06	4.67
0.1575	0.1175D-15	6.35	0.1179D-15	6.36	0.7000	0.1645D-06	4.64	0.1646D-06	4.64
0.1600	0.1567D-15	6.26	0.1573D-15	6.27	0.7500	0.3404D-06	4.60	0.3401D-06	4.60
0.1625	0.2077D-15	6.19	0.2085D-15	6.20	0.8000	0.6618D-06	4.55	0.6600D-06	4.56
0.1650	0.2737D-15	6.12	0.2749D-15	6.14	0.8500	0.1220D-05	4.51	0.1214D-05	4.53
0.1675	0.3587D-15	6.07	0.3603D-15	6.09	0.9000	0.2147D-05	4.47	0.2133D-05	4.51
0.1700	0.4674D-15	6.02	0.4697D-15	6.04	0.9500	0.3628D-05	4.42	0.3600D-05	4.49
0.1725	0.6059D-15	5.98	0.6090D-15	6.00	1.0000	0.5919D-05	4.37	0.5866D-05	4.46
0.1750	0.7815D-15	5.94	0.7856D-15	5.97	1.1250	0.1768D-04	4.23	0.1751D-04	4.34
0.1775	0.1003D-14	5.91	0.1008D-14	5.94	1.2500	0.4560D-04	4.06	0.4527D-04	4.13
0.1800	0.1281D-14	5.89	0.1288D-14	5.91	1.3750	0.1054D-03	3.85	0.1050D-03	3.87
0.1825	0.1629D-14	5.86	0.1638D-14	5.89	1.5000	0.2238D-03	3.61	0.2240D-03	3.61
0.1850	0.2062D-14	5.84	0.2073D-14	5.87	1.6250	0.4453D-03	3.35	0.4470D-03	3.37
0.1875	0.2599D-14	5.82	0.2613D-14	5.85	1.7500	0.8397D-03	3.07	0.8439D-03	3.11
0.1900	0.3261D-14	5.80	0.3279D-14	5.83	1.8000	0.1068D-02	2.96	0.1073D-02	3.00
0.1925	0.4077D-14	5.79	0.4098D-14	5.81	1.9000	0.1693D-02	2.75	0.1700D-02	2.78
0.1950	0.5076D-14	5.77	0.5102D-14	5.79	2.0000	0.2615D-02	2.54	0.2622D-02	2.55
0.1970	0.6033D-14	5.76	0.6062D-14	5.78	2.1000	0.3943D-02	2.36	0.3947D-02	2.36
0.1980	0.6571D-14	5.76	0.6602D-14	5.78	2.2500	0.7003D-02	2.12	0.6995D-02	2.12
0.1990	0.7152D-14	5.75	0.7186D-14	5.77	2.5000	0.1650D-01	1.85	0.1646D-01	1.87
0.2000	0.7781D-14	5.75	0.7817D-14	5.76	2.7500	0.3496D-01	1.73	0.3490D-01	1.73

0.2010	0.8460D-14	5.74	0.8499D-14	5.76	3.0000	0.6791D-01	1.70	0.6791D-01	1.70
0.2020	0.9193D-14	5.74	0.9234D-14	5.75	3.2500	0.1230D+00	1.78	0.1231D+00	1.78
0.2030	0.9984D-14	5.73	0.1003D-13	5.75	3.5000	0.2105D+00	2.19	0.2107D+00	2.19
0.2050	0.1176D-13	5.72	0.1181D-13	5.74	3.7500	0.3441D+00	3.37	0.3439D+00	3.37
0.2075	0.1438D-13	5.71	0.1443D-13	5.72	3.8000	0.3777D+00	3.74	0.3775D+00	3.74
0.2100	0.1752D-13	5.70	0.1759D-13	5.71	3.8500	0.4141D+00	4.15	0.4138D+00	4.15
0.2125	0.2129D-13	5.69	0.2137D-13	5.70	3.9000	0.4534D+00	4.62	0.4529D+00	4.62
0.2150	0.2579D-13	5.67	0.2587D-13	5.68	3.9500	0.4956D+00	5.13	0.4951D+00	5.13
0.2175	0.3115D-13	5.66	0.3123D-13	5.67	4.0000	0.5411D+00	5.70	0.5404D+00	5.70
0.2200	0.3750D-13	5.65	0.3760D-13	5.66	4.0500	0.5900D+00	6.32	0.5892D+00	6.32
0.2225	0.4502D-13	5.64	0.4512D-13	5.65	4.1000	0.6424D+00	6.99	0.6416D+00	6.99
0.2250	0.5390D-13	5.63	0.5401D-13	5.63	4.2500	0.8236D+00	9.34	0.8228D+00	9.34
0.2275	0.6436D-13	5.62	0.6447D-13	5.62	4.5000	0.1218D+01	14.38	0.1220D+01	14.38
0.2300	0.7664D-13	5.61	0.7674D-13	5.61	4.7500	0.1758D+01	20.75	0.1768D+01	20.76
0.2325	0.9103D-13	5.60	0.9113D-13	5.60	5.0000	0.2480D+01	28.33	0.2512D+01	28.36
0.2350	0.1079D-12	5.59	0.1079D-12	5.59	5.5000	0.4647D+01	46.13	0.4803D+01	46.24
0.2375	0.1275D-12	5.58	0.1275D-12	5.58	6.0000	0.8127D+01	65.65	0.8600D+01	65.88
0.2400	0.1503D-12	5.57	0.1503D-12	5.57	6.5000	0.1339D+02	85.12	0.1450D+02	85.46
0.2425	0.1768D-12	5.56	0.1768D-12	5.56	7.0000	0.2096D+02	103.43	0.2314D+02	103.86
0.2450	0.2075D-12	5.55	0.2074D-12	5.55	7.5000	0.3135D+02	120.07	0.3514D+02	120.55
0.2475	0.2430D-12	5.54	0.2429D-12	5.54	8.0000	0.4507D+02	134.89	0.5104D+02	135.40
0.2500	0.2839D-12	5.53	0.2837D-12	5.53	8.5000	0.6254D+02	147.96	0.7129D+02	148.47
0.2525	0.3310D-12	5.52	0.3307D-12	5.52	9.0000	0.8409D+02	159.43	0.9620D+02	159.93
0.2550	0.3852D-12	5.51	0.3848D-12	5.51	9.5000	0.1099D+03	169.47	0.1260D+03	169.95
0.2575	0.4473D-12	5.50	0.4467D-12	5.50	10.0000	0.1399D+03	178.26	0.1606D+03	178.72
0.2600	0.5184D-12	5.49	0.5177D-12	5.49	10.5000	0.1739D+03	185.94	0.2001D+03	186.41
0.2625	0.5996D-12	5.48	0.5987D-12	5.48	11.0000	0.2113D+03	192.67	0.2442D+03	193.15

Appendix. V. 3. The calculated STOT factor and its error of RAC2015 at 660Ecm

Ecm/ MeV	Stot/ keV b	STD/ keV b	E_{cm}/ MeV	Stot/ keV b	STD/ keV b	E_{cm}/ MeV	Stot/ keV b	STD/ keV b	E_{cm}/ MeV	Stot/ keV b	STD/ keV b
0.0037	7138.90	667.06	0.8700	42.86	4.66	2.7150	37.06	8.26	5.9100	1093.00	91.74
0.0075	4214.80	569.83	0.8775	42.48	4.65	2.7300	29.11	5.78	5.9325	1333.60	152.95
0.0112	3305.50	463.25	0.8850	42.11	4.65	2.7450	25.50	4.57	5.9550	1614.60	260.77
0.0150	2919.50	416.15	0.8925	41.76	4.64	2.7600	23.51	3.69	5.9775	1767.70	368.74
0.0188	2552.50	313.38	0.9000	41.41	4.64	2.7750	22.04	3.09	6.0000	1460.80	431.24
0.0225	1587.30	336.79	0.9075	41.07	4.63	2.7900	20.80	2.63	6.0300	1011.60	505.89
0.0263	2035.90	347.86	0.9150	40.73	4.63	2.8050	19.83	39.90	6.0600	880.35	441.61
0.0300	1871.20	377.25	0.9225	40.41	4.62	2.8200	19.48	3.16	6.0900	1355.80	477.33

0.0338	1730.80	17.12	0.9300	40.09	4.62	2.8350	18.98	2.43	6.1230	2282.40	412.96
0.0375	1564.00	16.60	0.9375	39.78	4.61	2.8500	18.57	1.74	6.1500	267.77	429.40
0.0412	1444.40	38.04	0.9450	39.48	4.61	2.8650	18.24	1.60	6.1800	98.52	448.11
0.0450	1289.20	45.78	0.9525	39.18	4.60	2.8800	18.06	1.58	6.2100	65.79	170.22
0.0487	1160.20	45.36	0.9600	38.89	4.60	2.8950	17.90	1.58	6.2400	52.83	59.13
0.0525	1166.30	20.40	0.9675	38.61	4.59	2.9100	17.90	1.64	6.2700	45.39	34.50
0.0563	1095.30	8.95	0.9750	38.33	4.59	2.9250	18.15	2.34	6.3000	40.30	41.35
0.0600	1041.30	10.10	0.9825	38.06	4.58	2.9400	18.37	1.71	6.3300	36.53	46.77
0.0637	926.46	6.90	0.9900	37.80	4.57	2.9550	18.69	1.84	6.3600	33.60	48.80
0.0675	884.95	19.76	0.9975	37.54	4.57	2.9700	19.08	1.96	6.3900	31.26	48.82
0.0712	866.58	11.62	1.0050	37.29	4.56	2.9850	19.75	2.87	6.4200	29.38	47.82
0.0750	838.44	9.11	1.0125	37.04	4.55	3.0000	20.95	1.64	6.4500	27.82	46.31
0.0787	676.43	9.30	1.0200	36.80	4.55	3.0150	22.16	1.73	6.4800	26.53	44.59
0.0825	676.16	6.61	1.0275	36.56	4.54	3.0300	23.82	1.45	6.5100	25.45	42.83
0.0862	649.54	13.51	1.0350	36.33	4.53	3.0450	26.00	1.40	6.5400	24.52	41.12
0.0900	614.82	20.55	1.0425	36.11	4.52	3.0600	28.95	1.36	6.5700	23.72	39.51
0.0938	564.41	29.42	1.0500	35.89	4.52	3.0750	32.42	1.42	6.6000	23.00	38.10
0.0975	496.35	28.42	1.0575	35.68	4.51	3.0900	39.37	1.28	6.6300	22.31	37.00
0.1013	443.75	77.95	1.0650	35.47	4.50	3.1050	48.29	1.23	6.6600	21.57	36.38
0.1050	539.22	4.57	1.0725	35.26	4.49	3.1200	61.74	1.17	6.6900	20.63	36.75
0.1088	523.99	6.09	1.0800	35.06	4.48	3.1350	86.41	1.13	6.7200	19.43	38.78
0.1125	512.34	7.58	1.0875	34.87	4.47	3.1500	135.71	1.07	6.7500	20.61	36.95
0.1163	491.63	9.04	1.0950	34.68	4.47	3.1650	258.90	1.01	6.7800	22.13	36.05
0.1200	450.05	8.35	1.1025	34.49	4.46	3.1800	620.49	0.97	6.8100	22.85	38.58
0.1238	457.59	5.06	1.1100	34.31	4.45	3.1950	1471.40	0.77	6.8400	22.80	45.34
0.1275	450.43	6.27	1.1175	34.13	4.44	3.2100	713.25	0.84	6.8700	22.80	56.20
0.1312	442.33	7.26	1.1250	33.96	4.43	3.2250	258.92	0.93	6.9000	22.92	72.75
0.1350	430.27	7.38	1.1363	33.71	4.41	3.2400	122.98	0.96	6.9300	23.02	97.70
0.1388	415.57	7.34	1.1475	33.47	4.40	3.2550	72.57	1.00	6.9600	23.69	129.58
0.1425	402.01	7.19	1.1587	33.23	4.38	3.2700	48.34	1.06	6.9900	23.90	167.11
0.1462	387.70	7.17	1.1700	33.01	4.36	3.2850	36.61	1.09	7.0200	23.91	182.96
0.1500	370.07	8.38	1.1813	32.79	4.35	3.3000	28.20	1.17	7.0500	23.19	153.58
0.1538	294.74	27.95	1.1925	32.58	4.33	3.3150	23.31	1.26	7.0800	22.26	99.81
0.1575	303.21	23.22	1.2038	32.39	4.31	3.3300	20.03	1.49	7.1100	21.60	57.12
0.1612	299.22	23.23	1.2150	32.19	4.29	3.3450	17.75	1.58	7.1400	21.29	35.08
0.1650	294.75	24.23	1.2262	32.01	4.27	3.3600	16.10	1.90	7.1700	21.12	28.83
0.1687	291.39	21.06	1.2375	31.83	4.25	3.3750	14.92	1.81	7.2000	21.06	29.90
0.1725	289.12	16.08	1.2487	31.67	4.23	3.3900	14.06	1.33	7.2300	21.03	31.90
0.1762	287.91	11.57	1.2600	31.51	4.21	3.4050	13.40	1.33	7.2600	21.12	33.34
0.1800	281.68	10.39	1.2713	31.35	4.19	3.4200	12.90	1.32	7.2900	20.73	35.01

0.1838	278.81	31.79	1.2825	31.21	4.17	3.4350	12.51	1.31	7.3200	20.82	35.55
0.1875	274.77	5.83	1.2938	31.07	4.14	3.4500	12.23	1.30	7.3500	21.00	35.72
0.1912	217.52	95.90	1.3050	30.94	4.12	3.4650	12.03	1.29	7.3800	21.28	35.58
0.1950	236.10	45.80	1.3162	30.81	4.10	3.4800	11.83	1.40	7.4100	21.32	35.73
0.1987	244.78	22.65	1.3275	30.70	4.07	3.4950	11.72	1.37	7.4400	21.37	36.02
0.2025	249.04	9.58	1.3388	30.59	4.05	3.5100	11.66	1.26	7.4700	21.62	35.06
0.2063	247.79	4.75	1.3500	30.48	4.03	3.5250	11.67	1.23	7.5000	21.73	34.86
0.2100	246.27	3.94	1.3613	30.39	4.00	3.5400	11.71	1.20	7.5300	21.84	34.63
0.2138	242.31	4.49	1.3725	30.30	3.97	3.5550	11.73	1.30	7.5600	21.98	34.39
0.2175	238.87	5.19	1.3837	30.22	3.95	3.5700	11.77	1.45	7.5900	22.29	33.88
0.2212	236.05	6.54	1.3950	30.14	3.92	3.5850	11.80	1.77	7.6200	22.41	33.64
0.2250	231.08	6.50	1.4062	30.07	3.90	3.6000	12.06	1.28	7.6500	22.53	33.39
0.2288	226.28	6.47	1.4175	30.01	3.87	3.6150	12.18	1.24	7.6800	22.11	33.85
0.2325	221.65	6.42	1.4288	29.96	3.84	3.6300	12.34	1.79	7.7100	22.24	33.61
0.2362	217.19	6.39	1.4400	29.91	3.81	3.6450	12.50	1.19	7.7400	22.36	33.37
0.2400	212.87	6.35	1.4512	29.87	3.78	3.6600	12.85	1.17	7.7700	22.49	33.15
0.2437	208.70	6.32	1.4625	29.84	3.75	3.6750	13.09	1.18	7.8000	22.62	32.93
0.2475	204.66	6.30	1.4737	29.81	3.72	3.6900	13.34	1.20	7.8300	22.75	32.72
0.2512	200.76	6.26	1.4850	29.79	3.70	3.7050	13.58	1.23	7.8600	22.96	32.42
0.2550	196.98	6.23	1.4963	29.78	3.66	3.7200	13.87	1.27	7.8900	23.11	32.19
0.2587	193.33	6.19	1.5075	29.78	3.63	3.7350	14.17	1.32	7.9200	23.25	32.00
0.2625	189.79	6.16	1.5188	29.78	3.60	3.7500	14.52	2.02	7.9500	23.39	31.82
0.2662	186.35	6.14	1.5300	29.79	3.57	3.7725	15.08	2.60	7.9800	23.53	31.64
0.2700	183.03	6.11	1.5412	29.81	3.54	3.7950	15.75	2.01	8.0100	23.40	31.78
0.2738	179.80	6.08	1.5525	29.84	3.51	3.8175	16.15	1.24	8.0400	23.55	31.78
0.2775	176.67	6.05	1.5638	29.88	3.48	3.8400	16.94	1.90	8.0700	23.69	31.62
0.2812	173.63	6.03	1.5750	29.92	3.44	3.8625	17.77	1.25	8.1000	23.83	31.46
0.2850	170.68	6.01	1.5863	29.98	3.41	3.8850	18.83	1.28	8.1300	23.97	31.31
0.2887	167.82	5.98	1.5975	30.04	3.38	3.9075	20.11	1.50	8.1600	24.11	31.17
0.2925	165.04	5.95	1.6087	30.11	3.34	3.9345	332.39	9.97	8.1900	24.26	31.03
0.2963	162.34	5.93	1.6200	30.19	3.31	3.9525	22.13	1.72	8.2200	24.41	30.89
0.3000	**159.71**	**5.90**	1.6312	30.28	3.27	3.9750	23.65	1.48	8.2500	24.56	30.76
0.3038	157.16	5.88	1.6425	30.38	3.24	3.9975	25.42	1.50	8.2800	24.70	30.81
0.3075	154.67	5.86	1.6537	30.49	3.21	4.0200	27.26	1.44	8.3100	24.94	30.57
0.3113	152.25	5.84	1.6650	30.61	3.17	4.0425	29.68	1.52	8.3400	25.20	30.35
0.3150	149.90	5.81	1.6762	30.75	3.14	4.0650	32.44	1.15	8.3700	25.35	30.22
0.3188	147.61	5.79	1.6875	30.89	3.10	4.0875	34.78	1.25	8.4000	25.53	30.16
0.3225	145.38	5.77	1.6988	31.05	3.06	4.1100	38.74	1.11	8.4300	25.67	29.96
0.3263	143.21	5.75	1.7100	31.22	3.03	4.1325	43.23	1.14	8.4600	25.86	30.04
0.3300	206.23	5.63	1.7213	31.40	2.99	4.1550	49.31	1.12	8.4900	26.01	29.95

0.3338	139.03	5.71	1.7325	31.59	2.95	4.1775	55.77	1.11	8.5200	26.16	30.02
0.3375	137.02	5.69	1.7438	31.80	2.91	4.2000	65.67	1.11	8.5500	26.32	29.76
0.3413	135.07	5.67	1.7550	32.03	2.87	4.2225	88.30	0.99	8.5800	26.45	29.56
0.3450	133.15	5.65	1.7663	32.27	2.84	4.2450	115.56	0.98	8.6100	26.67	29.48
0.3487	131.29	5.63	1.7775	32.53	2.80	4.2675	160.78	0.96	8.6400	27.37	28.93
0.3525	129.47	5.61	1.7887	32.80	2.76	4.2900	238.77	0.94	8.6700	27.62	28.94
0.3562	127.70	5.60	1.8000	33.09	2.72	4.3125	392.54	1.15	8.7000	27.86	28.76
0.3600	125.97	5.58	1.8112	33.40	2.68	4.3350	680.07	0.98	8.7300	28.08	28.75
0.3638	124.28	5.56	1.8225	33.73	2.64	4.3575	746.04	1.21	8.7600	28.34	28.71
0.3675	122.62	5.54	1.8338	34.08	2.60	4.3800	546.89	1.25	8.7900	28.60	28.68
0.3713	121.01	5.52	1.8450	34.46	2.56	4.4025	301.93	2.41	8.8200	28.81	28.78
0.3750	119.44	5.51	1.8562	34.85	2.51	4.4250	199.76	1.63	8.8500	29.04	28.68
0.3825	116.39	5.47	1.8675	35.27	2.47	4.4475	129.00	1.94	8.8800	28.82	28.89
0.3900	113.49	5.44	1.8788	35.72	2.43	4.4700	95.89	2.04	8.9100	28.99	28.86
0.3975	110.71	5.41	1.8900	36.19	2.39	4.4925	73.68	2.25	8.9400	29.11	28.74
0.4050	108.05	5.38	1.9013	36.70	2.34	4.5150	57.28	2.56	8.9700	29.25	28.37
0.4125	105.50	5.35	1.9125	37.23	2.30	4.5375	42.44	8.55	9.0000	29.32	27.67
0.4200	103.06	5.32	1.9238	37.80	2.26	4.5600	38.31	4.15	9.0375	29.35	28.71
0.4275	100.72	5.30	1.9350	38.40	2.21	4.5825	35.18	3.71	9.0750	29.34	29.94
0.4350	98.47	5.27	1.9462	39.05	2.17	4.6050	32.46	3.51	9.1125	29.28	30.49
0.4425	96.32	5.25	1.9575	39.73	2.12	4.6275	29.25	5.00	9.1500	29.19	30.83
0.4500	94.25	5.22	1.9688	40.45	2.07	4.6500	27.50	4.04	9.1875	29.05	31.67
0.4575	92.26	5.21	1.9800	41.22	2.03	4.6725	26.18	4.12	9.2250	28.88	32.31
0.4650	90.35	5.18	1.9913	42.04	1.98	4.6950	24.95	4.35	9.2625	28.64	32.88
0.4725	88.50	5.16	2.0025	42.90	1.93	4.7175	24.06	4.59	9.3000	28.35	33.39
0.4800	86.73	5.14	2.0138	43.83	1.89	4.7400	23.41	4.84	9.3375	27.99	33.72
0.4875	85.03	5.11	2.0250	44.81	1.84	4.7625	23.01	5.12	9.3750	27.57	34.37
0.4950	83.38	5.09	2.0362	45.85	1.79	4.7850	22.84	5.43	9.4125	27.05	34.97
0.5025	81.80	5.08	2.0475	46.95	1.74	4.8075	22.90	5.80	9.4500	26.45	36.34
0.5100	80.27	5.05	2.0587	48.13	1.69	4.8300	23.18	6.23	9.4875	25.75	37.42
0.5175	78.80	5.05	2.0700	49.38	1.64	4.8667	88.99	22.77	9.5250	24.96	38.59
0.5250	77.37	5.03	2.0813	50.71	1.59	4.8750	23.62	10.42	9.5625	24.13	40.06
0.5325	76.00	5.00	2.0925	52.13	1.54	4.8975	25.28	8.08	9.6000	23.30	41.49
0.5400	74.67	4.99	2.1037	53.64	1.49	4.9200	26.92	8.89	9.6375	22.62	43.31
0.5475	73.39	4.97	2.1150	55.24	1.44	4.9425	28.90	10.13	9.6750	22.20	41.75
0.5550	72.14	4.96	2.1263	56.94	1.39	4.9650	31.80	11.76	9.7125	22.26	44.01
0.5625	70.94	4.94	2.1375	58.75	1.34	4.9875	33.26	8.88	9.7500	22.88	46.28
0.5700	69.78	4.93	2.1488	60.66	1.29	5.0100	37.03	9.59	9.7875	24.03	44.96
0.5775	68.66	4.92	2.1600	62.69	1.24	5.0325	42.09	9.85	9.8250	26.01	42.50
0.5850	67.57	4.91	2.1712	64.82	1.18	5.0550	48.78	10.18	9.8625	27.71	40.25

0.5925	66.52	4.90	2.1825	67.06	1.13	5.0775	57.74	10.51	9.9000	29.34	38.18
0.6000	65.50	4.89	2.1937	69.42	1.08	5.1000	69.95	10.90	9.9375	30.86	36.68
0.6075	64.51	4.87	2.2050	71.87	1.03	5.1225	87.14	11.25	9.9750	32.19	35.20
0.6150	63.55	4.86	2.2162	74.42	0.99	5.1450	112.06	11.60	10.0125	33.35	34.09
0.6225	62.62	4.85	2.2275	77.04	1.00	5.1675	149.57	11.94	10.0500	34.37	33.30
0.6300	61.71	4.84	2.2387	79.71	1.06	5.1900	208.49	12.26	10.0875	35.25	32.73
0.6375	60.84	4.83	2.2500	82.41	1.35	5.2125	305.79	12.55	10.1250	36.02	32.32
0.6450	59.99	4.82	2.2650	86.00	2.63	5.2350	474.42	12.80	10.1625	36.71	31.97
0.6525	59.16	4.82	2.2800	89.52	0.81	5.2575	770.73	12.96	10.2000	37.32	31.77
0.6600	58.36	4.81	2.2950	92.76	0.67	5.2800	1229.30	12.94	10.2375	37.87	31.63
0.6675	57.58	4.80	2.3100	95.58	0.58	5.3025	1611.50	12.65	10.2750	38.17	31.68
0.6750	56.82	4.79	2.3250	97.82	0.52	5.3250	1477.60	12.31	10.3125	38.40	31.78
0.6825	56.09	4.78	2.3400	99.26	0.50	5.3475	1067.70	12.25	10.3500	38.83	31.74
0.6900	55.37	4.78	2.3550	99.78	0.56	5.3700	738.94	12.37	10.3875	39.23	31.71
0.6975	54.68	4.77	2.3700	99.25	4.07	5.3925	531.61	12.52	10.4250	39.62	31.70
0.7050	54.00	4.76	2.3850	97.63	0.47	5.4150	403.74	12.68	10.4625	39.99	31.70
0.7125	53.34	4.76	2.4000	94.95	0.47	5.4375	322.45	12.84	10.5000	40.32	31.71
0.7200	52.70	4.75	2.4150	91.31	0.49	5.4600	268.72	13.00	10.5375	40.67	31.62
0.7275	52.08	4.75	2.4300	86.91	0.52	5.4825	232.37	13.17	10.5750	41.00	31.64
0.7350	51.47	4.74	2.4450	81.95	0.55	5.5050	207.22	13.36	10.6125	41.32	31.66
0.7425	50.88	4.74	2.4600	76.65	0.59	5.5275	189.84	13.58	10.6500	41.65	31.68
0.7500	50.31	4.73	2.4750	71.23	0.65	5.5500	178.12	13.85	10.6875	41.96	31.71
0.7575	49.75	4.73	2.4900	65.86	0.71	5.5725	170.79	14.18	10.7250	42.27	31.73
0.7650	49.20	4.72	2.5050	60.68	0.78	5.5950	167.10	14.60	10.7625	42.58	31.76
0.7725	48.67	4.72	2.5200	55.79	0.87	5.6175	166.70	15.14	10.8000	42.88	31.79
0.7800	48.15	4.71	2.5350	51.24	0.98	5.6400	169.45	15.82	10.8375	43.19	31.82
0.7875	47.65	4.71	2.5500	47.07	1.10	5.6625	175.56	16.68	10.8750	43.49	31.86
0.7950	47.16	4.70	2.5650	43.28	1.26	5.6850	185.43	17.76	10.9125	43.79	31.89
0.8025	46.68	4.70	2.5800	39.88	1.47	5.7075	199.85	19.15	10.9500	44.08	31.93
0.8100	46.21	4.69	2.5950	36.87	1.76	5.7300	220.03	20.89	10.9875	45.44	31.38
0.8175	45.75	4.69	2.6100	34.25	2.16	5.7525	247.90	23.07	11.0250	45.48	31.58
0.8250	45.31	4.68	2.6250	32.11	2.77	5.7750	286.54	25.77	11.0625	45.78	31.61
0.8325	44.87	4.68	2.6400	30.75	3.83	5.7975	340.17	29.21	11.1000	46.10	31.66
0.8400	44.45	4.67	2.6550	31.55	6.04	5.8200	416.13	33.47	11.1375	46.40	31.70
0.8475	44.04	4.67	2.6700	46.07	11.99	5.8425	522.83	39.34	11.1750	46.70	31.75
0.8550	43.63	4.66	2.6835	597.17	18.69	5.8650	671.01	48.03	11.2125	47.00	31.79
0.8625	43.24	4.66	2.7000	75.33	14.41	5.8875	865.47	62.76	11.2500	47.43	31.75

Appendix. VI. Basic formulae used in RAC2015 (Lane1958)

The practical formulas of RAC are introduced from the literature (Lane1958), (Smith1991), (Barker1991) and (Chen2003), and so on. On the R-matrix and the reaction cross sections, the codes were strictly compiled in accordance with the formula of classic literatures (Lane1958), without any approximation. Here only introduce the part of development.

For the positive energy channel, the incoming (I) and outgoing wave (O) function as follow

$$I_c^+ = (G_c - iF_c)\exp(i\omega_c)\,;\; O_c^+ = (G_c + iF_c)\exp(-i\omega_c)\ , \qquad \text{S-AP.VI.1}$$

For the negative energy channel, the only outgoing wave (O) function

$$O_c^- = W\left(-\eta_\alpha, l+\frac{1}{2}; 2\rho_\alpha\right)\ , \qquad \text{S-AP.VI.2}$$

$$\omega_c \equiv \omega_{\alpha l} = \sigma_{\alpha l} - \sigma_{\alpha 0} = \textstyle\sum_{n=1}^{l} tan^{-1}(\eta_\alpha/n). \qquad \text{S-AP.VI.3}$$

The logarithmic derivative of O-type wave function is designated as

$$L_c \equiv \left(\frac{\rho_c O_c'}{O_c}\right)_{r_c=a_c} = S_c + iP_c\ . \qquad \text{S-AP.VI.4}$$

The real and imaginary parts of which are, according to (4.1.1b), (4.1.2), respectively,

$$S_c^+ = \left[\frac{\rho_c(F_cF_c' - G_cG_c')}{F_c^2+G_c^2}\right]_{r_c=a_c} \qquad \text{S-AP.VI.5}$$

$$S_c^- = \left(\frac{\rho_c W_c'}{W_c}\right)_{r_c=a_c}\ , \qquad \text{S-AP.VI.6}$$

$$P_c^+ = \left[\frac{\rho_c}{F_c^2+G_c^2}\right]_{r_c=a_c}, \qquad \text{S-AP.VI.7}$$

$$P_c^- = zero, \qquad \text{S-AP.VI.8}$$

In the case of the positive energy channels, the ratio

$$\Omega_c^+ = (I_c/O_c)^{1/2}_{r_c=a_c}\ . \qquad \text{S-AP.VI.9}$$

It is a unit-modulus complex number which is expressible as

$$\Omega_c^+ \equiv \Omega_{\alpha l}^+ = exp\, i(\omega_c - \phi_c^+)\ ,$$

$$\phi_c^+ \equiv \phi_{\alpha l}^+ = tan^{-1}(F_c/G_c), \qquad \text{S-AP.VI.10}$$

We also introduce $\mathfrak{L}_c = (\rho_c I_c'/I_c)_{r_c=a_c};\ \mathfrak{B}_c = (\rho_c/I_c O_c)_{r_c=a_c}\ .$ S-AP.VI.11

The Wronskian $\omega = (O_c'I_c - I_c'O_c)_{r_c=a_c}$ S-AP.VI.12

The relation between the R-matrix and the collision matrix U is

$$\mathrm{U^J} = \Omega \mathrm{W^J} \Omega; \qquad \text{S-AP.VI.13}$$

$$\mathrm{W}^J = 1 + \mathfrak{B}^{\frac{1}{2}}(1 - \mathrm{R^J L^0})^{-1}\mathrm{R^J} L \mathfrak{B}^{\frac{1}{2}} w \qquad \text{S-AP.VI.14}$$

Where, $\mathrm{L^0} = \mathrm{L} - \mathrm{B},$ S-AP.VI.15

$$B_c \equiv \frac{\delta_{\lambda c}}{\gamma_{\lambda c}} = \frac{D_{\lambda c}}{V_{\lambda c}} \qquad \text{S-AP.VI.16}$$

The formula of R-matrix, level matrix and energy shift

$$(\mathrm{R}^J_{(E)})_{\alpha' s' l', \alpha s l} = \textstyle\sum_{\lambda\mu}^{N} \gamma^J_{\alpha' s' l'} \gamma^J_{\alpha s l} A_{\lambda\mu} \delta_{JJ_0} \qquad \text{S-AP.VI.17}$$

$$[A^{-1}]_{\lambda\mu} = \left[E_\lambda^r - E - \Delta^r_{\lambda\mu}(E_\lambda^r)\right]\delta_{\lambda\mu} + \Delta^e_{\lambda\mu}(E_\lambda^r) - \frac{i}{2}\Gamma^e_{\lambda\mu}, \qquad \text{S-AP.VI.18}$$

$$\Delta_{\lambda\mu} = -\textstyle\sum_{\alpha s l}^{N} (\mathrm{S}_{\lambda\mu} - \mathrm{B}_\alpha)\gamma_{\alpha' s' l'}\gamma_{\alpha s l} \qquad \text{S-AP.VI.19}$$

With the relation between T-matrix and U-matrix of formula the cross section formulae are:

$$T^J_{\alpha' s' l', \alpha s l} = e^{2i\omega_{\alpha l}}\delta_{\alpha' s' l', \alpha s l} - U^J_{\alpha' s' l', \alpha s l} \qquad \text{S-AP.VI.20}$$

$$\sigma_{\alpha',a} == \frac{\pi}{k_\alpha^2}\sum_{sl's'lJ} g_J \left|T^J_{\alpha's'l',asl}\right|^2 \quad \text{S-AP.VI.21}$$

$$\sigma_{tot} = \frac{\pi}{k_\alpha^2}\sum_{slJ} 2g_J\,(1 - \mathrm{Re}U^J_{asl,asl}) \quad \text{S-AP.VI.22}$$

$$g_J = \frac{(2J+1)}{(2I_1+1)(2I_2+1)} \quad \text{S-AP.VI.23}$$

$$\frac{d\sigma_{\alpha\alpha'}}{d\Omega_{\alpha'}} = \frac{1}{(2I_1+1)(2I_2+1)}\sum_{ss'\nu\nu'}\left|A_{\alpha's'\nu',as\nu}(\Omega_{\alpha'})\right|^2 \quad \text{S-AP.VI.24}$$

$$A_{\alpha's'\nu',as\nu} = \frac{\sqrt{\pi}}{k_\alpha}(-C_{\alpha'}(\theta_{\alpha'})\delta_{\alpha's'\nu',as\nu} + i\sum_{JMll'm'}\sqrt{2l+1}(sl\nu 0|JM)(s'l'\nu'm'|JM)T^J_{\alpha's'l',asl}Y^{(l')}_{m'}(\Omega_{\alpha'})) \quad \text{S-AP.VI.25}$$

Appendix. VII. Review for theory models, experiment data, previous analysis works

Appendix. VII. 1. The develop process of R-matrix Models for γ capture

A. Formulae and its parameterization in (Holt1978)

During the research of photodisintegration ^{17}O (γ, n) ^{16O} reaction with R matrix, the detailed derivation of the collision matrix element have been demonstrated in the paper (Holt1978). However, in the concrete analysis of ED, the specific formula of channel capture was turned down. The channel contributions component can be identified as the adjustable parameter of$(\delta\Gamma_{\mu f,c})^{1/2}$, reduced radiative width for the channel capture. The following is the derivation of this method.

The collision matrix will be expressed in terms of that part of the Hamiltonian H, which electromagnetically couples the photon to the nucleons. In order to calculate that matrix element it is necessary to introduce the wave function $\psi_{E(J)}$ which describes the neutrons, -nucleus state and a final wave function $\psi_{f(J_f)}$ which describes the nucleus with all nucleons in its ground state. The collision matrix is

$$U^{(J)}_{\gamma\mathcal{L}f,c} = \left[\frac{8\pi(\mathcal{L}+1)}{\mathcal{L}\hbar}\right]^{1/2}\frac{k_\gamma^{\mathcal{L}+1/2}}{(2\mathcal{L}+1)!!}\frac{\langle\psi_{f(J_f)}\|H^{(\mathcal{L})}\|\psi_{E(J)}\rangle}{(2J+1)^{1/2}}$$

Where, $k_\gamma = E_\gamma/\hbar$c is the photon wave number and the subscript c refers to the final particle channel with the quantum number(slJ). Here, s is the channel spin, l is the orbital angular momentum, $\boldsymbol{J} = \boldsymbol{s} + \boldsymbol{l}$ is the total angular momentum, and is the multi-polarity. The radial integration implied by Eq. (2) must be performed in two parts: from the origin to the channel radius and from the channel radius to infinity. Inside the channel radius R the wave function $\psi_{E(J)}$can be expanded in terms of a complete set of states X_λ

$$\psi_{E(J)} = i\hbar e^{-i\phi_c}\sum_{\lambda\mu} A_{\lambda\mu}\Gamma^{1/2}_{\mu c}X_{\lambda(J)}\,,\ \mathrm{r} < a_c$$

Where, $\phi_c$is the hard-sphere phase shift, $\Gamma_{\mu c}$is the width of the level μ in channel c. Equation (3) corresponds to unit incoming flux in channel c. $A_{\lambda\mu}$is the matrix transformation which relates the internal wave function and the observed resonances.

$$(A^{-1})_{\lambda\mu} = (E_\lambda - E) - \sum_c[(S_c - B_c) + iP_c]\,\gamma_{\lambda c}\gamma_{\mu c}$$

Where, E_λ is a level energy, the shift factorS_c, the boundary condition constantB_c, P_c is the penetration factor and $\gamma_{\lambda c}$ are the reduced width amplitudes. In the exterior region the wave function $\psi_{E(JM)}$ can be written in the customary manner in terms of the incomingI_c, and outgoing $O_c$spherical waves

$$\psi_{E(JM)} = v_c^{1/2}\left[I_c(k_c r) - U^{(J)}_{cc}O_c(k_c r)\right]\varphi_{c(JM)},\ \mathrm{r} \geq a_c$$

Where, we have assumed that c is the only open particle channel and have neglected contributions from closed channels. Here, v_c is the particle speed, $\varphi_{c(JM)} = r^{-1}(i^l Y_{lM})\psi_c$ is the surface function. U_{cc}Is the collision function for elastic scattering in channel c. For the moment we write the collision function in the form

$$U^{(J)}_{cc} = e^{-2i\phi_c}(1 + \sum_{\lambda\mu} A_{\lambda\mu}\Gamma^{1/2}_{\mu c}\Gamma^{1/2}_{\lambda c})$$

The last expression implies that we include all possible resonances in the analysis. Substitute Eq. (5) into Eq. (4) and then Eq. (3) and (4) into Eq. (2); the integration naturally splits into an internal segment ($\mathrm{r} < a_c$) and an external region ($\mathrm{r} \geq a_c$), the collision matrix becomes

$$U^{(J)}_{\gamma\mathcal{L}f,c} = ie^{-i\phi_c}\sum_{\lambda\mu} A_{\lambda\mu}\Gamma^{1/2}_{\lambda c}\Gamma^{1/2}_{\mu\gamma f}$$
$$+\left[\frac{8\pi(\mathcal{L}+1)}{\mathcal{L}\hbar v_c}\right]^{1/2}\frac{k_\gamma^{\mathcal{L}+1/2}}{(2\mathcal{L}+1)!!}(2J+1)^{-1/2}\langle\psi_{f(J_f)}\|H^{(\mathcal{L})}\|(I_c - e^{-2i\phi_c}O_c)\varphi_{c(J)}\rangle$$
$$-\left[\frac{8\pi(\mathcal{L}+1)}{\mathcal{L}\hbar v_c}\right]^{1/2}\frac{k_\gamma^{\mathcal{L}+1/2}}{(2\mathcal{L}+1)!!}(2J+1)^{-1/2}ie^{-2i\phi_c}\sum_{\lambda\mu}A_{\lambda\mu}\Gamma^{1/2}_{\mu c}\Gamma^{1/2}_{\lambda c}\langle\psi_{f(J_f)}\|H^{(\mathcal{L})}\|O_c\varphi_{c(J)}\rangle$$

Where we have made the identification that

$$\Gamma^{1/2}_{\mu\gamma f} = \left[\frac{8\pi(\mathcal{L}+1)}{\mathcal{L}}\right]^{1/2}\frac{k_\gamma^{\mathcal{L}+1/2}}{(2\mathcal{L}+1)!!}\frac{\langle\psi_{f(J_f)}\|H^{(\mathcal{L})}\|X_{\lambda(J)}\rangle}{(2J+1)^{1/2}}$$

This γ-ray width is that portion of the radiative capture strength that is due to the matrix element in the interior region. We note that this width has a real value. This width is sometimes referred to as the compound nuclear part of the radiative capture. It is expected that these radiative widths, in general, will not be correlated with the particle widths as in the case of direct capture resonances. Nevertheless, the first term in Eq. (6) is a resonant component. The second term contains no pole terms, and therefore, gives rise to a non-resonant component. This term is referred to as hard-sphere capture, since it depends only on the hard-sphere phase shift. The final term is due to resonant capture which occurs in the external region, i.e., outside the channel radius. This process is referred to as channel capture. The contribution from the last two terms in Eq (6) is due to the long-range nature. Of the electromagnetic interaction. The reduced radiative width for the channel capture component can be identified as

$$(\delta\Gamma_{\mu f,c})^{1/2} = \left[\frac{8\pi(\mathcal{L}+1)}{\mathcal{L}\hbar v_c}\right]^{1/2}\frac{k_\gamma^{\mathcal{L}+1/2}}{(2\mathcal{L}+1)!!}e^{-i\phi_c}(2J+1)^{-1/2}\Gamma^{1/2}_{\mu c}\langle\psi_{f(J_f)}\|H^{(\mathcal{L})}\|O_c\varphi_{c(J)}\rangle$$

Then the form for the collision matrix becomes

$$U^{(J)}_{\gamma\mathcal{L}f,c} = ie^{-i\phi_c}\sum_{\lambda\mu}A_{\lambda\mu}\Gamma^{1/2}_{\lambda c}\left[\Gamma^{1/2}_{\mu\gamma f} - (\delta\Gamma_{\mu f,c})^{1/2}\right] + U^{J}_{\gamma\mathcal{L}f,c}(H.S.)$$

Where $U^{J}_{\gamma\mathcal{L}f,c}(H.S.)$ is the hard-sphere component? Here $(\delta\Gamma_{\mu f,c})^{1/2}$is in general a complex quantity, since the outgoing wave function O is complex. It will be shown that the complex nature of $(\delta\Gamma_{\mu f,c})^{1/2}$ gives rise to unique features of radiative

$$\Gamma_{\gamma 0} = \left|\Gamma^{1/2}_{\mu\gamma f} - (\delta\Gamma_{\mu f,c})^{1/2}\right|^2$$

Comment： This paper made a big contribution for the old model to calculate γ transition. But it did not give out any special results.

B.The direct capture model of (Kettner1982)

The possible radiative capture amplitudes into the^{16}O ground state ($J^\pi = 0^+$) can be classified according to the orbital angular momentum *l* of the initial ^{4}He+ ^{12}C state (or equivalently the multipolarity L of the γ0-ray transition). Capture amplitudes with *l* =0 are expected to be small compared with other multipolarities, since they cannot proceed by single photon emission. Since multipolarities with L≥3 are extremely weak, the capture amplitudes are restricted to orbital angular momenta (multipolarities) of *l*= 1 (El) and *l* =2 (E2). The capture data were fitted with the expression:

$$\mathrm{S(E)} = S_{R1}(l=1,E) + S_{R2}(l=1,E) + 2\sqrt{S_{R1}(E)S_{R2}(E)}cos\alpha + S_{R3}(l=2,E) + S_{DC}(l=2,E) + 2\sqrt{S_{R3}(E)S_{DC}(E)}cos\beta$$

Where, the quantitiesS_{R1}, S_{R2} and S_{R3} refer to the S-factors of the resonances at$E_\gamma = -0.045(l=1), 2.418(l=1)$ and $E_\gamma = -0.245(l=2)$, respectively. These S-factors are given by

$$S_R(l,E) = Eexp(2\pi\eta)\pi\lambda^2(2l+1)\frac{\Gamma_\alpha(l,E)\Gamma_\gamma(l,E)}{(E_l+\Delta_l-E)^2+(\Gamma(E)/2)^2}$$

With the partial width$\Gamma_\alpha(l,E)$, $\Gamma_\gamma(l,E)$ and the total width $\Gamma(E)$

$$\Gamma_\alpha(l,E) = 2\gamma^2_{max}\theta^2_\alpha(l)P_l(E)$$
$$\Gamma_\gamma(l,E) = ((Q+E)/E_x)^{2L+1}\Gamma_\gamma(l,E_\gamma)$$
$$\Gamma(E) = \Gamma_\alpha(l,E) + \Gamma_\gamma(l,E)$$

The S-factor of the direct capture process is described by the nearly energy independent term (**Rolfs1973**)

$$S_{DC}(l=2,E)=(36.18+1.46\times E-1.36\times E^2)\times 10^{-3}\theta_\alpha^2(g.s.)\ \text{MeV.b}$$

The phase difference α of the two interfering l= 1 resonance amplitudes is given by the difference of their resonance phase shifts,

$$\alpha=\varepsilon_{R_1}(l=1)-\varepsilon_{R_2}(l=1)$$

And the phase difference β of the interfering l= 2 resonant and direct capture amplitudes by

$$\beta=\varepsilon_{R_3}(l=2)$$

Of course, the sign +of both interference terms in the above expression must be determined from the ED.).

Comment： This paper made a big contribution for direct capture process. The results show that the contribution from direct capture is a small part of total γ transition.

C.The detail calculation in (Barker1991)

On the basis of (Holt1978), the derivation and analytical process of three contributions to the collision matrix element are given in the paper (Barker1991), because isospin is expected to be a good quantum number in the channel region, one can neglect the channel contributions to El capture of $^{12}C(\alpha,\gamma)^{16}O$ reaction, and three contributions of E2 capture consideration.

Since the coupling of the nucleons to the electromagnetic field is weak, first-order perturbation theory is used, and the photon channel is treated in a different way from a normal particle channel. Here it give the formula only for the case of electric multipole radiation, the initial stateJ_i and final state $J_f$are described by R-matrix formulae.

For EL radiation to the final stateJ_f, the total cross section may be written

$$\sigma_{J_f}=\sum_{J_i}\sigma_{J_iJ_f}$$

$$\sigma_{J_iJ_f}=\frac{\pi}{k_a^2}\frac{2J_i+1}{(2I_a+1)(2I_A+1)}\sum_{S_el_i}\left|U^{J_i}_{S_el_i,l_f}\right|^2$$

Where,

$$U^{J_i}_{S_el_i,l_f}=-\mathrm{i}e^{i(\omega_i-\phi_i)}2P_{l_i}^{1/2}k_\gamma^{L+1/2}\left[\sum_{\lambda\mu}\gamma^{J_i}_{\lambda s_e l_i}\gamma^{J_i}_{\mu\gamma J_f}A^{J_i}_{\lambda\mu}+\frac{2\mu_e^{1/2}e_L}{\hbar k_a}\left\{\frac{(L+1)(2L+1)}{L}\right\}^{1/2}\frac{1}{(2L+1)!!}N_f^{1/2}a_e^L F_{l_i}(a_e)G_{l_i}(a_e)\right.$$

$$\left.\times\sum_{l_f}i^{l_i+L-l_f}\theta^{l_f}_{f\alpha_e s_e l_f}(l_iL00|l_f0)U(Ll_fJ_is_e;l_il_f)J'_L(l_i,l_f)\right]$$

Here the level matrix A^{J_i} is defined by its inverse

$$[(A^{J_i})^{-1}]_{\lambda\mu}=(E^{J_i}_\lambda-E)\delta_{\lambda\mu}-\sum_c(S_l-B_l+iP_l)\gamma^{J_i}_{\lambda c}\gamma^{J_i}_{\mu c}\quad(c=\alpha sl)$$

The photon reduced-width amplitude has internal and channel contributions

$$\gamma^{J_i}_{\mu\gamma J_f}=\gamma^{J_i}_{\mu\gamma J_f}(int)+\gamma^{J_i}_{\mu\gamma J_f}(ch)$$

Where,

$$\gamma^{J_i}_{\mu\gamma J_f}(int)=\left\{\frac{4\pi(L+1)}{L}\right\}^{1/2}\frac{1}{2L+1!!}\sum_{M_f}(J_f\mathrm{L}M_fM_i-M_f|J_iM_f)\times\left(X_{\mu J_iM_i}\left|\mathcal{H}^{(L)}_{EM_i-M_f}\right|\Phi_{fJ_fM_f}\right)_{\text{int}}$$

$$\mathcal{H}^{(L)}_{EM}=\sum_{i=1}^{A}e_ir_i^Li^LY_{LM}(\theta_i\phi_i)$$

$$\gamma_{\mu\gamma J_f}^{J_i}(ch) = \frac{2e_L}{\hbar}\left\{\frac{(L+1)(2L+1)}{L}\right\}^{1/2}\frac{1}{(2L+1)!!}N_f^{1/2} \times \sum_{cl_f'} \mu_c^{1/2} a_c^{L+1} \gamma_{\mu c}^{J_i} i^{l+L-l_f'} \theta_{f\alpha s l_f'}^{J_f}(lL00|l_f'0) U(Ll_f' J_i s; l l_f) J_{Lc}(l, l_f')$$

The normalization factor N_f for the final state is defined by

$$N_f^{-1} = 1 + \sum_{\alpha s l_f'} \frac{2(\theta_{f\alpha s l_f'}^{J_f})^2}{a_\alpha}\int_{a_\alpha}^{\infty} d\mathrm{r}\left[\frac{W_{\alpha s l_f'}(\mathrm{r})}{W_{\alpha s l_f'}(a_\alpha)}\right]^2$$

For energies *E* at which channel c is open, one has

$$J_{Lc}(l, l_f') = J_L''(l, l_f') + i\frac{F_l(a_c)G_l(a_c)}{F_l^2(a_c) + G_l^2(a_c)} J_L'(l, l_f')$$

Where,

$$J_L'(l, l_f') = \frac{1}{a_c^{L+1}}\int_{a_c}^{\infty} d\mathrm{r} r^L \frac{W_{\alpha s l_f'}(\mathrm{r})}{W_{\alpha s l_f'}(a_c)}\left[\frac{F_l(r)}{F_l(a_c)} - \frac{G_l(r)}{G_l(a_c)}\right]$$

$$J_L''(l, l_f') = \frac{1}{a_c^{L+1}}\int_{a_c}^{\infty} d\mathrm{r} r^L \frac{W_{\alpha s l_f'}(\mathrm{r})}{W_{\alpha s l_f'}(a_c)}\frac{F_l(a_c)F_l(r) + G_l(a_c)G_l(r)}{F_l^2(a_c) + G_l^2(a_c)}$$

And for energies E at which channel c is closed,

$$J_{Lc}(l, l_f') \equiv J_L^-(l, l_f') = \frac{1}{a_c^{L+1}}\int_{a_c}^{\infty} d\mathrm{r} r^L \frac{W_{\alpha s l_f'}(\mathrm{r}) W_{\alpha s l}(\mathrm{r})}{W_{\alpha s l_f'}(a_c) W_{\alpha s l}(a_c)}$$

Additional formulae for the dimensionless reduced width amplitude, reduced mass and effective charge are

$$\theta_{\lambda c}^J = \gamma_{\lambda c}^J (\hbar^2/\mu_c a_c^2)^{-1/2}$$

$$\mu_e = \frac{M_a M_A}{M_a + M_A}$$

$$e_L = \mu_e^L\left[\frac{Z_a}{M_a^L} + (-)^L\frac{Z_A}{M_A^L}\right]e$$

There are three contributions to the collision matrix element (4). The part of the photon reduced-width amplitude arising from integration over the internal region, $\gamma_{\mu\gamma J_f}^{J_i}(int)$ given by equation (7), leads to a resonant contribution of the standard R-matrix form (since $\gamma_{\mu\gamma J_f}^{J_i}(int)$ is real and constant). Another resonant contribution comes from integrations over the various channels, leading to $\gamma_{\mu\gamma J_f}^{J_i}(ch)$ given by equation (9), but in general $\gamma_{\mu\gamma J_f}^{J_i}(ch)$is neither real nor constant. There is also a no resonant contribution coming from the entrance channel only, which is often referred to as the hard-sphere capture amplitude.

Specialization to ^{12}C (α,γ) ^{16}O

Because isospin is expected to be a good quantum number in the channel region, one can neglect the channel contributions to El capture (note that e_L = 0 if the ^{4}He mass excess is neglected). Thus standard R-matrix formulae can be applied to the El component.

For low-energy a-particles (*E* < 4·44 MeV), the only open particle channel is ^{12}C (g.s.) +α, and we neglect contributions from all other channels. Then, omitting indices that have fixed values or are otherwise superfluous, we can write the formulae as

$$\sigma_{J_i J_f} = \frac{\pi}{k_a^2}(2J_i + 1)\sum_{S_e l_i}\left|U_{l_f}^{J_i}\right|^2$$

Where,

$$U_{l_f}^{J_i} = -\mathrm{i}e^{i(\omega_i - \phi_i)} 2P_{J_i}^{1/2} k_\gamma^{5/2}\sum_{\lambda\mu}\gamma_\lambda^{J_i}\gamma_{\mu\gamma J_f}^{J_i} A_{\lambda\mu}^{J_i} + \frac{3}{\sqrt{10}}\frac{M_n^{1/2} e}{\hbar k} N_f^{1/2} a^2 F_{J_i}(a) G_{J_i}(a)\theta_f^{J_f}(J_i 200|J_f 0) J_{L2}'(J_i, l_f)$$

With

$$[(A^{J_i})^{-1}]_{\lambda\mu} = (E_\lambda^{J_i} - E)\delta_{\lambda\mu} - \sum_c (S_{J_i} - B_{J_i} + iP_{J_i})\gamma_\lambda^{J_i}\gamma_\mu^{J_i}$$

$$\gamma_{\mu\gamma J_f}^{J_i}(ch) = \frac{3}{\sqrt{10}}\frac{M_n^{1/2}e}{\hbar k}N_f^{1/2}a^3 i^{J+2-J_f}\gamma_\mu^{J_i}\theta_f^{J_f}(J_i 200|J_f 0)\times\left[J'_{L2}(J_i,l_f) + i\frac{F_{J_i}(a)G_{J_i}(a)}{F_{J_i}^2(a)+G_{J_i}^2(a)}J'_{L2}(J_i,l_f)\right]$$

$$N_f^{-1} = 1 + \frac{2(\theta_f^{J_f})^2}{a}\int_a^\infty dr\left[\frac{W_{J_f}(r)}{J_f(a)}\right]^2$$

Because of the one-channel approximation, the resonant term in equation (***) can be written as

$$\sum_{\lambda\mu}\gamma_\lambda^{J_i}\gamma_{\mu\gamma J_f}^{J_i}A_{\lambda\mu}^{J_i} = \frac{\sum_\lambda \gamma_\lambda^{J_i}\gamma_{\mu\gamma J_f}^{J_i}/(E_\lambda^{J_i}-E)}{1-(S_{J_i}-B_{J_i}+iP_{J_i})\sum_\lambda(\gamma_\lambda^{J_i})^2/(E_\lambda^{J_i}-E)}$$

Comment： This paper made a big contribution for the old model to calculate γ carpture reaction. But, the results of calculation in this paper are far from the experimental data. Table S1.1 shows that the results are too higher to belive, the uncetainty are very larger.

RAC2015	**159±7.3**	**≈94**	**≈61**			
Schurman2012	161±21	83.4	73.4			
		Barker1991		$280^{\pm 230}_{-140}$	$150^{\pm 170}_{-50}$	$120^{\pm 60}_{-70}$

D.The simply application in (Angulo2000)

The capture cross section of order *L* from an initial state with spin $J_i\pi_i$ to a final state with spin $J_f\pi_f$ reads, in the *R*-matrix formalism

$$\sigma_L(E, J_i\pi_i \to J_f\pi_f) = \frac{8\pi(L+1)}{\hbar L(2L+1)!!}\frac{2J_f+1}{2J_i+1}k_\gamma^{2L+1}\times\left|\langle\psi^{J_f\pi_f}\middle|\mathcal{M}_L^E\middle|\psi_{int}^{J_i\pi_i}(E)\rangle_{int} + \langle\psi^{J_f\pi_f}\middle|\mathcal{M}_L^E\middle|\psi_{ext}^{J_i\pi_i}(E)\rangle_{ext}\right|^2$$

Where, $\psi^{J_f\pi_f}(\psi^{J_i\pi_i})$is the final (initial) wave function, k_γ is the photon wave number, and $\mathcal{M}_L^E$ is the electric multipole operator of order *L*. In definition (**), the first term of the right-hand side represents the internal contribution, while the second term represents the external part (subscript int (ext) refers to integration performed over the internal (external) region only). Notice that this latter contribution indirectly depends on the nuclear interaction through the collision matrix which appears in$\psi_{ext}^{J_i\pi_i}$. The relative importance of both components depends on the reaction and on the energy. For weakly bound systems, such as 7Be+*p*, the external contribution is strongly dominant, and Eq. (***) reduces to the extra nuclear capture approximation (Christy1961). In the present case, the binding energy of ^{16}O with respect to the α+^{12}C threshold in fairly large (7.16 MeV) and, up to a very good approximation, the external part can be neglected. In this approximation, the cross section reads

$$\sigma_L(E, J_i\pi_i \to J_f\pi_f) = \frac{\pi}{k^2}(2J_i+1)\frac{\left|\sum_\lambda \varepsilon_\lambda\left[\check{\Gamma}_\lambda^\alpha(E)\check{\Gamma}_\lambda^\gamma(E)\right]^{1/2}/(E_\lambda - E)\right|^2}{|1-LR^{J_i\pi_i}|^2}$$

Where, the formal α and γ widths are defined by

$$\check{\Gamma}_\lambda^\alpha(E) = 2\check{\gamma}_\lambda^\alpha P_J(E)$$

$$\check{\Gamma}_\lambda^\gamma(E) = \frac{8\pi(L+1)}{\hbar L(2L+1)!!}\frac{2J_f+1}{2J_i+1}k_\gamma^{2L+1}\times\left|\langle\psi^{J_f\pi_f}\middle|\mathcal{M}_L^E\middle|\chi_\lambda^{J_i\pi_i}(E)\rangle_{int}\right|^2$$

And $\varepsilon_\lambda$is a phase coefficient, equal to +1 or -1. The phase coefficients are written explicitly to account for the sign of the electromagnetic matrix elements. With this definition, the square root in Eq. (***) is always positive. The energy dependence of reads

$$\check{\Gamma}_\lambda^\gamma(E) = \check{\Gamma}_\lambda^\gamma(E_\gamma)\left(\frac{E-E_f}{E_\gamma - E_f}\right)^{2L+1}$$

Where, E_f is the energy of the final state and E_γ the resonance energy, in the following will be denoted as$\check{\Gamma}_\lambda^\gamma$, again $\check{\Gamma}_\lambda^\gamma$ must be considered either as a parameter, or as the result of a vibrational calculation involving basis states $\chi_\lambda^{J_i\pi_i}$.

Comment： This paper made a big contribution for explain of that the external contribution of ^{12}C (α, γ) ^{16}O is very small, and it can be ignored.

E. AZUMA: An *R*-matrix code for nuclear astrophysics

(PHYSICAL REVIEW C **81**, 045805 (2010))

On the models mentioned above (Lane1958, Lana1960, Hold1978, Barker1991), R. E. Azuma, *et.al.* Published the R-matrix code AZURE which allows simultaneous analysis the integrated and differential data. The part about elastic scattering is a copy of (Lane1958), here just list the part about ***Photon channels.***

The R-matrix theory described above is appropriate only for particle-particle reactions. In the internal region (enclosed by the boundary surface), photon channels can be included symmetrically with particle channels (21); however, it has often been found necessary to include an additional capture component attributed to the external region (beyond the boundary radius).

In A-matrix formalism, the internal transition matrix element connecting a particle channel c to a photon channel $p = \epsilon L \lambda_f$ takes the form

$$T_{cp}^{J,int} = -i \sum_{\lambda\lambda'} \Omega_c \Omega_p A_{\lambda\lambda'} \Gamma_{\lambda c}^{1/2} \Gamma_{\lambda' p}^{1/2} \tag{1.5}$$

Where

$$\Omega_p = 1, \Gamma_{\lambda' p} = 2 k_\gamma^{2L+1} \gamma_{\lambda' p}^{int\,2} \tag{1.6}$$

In the above expression, the term λ_f indicates the final state with some defined energy and total spin J_f and L is the multipolarity of the γ -ray. The symbol ϵ has been introduced to indicate the mode of the emitted radiation, where ϵ= 0 for magnetic transitions and ϵ = 1 for electric transitions. It should be noted that the internal transition matrix can also be written in *R*-matrix formalism if photon channels are included in the definition of the *R* matrix, and the photon penetrability is defined to be $P_\gamma = k_\gamma^{2L+1}$. Additionally, it is also often assumed that the resonant state is not significantly dampened by the γ decay, therefore the elements of the diagonal matrix **L0** are ignored for photon channels. In *A*-matrix formalism, this is tantamount to neglecting the photon channel from the channel sum in the definition of the *A* matrix. Such an assumption is not justified if the photon widths are appreciable compared to the particle widths, and in these cases proper photon channel Damping must be included.

In the external region, the scattering state contains contributions from both resonant and hard-sphere phase shifts (Lane1960, Holt1978). Throughout the remainder of this paper, the term EC will be associated with this no resonant portion, while the external resonance contribution will be designated by ERC. No resonant capture has been treated historically in two distinct but analogous ways. The term direct capture (DC) often refers specifically to the formulation in (Rolfs1973), while the term EC, defined above, is associated with the hard-sphere formulation. With the assumption of the hard-sphere phase shift and a square-well bound-state potential in DC, the two formalisms become identical.

A full multilevel multichannel external capture theory was introduced in Ref. (Barker1991), and the formalism used in AZURE is based on that work. This approach allows resonant and direct or external capture contributions to be combined in a self-consistent manner. Additionally, we follow Ref. (Angulo2001) and express the external capture in terms of the asymptotic normalization coefficient (ANC).

The following external capture equations apply for electric-multipole (EL) external capture transitions only, which are typically the most important cases in practice. The external portion of the transition matrix element is defined as

$$T_{cp}^{J,ext} = -i\Omega_c \sqrt{\frac{8(2L+1)(L+1)}{L\hbar}} \frac{k_\gamma^{L+1/2}}{(2L+1)!!}$$

$$\times\left[\sum_{l_f}\frac{i^{l+L-l_f}\bar{e}_\alpha^L}{v_\alpha^{1/2}}(l0L0|l_f0)U(Ll_fJs;lJ_f)R_{cl_fL}^{EC}+\sum_{c'l_f'}\frac{i^{l'+L-l_f'}\bar{e}_{\alpha'}^L}{v_\alpha^{1/2}}(l'0L0|l_f'0)(Ll_f'Js';l'J_f)R_{cc'l_f'L}^{ERC}\right] \quad (1.7)$$

Where

$$\bar{e}_\alpha^L = e\left[Z_{\alpha1}(\frac{M_{\alpha2}}{A_a})^L + Z_{\alpha2}(\frac{-M_{\alpha1}}{A_a})^L\right] \quad (1.8)$$

Is the effective charge term, with e the fundamental charge, $M_{\alpha i}$ and $Z_{\alpha i}$ are the constituent masses and charges of particle pair α, $A_\alpha = M_{\alpha1} + M_{\alpha2}$, and

$$U(Ll_fJs;lJ_f) = (2l+1)^{1/2}(2J_f+1)^{1/2}W(Ll_fJs;lJ_f) \quad (1.9)$$

Is the normalized Racah coefficient. All quantities appearing with a subscript f refer to the final state configuration. It should be noted that our Eqs. (1.5) and (1.6) follow the sign convention of Refs. (lane1958, Holt1978) and consequently differ from those in (barker1991) by an overall minus sign (which has no effect upon observables). We have also allowed $\bar{e}_\alpha^L$ to depend upon the particle pairα, as it must if more than one pair type is present in the problem.

The integrals $R_{cl_fL}^{EC}$ and $R_{cc'l_f'L}^{ERC}$ contain the hard-sphere and resonant portions of the initial scattering wave function, respectively. The hard-sphere integral is given by

$$R_{cl_fL}^{EC} = C_{\alpha sl_f}\int_{a_c}^{\infty} drr^L[F_{\alpha l}(k_\alpha r)cos\delta_c^{hs} + G_{\alpha l}(k_\alpha r)sin\delta_c^{hs}]\times W_{-\eta\alpha,l_f+1/2}(k_{\alpha f}r) \quad (1.10)$$

In the above equation, the asymptotic normalization (ANC) is represented by Cαslf , the functions Fαl (kαr) and Gαl (kαr)are normal Coulomb functions, W−ηα , lf +1/2(2kαf r) is a Whittaker function, and δ^{hs} is the hard-sphere phase shift given by

$$\delta_c^{hs} = -tan^{-1}\left[\frac{F_{\alpha l}(k_\alpha a_c)}{F_{\alpha l}(k_\alpha a_c)}\right] \quad (1.11)$$

The resonant external integral $R_{cc'l_f'L}^{ERC}$includes contributions from all channels. For open channels, we define

$$K_{Lcl_f} = \exp(i\delta_c^{hs})P_c^{1/2}\int_{a_c}^{\infty} drr^L\,[G_{\alpha l}(k_\alpha r) + iF_{\alpha l}(k_\alpha r)]\times W_{-\eta\alpha,l_f+1/2}(2k_{\alpha f}r) \quad (1.11)$$

And for closed channels

$$K_{Lcl_f} = (k_\alpha a_c)^{1/2}\int_{a_c}^{\infty} drr^L\frac{W_{-\eta\alpha,l+1/2}(2k_\alpha r)}{W_{-\eta\alpha,l+1/2}(2k_\alpha r)}\times W_{-\eta\alpha,l_f+1/2}(2k_{\alpha f}r) \quad (1.12)$$

In R–matrix formalism, the resonant external integral is given by

$$R_{cc'l_f'L}^{ERC} = P_c^{1/2}[(1-RL)^{-1}R]_{cc'}C_{\alpha's'l_f'}K_{Lc'l_f'} \quad (1.13)$$

While for the A–matrix formalism the term takes the form

$$R_{cc'l_f'L}^{ERC} = P_c^{1/2}\sum_{\lambda\mu}\gamma_{\lambda c}\gamma_{\mu c'}A_{\lambda\mu}\,C_{\alpha's'l_f'}K_{Lc'l_f'} \quad (1.14)$$

The above integrals can also be parameterized in terms of the dimensionless reduced width amplitude (DRWA), θαslf, by substituting for the ANC the expression

$$C_{\alpha sl_f} = \sqrt{\frac{2}{a_{\alpha sl_f}}}\theta_{\alpha sl_f}\frac{N_f^{1/2}}{W_{-\eta\alpha,l_f+1/2}(2k_{\alpha f}a_c)} \quad (1.15)$$

The normalization factor N_f results from the fact that R-matrix Eigen functions are normalized to unity inside the channel radii. It is given by

$$N_f^{-1} = 1 + \sum_{\alpha s l_f} \frac{2\theta_{\alpha s l_f}^2}{a_{\alpha s l_f}} \int_{a_c}^{\infty} \left[\frac{W_{-\eta\alpha, l+1/2}(2k_\alpha r)}{W_{-\eta\alpha, l+1/2}(2k_{\alpha f} a_{\alpha s l_f})} \right]^2 dr \tag{1.16}$$

If the level shift of the final state vanishes, the dimensionless reduced width can be related to the R-matrix reduced width $\gamma_{\alpha s l_f}$ for that state via Eq. IV.3.10in (lane1985):

$$\theta_{\alpha s l_f} = \frac{a_{\alpha s l_f} \sqrt{\mu_\alpha}}{\hbar} \gamma_{\alpha s l_f} \tag{1.17}$$

And using Eq. A.29in (lane1985) the normalization factor can be written

$$N_f^{-1} = 1 + \sum_{\alpha s l_f} \gamma_{\alpha s l_f}^2 \left(\frac{dS_{\alpha s l_f}}{dE} \right)_{a_{\alpha s l_f}} \tag{1.18}$$

Alternative definitions of the dimensionless reduced width amplitude also exist.

Defining the total transition matrix element for capture as

$$T_{cp}^J = T_{cp}^{J,int} + T_{cp}^{J,ext}$$

It can be shown that the AD is given as

$$\frac{d\sigma_{a\to\lambda_f}}{d\Omega} = \frac{1}{(2I_{\alpha 1}+1)(2I_{\alpha 2}+1)} \frac{1}{k_\alpha^2} \sum_k B_k P_k(\theta) \tag{1.19}$$

With the definitions

$$B_k = \sum_{s,L,L',l,l',J,J',\epsilon,\epsilon'} ( ) \frac{(-1)^{1+s-J_f}}{4} Z_1(l,J,l',J';sk) \times Z_2(L,J,L',J';J_f k) T^{*J'}_{asl',\epsilon',L'\lambda_f} T^J_{asl',\epsilon,L\lambda_f} \tag{1.20}$$

And

$$Z_1(l,J,l',J';sk) = \hat{l}\hat{l}'\hat{J}\hat{J}'(l0l'|k0) W(lJl'J';sk) \tag{1.21}$$

$$Z_2(L,J,L',J';J_f k) = \hat{L}\hat{L}'\hat{J}\hat{J}'(L1L'|k0) W(LJL'J';J_f k) \tag{1.22}$$

Where the symbol ( ) indicates a parity restriction defined by

$$[\,] = \frac{1}{2}\left[1 + (-1)^{L'+L+k+\epsilon+\epsilon'}\right] \tag{1.23}$$

These equations are identical to those given in Ref. (Seyler1979). Integrating over the solid angle gives the usual expression for the total cross section:

$$\sigma_{a\to\lambda_f} = \frac{\pi}{k_\alpha^2} \sum_{JlsL\epsilon} g_J \left| T_{cp}^J \right|^2 \tag{1.24}$$

Comment： This paper made a big contribution for making a code AZURE which can make gloable fitting for ^{12}C (α, γ) ^{16}O at first. But the code AZURE has not been used to produce the SF of ^{12}C (α, γ) ^{16}O down to 0.3 MeV.

Appendix.VII. 2. Evaluation for ED

Table Appendix.VII. 2. 1 shows the Conditions for experimnts about ^{12}C (α, γ) ^{16}O.

Table Appendix.VII. 2. 1 Conditions for experimnts about ^{12}C (α, γ) ^{16}O

Expt	Beam Curr. (μA)	Det.type, Effic. (%)	Target	Meas. time(h)	Ang.Data points	Energy range Ecm (MeV)	S(E) Data points
Dyer 1974	0.3	NaI(Tl), 3	^{12}C	1000	9	1.41-2.94	24, 4(E1, E2)
Redde1987	700	Ge, 14-35	^{12}C, Au	900	3(6)	0.94-2.84	24, 24(E1, E2)

							25, 25(SCG3, 4)
Ouellet1996	20-35	Ge, 18-30	^{12}C, Au	1950	5(6)	1.37-2.98	9, 9(E1, E2)
Kunz2001, 2002	450	4πGe, 100	^{12}C, Au	700	8-9	0.95-2.80	20, 20(E1, E2) 16, 16(SCG3, 4)
Assuncao2006	340	4πGe, 100	^{12}C, Au	720	9-10	1.3-2.78	25, 25(E1, E2)
Makii2009	8, 4MHz	NaI(Tl),	^{12}C, Au	400	3-4	1.225-1.591	4, 4(E1, E2)
Plag2012	6, 1MHz	4πBaF$_2$, 100	^{12}C, Au	270	12	1.002-1.51	4, 4, 4(STOT, E1, E2)

The article (Ouellet1996) reports that;

The excitation function of the $^{12}C(\alpha,\gamma)^{16}O$ reaction and the AD of its γ rays were measured at nine center-of-mass energies ranging from *E*=1.37 MeV to 2.98 MeV. These measurements allowed the separation of the *E*1 and *E*2 contributions and their extrapolation to the region of astrophysical interest. The analysis of all the available *E*1 cross sections with the *K*-matrix method and with a three-level *R*-matrix method yields a consistent prediction of 79.6±16 keV b for the *E*1 *SF* at 0.3 MeV. The *E*2 contribution at the same energy is 36.6±6 keV b from a cluster model analysis of the present data. The best estimate of the total *SF* at 0.3 MeV is 120 keV b, and it is unlikely that it will fall outside the range of 80–160 keV b.

The article (Kunz2001) and (Kunz2002) report that:

The ADs of gamma rays from the ^{12}C (Alpha, gamma) ^{16}O reaction have been measured at 20 energy points in the energy range E-cm = 0.95 to 2.8 MeV. The sensitivity of the present experiment compared to previous direct investigations was raised by 1-2 orders of magnitude, by using an array of highly efficient (100%) Ge detectors shielded actively with BGOs, as well as high beam currents of up to 500 muA that were provided by the Stuttgart DYNAMITRON accelerator. The SE1 and SE2 factors deduced from the gamma ADs have been extrapolated to the range of helium burning temperatures applying the R-matrix method, which yielded S-E1(300) = (76 ± 20) keV b and S-E2(0.3 MeV) = (85 ± 30) keV b. A new astrophysical reaction rate of ^{12}C (α, γ) ^{16}O has been calculated based on our recent determination of the E1- and E2-capture cross sections. The ***R***-matrix method has been applied to describe the SE1 and functions as well as the data of elastic a scattering and the β-delayed a decay of ^{16}N - SE2-factor

From other experiments. The resulting reaction rate for stellar temperatures is presented in both tabular form and an analytic expression. A new temperature dependence of the reaction rate was obtained when compared with reported evaluations. The associated uncertainties were reduced considerably in comparison to previous determinations.

The article (Assuncao06) reports that:

A new experiment to determine the thermonuclear cross section of the ^{12}C(α, γ)^{16}O reaction has been performed in regular kinematics using an intense α-particle beam of up to 340 μA from the Stuttgart DYNAMITRON. For the first time, a 4π-germanium-detector setup has been used to measure the AD of the γ rays at all angles simultaneously. It consisted of an array of nine EUROGAM high-purity Ge detectors in close geometry, actively shielded individually with bismuth germinate crystals. The ^{12}C targets were isotopic ally enriched by magnetic separation during implantation. The depth profiles of the implanted carbon in the ^{12}C targets were determined by Rutherford backscattering for purposes of cross-section normalization and absolute determination of the *E*1 and *E*2 *SF*s. ADs of the γ decay to the ^{16}O ground state were measured in the energy range *E*c.m. = 1.30–2.78 MeV and in the angular range (Lab.) 30°–130°. From these distributions, astrophysical *E*1 and *E*2 *S*-factor functions vs energy were calculated, both of which are indispensable to the modeling of this reaction and the extrapolation toward lower energies. The separation of the *E*1 and *E*2 capture channels was done both by taking the phase value φ12 as a free parameter and by fixing it using the results of elastic α-particle scattering on ^{12}C in the same energy range.

The article (Makii2009) reports that:

We measured the γ -ray AD from ^{12}C (α, $\gamma 0$)^{16}O to the ground state of ^{16}O using a pulsed αbeam at *E*eff = 1.6 and 1.4 MeV. True events of ^{12}C (α, $\gamma 0$)^{16}O were discriminated from background events with a time-of-flight method because of neutrons from ^{13}C (α, n) ^{16}O. The obtained γ -ray spectrum with anti-Compton NaI (Tl) spectrometers showed a characteristic line shape from ^{12}C (α, γ_0) ^{16}O: the Doppler broadening and energyloss of α particles in ^{12}C targets. A Rutherford backscattering spectrum of α particles from enriched ^{12}C targets was measured during beam irradiation to obtain the target thickness and incident α-beam intensities. Theastrophysical *SF*s for *E*1 and *E*2, *SE*1(γ0 : *E*eff) and *SE*2(γ0 : *E*eff), derived from the present cross sectionsare in excellent agreement with the values derived by *R*-matrix calculation of the β-delayed α spectrum of ^{16}N, and by using the asymptotic normalization constant in the *R*-matrix fit.

The article (Plag2012) reports that:

The ^{12}C(α, γ)^{16}O reactionED, are still subject to large uncertainties due to the almost vanishing cross section at stellar energies. So far, most measurements have been performed with germanium detectors. To compensate for their low efficiency, the highest beam currents had to be used, resulting in target degraADtion and beam-induced backgrounds. Instead, the present measurement was performed with high-efficiency detectors and low beam currents, using the Karlsruhe 4π BaF2 detector and the pulsed 3.7-MV Van de Graaff accelerator at Karlsruhe Institute of Technology. The ^{12}C(α, γ)^{16}O cross sections have been measured at center-of-mass energies *E* between 1002 and 1510 keV, and the *E*1 and *E*2 components were derived with an accuracy comparable to the previous best data obtained with HPGe detectors.

APPENDIX.VII. 2.2 Experiments with Recoil Mass Separator (RMS)

The experiments with this kinds of method to measure $^{12}C(\alpha,\gamma)^{16}O$ cross sections includes (Schumann2005), (Schumann2011), (Fuji2010), and so on. Table Appendix.VII. 2. 2 shows Conditions for experimnts about ^{12}C (α, γ) ^{16}O with Recoil Mass Separator (RMS)

Table Appendix.VII. 2. 2 Conditions for experimnts about ^{12}C (α, γ) ^{16}O with Recoil Mass Separator (RMS)

Expt	Beam Curr.(μA)	Det.type, Effic. (%)	Target	Meas. Time(h)	Ang.Data points	Ecm range (MeV)	S (E). Data points
Ketter1982	50	NaI(Tl), 20	^{4}He, gas	1000	4	1.44-3.38	48-SCG0, SCG3
Roters1999	20	BGO, 270	^{4}He, gas	5000	2	0.94-3.39	13, 13(E1,E2)
Matei2006	30-50	γ:BGO, ^{16}O: Si(DSSSD)	^{4}He, gas			2.22-5.42	32-SCG1
Schumman2005	10	^{16}O:ΔE-E telescope	^{4}He, gas			1.903-4.917	75-STOT
Fuji2010	12	^{16}O: Si-SSD	^{4}He, gas	40		1.5-2.4	2-STOT

The article (Schumann2005) is the respective one.

It reports that Most of the existing data on these reactions have been gained by means of gamma-ray spectroscopy, where the measurements are very difficult in view of the low cross sections and the relatively high background in the detectors. Since some decades a new technique has been exploited, based on the direct detection of the nuclei produced during the reaction using a Recoil Mass Separator (RMS) able to collect the recoil ions keeping the reaction kinematic information, while suppressing the projectile beam emerging from a thin target. A pioneering work was done at Caltech (2), where $^{12}C(\alpha,\gamma)^{16}O$ was measured using a recoil mass separator and a NaI (Tl) detection setup. Here the insufficient beam suppression required a coincidence condition between gamma-rays and recoils, thus reducing the advantages of the use of a recoil mass separator. Later started the NABONA (NAples BOchum Nuclear Astrophysics) collaboration between the Institut für Experimentalphysik III of the Ruhr-Universität Bochum, the INFN-Sezione di Napoli and Dipartimento di Scienze

Fisiche of the University of Naples Federico II, and for some experiments, the group of the ATOMKI, Debrecen . The aim of this collaboration was to measure the cross section of ^{7}Be (p, g) ^{8}B. This experiment was performed using a ^{7}Be beam and a windowless hydrogen gas target in combination with a recoil separator with sufficient beam suppression and acceptance to detect the recoil without the need of the coincidence condition with gamma-rays. As a follow-up of the NABONA collaboration, a new collaboration between the same groups started, called ERNA, whose aim was to study $^{12}C(\alpha,\gamma)^{16}O$ and ^{3}He(^{4}He, γ)^{7}Be using a new recoil separator installed at the 4MV Dynamitron Tandem Laboratorium of the Ruhr-Universität Bochum. At the same time a recoil mass separator named DRAGON was designed and installed at TRIUMF, where several reactions have been studied involving both radioactive (10) and stable beams (11), (12), (13). Other similar systems have been developed or are in course of development at different laboratories in Japan and USA (14). A general review of the field is beyond the scope of the present work. We rather focus on some peculiar aspects of this experimental approach and the description of the ERNA RMS. We consider then the case of $^{12}C(\alpha,\gamma)^{16}O$ that, besides its enormous interest in nuclear astrophysics, presents the typical difficulties encountered in this kind of experiments.

The article (Schumann2011) reports that:

The radiative capture reaction ^{12}C (α, γ) ^{16}O has been investigated in the energy range E = 3.3 to 4.5 MeV. This experiment focused in particular on the cascade transition to the 0+ state at Ex = 6.05 MeV in ^{16}O and was performed by detecting the capture γ -rays with a NaI detector array at the windowless 4He gas target of the recoil mass separator ERNA in coincidence with the ^{16}O ejectiles. The 6.05 MeV transition has been considered recently as a component accounting for up to 15% of the ^{12}C (α, γ) ^{16}O total cross section at astrophysical energies. The arrangement of the detector array yielded additional information on the γ -ray multipolarity, i.e. the ratio σE2/σE1, and it was found that the 6.05 MeV transition is entirely E2 in the studied energy range. The results for this transition are analyzed in an R-matrix formalism and extrapolated to the relevant Gamow energy of stellar helium burning, E0 _ 300 keAPPENDIX.VII. In contrast to a previous analysis, the present extrapolation suggests a negligible contribution from this amplitude, $S_{6.05(300)}$ < 1 keV b. Additional data for cascade transitions to excited states at Ex = 6.13, 6.92, and 7.12 MeV, respectively, as well as to the ground state were obtained and the corresponding SFs in the studied energy range are given.

The article (Matei2006) reports that:

Radiative particle capture into the first excited, 0^{+} state of ^{16}O at 6.049 MeV excitation energy has rarely been discussed as contributing to the $^{12}C(\alpha,\gamma)^{16}O$ reaction cross section due to experimental difficulties in observing this transition. We report here measurements of this radiative capture in $^{12}C(\alpha,\gamma)^{16}O$ for center-of-mass energies of E=2:22 MeV to 5.42 MeV at the DRAGON recoil separator. To determine cross sections, the acceptance of the recoil separator has been simulated in GEANT as well as measured directly. The transition strength between resonances has been identified in R-matrix fits as resulting both from E2 contributions as well as E1 radiative capture. Details of the extrapolation of the total cross section to low energies are then discussed $S_{6:05}$(0.3 MeV) = 25^{+16}_{-15} keV b) showing that this transition is likely the most important cascade contribution for $^{12}C(\alpha,\gamma)^{16}O$

The article (Fuji2010) reports that:

A cross section measurement with a direct O-16 detection method for the reaction energy from E_{cm} = 2.4 down to 0.7 MeV is planned at Kyushu University Tandem Laboratory (KUTL). To perform the experiment successfully and to get the quantitative information of the cross section within the 10% error, we have newly developed several instruments in 2009, such as a blow-in type windowless gas target and movable slit system placed in the recoil mass separator. By using the windowless blow-in gas target, a pressure of 24 Torr was achieved. The effective thickness along the beam axis was measured by p+^{4}He scattering. Thanks to the movable slits installed in a recoil mass separator and the trajectory analysis, we found effective reduction of background conditions from the C-12 beam.

APPENDIX.VII. 2.3. Transfer reaction

TABLE APP.VII. 2.3.1 Comparison of the α-spectroscopic factors

Experi-ment	$S\alpha$ 6.92 , 2^+	$S\alpha$ 7.12 , 1^-	$S\alpha$ 6.05 , 0^+	$S\alpha$ 6.13 , 3^-	$S\alpha$ 9.58 , 1^-	$S\alpha$ 10.35 , 4^+	Reaction Energy (MeV)
Oulebsir2012	0.15±0.05	0.07±0.03	$0.13^{-0.06}_{+0.07}$	0.06±0.04	$0.10^{+0.08}_{-0.06}$	$0.19^{+0.17}_{-0.08}$	^{12}C+^{7}Li, 28, 34
Belhout 2007	0.37±0.11	0.11±0.03	0.12±0.04	0.29±0.15	0.34±0.10	0.11±0.06	^{12}C+^{7}Li, 48
Becchetti2005	$0.37^{-0.04}_{+0.06}$	$0.17^{+0.06}_{-0.04}$	$0.08^{+0.04}_{-0.06}$	$0.11^{+0.05}_{-0.02}$	$0.09^{+0.03}_{-0.06}$	$0.17^{+0.06}_{-0.03}$	^{12}C+^{7}Li, 34

TABLE APP.VII. 2.3.2 The α-reduced widths and SF

Experiment	$\gamma^2\alpha$ (0^+) /(keV)	$\gamma^2\alpha$ (3^-) /(keV)	$\gamma^2\alpha$ (2^+) /(keV)	$\gamma^2\alpha$ (1^-) /(keV)	SE10/ keV b	SE20/ keV b
Oulebsir2012	19.7±5.5	2.35±0.8	26.7±10.3	7.8±2.7	100±28	50±19
Belhout2007	/	/	$26.6^{+19.2}_{-17.2}$	4.59 ± 2.91	80.6^{+17}_{-16}	

The article (Oulebsir2012) reports that:

The extrapolation of the measured cross sections to stellar energies ($E \sim 0.3$ MeV) is made particularly difficult by the presence of the 2^+ (Ex = 6.92 MeV) and 1^- (Ex = 7.12 MeV) subthreshold states of ^{16}O. To further investigate the contribution of these two subthreshold resonances to the ^{12}C (α, γ) ^{16}O cross section, their α-reduced widths can be determined via a measurement of the transfer reaction ^{12}C (^{7}Li, t) ^{16}O. The uncertainties on the determined α-spectroscopic factors and the α-reduced widths maybe reduced by a detailed distorted-wave Born approximation analysis of the transfer ADs. The R-matrix calculations of ^{12}C (α, γ) ^{16}O cross section can be used the obtained α-reduced widths for the 2^+ and 1^-subthreshold resonances.

The article (Belhout2007) reports that:

The ADs for low lying states of ^{16}O produced in the ^{12}C (^{6}Li, d) ^{16}O α-transfer reaction have been measured using a high energy resolution position sensitive detection system. The measured cross section data have been analyzed by the FRDWBA theory with a particular emphasis put on the states of astrophysical interest mainly the 1^- (7.12 MeV) state. Extracted values of nuclear level parameters (excitation energy, Ex, line width, Γc.m., α-spectroscopic factor, $S\alpha$, and reduced α-width, suggesting that the channel radius a = 6.5 fm is likely suitable for the calculations of reduced α-widths near the nuclear surface. However, given that previous DWBA results are available for comparison only near the channel radius a =5.5 fm, calculations have been carried out here for both three preceding a values. Formal values $0.0036 \leq \theta\alpha^2(7.12) \leq 0.152$, which is consistent with the preceding DWBA interval, and to a result for the E1 component of the reaction astrophysical factor, G-SE10=80.6^{+17}_{-16} , very consistent with most constrained values previously reported in the literature.

The article (Brune1999) reports that:

The ^{12}C (a, g) ^{16}O reaction is crucial for the understanding of He burning in massive stars, but the low-energy cross section is highly uncertain. To address this problem we have measured at sub-Coulomb energies total cross sections for the ^{12}C (^{6}Li, d) ^{16}O and ^{12}C (^{7}Li, t) ^{16}O reactions to the bound

2^+ and 1^- states of ^{16}O. The data are analyzed to obtain the reduced a widths of these states. Together with capture and phase-shift data, these results provide for a more accurate determination of the low energy ^{12}C (a, g) ^{16}O SF: $SE1$ (0.3 MeV) = 101^{+17}_{-17} keV b and $SE2$ (0.3 MeV) = 42^{+16}_{-23} keV b for the $E1$ and $E2$ multipole components of the reaction.

In this way the SF results obtained maybe have large difference and lager uncertainty due to that it is very hard to get the closedα-spectroscopic factors, see Table as follow. The α-reduced widths of (Oulebsir2012) have been taken as experimential data for fitting.

APPENDIX.VII. 2.4 Mesherments for $^{12}C(\alpha,\alpha)^{12}C$

Table Appendix.VII. 2. 4 Conditions for experimnts about $^{12}C(\alpha,\alpha)^{12}C$

Expt	Beam Cur.(mA)	Det.type, effic. (%)	Target	Ang. Num.	Eα range(MeV)	Data points
Plag1987	α, 0.1-1	Surface , barrier	^{12}C, Au	35	1.0-6.6	51×35
Tischhaus2002	α, 0.2	Si	^{12}C, Au	32	2.6-8.2	12864
Brune1975	α, 0.15	solid-state detector	^{12}C		3.0-10.0	
Morris1968	α	gas cell	CO2, Gas	28	6.6-8.5	639

The article (Plag1987) reports that:

The elastic scattering of Alpha particles from ^{12}C has been investigated for 35 angles in the range elab = 22^o to 163^o and for 51 energies at E = 1.0 to 6.6 MeV. The extracted phase shifts for I=0 to 6 partial waves have been parametrized in terms of the multilevel R-matrix formalism. Information on the deduced parameters of states in ^{16}O is reported. The data reveal reduced a-particle widths for the 6.92 and 7.12 MeV subthreshold states consistent with recent work. The implications for the stellar reaction rate of ^{12}C (α, γ) ^{16}O are discussed.

The article (Tischhaus2002) reports that:

ADs of ^{12}C (a, a) ^{12}C have been measured for E_α (2.6 to 8.2 MeV), at angles from 24^O to 166^O, yielding 12 864 data points. *R*-matrix analysis of the ratios of elastic scattering yields a reduced width amplitude of γ_{12} = 0.47± 0.06 MeV$^{0.5}$ for the *Ex* = 6.917 MeV (2^+) state in ^{16}O (*a*=5.5 fm). The dependence of the x2 surface on the interaction radius *a* has been investigated and a deep minimum is found at *a*= $5.42^{+0.16}_{-0.27}$ fm. Using this value ofγ_{12}, radiative a capture and ^{16}N β-delayed α-decay data, the *SF* is calculated at *E*cm (0.3 MeV) to be *SE*2 (0.3 MeV) 53^{+13}_{-18} keVb for destructive interference between the subthreshold resonance tail and the ground state *E*2 direct capture.

APPENDIX.VII. 2.5 $\beta-\alpha$ delay for ^{16}N

Table Appendix.VII. 2. 5 Conditions for experimnts about $\beta-\alpha$ delay for ^{16}N

Ref	Hatt1970	Azuma1994	Zhao1993		France2007	Tang2010
Group	Mainz	TRIUMF	Yale1	Seattle	Yale 2	Argonne
^{16}N production	^{15}N(*d*, *p*)	Isotope separator	^{15}N(*d*, *p*)	^{15}N(*d*, *p*)	^{15}N(*d*, *p*)	^{15}N(*d*, *p*)
^{16}N implantation speed	Low	Low	High	High	High	High
Mass/composition Of ^{16}N catcher	30μg/cm^2$C_6H_7N_{.5}O_{10}$+ 6–8 Torr $^{15}N_2$	10 μg/cm^2 C	180 μg/cm^2 Al	10/20 μg/cm^2 C	180 μg/cm^2 Al	17 μg/cm^2 C
Detectors	<35 μm Si	10.4–15.8 μm Si	50 μm Si	15–20 μm Si	50 μm Si	Ion chamber
Background (measured)	β tail	^{18}N, ^{17}N	None	Unknown	None	Maybe

Degraded event suppression	None	α-^{12}C	β-α	α-^{12}C	β-α	α-^{12}C
Efficiency corrections	None	None	β	Unknown	β	None
Energy calibration	^{10}B(n, α)	^{18}N, ^{20}Na	^{10}B(n, α)	Unknown	^{10}B(n, α)	^{10}B(n, α)
Deconvolution applied	None	None	Division (see text)	Unknown	Division (see text)	None
Cut off Energy (MeV)	1.08	0.59	0.835	0.626	0.73	0.45
Total counts	2×10^6	1×10^6	6×10^4	1×10^5	2.8×10^5	2.7×10^5

The article (Aruma1994) reports that:

The shape of the low-energy part of the β-delayed α-particle spectrum of ^{16}N is very sensitive to the α+^{12}C reduced width of the 7.117 MeV subthreshold state of ^{16}O. This state, in turn, dominates the low-energy *p*-wave capture amplitude of the astrophysically important ^{12}C (α, γ) ^{16}O reaction. The α spectrum following the decay of ^{16}N has been measured by producing a low-energy ^{16}N^{14}N^{+} beam with the TRIUMF isotope separator TISOL, stopping the molecular ions in a foil, and counting the α particles and ^{12}C recoil nuclei in coincidence, in thin surface-barrier detectors. In addition to obtaining α spectrum, this procedure determines the complete detector response including the low-energy tail. The spectrum, which contains more than 10^6 events, has been fitted by *R*- and *K*-matrix parametrizations which include the measured ^{12}C (α, γ) ^{16}O cross section and the measured α+^{12}C elastic scattering phase shifts. The model space appropriate for these parametrizations has been investigated. For S_{E1}(300), the *E*1 part of the astrophysical *SF* for the ^{12}C (α, γ) ^{16}O reaction at $E_{\text{c.m.}}$ = 0.3 MeV, values of 79±21 and 82±26 keV b have been derived from the *R*- and *K*-matrix fits, respectively.

The article (Tang2010) reports that:

A measurement of the β-delayed α decay of ^{16}N using a set of twin ionization chambers is described. Sources were made by implantation, using a ^{16}N beam produced via the In-Flight Technique. The energies and emission angles of the ^{12}C and α particles were measured in coincidence and very clean α spectra, down to energies of 450 keV, were obtained. The structure of the spectra from this experiment is in good agreement with results from previous measurements. An analysis of our data with the same input parameters as used in earlier studies gives *SE*1 (300) = 86 ± 22 keVb for the *E*1 component of the *S*-factor. This value is in excellent agreement with results obtained from various direct and indirect measurements. In addition, the influence of new measurements including the phase shift data from Tischhauser *et al.* on the value of *SE*1 (300) is discussed.

The article (Buchmann2009)

Published a review about that the β-delayed α decay of ^{16}N has been used to restrict the *E*1 fraction of the ground state γ transition in theastrophysically important ^{12}C (α, γ) ^{16}O reaction in several experiments. A review of the published measurements is given, and GEANT4 simulations and *R*-matrix calculations are presented to further clarify the observedα spectra. A clear response function, in the form of a low-energy tail from the scattering of α particles in the catcher foil, is observed in these simulations for any foil thickness. Contrary to claims in the literature, the simulations show that the TRIUMF measurement and those performed at Yale and Mainz originate from the same underlying spectrum. The simulations suggest that the discrepancies between the Yale and TRIUMF final results can be attributed to incorrect deconvolution methods applied in the former case. The simulations show in general that the form (width) of the spectrum is very sensitive to the catcher foil thickness. It is concluded that the TRIUMF measurement most likely represents the currently closest approximation to the true β-delayed α-decay spectrum of ^{16}N.

Appendix.VII. 3. Evaluation for previous analysis works

0. deBoer2013 PHYSICAL REVIEW C **87**, 015802 (2013) ***R*-matrix analysis of ^{16}O compound nucleus reactions**

Background: Over the past 60 years, a large amount of experimental nuclear data have been obtained for reactions which probe the $_{16}$O compound nucleus near the α and proton separation energies, the energy regimes most important for nuclear astrophysics. Difficulties and inconsistencies in *R*-matrix fits of the individual reactions prompt a more complete analysis.

Purpose: Determine the level of consistency between the wide varieties of experimental data using a multiple entrance/exit channel *R*-matrix framework. Using a consistent set of data from multiple reaction channels, attain an improved fitting for the $_{15}$N(p, γ_0)$_{16}$O reaction data. **Methods:** Reaction data for all available reaction channels were fit *simultaneously* using a multichannel *R*-matrix code.

Results: Over the wide range of experimental data considered, a high level of consistency was found, resulting in a single consistent *R*-matrix fit which described the broad level structure of $_{16}$O below E_x = 13.5 MeV. The resulting fit was used to extract an improved determination of the low-energy S factor for the reactions ^{15}N (p, γ) ^{16}O and ^{15}N (p, α) ^{12}C.

Conclusion: The feasibility and advantages of a complete multiple entrance/exit channel *R*-matrix description for the broad level structure of $_{16}$O has been achieved. A future publication will investigate the possible effects of the multiple-channel analysis on the reaction $_{12}$C(α,γ)$_{16}$O.

Problem: The low-energy S factor for $_{12}$C(α,γ)$_{16}$O have not been published until now.

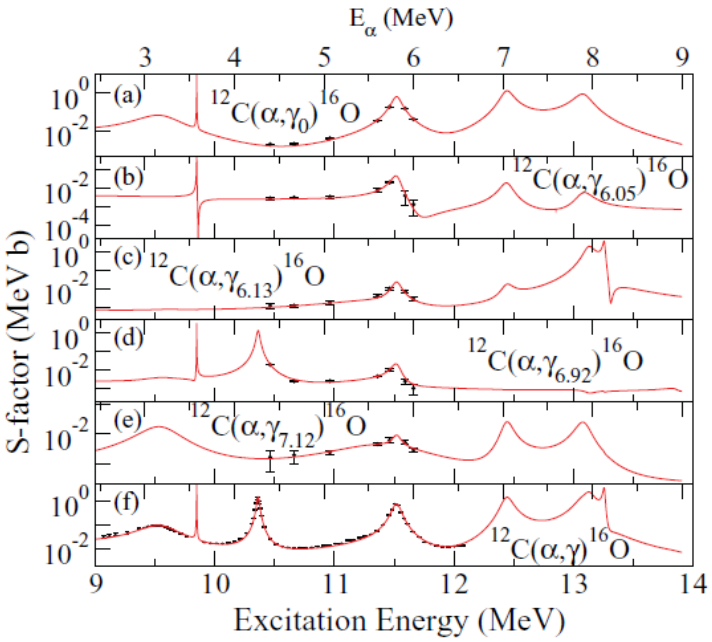

A. Dyer 1974

While there were a few experiments earlier, the 1974 measurement (Dyer1974) of Dyer and Barnes of the ^{12}C(α, γ)^{16}O ground state E1 reaction cross section may be the first which led to serious work in understanding the reaction mechanism. The cross section for the reaction ^{12}C(α, γ)^{16}O has been measured for a range of c.m. energies extending from 1.41 MeV to 2.94 MeV, by using^{12}C targets of high

isotopic purity, large NaI(TI) crystals, and the time-of-flight technique for the suppression of prompt neutron background and time-independent background. Gamma-ray AD have also been measured at c.m. energies of 2.18, 2.42, 2.56 and 2.83 MeV. Two methods are discussed for extrapolating to low energies the electric dipole contribution to the cross sections.

Problem:

By means of theoretical fits, which include the coherent effects of the 1^- states of 160 at 7.12 MeV, 9.60 MeV, and those at higher energies, the electric-dipole portion of the cross section at astrophysically relevant energies has been determined. A three-level R-matrix parametrization of the data yields an S-factor at Ec.m. =300keV, S (300keV) $=140^{+140}_{-120}$ keVb. A "hybrid" R-matrix optical-model parameterization yields S (300KeV) $=80^{+50}_{-40}$ keVb. It is seen that the two methods of parametrizing the data give consistent results, but that the error obtained from the three-level R-matrix analysis is much larger than that obtained from the hybrid R-matrix optical-model parametrization. The principal reason for this appears to be that the γ-width of the fictitious background level in the three-level R-matrix parametrization is free to vary in the fit to the $^{12}C(\alpha, \gamma)^{16}O$ ***data***. The effect of varying $\Gamma_{\gamma 3}$ is somewhat similar to the effect of varying the reduced α width of the 7.12 MeV state, i.e. to increase or decrease the constructive interference on one side of the resonance corresponding to the 9.60 MeV state, and the destructive interference on the other side. Thus, both of these parameters must be assigned rather large errors, and the S-factor at 0.3 MeV, which is more strongly dependent on the reduced α-width of the 7.12 MeV state, becomes uncertain by a correspondingly large amount. In the case of the hybrid R-matrix optical-model parametrization, the background contribution is constrained by the choices of ***d*** and V(r), the optical model potential, which is determined by the fit to the ***$^{12}C(a, a)^{12}C$*** p-wave phase shifts. This is certainly a physically plausible method of specifying the background strength, but it cannot be verified experimentally unless the background El radiation can be separated with high precision from the wealth of radiation arising from other multipoles at energies above the range of the present experiment (a task which appears to be even more difficult than the present low-energy cross-section measurements).

B. Kettner1982

A measurement in inverted kinematics (with a ^{12}C beam on a helium gas target) of ^{12}C (α, γ) ^{16}O reaction has been reinvestigated by Kettner et al. (Kettner1982) over the energy range Ec.m. = l.34-3.38 MeV in 1982. In order to avoid the neutron-induced γ-ray background due to the ^{13}C (α, n) ^{16}O contaminant reaction, the role of projectiles and target nuclei has been interchanged: 4He target nuclei contained in a windowless and recirculating gas target system were bombarded with the intense ^{12}C beam from the Bochum Dynamitron tandem. A large area plastic detector was used for the suppression of time-independent background. With the use of γγ-coincidences between NaI (Tl) crystals, Kettner et al. found cascade γ-ray transitions via the (6.92±7.12) MeV excited states of ^{16}O. Due to the lack of good energy resolution, the individual contributions via these two states could not be resolved. In the analyses of these data it was asumed that the observed yields arise predominantly from the cascade via the 6.92 MeV state. The extrapolation used a simplified model, but pointed to the importance of the E2 ground state transition.

Problem:

The extrapolation used a simplified model, and the extrapolated S-factors at E. = 0.3 MeV for the ^{12}C (α, γ) ^{16}O and ^{12}C (α, γ3)^{16}O reactions are found to be S (300KeV) $=420^{+160}_{-120}$ keVb and 12 ± 2 keVb, respectively, leading to a total value of STOT (300KeV) $=430^{+160}_{-120}$ keV*b. As a result, the astrophysical S-factor, SE10 (300KeV) = 250keVb, determined by this paper is some fourfold higher than that obtained from the data of (Dyer1974). Since the absolute cross sections, near the maximum of the ER = 2.39 Mev (Jπ = 1-) resonance, between the two data sets differ only by about 25%, it has been suggested that the above discrepancy might lie to a large extent in the difference between the partial (El) and the total (El + E2) capture yields. It was pointed out previously by Dyer and Barnes (Dyer1974) that E2 resonant capture through the tail of the $J\pi=2^+$, 6.92 MeV state may be significant in the astrophysical energy region. This work confirms this expectation and leads to an E2 portion of the cross section of SE20 (300KeV) = 180keV.b.

C. Redder1987

A measurement employing an implanted ^{12}C target of high isotopic purity in gold, an intense α current approaching 1 mA, and three high resolution germanium detectors, was published by (Redder1987) in 1987. The data provide information on the El and E2 capture amplitudes involved in the transition to the ground state as well as to excited states. The summed yields for both transitions, 6.92→0 and 7.12 → 0 MeV, are in good agreement with previous coincidence work using NaI (T1) crystals (Kettner1982).

Problem:

To analyze quantitatively the El capture data, the many-level R-matrix formalism of (Weisser1974) is used in the work. The final parameters obtained from a fit to the combined data sets were used to extrapolate the S(E)-factor curve to stellar energies: SE10(E0 = 0.3 MeV) = 200 (+280, - 180) keV. b. It is seen that the three-level R-matrix Fits to the AD of ^{12}C (α, γ) ^{16}O E l capture data alone give SE10 (E0 = 0.3 MeV) values with rather large uncertainties. As pointed out above, the reason for these uncertainties is due to the fact that the γ-ray width of the fictitious background level is free to vary in the three-level R-matrix parametrization. To reduce the error in SE10, the hybrid R-matrix Model of (Koonin1974) was applied in the analysis. The best fit to the combined El capture data using the Woods-Saxon potential ($\chi 2$ = 1.5) was obtained for d = 9.5 and $\gamma_{1\alpha}$ = -0.37 $MeV^{1/2}$, leading to SE10 (E0) = 90 (+100, -60) keV b. The gaussian potential resulted in$\chi 2$ = 2.0, d = 4.2, $\gamma_{1\alpha}$ = -0.56 MeV1/2 and SE10 (E0) =140 (+120, - 80) keV b. These results are consistent with previous hybrid R-matrix parametrizations of the original data of (Dyer1974): Woods-Saxon potential with SE10 (E0) =80 (+50, -40) KeV.b (Koonin1974). The fit to the S-factor data for the *6.92 →0* and *7.12 → 0* MeV secondary transitions lead to S6.92 (*E0)* = (7 ±2) keV.b and S7.12 (*E0) =1.3* (+0.5, -1.0), KeV.b (statistical errors only), respectively.

D. Zhao1993

The measurement of the β-delayed α-spectrum of ^{16}N done at Yale University is described in (Zhao1993), with ^{16}N nuclei produced using 80 MeV /nucleon ^{18}O beams on ^{9}Be targets. The ^{16}N secondary nuclei were mass analyzed and separated from the reaction products using the Michigan State University Al200 isotope separator. A detector array, including four thin surface barrier detectors, a *p-i-n* diode, a Ge gamma-ray detector, and a two dimensional position sensitive parallel plate avalanche counter, was used for implantation and study of the separated nuclei. The unfolded spectrum of beta-delayed Alpha-particle emission of ^{16}N was fit simultaneously with elastic scattering data and the ^{12}C (α, γ) ^{16}O data, using the R-matrix formalism developed in Ref. (Ji19901. (Zhao1993) used these data to extract the *SF* for the ^{12}C (α, γ) ^{16}O capture reaction to yield SE10 (0.3) = 95± 6(stat) ±28 (syst) keV.b.

E. Azuma1994

The α spectrum following the decay of ^{16}N has been measured in Ref. (Azuma1994) by producing a low-energy $^{16}N^{14}N+$ beam with the TRIUMF isotope separator TISOL, stopping the molecular ions in a foil, and counting the α particles and ^{12}C recoil nuclei in coincidence, in thin surface-barrier detectors. In addition to obtaining α spectrum, this procedure determines the complete detector response including the low-energy tail. The ^{16}N spectrum, which contains more than 106 events, has been employed in *R*- and K-matrix fits, together with the $^{12}C(\alpha, \gamma)^{16}O$ data and the elastic-scattering data for α particles on ^{12}C, to derive *SE1(300)* , the *E1 SF* of the $^{12}C(\alpha, \gamma)^{16}O$ reaction at *E* = 0.3 MeV.The R-matrix and K-matrix Fits to the AD of data result in *SE10(0.3)* = 79 ±21 keV.b and *SE10(0.3)* = 82 ±26 keV.b, respectively.

Comment: Fitting procedure shows that this work has the best α spectrum.

F. Ouellet1996

The paper (Ouellet1996) report a measurement of the^{12}C (α, γ) ^{16}O cross section in which full AD were measured at nine energies between 1.36 and 2.98 MeV. Six highefficiency germanium detectors were used in fixed geometry at all energies and the targets were ^{12}C implanted in gold. These measurements allowed the separation of the *E*1 and *E*2 contributions and their extrapolation to the region of astrophysical interest. The analysis of the *E*1 cross sections with a three-level R-matrix method yields a prediction of 79±16 keV b for the SF at Ec.m. =0.3 MeV, along with the phase shifts from elastic scattering and the β-delayed α spectrum from the decay of ^{16}N. The procedure used for the extrapolation of *E2* transitions is based on the formalism developed by Langanke and Koonin (). As opposed to the *E*1 situation, a more microscopic approach is useful here because of the relatively smooth behavior of the *E*2 cross section at low energy.

There is only one resonance, at subthreshold, contributing to the *SF* in a significant way. The contribution of *E2* transitions at the same energy is 36±6 keV b from the cluster-model analysis of the present data.

Comment: The SF of this work is absolute walue. Fitting procedure shows that taking NF=1 can get good fitting.

G. Roter1999

In 1999, Roters et al. (Roter1999) published a measurement of the ^{12}C (α, γ) ^{16}O reaction. Excitation functions of the γ_0 capture transition in ^{12}C (α, γ) ^{16}O at θ_γ = 90 degree were obtained using a 4 × 4'' BGO crystal in close geometry (*E* = 0.94 to 3.39 MeV) and a 2 × 2''BGO crystal in far geometry (*E* = 1.69 to 3.29 MeV), where the study of the reaction was initiated in inverse kinematics involving a windowless gas target. The small crystal detected essentially the *E*10 multipole component in the γ_0 capture transition, while the large crystal observed approximately the angle-integrated sum of the *E*10 and *E*20 multipole components. A careful analysis of the data then produces the ratio σE20/σE10. The *S*E10 data agree with previous data; however, the σE20/σE10 data shown in Fig. 13 of (Roter1999) show some problems relative to the fit applied in the high energy region above *E* >2.8 MeV.

H. Gialanella2001

An excitation function of the ground-state γ0-ray capture transition in $^{12}C(\alpha, \gamma)^{16}O$ at $\theta\gamma$ =90° was obtained in far geometry using six Ge detectors(Gialanella2001), where the study of the reaction was initiated in inverse kinematics involving a windowless gas target. The detectors observed predominantly the *E*1 capture amplitude. The data at *E* = 1.32 to 2.99 MeV lead to an extrapolated astrophysical *SF* *SE*1 (*E*0) = 90 ± 15 keV b at *E*0 = 0.3 MeV (for the case of constructive interference between the two lowest *E*1 sources), in good agreement with previous works. However, a novel Monte Carlo approach in the data extrapolation reveals systematic differences between the various data sets such that a combined analysis of all available data sets could produce a biased estimate of the *SE*1 (*E*0) value. As a consequence, the case of destructive interference between the two lowest *E*1 sources with *SE*1 (*E*0) = 8±3 keV b cannot be ruled out rigorously.

I. Kunz2001

Direct ^{12}C (α, γ) ^{16}O radiative capture measurements have been carried out at the Institut für Strahlenphysik of the University of Stuttgart. The AD of γ rays from the reaction have been measured at 20 energy points in the energy range *E* =0.95 to 2.8 MeV. The sensitivity of the present experiment compared to previous direct investigations was raised by 1–2 orders of magnitude, by using an array of highly efficient (100%) Ge detectors shielded actively with BGOs, as well as high beam currents of up to 500 mA that were provided by the Stuttgart DYNAMITRON accelerator. The *R*-matrix method has been applied to describe the SE1- and SE2-factor deduced from the γ AD as well as the data *of elastic α scattering and the β-delayed α decay* of ^{16}N from other experiments. The *S*-factor curves are extrapolated into the range of burning temperature. The following values for the *E*1, the *E*2 part of the *SF*, the contribution due to γ cascades, and the total *SF* at E0 =0.3 MeV have been extracted: SE10(E0) = 76 ± 20 keV b, SE20(E0) = 81 ± 22 keVb, *S*casc =4±4 keVb and *STOT*=165±50 keVb.

Comment: This work Kunz2001 and Kunz2002 are very important experimental and analysis works, which produced total SF from 0.3 MeV to 8 MeV.

J. Schurmann2005

A new experimental approach (Schurmann2005) has been developed at the 4 MV Dynamitron tandem accelerator ERNA in Bochum. This measurement in inverse kinematics using the recoil mass separator in combination with a windowless He gas target allowed to collect data with high precision in the energy range E = 1.9 to 4.9 MeV. The total cross-section of ^{12}C (α, γ) ^{16}O was measured for the first time by a direct and ungated detection of the ^{16}O recoils. The data represent new information for the determination of the astrophysical S (E) factor.

Comment: This work is the most important experimental measurement for toal SF in ^{12}C (α, γ) ^{16}O, and it play the most important effect in gloable ftting.

K. Assuncao2006

A new experiment(Assuncao2006) to determine the thermonuclear cross section of the $^{12}C(\alpha, \gamma)^{16}O$ reaction has been performed in regular kinematics using an intense α-particle beam of up to 340μA from the Stuttgart DYNAMITRON. The outstanding characteristic of this experiment was the simultaneous use of nine HPGe detectors in a 4π geometry to measure, for the first time in a single run, the complete AD of the emittedγ rays. The HPGe detectors were individually shielded by BGO detectors which reduced the background by a large factor. AD of the γ decay to the ^{16}O ground state were measured in the energy range Ec.m. = 1.30-2.78 MeV and in the angular range (Lab.) 30°–130°. From these distributions, astrophysical E1 and E2 S-factor functions vs energy were calculated, both of which are indispensable to the modeling of this reaction and the extrapolation toward lower energies. The separation of the E1 and E2 capture channels was done both by taking the phase value φ12 as a free parameter and by fixing it using the results of elastic α-particle scattering on ^{12}C in the same energy range.

Comment: This work is the most important experimental measurement for DA in $^{12}C\ (\alpha, \gamma_0)\ ^{16}O$, The DA and integrated $S_{g.s}$ at 3.570 MeV play a stdndard function for ftting of $^{12}C\ (\alpha, \gamma_0)\ ^{16}O$.

L. Matei2006

Among the cascade transitions of $^{12}C\ (\alpha, \gamma)\ ^{16}O$ reaction, some attention has been paid to the cascade transition via the 6.92 MeV and 7.12 MeV excited states in ^{16}O, however, no consideration has been given to a possible cascade via the first excited state of ^{16}O at 6.049 MeV as contributing to the $^{12}C\ (\alpha, \gamma)\ ^{16}O$ reaction cross section due to experimental difficulties in observing this transition. This excited 0+ state decays exclusively by e+e− transition (E0) to the 0+ ground state and only the primary γ-ray line can be observed. Ref. (Matei2006) report measurements of this radiative capture in $^{12}C\ (\alpha, \gamma)\ ^{16}O$ for center-of-mass energies of E=2.22 MeV to 5.42 MeV at the DRAGON recoil separator. To determine cross sections, the acceptance of the recoil separator has been simulated in GEANT as well as measured directly. The transition strength between resonances has been identified in R-matrix fits as resulting both from $E2$ contributions as well as $E1$ radiative capture, following the procedure described by Barker and Kajino (Barker1991). Details of the extrapolation of the total cross section to low energies are then discussed ($S_{6.05}(300) = 25^{+16}_{-15}$ keV b) showing that this transition is likely the most important cascade contribution for $^{12}C\ (\alpha, \gamma)\ ^{16}O$. This is one of the most important problems have to be resolved in this work.

M. Matei2008

In the experiment performed at Ohio University gamma-ray branching ratios of the 7.12-MeV state in ^{16}O have been measured using the γ-γ coincidence technique. An upper limit on the 7.12 → 6.92 MeV transition was set at 2×10^{-5}. These data reduce the uncertainty in both the extrapolation of the cascade cross section through the 6.92-MeV state and the extracted value. In the same experiment, relative cross sections and AD of the 7.12-, 6.92-, and 6.13-MeV to ground-state transitions have been studied for the $^{19}F(p, \alpha\gamma)$ reaction at several energies near Ep = 2 MeV. The available ED for the cascade through the 6.92-MeV state have been fitted with the R-matrix formalism, leading to $S_{6.92}$ (0.3) = 7.1 ± 1.6 keV b.

N. Tang2010

A measurement of the β-delayed α decay of ^{16}N using a set of twin ionization chambers is described in Ref. (Tang2010). Sources were made by implantation, using a ^{16}N beam produced via the In-Flight Technique. The energies and emission angles of the ^{12}C and α particles were measured in coincidence and very clean α spectra, down to energies of 450 keV, were obtained. The structure of the spectra from this experiment is in good agreement with results from previous measurements. Extracting the relevant SFof SE1 from the data is done using the R-matrix formalism through a least-squares by a simultaneous fit to data from the β-delayed α decay of ^{16}N, in combination with experimental results from the capture reaction $^{12}C\ (\alpha, \gamma)\ ^{16}O$ performed at higher energies, as well as with phase shift parameters obtained from elastic scattering of $^{12}C\ (\alpha, \alpha)\ ^{12}C$. The SE1 (0.3) value of 86 ± 22 keVb obtained in this experiment agrees within the uncertainties with data obtained during the last 15 years.

O. Schurmann2011

The radiative capture reaction ^{12}C (α, γ) ^{16}O has been investigated in the energy range E = 3.3 to 4.5 MeV in Ref. (Schurmann2011). This experiment focused in particular on the cascade transition to the 0+ state at Ex = 6.05 MeV in ^{16}O and was performed by detecting the capture γ -rays with a NaI detector array at the windowless ^{4}He gas target of the recoil mass separator ERNA in coincidence with the ^{16}O ejectiles. The 6.05 MeV transition has been considered recently as a component accounting for up to 15% of the ^{12}C (α, γ) ^{16}O total cross section at astrophysical energies. The arrangement of the detector array yielded additional information on the γ -ray multipolarity, i.e. the ratio σE2/σE1, and it was found that the 6.05 MeV transition is entirely E2 in the studied energy range. The results for this transition are analyzed in an R-matrix formalism and extrapolated to the relevant Gamow energy of stellar helium burning, E0 = 0.3 MeV. In contrast to a previous analysis (Matei2006), the present extrapolation suggests a negligible contribution from this amplitude, $S_{6.05}(0.300)$ < 1 keV b. Additional data for cascade transitions to excited states at Ex = 6.13, 6.92, and 7.12 MeV, respectively, as well as to the ground state were obtained and the corresponding SFs in the studied energy range are given.

P. Buchmann2006

For transitions to the ground state, only E1 and E2 (and higher electric multipole) radiative capture is allowed as only natural parity states can be populated by α-capture on ^{12}C. Only the radiative capture from the p- (l=1, E1) and d- (l=2, E2) waves are therefore important here for radiative capture into the $J^{\pi} = 0^{+}$ ^{16}O ground state. These two transitions mix in the AD11 following Eq. (1), while they add incoherently in the total cross section. The ways to distinguish E1 and E2 transitions experimentally are either to measure γ AD and evaluate the data by Eq. (1) or, for the E1 transition, to measure at 90°only as the E1 distribution peaks at 90◦, while the E2 distribution peaks at 45°and 135°, with no photons being emitted at 90°. With admixtures of E1and E2 components the distributions are asymmetric with respect to 90°. Note that while the E1 and E2 components for the ground state transition are thus separable, the errors (typically on S(300)) derived in fits to these individual components stay correlated in a complicated way which has never been taken into account.

P. Transfer reaction

The article (Oulebsir2012) reports that:

The extrapolation of the measured cross sections to stellar energies (E ∼ 0.3 MeV) is made particularly difficult by the presence of the 2^{+} (Ex = 6.92 MeV) and 1^{-} (Ex = 7.12 MeV) subthreshold states of ^{16}O. To further investigate the contribution of these two subthreshold resonances to the ^{12}C (α, γ) ^{16}O cross section, their α-reduced widths can be determined via a measurement of the transfer reaction ^{12}C (^{7}Li, t) ^{16}O. The uncertainties on the determined α-spectroscopic factors and the α-reduced widths maybe reduced by a detailed distorted-wave Born approximation analysis of the transfer AD. The R-matrix calculations of ^{12}C (α, γ) ^{16}O cross section can be used the obtained α-reduced widths for the 2^{+} and 1^{-}subthreshold resonances.

The article (Belhout2007) reports that:

The AD for low lying states of ^{16}O produced in the ^{12}C (^{6}Li, d) ^{16}O α-transfer reaction have been measured using a high energy resolution position sensitive detection system. The measured cross section data have been analyzed by the FRDWBA theory with a particular emphasis put on the states of astrophysical interest mainly the 1^{-} (7.12 MeV) state. Extracted values of nuclear level parameters (excitation energy, Ex, line width, Γc.m., α-spectroscopic factor, $S\alpha$, and reduced α-width, suggesting that the channel radius a = 6.5 fm is likely suitable for the calculations of reduced α-widths near the nuclear surface. However, given that previous DWBA results are available for comparison only near the channel radius a =5.5 fm, calculations have been carried out here for both three preceding a values. Formal values $0.0036 \leq \theta\alpha^{2}(7.12) \leq 0.152$, which is consistent with the preceding DWBA interval, and to a result for the E1 component of the reaction astrophysical factor, GTE10=80.6^{+17}_{-16} , very consistent with most constrained values previously reported in the literature.

The article (Brune1999) reports that:

The ^{12}C (α, γ) ^{16}O reaction is crucial for the understanding of He burning in massive stars, but the low-energy cross section is highly uncertain. To address this problem we have measured at sub-Coulomb energies total cross sections for the ^{12}C (^{6}Li, d) ^{16}O and ^{12}C (^{7}Li, t) ^{16}O reactions to the bound 2^{+} and 1^{-} states of ^{16}O. The data are analyzed to obtain the reduced a widths of these states. Together with

capture and phase-shift data, these results provide for a more accurate determination of the low energy ^{12}C (α, γ) ^{16}O *SF*: *SE*1 (0.3 MeV) = 101^{+17}_{-17} keV b and *SE*2 (0.3 MeV) = 42^{+16}_{-23} keV b for the *E*1 and *E*2 multipole components of the reaction.

In this way the SF results obtained maybe have large difference and lager uncertainty due to that it is very hard to get the closedα-spectroscopic factors, see Table as follow. The α-reduced widths of (Oulebsir2012) have been taken as experimental data for fitting.

References and notes

1. $S(E) = E \times \mathrm{Exp}(2\pi\eta) \times \sigma(E)$, $\eta = Z_1 Z_2 e^2 M/\hbar k$. In this paper, all E in CM system, all SF in KeV b.
2. Arnett1973. W. Arnett, Annu. Rev. Astron. Astrophys. 11, 73 (1973).
3. Tur2007 C. Tur, A. Heger, S. M. Austin, Astrophys. J. 671, 821 (2007).
4. Austin2011. S. M. Austin, A. Heger, C. Tur, Phys. Rev. Lett. 106, 152501 (2011).
5. Tur2010 C. Tur, A. Heger, S. M. Austin, Astrophys. J. 718, 357 (2010).
6. Inma2001 D. Inma, H. Peter, S. Osca, Astrophys. J. 557, 279 (2001).
7. Pignatari2010. M. Pignatari et al., Astrophys. J. 710, 1557 (2010).
8. Metcalfe2002 T. S. Metcalfe, M. Salaris, D. E. Winget, Astrophys. J. 573, 803 (2002).
9. Brown2001 G.E. Brown et al., New Astronomy 6, 457 (2001).
10. Fowler1984. W. A. Fowler, *Rev. Mod. Phys*. 56, 149 (1984).
11. Woosley2007. S. E. Woosley, A. Heger, *Phys. Rep*. 442. 269 (2007).
12. Rolfs1988C. E. Rolfs, W. S. Rodney, Cauldrons in the Cosmos (The Univ. of Chicago Press, 1988), pp. xi-xii.
13. Kirsebom2012. O. S. Kirsebom, M. Alcorta, M. J. G. Borge, M. Cubero, C. A. Diget, et al., *Phys. Rev. Lett.*, 108, 202501 (2012).
14. Xu2007. Y. Xu, W. Xu, Y.G. Ma, W. Guo, J.G. Chen, *et al*., *Nucl. Instrum. Methods in Physics Research A* 581 (2007).
15. Lane1958 A. M. Lane, R.G. Thomas, *Rev. Mod. Phys*. 30, 257 (1958).
16. Lane1960. A. Lane and J. Lynn, *Nucl. Phys*. **17**, C563 (1960).
17. Holt1978. R. J. Holt, H. E. Jackson, R. M. Laszewski, J. E. Monahan, J. R. Specht, *Phys. Rev. C* 18, 1962 (1978).
18. Barker1991. F. C. Barker, T. Kajino, *Aust. J. Phys*. 44, 36 (1991).
19. Azuma2010. R. E. Azuma, E. Uberseder, E. C. Simpson, C. R. Brune, H. Costantini, et al., *Phys. Rev. C* 81, 045805 (2010).
20. deBoer2013. R. J. deBoer, J. Görres, G. Imbriani, P. J. LeBlanc, et al., *Phys. Rev. C* 87, 015802 (2013)
21. Schurmann2012. D. Schürmann, L. Gialanella, R.Kunz, F. Strieder, *Phys. Lett. B* 711, 35 (2012).
22. Angulo2000. C. Angulo, P. Descouvemont, *Phys. Rev. C* 61, 064611 (2000).
23. Dufour2008. M. Dufour, P. Descouvemont, *Phys. Rev. C* 78, 015808 (2008).
24. Buchmann1996. L. Buchmann, R. E. Azuma, C. A. Barnes, J. Humblet, K. Langanke. *Phys. Rev. C* 54, 1(1996)
25. Kettner1982. K. U. Kettner, H.W. Becker, L. Buchmann, J.Görres, H. Kräwinkel, et al., *Z. Phys. A* 308, 73 (1982)
25. Tilley1993. D.R. Tilley, H.R. Weller, C.M. Cheves, *Nucl. Phys. A* 565, C1 (1993).
27. Carlson2009. A. D. Carlson, V. G. Pronyaev, D. L. Smith, N. M. Larson, Z. P. Chen *et al*., *Nucl. Data. Sheets* **110**, 3215 (2009).
28. NDS-IAEA2007. *Neutron cross section standards, IAEA* (2007)
29. Tang2010. X. D. Tang, K. E. Rehm, I. Ahmad, C. R. Brune, A. Champagne, et al., *Phys. Rev. C* 81, 045809 (2010).
30. Smith1991. D. L. Smith, *Probability, Statistics, and data Uncertainties in Nuclear Science and Technology* (Amer Nuclear Society, Chicago, 1991).
31. Welton1963. T. A. Welton, in Fast Neutron Physics, edited by J. B. Marion and J. L. Fowler (Interscience, New York, 1963), Vol. II, p. 1317.
32. Seyler1979. R. G. Seyler and H. R. Weller, Phys. Rev. C **20**, 453 (1979)
33. Chen2003. Z. P. Chen, R. Zhang, Y. Y. Sun, T. J. Liu, *Science in China* (Series G) 46, 225 (2003).
34. Barnett1974. A. R. Barnett, D. H. Feng, J. W. Steed, L. J. B. Goldfarb, *Comput. Phys. Commun. 8, 377 (1977).*
35. Oulebsir2012. N. Oulebsir, F. Hammache, P. Roussel, M. G. Pellegriti, L. Audouin, et al., *Phys. Rev. C* 85, 035804 (2012).
36. Belhout2007. Belhout A., Kiener J., Coc A., Duprat J., Engrand C. et al, *Nucl. Phys. A* **793**, 178 (2007)
37. Schurmann2005. D Schürmann, A. Di Leva, L. Gialanella, D.Rogalla, F.Strieder, et al., *Eur. Phys. J*. A 26, 301 (2005).
38. Schurmann2011. D. Schurmann, A. Di Leva, L. Gialanella, R. Kunz, F. Strieder, et al., *Phys. Lett. B* 703, 557 (2011).
39. Brochard1975. F. Brochard, P. Chevallier, D. Disdier, *J. Phys*. (Paris) 36, 113 (1975).
40. Redder1987. A.Redder, H.Becker, C.W.Rolfs, H.Trautvetter, T. R, P. Donoghue, et al., *Nucl. Phys. A* 462, C385 (1987).
41. Ouellet1996. J. M.Ouellet, M.L.Butler, H.N.Evans, H.C.Lee, J. R.W.Leslie, et al., *Phys. Rev. C* 54, 1982 (1996).
42. Kunz2001. R. Kunz, M. Jaeger, A.Mayer, J. Hammer, G. W. Staudt, et al., *Phys. Rev. Lett*. 86, 3244 (2001).
43. Assuncao2006. M. Assuncao, M. Fey, M. Lefebvre-Schuhl, J. Kiener, V. Tatischeff, et al., *Phys. Rev. C* 73, 055801 (2006).
44. Makii2009. H. Makii, Y. Nagai, T. Shima, M. Segawa, K. Mishima, et al., *Phys. Rev. C* 80, 065802 (2009).
36. Plag2012. R. Plag, R. Reifarth, *Phys. Rev*. C 86, 015805 (2012).
45. Kunz2002. R. KUNZ, M. FEY, M. JAEGER, *THE ASTROPHYSICAL JOURNAL*, 567:643-650 (2002)
46. Katsuma2008. M. Katsuma, *Phys. Rev. C* 78, 034606 (2008).
47. Xu2013. Y. Xu, K. Takahashi, S. Goriely, M. Arnould, M. Ohta, et al., *Nucl. Phys. A* 918, C61 (2013) (NACREII).
48. Brune1999. C. R. Brune, W. H. Geist, R. W. Kavanagh, K. D. Veal, *Phys. Rev. Lett.* 83, 4025 (1999).

49. Angulo1999. C. Angulo, M. Arnould, M. Rayet, P. Descouvemont, D. Baye, et al., *Nucl. Phys. A* 656, C3 (1999) (NACRE).
50. Hammer2005. J. W. Hammer, M. Fey, R. Kunz, J. Kiener, V. Tatischeff, et al., *Nucl. Phys. A* 752, C514 (2005).
51. Dyer1974. P. Dyer, C. A. Barnes, *Nucl. Phys. A* 223, C495 (1974).
52. Fey2004, PhD thesis, University Stuttgart, Germany, (2004).
53. Larson1964. J. D. Larson and R. H. Spear, *Nucl. Phys*. **56**, 497 (1964).
54. Plaga1987. R. Plaga, H. W. Becker, A. Redder, C. Rolfs, H. P. Trautvetter, *J, NP/A*, 465, 291, (1987)
55. Tischhauser2009. P. Tischhauser, A. Couture, R. Detwiler, J. Görres, C. Ugalde, et al., *Phys. Rev*. C 79, 055803 (2009).
56. Morris1968. J.M.Morris, G.W.Kerr, T.R.Ophel, *J, NP/A*, 112, 97, 1968
57. Brune1999. C. R. Brune, W. H. Geist, H. J. Karwowski, E. J. Ludwig, K. D. Veal, et al., *Phys. Rev.* Lett. **83**, 4025 (1999).
58. Zhao1993. Z. Zhao, R. H. France, III, K. S. Lai, S. L. Rugari, M. Gai, et al., *Phys. Rev. Lett*. 70, 2066 (1993).
59. Azuma1994. R. E. Azuma, L. Buchmann, F. C. Barker, C. A. Barnes, J. M. D'Auria, et al., *Phys. Rev.* C 50 1194 (1994).
60. Mitchell1964. I. V. Mitchell, T. R. Ophel, *Nuclear Physics* 58 (1964)
61. deBoer2012. R.J.Deboer, et al., Physical Review, Part C, Nuclear Physics, Vol.85, p.045804 (2012)
62. Fujita2013. K. Fujita, K. Sagara, T. Teranishi, W. Iwasaki, D. KaADma, et al., *Few-Body Systems* 54, 1603 (2013).
63. Ophel1976. T. R. Ophel, A. D. Frawley, P. B. Treacy, K. H. Bray, *Nucl. Phys. A* 273, C397 (1976).
64. Buchmann1996. L. Buchmann, *Astrophys*. J. 468, 127 (1996).
65. Caughlan1988. G.R. Caughlan, W.A. Fowler, At. *Nucl. Data. Tables* 40, 283 (1988) (CF88).
66. J. Ferguson, Angular Correlation Methods in Gamma-Ray Spectroscopy (North-Holland, Amsterdam),1965.
67 M. Gai et al., UConn-Yale-Duke-Weizmann-PTB-UCL Collaboration,., J. Phys. Conf. Ser. 337, 012054 (2012).
68. K. E. Rehm, J. Phys. Conf. Ser. 337, 012006 (2012).
69. Y. Xu et al. Nucl. Instrum. Methods Phys. Res., Sect. A581, 866 (2007).